The University Of Sheffield.

Access To Thesis.



- A bound copy of every thesis which is accepted as worthy for a higher degree, must be deposited in the University of Sheffield Library, where it will be made available for borrowing or consultation in accordance with University Regulations.
- All students registering from 2008–09 onwards are also required to submit an electronic copy of their final, approved thesis. Students who registered prior to 2008–09 may also submit electronically, but this is not required.

Author: Lindsey Dew Dept: Materials Science and Engineering

Thesis Title: Development of angiogenic models to investigate neovascularisation for tissue engineering applications Registration No: 110228507

**For completion by all students:**

Submit in print form only (for deposit in the University Library): ☐

Submit in print form and also upload to the *White Rose eTheses Online* server: In full ☑

Edited eThesis ☐

**Please indicate if there are any embargo restrictions on this thesis. Please note that if no boxes are ticked, you will have consented to your thesis being made available without any restrictions.**

| Embargo details: (complete only if requesting an embargo to either your print and/or eThesis) | Embargo required? | | Length of embargo (in years) |
|---|---|---|---|
| Print Thesis | Yes ☐ | No ☑ | ____ |
| eThesis | Yes ☐ | No ☑ | ____ |

**Supervisor:** I, the supervisor, agree to the named thesis being made available under the conditions specified above.

Name: Professor Sheila MacNeil Dept: Materials Science & Engineering

Signed:  Date: 21.10.15

**Student:** I, the author, agree to the named thesis being made available under the conditions specified above.

I give permission to the University of Sheffield to reproduce the print thesis in whole or in part in order to supply single copies for the purpose of research or private study for a non-commercial purpose.

I confirm that this thesis is my own work, and where materials owned by a third party have been used copyright clearance has been obtained. I am aware of the University's *Guidance on the Use of Unfair Means* (www.sheffield.ac.uk/lets/design/unfair)

I confirm that all copies of the thesis submitted to the University (including electronic copies on CD/DVD) are identical in content.

Name: Lindsey Dew Dept: Materials Science and Engineering

Signed:  Date: 21.10.15

**For completion by students also submitting an electronic thesis (eThesis):**

I, the author, agree that the University of Sheffield's eThesis repository (currently WREO) will make my eThesis available over the internet via an entirely non-exclusive agreement and that, without changing content, WREO may convert my thesis to any medium or format for the purpose of future preservation and accessibility.

I, the author, agree that the metadata relating to the eThesis will normally appear on both the University's eThesis server and the British Library's EThOS service, even if the thesis is subject to an embargo. I agree that a copy of the eThesis may be supplied to the British Library.

I confirm that the upload is identical to the final, examined and awarded version of the thesis as submitted in print to the University for deposit in the Library (unless edited as indicated above).

Name: Lindsey Dew Dept: Materials Science and Engineering

Signed: 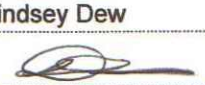 Date: 21.10.15

**THIS SHEET MUST BE BOUND IN THE FRONT OF THE PRINTED THESIS BEFORE IT IS SUBMITTED**


The University Of Sheffield.

# Development of angiogenic models to investigate neovascularisation for tissue engineering applications

*Author:*

Lindsey Dew

*Supervisors:*

Professor Sheila MacNeil
Dr Frederik Claeyssens
Dr CK Chong

*A report submitted in fulfilment of the requirements for the degree of Doctor of Philosophy in the*

Department of Materials Science and Engineering

February 21, 2015

University of Sheffield

# *Abstract*

Kroto Research Institute

Department of Materials Science and Engineering

by Lindsey Dew

The aim of this project was to develop *in vitro* models for angiogenesis that have the capability of combining pro-angiogenic cells with an extracellular matrix (ECM) component that can be monitored under flow conditions to learn more about the 'rules' of angiogenesis.

Significant advancement has been made in the field of tissue engineering in recent years, however one of the current obstacles limiting progression is the production of thick, complex tissues due to the lack of rapid neovascularisation of the constructs upon implantation. Blood vessel formation is tightly regulated and relies on the chronologically precise adjustment of vessel growth, maturation and suppression of endothelial cell growth - all of which are controlled by a large number of factors which influence each other. To induce vascularisation within tissue-engineered (TE) substitutes the same processes need to occur. A number of different vascularisation strategies have been investigated in an attempt to overcome this issue but as yet there is no unified solution to this problem. The most promising attempts have used scaffolds with vascular architectures, perfusion conditions and relevant cell types. Although it is recognised that perfusion conditions, the cell type and scaffold architecture are important with regards to vascularisation strategies many of the techniques fail to consider them in combination. It is therefore important to take a step back and understand how these factors work together to

promote angiogenesis in order to advance this crucial area. This lack of understanding is further compounded by the deficiencies of current angiogenesis models. Current *in vitro* models fail to combine the use of supporting cells, the extracellular matrix and fluid flow in 3D. Although this complexity exists within *in vivo* models such assays are primarily limited by the species used, organ sites available and complicated analysis techniques.

In this project two *in vitro* angiogenesis models were developed. The first was derived from the decellularisation of a rat jejunum. Characterisation showed the retention of key extracellular matrix (ECM) components and the removal of almost all cellular material. Re-endothelialisation with human dermal endothelial cells (HDMECs) of the patent vascular network showed enhanced results when co-cultured with human dermal fibroblasts (HDFs). In an attempt to induce angiogenesis, vascular endothelial growth factor (VEGF) loaded gels were placed on top of the scaffold whilst being continuously perfused with media. Placing VEGF loaded gels onto the recellularised jejunum led to the expression of the Notch ligand Delta-like-4 (DLL4) by HDMECs indicating their transformation into tip cells which are synonymous with sprouting angiogenesis.

The second was produced through the combination of robocasting and electrospinning. Nanofibrous poly(3-hydroxybutyrate-*co*-3-hydroxyvalerate) (PHBV) scaffolds with hollow channels capable of perfusion were produced that could be re-endothlialised with HDMECs. Again the addition of HDFs enhanced cellular distribution in the channels. Placing VEGF loaded gels onto the surface of the scaffolds led to the outgrowth of HDMECs into the gel, forming perfusable tubules.

Overall these two models overcome limitations of current *in vitro* models since they offer the capability of combining pro-angiogenic cells with ECM components that can be monitored under flow conditions. With further development they could provide more sophisticated platforms upon which to investigate the angiogenic process.

# *Acknowledgments*

I would like to first of all thank my primary supervisor Professor Sheila MacNeil for all of her support and guidance throughout this project. From my first terrified day she made me feel instantly welcome in her group and continued to help me throughout my time at the Kroto Research Institute. Her overwhelming enthusiasm and vision spurred me on even through the toughest of experiments. I would also like to thank my secondary supervisor Dr Fred Claeyssens for all of his input into the project, his great ideas and his excellent sense of fun. Thanks also goes to Dr Will English who treated me like one of his own PhD students, spending hours chatting about the project over tea and for generally being a font of angiogenesis knowledge. I would also like to thank all of those at the Kroto Research Institute who have helped me along the way. In particular, Dr Anthony Bullock who taught me the art of cell culture, Dr Frazer Bye who showed me the ropes of the lab when I first arrived, Dr Julio Bissoli who spent hours teaching me how to cannulate and be a pseudo-surgeon, Mark Wagner and Robert Dickinson who know everything about anything Kroto related (and I'm sure much more) and Dr Ilida Ortega who was a great teacher showing me how to be an efficient researcher and who has become a great friend. My partners in PhD crime, Giulia Gigliobianco and Leyla Zilic have become like sisters to me, sharing in the ups and downs and for this I am truly grateful. A very special thank you goes to my family for all of their continued support, who I am sure could describe each of my experiments and answer questions related to any part of my PhD in great detail. I am very grateful to my parents Karen and John, my sister Stacey and my aunty Lynn who have always encouraged me to pursue what makes me happy and who have had to learn how to become my emotional counsellors and motivators. I am so fortunate to have such a great bunch of fun and loyal people to call my family. Lastly a massive thank you to my boyfriend Dr Chris Reynolds who makes me laugh every day. He has patiently listened to me endlessly talk about my project and my worries to the point where he could have joined my supervisory team. I am truly lucky to have found such an amazing person to share my life with.

*This thesis is dedicated to Karen, John and Stacey Dew, Christopher Reynolds, Lynn Jobson and my beloved nanna the late Maria Jobson.*

# *Outputs*

## Publications

**Dew L.**, MacNeil S. and Chong CK. (2015). Vascularization strategies for tissue engineers. Regenerative Medicine 10(2), 211-224.

Ortega I. †, **Dew L.** †, Kelly AG., Chong CK., MacNeil S. and Claeyssens F. (2015). Fabrication of biodegradable synthetic perfusable vascular networks via a combination of electrospinning and robocasting. Biomaterials Science 00, 1-5. † These authors have contributed equally to this work.

## Publications in preparation

**Dew L.**, English WR., Chong CK. and MacNeil S. Investigating neovascularization in rat decellularized intestine - an in vitro platform for studying angiogenesis.

**Dew L.**, English WR., Ortega I., Claeyssens F. and MacNeil S. Fabrication of biodegradable synthetic vascular networks and their use as a model of angiogenesis. Submitted to Cells Tissues Organs journal (04/10/2015).

## Presentations

**Enabling the induction of neovascularisation in tissue-engineered skin**. TERMIS-EU Meeting, 17/6/2013 - 20/6/2013, Istanbul, Turkey.

**Decellularised rat liver and jejunum bioscaffolds for neovascularisation in tissue engineering.** TCES Meeting, 23/7/2013 - 25/7/2013, Cardiff, UK.

**Decellularised organs: a tool to enable neovascularisation in tissue engineering.** The 15th International Conference on Biomedical Engineering (ICBME), 4/12/2013 - 7/12/2013, Singapore.

**Enabling neovascularisation in tissue engineering.** DTC Joint Conference, 11/7/2014, Nottingham, UK.

**Development of angiogenic models to investigate neovascularisation for tissue engineering applications.** DTC Joint Conference, 21/7/2015, Leeds, UK.

**Development of an angiogenic models to investigate neovascularisation in tissue engineering.** ESB, 30/8/2015 – 3/9/2015, Poland.

## Posters

**Enabling the induction of neovascularisation for tissue engineering applications.** DTC Joint Conference, 10/7/2012, Keele, UK.

**Induction of neovascularisation in tissue engineering.** BITEG Work in Progress Meeting, 17/12/2012, York, UK.

**Decellularisation: enabling neovascularisation in tissue engineering.** DTC Joint Conference, 12/7/2013, Sheffield, UK.

**Decellularised jejunum: A tool to enable neovascularisation in tissue engineering.** BITEG Work in Progress Meeting, 19/12/2013, Leeds, UK.

**Towards the modelling of neovascularisation in tissue engineering.** The University of Sheffield Engineering Symposium (USES), 24/6/2014, Sheffield, UK.

**Towards the prevascularisation of tissue-engineered skin substitutes.** TCES Meeting, 2/7/2014 - 4/7/2014, Newcastle, UK.

**Modelling neovascularisation in tissue engineering.** Angiogenesis and Vascular Remodelling: New Perspectives, 14/7/2014 - 16/7/2014, Chester, UK.

**Investigating neovascularisation in rat decellularised intestine – an *in vitro* platform for studying angiogenesis.** ESB, 30/8/2015 – 3/9/2015, Poland.

**Development of a three-dimensional *in vitro* model to study neovascularisation.** TERMIS-World Congress, 8/9/2015 – 11/9/2015, Boston, USA.

# Table of Contents

# List of Figures

# List of Tables

# Glossary

| | |
|---|---|
| ADMSC | Adipose derived mesenchymal stem cells |
| BMMSC | Bone marrow derived mesenchymal stem cells |
| BPT | British Pipe Thread |
| BSA | Bovine serum albumin |
| CAM | Chorioallantoic membrane |
| CC | Cardiac construct |
| CM | Cardiomyocyte |
| $CO_2$ | Carbon dioxide |
| CTF | Cell traction forces |
| DAPI | 4',6-diamidino-2-phenylindole |
| DCM | Dichloromethane |
| DMB | Dimethylmethylene blue |
| DMEM | Dulbecco's Modified Eagle Medium |
| DTC | Doctoral training centre |
| EC | Endothelial cells |
| ECM | Extracellular matrix |
| EDTA | Ethylenediaminetetraacetic acid |
| EPC | Endothelial progenitor cells |
| ESC | Embryonic stem cells |
| FCS | Fetal calf serum |
| FGF | Fibroblast growth factor |
| FITC | Fluorescein isothiocyanate |
| GAG | Glycosaminoglycan |
| GFP | Green fluorescent protein |
| GM | Genetically modified |
| H&E | Hematoxylin and Eosin |
| HBSS | Hanks Balanced Salt Solution |
| HC | Hepatocyte |
| HDF | Human dermal fibroblasts |
| HDMEC | Human dermal microvascular endothelial cells |
| HMDS | Hexamethyldisilazane |
| HMW | High molecular weight |

| | |
|---|---|
| HSC | Hematopoietic stem cells |
| HUVEC | Human umbilical vein endothelial cells |
| IgG | Immunoglobulin G |
| IMS | Industrial methylated spirits |
| iNOS | Inducible nitric oxide synthase |
| MEF | Mouse embryonic fibroblasts |
| MEMS | Microelectromechanical systems |
| MMPs | Metalloproteinases |
| MSC | Mesenchymal stem cell |
| MV | Microvascular |
| NO | Nitric oxide |
| $O_2$ | Oxygen |
| PA | Peracetic acid |
| PBMC | Peripheral blood mononuclear cells |
| PBS | Phosphate buffered saline |
| PDGF | Platelet derived growth factor |
| PDO | Polydioxanone |
| PEG | Polyethylene glycol |
| PEUU | Polyether urethane urea |
| PFA | Paraformaldehyde |
| PHBV | Poly 3-hydroxybutyrate-*co*-3-hydroxyvalerate |
| PVA | Polyvinyl alcohol |
| RBC | Red blood cells |
| RFP | Red fluorescent protein |
| ROCK | Rho-associated kinase |
| RPM | Revolutions per minute |
| RT | Room temperature |
| SDS | Sodium dodecyl sulphate |
| SEM | Scanning electron microscopy |
| SIS | Small intestinal submucosa |
| SMA | Superior mesenteric artery |
| SMC | Smooth muscle cells |
| TCP | Tissue culture plastic |
| TE | Tissue-engineered |
| UTS | Ultimate tensile stress |
| VEGF | Vascular endothelial growth factor |

| | |
|---|---|
| VPPG | Vascular pattern path generator |

# Chapter 1

# Introduction

## 1.1. Structure and function of the vascular system

Diffusion is a mechanism used widely throughout the body to transport substances from regions of higher concentrations to those of lower concentrations. However, beyond a distance of a few cell diameters, it is too slow to meet the metabolic requirements of cells. As a result the circulatory system provides an alternative mechanism to transport molecules rapidly over long distances between cells and the body's surface and also between various specialised tissues and organs in large, multi-cellular organisms.

The blood vessels of the circulatory system form a detailed network of interconnected tubes that transport blood, pumped by the heart, throughout the entire body. The three main types of blood vessel present in the body are the arteries, veins and capillaries; all of which are composed of several layers (Figure 1). All vessels consist of a single cell thick inner layer of endothelial cells (ECs) known as the tunica intima that lines the lumen forming a smooth, friction reducing surface. Mural cells wrap around this structure stabilising the vascular tube and are contractile in nature in order to regulate vessel diameter and consequently blood flow. In smaller vessels (capillaries) mural cells are sparse and usually referred to as pericytes with little to no elastin present since the expansion and recoil of these vessels is low due to the small pressures present. In larger vessels (veins, arteries etc.) they are multi-layered and referred to as smooth muscle cells (SMCs) which are reinforced by organised layers of elastic tissue that form elastic laminae. This middle layer, or tunica media, is particularly thick in the arteries that must be elastic and strong enough to sustain large pulsatile pressures caused by the outflow of blood from the heart. The outermost layer, the tunica adventitia, is composed largely of

collagen fibres with SMCs present in larger vessels that are required to stretch and recoil, such as veins [1].

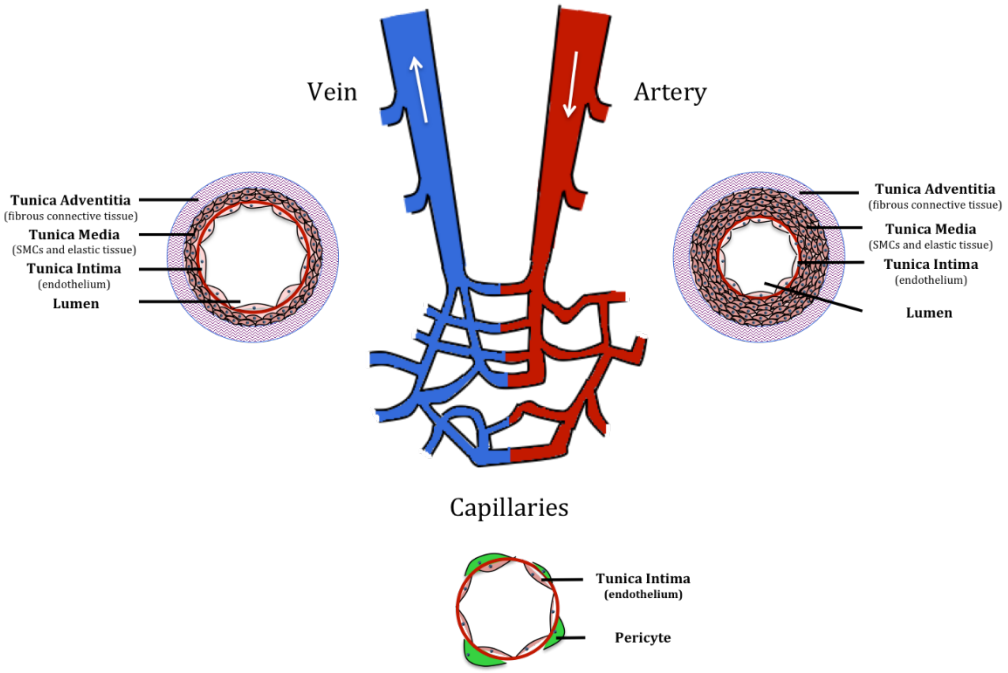


Figure 1 - Blood vessel hierarchy and structure

## 1.2. Formation of the vascular system

Since blood vessels are essential in providing tissues with nutrients and removing waste from these sites they begin to form in the early stages of embryonic development via three distinct processes: *vasculogenesis*, *angiogenesis* and *arteriogenesis* [2].

### 1.2.1. Vasculogenesis

The formation of the first capillaries takes place by vasculogenesis. Initially aggregations of cells called blood islands form in the embryonic yolk sac and contain a homogenous collection of cells called hemangioblasts, which are the precursors to blood and blood vessels. As

these cells develop, two distinct types of cells are formed: hematopoietic stem cells (HSCs) and endothelial progenitor cells (EPCs). As the blood islands merge, the HSCs which sit in the centre of the blood island develop into blood cells and the EPCs which occupy the periphery of the blood island develop into a primitive capillary plexus that grows towards the embryo [3] as illustrated in Figure 2.

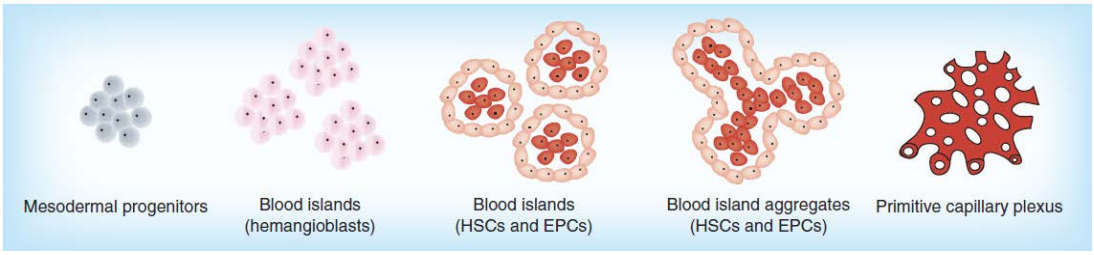


Figure 2 - Formation of primitive capillary plexus via vasculogenesis

### 1.2.2. Angiogenesis

The primitive network then grows and remodels via angiogenesis, invading target tissues and giving rise to the more developed capillary plexuses of embryonic organs. It does this through two distinct processes known as sprouting and non-sprouting angiogenesis.

Sprouting angiogenesis is a process whereby ECs branch out from an existing capillary extending through the surrounding matrix to form a new vessel. The steps involved in this process are outlined below and illustrated in Figure 3 [4]:

1. The basement membrane is dissolved and pericytes detach from the capillary
2. ECs migrate towards the extracellular space and form an endothelial sprout
3. ECs start to proliferate downstream of the leading edge of the sprout
4. A lumen forms in the endothelial sprout

5. A closed loop forms with another vessel (i.e. anastomoses)
6. Pericytes are recruited and the basement membrane forms around the new vessel

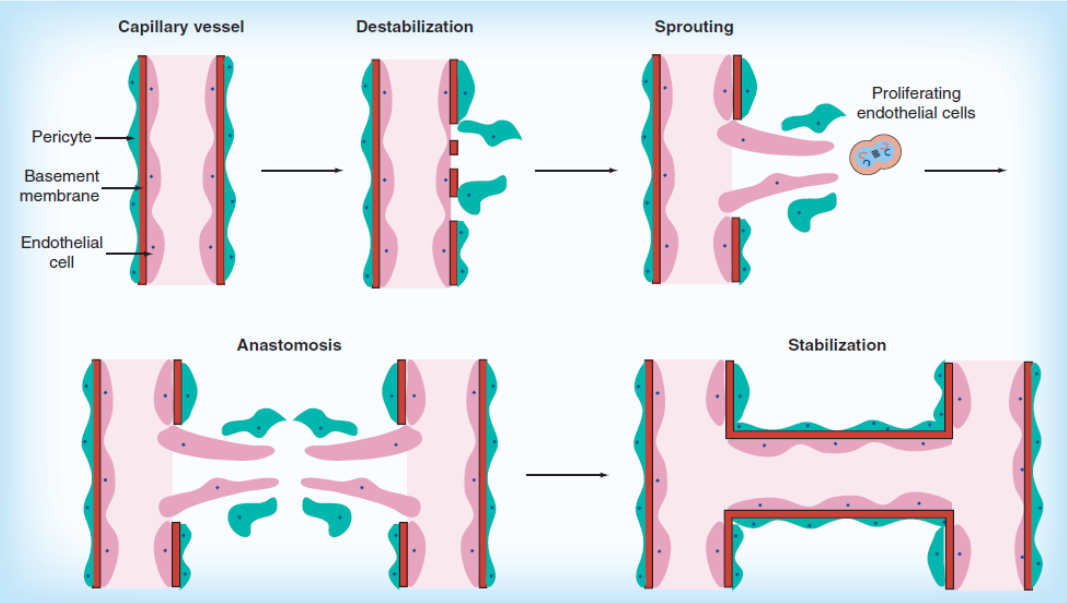


Figure 3 - Process of sprouting angiogenesis whereby ECs branch out from an existing capillary extending through the surrounding matrix to form a new vessel.

Non-sprouting angiogenesis refers to the process whereby a single capillary splits into two from within (Figure 4). The process takes place via several distinct steps [5]:

1. The endothelial walls of the opposite sides of a vessel migrate towards each other forming what is known as an 'intraluminal pillar'
2. A central perforation is then formed in the centre of the pillar
3. The pillar is invaded with pericytes and myofibroblasts that deposit extracellular matrix (ECM) into the pillar
4. Several pillars then increase in size and merge, splitting up the original capillary into two new capillaries.

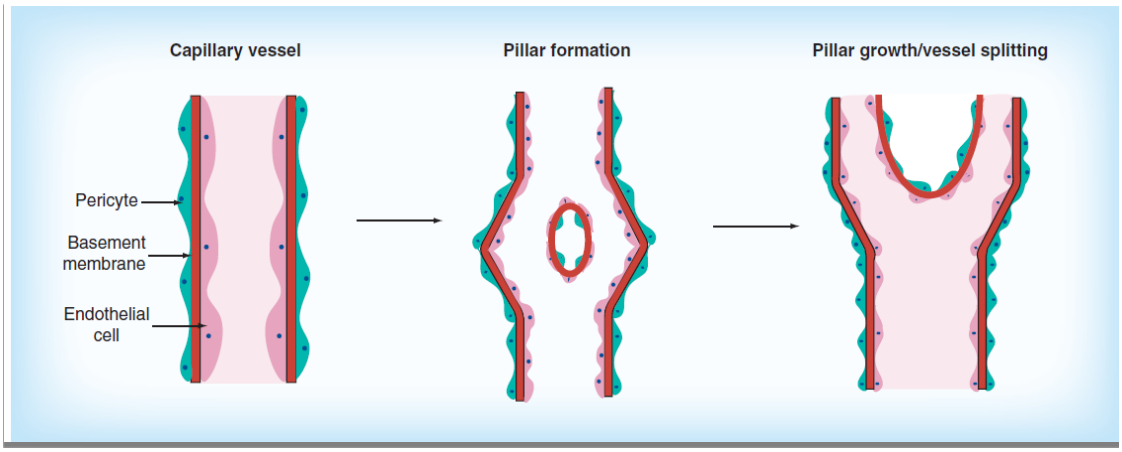


Figure 4 - Process of non-sprouting angiogenesis whereby a single capillary splits into two capillaries from within.

Key factors influencing angiogenesis have been identified and can be broadly split into molecular and mechanical mechanisms. It is important to note that most of the information presented has been attained through the study of extraembryonic sprouting angiogenesis and the work presented throughout refers to this type of angiogenesis [6].

## Molecular Mechanisms

Numerous endogenous biochemical factors capable of stimulating or inhibiting angiogenesis have been identified. These are mainly cytokines and their receptors, ECM constituents, cell-matrix adhesion molecules and matrix degrading enzymes. A brief overview of the roles these factors play in physiological angiogenesis is provided. Here, whilst the effect each factor has throughout the angiogenic process is summarised in Table 1 readers that require more details in these topics are referred to other sources [7–10].

### *Cytokines and their receptors*

Hypoxia occurs when the balance between the supply and demand of oxygen ($O_2$) is altered and the level of $O_2$ reaching the cells is depleted. The founding member of the hypoxia inducible factor (HIF), HIF-1α

regulates a broad spectrum of genes in response to $O_2$ deprivation. The HIF pathway is controlled by prolyl hydroxylase domain (PHD) enzymes. At physiological $O_2$ levels HIF-1α becomes hydroxylated by members of the PHD family. Hydroxylation generates a binding site for the von Hippel-Lindau (pVHL) tumour suppressor protein and as a result HIF-1α is polyubiquitylated and undergoes proteosomal degradation. When the environment is hypoxic and $O_2$ is depleted, the rate of hydroxylation is suppressed and so HIF-1α accumulates. It then dimerizes with a HIF-β family member, translocates into the nucleus and leads to gene activation [11][12,13] that promotes the short and long term adaptation to hypoxia. Long term adaptation to local hypoxia is controlled via stimulating angiogenesis. The HIF pathway regulates a host of angiogenesis related genes including vascular endothelial growth factor (VEGF), angiopoietin-1 (Ang-1) and angiopoietin-2 (Ang-2), platelet derived growth factor (PDGF), Tie-2, basic fibroblast growth factor (bFGF), transforming growth factor-β (TGF-β) etc. [14]. Pro-angiogenic growth factors signal through their receptors on ECs and activate endothelial nitric oxide synthase (eNOS). The action of shear stress also activates eNOS. Upon activation eNOS catalyses L-arginine to L-citrulline and nitric oxide (NO). Finally, NO release induces angiogenesis through EC migration, proliferation etc. [15] The effects of such aforementioned cytokines are discussed below.

Studies have shown that acidic fibroblast growth factor (aFGF) and bFGF induce the production of matrix proteases in ECs that break down the ECM and allow migration of ECs into the surrounding matrix allowing the formation of capillary like tubes [16]. Fibroblast growth factor (FGF) is not only specific to ECs but also acts on most cells derived from the embryonic mesoderm and neuroectoderm, including fibroblasts and pericytes [17]. It is believed that storage of FGF in the ECM is possible and when the matrix is degraded FGF can be released [18].

VEGF is known to be a key angiogenic stimulator. The VEGF family is composed of 7 members: VEGF-A, VEGF-B, VEGF-C, VEGF-D, VEGF-E, VEGF-F and placenta growth factor. VEGF-A in particular (referred to as VEGF herein) is known to be a major regulator of physiological and

abnormal angiogenesis and in turn has many isoforms including $VEGF_{121}$, $VEGF_{145}$, $VEGF_{165}$, $VEGF_{183}$, $VEGF_{189}$ and $VEGF_{206}$ [19]. Of these isoforms, $VEGF_{165}$ has been found to have optimal bioavailability combined with high biological potency and is therefore used in many angiogenesis studies [19,20]. Its effect is mediated by the receptor, VEGFR-2 which is expressed predominantly in ECs. VEGF binding causes VEGFR-2 activation, which in turn sets off multiple intracellular responses and leads to a complete angiogenic process [21,22]. VEGF is produced by many cells and a major regulator in its production is the local oxygen concentration. Cells that experience reduced oxygen levels upregulate the production of VEGF, which in turn acts on ECs causing them to proliferate and invade the hypoxic tissue in order to provide new blood vessels for increased oxygen transfer [14,23].

PDGF is produced by cells including platelets, fibroblasts, ECs and macrophages. The effects of PDGF are again mediated through its receptors, which can be found in ECs, pericytes and SMCs in blood vessel walls. Signalling via PDGF and its receptor are important in blood vessel maturation, causing vessels to stabilise and maintain their vascular integrity [24].

Members of the TGF-β family are multifunctional cytokines that affect many forms of cell behaviour including proliferation, recognition, differentiation, apoptosis, inflammation and angiogenesis [25,26]. As a result of its diverse nature, TGF-β and its receptors are expressed in a range of cells. Depending on the cell type and extracellular surrounding they mediate different and sometimes opposite effects on the same cells [25]. This has been observed in many angiogenesis studies where the effects of TGF-β have been found to be concentration/context driven [27]. At low concentrations TGF-β promotes angiogenesis by upregulating pro-angiogenic factors, stimulating EC proliferation and migration, and the production of proteinases that break down the local ECM. However, at high doses TGF-β inhibits EC growth and promotes the reformation of the basement membrane whilst stimulating SMC differentiation and recruitment to stabilise the vessels [28].

ECs have a specific receptor called Tie-2. The angiopoietins, Ang-1 and Ang-2 are ligands for Tie-2 and play antagonistic roles in angiogenesis [28]. Ang-1 activates the Tie-2 receptor and promotes the recruitment of pericytes and SMCs in order to stabilise and maintain vascular integrity. Ang-2 on the other hand competes with Ang-1 for binding of Tie-2 and blocks vessel stabilisation from Tie-2 signalling, thereby loosening the interactions between ECs and pericytes and the ECM [28].

*ECM, Integrins and matrix proteases*

The ECM is not only responsible for providing physical support for cellular components but it also provides biochemical and mechanical cues that regulate cellular function and can affect the angiogenic process [29]. In the case of biochemical regulation, studies show that matrix molecules found in the basement membrane (more specifically, decorin and tenascin C) cause ECs to establish and maintain capillary like structures throughout angiogenesis [30]. Molecules such as hyaluronan have been implicated in the inhibition of angiogenesis by reducing EC migration and adhesion when in its native high molecular weight (HMW) form. However under certain physiological and pathological instances HMW hyaluronan can be broken down into smaller segments, termed oligomers, which have been found to stimulate EC proliferation and promote angiogenesis. It has been found that hyaluronan oligomers compete with native HMW hyaluronan in binding to the receptor CD44 present on ECs. Unlike HMW hyaluronan, the oligomers can trigger intracellular signalling pathways that prompt cell proliferation [31].

The effects of ECM components are mediated by their adhesion to cell surface receptors, known as integrins. Of the more than 20 integrin types, $\alpha_v\beta_3$ has been studied extensively for its role in angiogenesis. It is heavily upregulated on ECs by the action of angiogenic growth factors such as bFGF, tumour necrosis factor-$\alpha$ (TNF-$\alpha$) and interleukin-8 (IL-8) and enhances EC survival as well as localising degradation proteins to the tips of sprouting blood vessels helping to increase cell migration speed and matrix degradation in this area [32]. Angiogenesis induced by VEGF

depends on another integrin, $\alpha_v\beta_5$ , which promotes EC migration and invasion [32,33]. It has been shown that these integrins promote distinct pathways in angiogenesis and drive distinct cellular behaviours [34].

When angiogenesis takes place the local ECM is degraded by matrix metalloproteinases (MMPs). Upon degradation they allow the release of angiogenic growth factors stored in the ECM. Their activity is tightly controlled by several mechanisms to prevent excessive breakdown of the ECM and to guide directional cell migration and invasion. Protease inhibitors are secreted by cells near areas of active matrix degradation in order to protect uninvolved matrices [2,35].

### Mechanical Mechanisms

All cells in the body are subjected to mechanical forces that are either self-generated or originated from their surrounding environment. In comparison to the wealth of knowledge regarding the molecular mechanisms of angiogenesis, there is limited research that investigates its mechanical regulation. This section aims to highlight the implications of intrinsic and extrinsic cellular forces on physiological angiogenesis.

Maintaining the structure and shape of a cell requires forces to be transmitted from the actin-myosin fibres, via integrins, to the ECM proteins and these forces are known as the cell traction forces (CTFs) [36]. Thus the adherent cell is under tension due to the ECM's resistance to deformation. As well as the cell–ECM contacts, cells also form cell-cell contacts with their neighbours and as a result a continuous cellular tissue is maintained. The amount of cytoskeletal tension can change by rearrangement of the cytoskeletal proteins and adhesion sites, whether it is in response to external biochemical or mechanical stimuli [37]. This can cause a multitude of results critical to angiogenesis such as cell migration, matrix remodelling etc.

With regards to cell migration, CTFs are the driving force behind cell movement. Initially the cell propels its membrane forward by orienting and reorganising the actin-myosin network at its leading edge. It then attaches to the ECM at the leading edge and releases its contact to the

substrate at the trailing edge of the cell pulling itself forward by the CTFs generated [38]. Rho is a member of the Ras family of small GTP binding proteins. The Rho GTPase family consists of 3 subfamilies – Rho (RhoA, RhoB and RhoC), Rac (Rac1, Rac2 and Rac3) and CDC42. RhoA is the most extensively studied Rho family member and it main target is Rho-associated kinase (ROCK) [39]. Activation of the Rho/ROCK pathway (by cell signalling, growth factors etc.) plays a key role in actin cytoskeleton organisation, whereby inhibiting the action of Rho or ROCK reduces the capacity of ECs to form tubular networks [40]. The inhibition of ROCK also substantially reduces the CTFs and subsequent migration speed of ECs [6]. This indicates that the Rho/ROCK pathway and resultant CTFs play a role in regulating angiogenesis.

With regards to matrix remodelling it has been found that cells such as fibroblasts and ECs distort and rearrange their surrounding ECM, via CTFs, when they move across it. The resultant ECM tends to align parallel to the migrating cell [41] and during angiogenesis, the production of an aligned ECM at the sprouting tip of a new vessel creates a track for the trailing ECs to follow [42].

Along with CTFs, the mechanical properties of the ECM also play an important role in the assembly and maintenance of the microvasculature. The form and function of ECs is highly influenced by the Young's Modulus of the surrounding ECM. For example, compliant matrices tend to induce network formation by allowing ECs to reorganise the ECM through CTFs [42]. However, there is believed to be an upper limit of flexibility a matrix can have with regards to angiogenesis [43]. It has been found that ECM properties are actively modified throughout the process of angiogenesis, via the production of MMPs [30]. A better understanding and control of such properties could therefore lead to improved vascularisation in both native and engineered tissues.

Blood vessels are constantly subjected to external mechanical forces originating from either blood flow or the extravascular environment. The action of blood flowing past ECs results in a drag force tangential to the apical surface of the cells known as shear stress. Studies have shown that capillaries exposed to higher blood flow velocities (and hence shear

stresses) had more sprouts, but capillaries with slow flow gradually narrowed and disappeared [44]. Stretching of muscle was also reported to stimulate capillary growth *in vivo* but via a different mechanism [45]. Studies show that capillaries formed in stretched muscle are produced mainly by sprouting angiogenesis, whereas increased shear stresses cause capillary growth via non-sprouting angiogenesis [46]. This implies that the molecular events that drive angiogenesis differ with stimuli. Although progress has been made in this area more work is necessary to fully understand the roles that externally applied forces play in angiogenesis.

Table 1 - Biochemical and mechanical regulators of angiogenesis.

| Event | Factor | Description |
|---|---|---|
| ***Angiogenic trigger*** 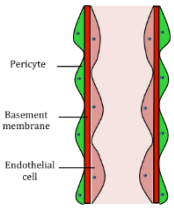  | Hypoxia | Reduction in $O_2$ pressure activates transcription of various angiogenesis related genes [14]. |
| | Shear stress | Evidence shows that increased shear stresses are related to an increased level of capillary formation [44]. |
| ***Destabilisation*** 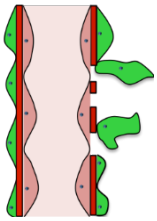 | VEGF | Leads to increased vessel permeability [21,22]. |
| | Ang-2 | Loosens interaction between ECs and pericytes [28]. |
| | MMPs | Locally breaks down ECM to provide space for migration of cells [35]. |
| ***Sprouting*** 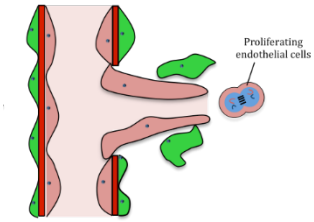  | VEGF | Leads to EC proliferation and invasion of hypoxic tissue [21,22]. |
| | Ang-2 | Maintains loosened interactions between ECs and pericytes [28]. |
| | FGF | Induce production of MMPs that break down ECM and allows migration of ECs [16]. |
| | MMPs | Break down ECM to provide space for migration of cells and releases stored FGF from ECM [2,35]. |
| | TGF-β (low concentration) | Stimulates EC proliferation and migration and upregulates MMPs to break down ECM [28]. |
| | Integrins | $\alpha_v\beta_3$ upregulated on ECs by action of bFGF and enhances EC survival as well as localising degradation proteins to tips of sprouting vessels, helping to increase migration speed and matrix degradation. $\alpha_v\beta_5$ upregulation induced by VEGF promotes EC migration and invasion [32,34]. |
| | CTFs | Aid in pulling cells forward [38]. |
| | ECM Modulus | Compliant matrices allow ECs to reorganise ECM through CTF during network formation [42]. |
| ***Anastomosis/Stabilisation*** 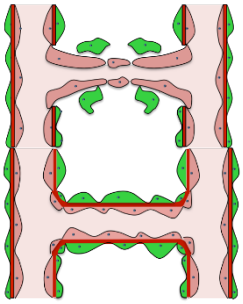 | TGF-β (high concentration) | At high doses TGF-β inhibits EC growth and promotes reformation of basement membrane. It also stimulates recruitment of pericytes to stabilise vessels [28]. |
| | PDGF | Causes vessels to stabilise and maintain their vascular integrity [24]. |
| | Ang-1 | Promotes recruitment of pericytes to stabilise and maintain vascular integrity [28]. |

### The Interplay between Molecular and Mechanical Mechanisms

It is important to note that although molecular and mechanical factors (summarised in Table 1) have been discussed separately, the activity of an angiogenic stimulus or inhibitor depends on the presence/concentration of other factors in the environment. These can vary both temporally and spatially throughout the angiogenic process and this may explain why angiogenic factors often display context/concentration dependent actions in various experimental setups [4]. Better understanding of the interplay between ECs, molecular and mechanical factors will certainly play an important role in understanding the fundamental regulation of angiogenesis.

## 1.2.3. Arteriogenesis

Once pericytes have been recruited, some vessels remain as capillaries and others are subsequently covered by a muscular coat endowing them with viscoelastic and vasomotor properties necessary to accommodate the changing needs in tissue perfusion. This process is known as arteriogenesis [4]. Readers interested in this topic are guided towards other sources [47,48].

Although this section is by no means an exhaustive review of all of the factors that influence blood vessel formation it does highlight the complex nature of the process.

## 1.3. The importance of vascularisation in tissue engineering

Tissue engineering was originally developed as an alternative therapy for the treatment of tissue loss or end-stage organ failure, resolving the shortage of tissues and organs available for transplantation therapy. It represents a biology driven approach by which constructs are engineered to replace damaged, injured or missing tissues through combining materials technology and biotechnology [49,50]. Significant progress has been made in recent years, however one of the current obstacles in the field is the production of thick (≥2 mm), complex tissues due to the lack of rapid neovascularisation of the constructs [51]. Blood vessel formation is tightly regulated and relies on the chronologically precise adjustment of vessel growth, maturation and suppression of EC growth - all of which are controlled by a large number of factors which influence each other. To induce vascularisation within tissue engineered (TE) substitutes these same processes need to occur. The complexity of these tightly regulated processes explains why this remains one of the major obstacles in the field of tissue engineering at present [51]. To overcome this the aim is to translate the basic principles of angiogenesis to produce a physiologically relevant TE construct fit for use in the clinic. This section describes the current vascularisation strategies that have been adopted for bladder, liver, myocardium and skin, the tissues where there have been considerable research efforts to overcome these problems for the introduction of materials into patients as summarised in Table 2. These are discussed under five headings as follows: prevascularisation systems; scaffold functionalisation; harnessing natural vascular architectures; production of a synthetic vascular architecture; integrating cellular components and are summarised in Figure 5.

### 1.3.1. Prevascularisation systems

This approach aims to produce TE constructs with a network of functional capillaries in order to accelerate anastomosis with the host tissue upon implantation. This has been attempted both *in vivo* and *in vitro*.

- *In vitro prevascularisation.* In this approach the construct is cultured *in vitro* with the aim of producing a three dimensional (3D) prevascularised structure that can be implanted and subsequently connected with the existing vasculature in the site of implantation. For example, Sekine *et al.* have attempted to prevascularise myocardial cell sheets *in vitro* using a vascular bed and bioreactor system for the reconstruction of heart tissue. Here tissue that contained an artery and vein was resected and connected to a perfusion bioreactor to establish a vascular bed. A tri-layer cardiac cell sheet produced with a co-culture of ECs was then overlaid onto the vascular bed. ECs were shown to connect to capillaries in the vascular bed forming tubular lumens and producing *in vitro* perfusable blood vessels in the cell sheet [52]. This method seems promising with the possibility of thicker constructs being developed by stacking cell sheets [53].

- *In vivo prevascularisation.* Some approaches have used the host's intrinsic vasculature to vascularise the constructs *in vivo*. For example, in the case of the reconstruction of the bladder autologous engineered bladder tissues have used the host omentum to vascularise the implanted tissues [54]. Here, urothelial and SMC from patient biopsies were grown *in vitro* and cultured onto biodegradable bladder-shaped scaffolds made of collagen, or composites of collagen and polyglycolic acid. The omentum was used as a wrap in some patients and not in others. Post-operatively patients who had this omental wrap, showed the greatest improvement in bladder function as it enhanced angiogenic ingrowth of vessels and subsequently supported and maintained the transplanted cells. Overall, it was suggested that this method can be used in patients who need cystoplasty but additional studies are needed before this procedure can be used widely [54]. In cases where wrapping the TE construct is impractical due to anatomical location, a two-staged approach has been suggested whereby the construct is firstly prevascularised by the intrinsic vasculature before implanting into the required area. In the case of heart tissue, Dvir *et al.* took neonatal cardiac cells and seeded them onto an alginate scaffold in combination with angiogenic factors. It was

then vascularised for 7 days on the omentum before transplantation onto infarcted rat hearts. After 28 days the scaffold showed both structural and electrical integration [55]. Although promising, this technique requires a two-step procedure and may suffer from complications. Alternatives to the omentum have also been studied and include the use of arteriovenous loops (AVs). These connect an artery and a vein through the use of either an autologous vein or synthetic equivalent and this is placed inside a chamber that houses a TE substitute to be vascularised which is subsequently placed into a well vascularised site within the recipient. Tanaka *et al.* successfully used an AV shunt within rats to vascularise a sheet of artificial skin dermis (PELNAC) [56]. It is suggested that new blood vessels are induced as a result of the increased shear stresses within the AV [57]. Although a promising technique, the need for several surgeries is a concern when considering its clinical application.

### 1.3.2. Scaffold functionalisation: applying growth factors

As discussed previously, growth factors play a key role in controlling angiogenesis and it is a therefore not surprising that a common approach to induce vascularisation in almost all TE substitutes is to harness this potential in order to recruit host vasculature. In the case of bladder regeneration the use of a 'smart patch' that alters a scaffold by incorporating growth factors such as VEGF [58], bFGF [59] or combinations of growth factors such as PDGF and VEGF [60] has been investigated to promote angiogenesis and cell proliferation. Although all of these studies report enhanced vascularisation when implanted into animal models, none describe the production of a robust and functional vascular supply. The same growth factors have been applied to scaffolds in an attempt to revascularise TE liver scaffolds. The use of VEGF alone showed a short term enhancement of hepatocyte (HC) survival as a result of increased vascularisation but this could not be maintained long term due to the high instability of the angiogenic growth factor [61]. Promising methods to overcome this have used new biomaterial strategies. One such approach uses a polymeric system to localise and control the delivery of

VEGF and PDGF from a scaffold [62]. An increase in angiogenic ingrowth and formation of mature vessels after implantation has been shown in animals but constructs of this type were relatively small and as such results may not be reproducible in larger constructs. Other groups have used growth factors to prime the implantation site. For instance, the pre-implantation of a bFGF releasing device which is later removed upon implantation of a monolayer sheet of hepatic tissue has been shown to improve engraftment and function of these cells when compared to HCs injected through the portal vein [63]. Although promising the scale up to larger functional cell sheets is yet to be shown and so the problem of vascularising a large TE liver substitute still remains. Similar approaches of controlled release of growth factors have been studied when trying to create TE skin substitutes [64–67] but some argue that the repeated administration of such approaches could become a practical issue [68]. As a result more sophisticated methods have been investigated, including the genetic modification of cells to overexpress important growth factors. A study carried out by Supp *et al.* describes the use of human keratinocytes genetically modified (GM) by transduction with a replication incompetent retrovirus to overexpress VEGF [69]. Skin substitutes consisting of a collagen-glycosaminoglycan substrate cultured with human fibroblasts and the GM keratinocytes were then implanted onto a full thickness wound on athymic mice. Results showed increased numbers of dermal blood vessels and decreased time to vascularise when compared with controls [69]. Whilst this may be an approach to improve vascularisation it is challenging to get GM cells approved for clinical use due to the potential of random viral integration into the genome, however alternative methods are being developed to overexpress genes without the need for random integration or integration at all [68,70].

### 1.3.3. Harnessing natural vascular architectures

The re-use of biological structures is another approach being used to produce TE constructs with intrinsic vasculature. By decellularising mammalian tissues a naturally derived 3D structure containing microvascular networks can be obtained. These matrices can then be repopulated with appropriate primary cells to produce perfusable

constructs [71]. A benefit of the decellularisation process is the retention of natural ECM components, which as described previously, can aid the angiogenic process. Such a technique has been used to produce TE bladder constructs [72]. Here, porcine small bowel segments were processed to produce acellular matrices which were then repopulated with parenchymal cells to restore tissue function and EPCs, due to their ability to differentiate into capillary, arterial and venous ECs. Implantation into pigs showed good perfusion with no issue of thrombosis in the short term and highlighted the potential of such a method which combines a natural vascular architecture with EPCs and perfusion conditions [73]. Furthermore, this approach has been used to decellularise porcine heart tissue with the retention of the natural vascular network and native ultrastructural properties. Recellularisation with human umbilical vein endothelial cells (HUVECs) showed the creation of a cell monolayer within the vessels with no cell infiltration into the bulk tissue [74]. This initial work is promising but it is not yet known whether the vessels can support parenchymal cells and whether they form an anti-thrombogenic lining when implanted *in vivo*. Decellularisation of rat livers to produce naturally derived 3D scaffolds with intact vascular trees which were then been reseeded with primary rat HCs and ECs via perfusion has also been used to produce a TE liver substitute. Microvascular ECs were used to provide vascular function whilst the cells were perfused constantly with cell culture media. Transplantation into rats showed that cell viability and function were maintained for 8 hours [75]. Similar work carried out by other groups also showed promising results [76–78]. Overall, such methods seem to overcome cell seeding and mass transport issues associated with commonly used techniques as the native vasculature enables nutrients and cells to be delivered throughout the entire tissue construct [77]. However large amounts of cells are required for such a method and this may be a limiting factor for its translation. It is also important to note that the majority of positive results obtained to date using decellularisation techniques have been related to simple, thin tissues such as skin, bladder etc. where it is relatively simple to remove and replace cells [79]. More challenging issues arise with increased tissue complexity. For instance when decellularising the heart questions arise such as:

- What is the most appropriate decellularisation technique to remove as many cells as possible from such a thick scaffold without causing detrimental effects to the ECM?
- What are the best type of cells to use when repopulating the scaffold?
- What developmental stage should the cells be at when repopulating the scaffold?
- How do you get the correct cell type back to the correct site within the decellularised heart?

All of these questions are yet to be answered and as a result research in this area is still active.

### 1.3.4. Production of a synthetic vascular architecture

Scaffolds should not only promote good cell attachment and allow for the storage and release of compounds, but should also be able to promote and guide vascularisation. This has led several groups to look at incorporating a vascular network imprint within scaffolds to try and promote neovascularisation. One example is the microelectromechanical systems (MEMS) approach whereby polymer moulding using micro-etched silicon is used to produce planar 3D channel networks with capillary dimensions [80]. These channels act as microfluidic bioreactors and are considered to be advantageous primarily because they provide a large surface-area-to-volume ratio and therefore provide adequate nutrient and oxygen supply throughout the construct. These channel networks have been used to culture HCs within the channels *in vitro* [81]. Liver sinusoids have also been mimicked using this 3D architecture and fluid perfusion approach, with reports stating that cells have maintained elevated liver function *in vitro* [82]. The use of hepatocytes was reported in this study but no mention of the use of any type of EC is made for the promotion of angiogenesis or even for the eventual prevention of thrombosis. Research is ongoing in this area, specifically in trying to scale the constructs to physiologically relevant sizes [80]. An alternative approach to fabricate intrinsic vascular channels within scaffolds for myocardial TE has also been studied. Marsano *et al.* produced an array of cubically packed

channels within porous poly(glycerol sebacate) scaffolds, using a laser, that were then seeded with rat cardiomyocytes (CMs) and transduced myoblasts releasing VEGF. Ten weeks after implantation into a mouse model of myocardial infarction the vascular ingrowth and contractility of the patch were greatly improved [83]. Although promising these scaffolds were only 1mm thick and the possibility of scale up to physiologically relevant sizes remains unknown. Miller *et al.* reported the 3D printing of filament networks of carbohydrate glass which was used to generate cylindrical networks that could be lined with ECs and perfused with blood under high pressure [84]. They demonstrated that vascular channels sustained the metabolic function of primary hepatocytes in engineered tissue constructs *in vitro*. This preliminary work seems promising but long term studies would be required to determine whether this technique could be translated *in vivo*.

### 1.3.5. Integrating cellular components

Another way to induce neovascularisation in TE substitutes is to incorporate angiogenic cellular components into the matrix material. Delivering cells of endothelial origin has been the focus of many studies aimed at enhancing neovascularisation since they are directly associated with contributing to vessel formation. Cells ranging from terminally differentiated ECs to pluripotent stem cells have been studied to observe their vascularisation potential [68]. However, the use of terminally differentiated ECs such as human dermal microvascular endothelial cells (HDMECs) and HUVECs alone has resulted in poor formation of functional vascular development *in vivo* [85,86] and this has led to the use of co-cultures of ECs with different cell types as well as the use of EPCs. Lesman *et al.* carried out a study comparing porous scaffolds seeded with only human embryonic stem cell derived cardiomyocytes (hESC-CM) to that seeded in combination with HUVECs and mouse embryonic fibroblasts. When implanted into an infarcted heart rat model the tri-culture scaffold demonstrated increased levels of vascularisation in comparison to the scaffold containing only hESC-CMs [87]. Other studies have also highlighted the need for 'helper' cells which are believed to secrete paracrine factors that enhance network morphogenesis [1,88,89].

There is evidence that EPCs, which can be derived from bone marrow, fat tissue and peripheral blood are potentially useful for tissue engineering applications. The use of EPCs derived from adult blood to vascularise a decellularised dermal skin substitute showed inosculation with the recipient murine circulation when implanted *in vivo* [85]. Other studies using bone marrow derived mesenchymal stem cells (BMMSCs) seeded in a collagen sponge showed increased vascularisation *in vivo* [90]. There are few reports of endothelial differentiation of BMMSCs *in vivo* [91] and their contribution is thought to be related to their trophic effect on host vessels [92]. However harvesting bone marrow is painful and not entirely risk free, raising questions over the suitability of such a source. The use of adipose derived mesenchymal stem cells (ADMSCs) has also led to increased vascularisation *in vivo* in a murine model [93]. Clinical trials using ADMSCs are currently ongoing to demonstrate the safety and feasibility of using such cells [94,95]. The use of pluripotent progenitor cells such as embryonic stem cells and induced pluripotent stem cells (iPSCs) have also been investigated. In a recent study Takebe *et al.* reported the generation of vascularised and functional human liver from human iPSCs by transplantation of liver buds created *in vitro*. Briefly, hepatic endoderm cells from human iPSCs were combined with HUVECs and MSCs *in vitro* to form liver buds. These were then transplanted into mice where human vasculature in the constructs became connected to the hosts within 48 hours. By using a combination of these three cell types the vasculature was reported to be similar to that of an adult liver, whereas transplants of only HUVECs and human MSCs showed much less dense vascular infiltration [96]. This proof of concept demonstration of organ bud transplantation appears promising but in order to determine the optimal cell type to use in patients further direct comparative and long term studies are required.

It is clear that vascularisation plays a vital role in the survival of TE constructs. The most promising ways to circumvent slow revascularisation have used scaffolds with vascular architectures, perfusion conditions and relevant cell types, whether this be through the use of the omentum, AV or a combination of an acellular natural scaffold with EPCs under perfusion. Although it is recognised that perfusion conditions, the cell type and scaffold architecture are important with regards to

vascularisation strategies many of the techniques fail to consider them in combination. It is important to take a step back and understand how these factors work together to promote angiogenesis in order to advance this crucial area.

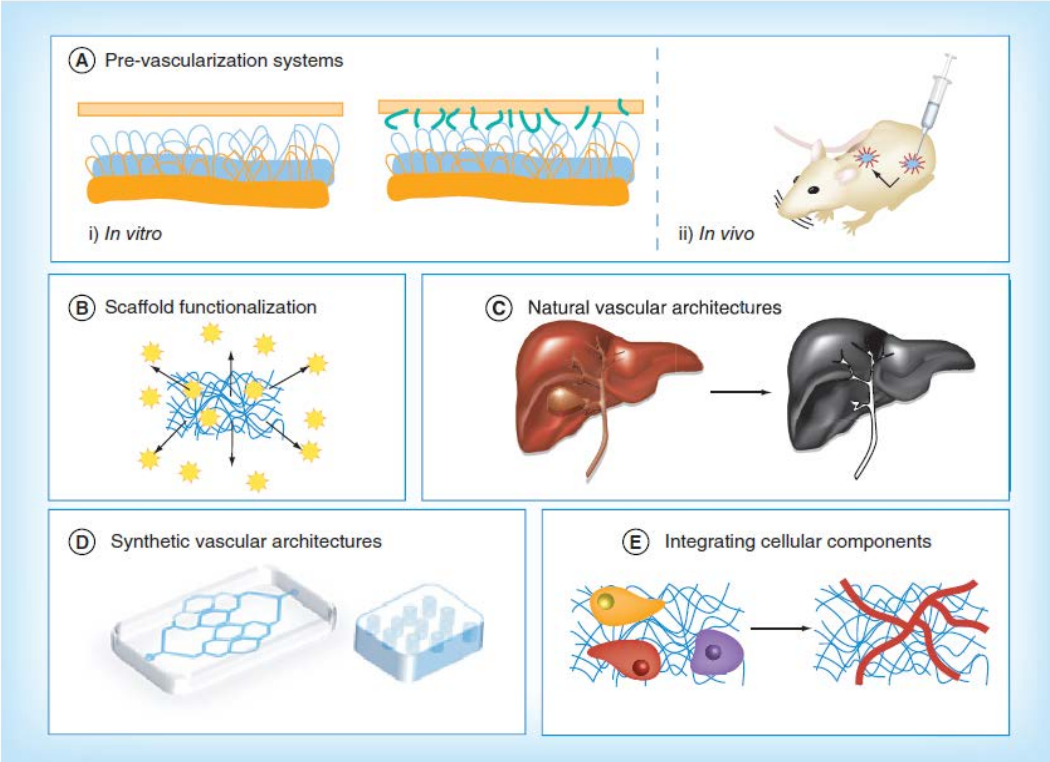


Figure 5 - The five main strategies used in an attempt to overcome vascularisation issues in tissue engineering. These include: (A) the use of (i) *in vitro* and (ii) *in vivo* prevascularisation systems; (B) the use of growth factors to stimulate blood vessel ingrowth; (C) the use of natural vascular architectures obtained by decellularisation; (D) the production of synthetic vascular architectures; and (E) the integration of cellular components to enhance vascularisation.

Table 2 - Summary of current tissue engineering approaches and methods that attempt to overcome neovascularisation problems.

| Tissue | Approaches to overcome neovascularisation issues | Vascular cells? | Perfusion? | Vascular architecture? | Current status |
|---|---|---|---|---|---|
| Bladder | Prevascularisation systems | ✓ | ✓ | ✓ | Omentum: Patients [54] |
| | Scaffold functionalisation: applying growth factors | × | × | × | Animals [58–60] |
| | Harnessing natural vascular architectures | ✓ | ✓ | ✓ | Animals [72] |
| Liver | Production of synthetic vascular architectures | × | ✓ | ✓ | Laboratory [81,82] |
| | Harnessing natural vascular architectures | ✓ | ✓ | ✓ | Animals [75–78] |
| | Scaffold functionalisation: applying growth factors | × | × | × | Animals [61,62] |
| Myocardium | Integrating cellular components | ✓ | × | × | Animals [1,87] |
| | Prevascularisation systems | ✓ | ✓ | ✓ | Omentum: Animals [55] Vascular bed/bioreactor: laboratory [52] |
| | Production of synthetic vascular architectures | × | × | ✓ | Animals [83] |
| | Harnessing natural vascular architectures | ✓ | ✓ | ✓ | Laboratory [74] |
| Skin | Scaffold functionalisation: applying growth factors | × | × | × | Animals [64–69] |
| | Integrating cellular components | ✓ | × | × | EPCs: Animals [85] BMMSCs: Animals [90] ADMSCs: Patients [93] |
| | Prevascularisation systems | ✓ | ✓ | ✓ | Animals [56] |

## 1.4. Established angiogenesis assays

As mentioned in the previous section blood vessel formation is a complex process that is controlled by a large number of inter-related factors and it is therefore not surprising that this remains a challenge in the tissue engineering field. To induce vascularisation within TE substitutes these same processes will need to occur and therefore an understanding of the basic principles and factors affecting angiogenesis is needed. Since the study of angiogenesis has increased rapidly over the last 40 years as a result of its connection with a number of pathologies including cancer, rheumatoid arthritis and retinopathies to name but a few [4], assays have been developed in an attempt to study the process. Ideally these would enable the assessment of multiple factors, providing reliable and reproducible results directly relating to those found in the clinic [97]. From the observations gleaned from tissue engineering strategies this would include the combination of a relevant vascular architecture, ability to incorporate the relevant cell combinations along with flow conditions and an appropriate ECM component. However, despite the increase in development of angiogenesis assays there is currently no single 'gold standard' assay. This section aims to provide an overview of the main assays that are presently available, with the advantages and disadvantages of each summarised in Table 3.

### 1.4.1. *In vitro* assays

#### Endothelial cell migration assays

During angiogenesis ECs are stimulated by a gradient of angiogenic factors to produce MMPs which subsequently break down the basement membrane and allow ECs to migrate into the surrounding matrix.

Transfilter assays are widely used *in vitro* to quantify EC migration. These are 3D assays consisting of a filter containing 8 μm diameter pores upon which ECs are seeded and can travel through. An attractant is placed in the lower chamber and EC migration is observed [98]. The filter can be coated with ECM proteins or more complex materials such as Matrigel in order to more closely mimic the *in vivo* microenvironment [99]. The advantages of this assay are that it is highly sensitive to changes in concentration of attractant, is readily reproducible and takes a relatively short amount of time to observe quantifiable effects [97,100]. However it has been noted to be difficult to set up, to maintain gradients for long time periods (as this reaches equilibrium throughout the chamber over time) and the user is unable to observe cell movement during the experiment [97,101,102].

Other migration assays, known as scratch assays, have been developed and use scraping tools to remove an area of confluent ECs from a surface before allowing peripheral ECs to migrate and refill the naked area [103]. The migratory response of the ECs can then be monitored using microscopy at different time points to determine the rate and extent of migration [104]. However it has been noted that identical confluence of ECs between experiments can be difficult to replicate and results may vary depending on the size of the denuded area [105,106]. In an attempt to overcome this issue the addition of a teflon 'fence' can be introduced whereby, upon removal, ECs grow into the area covered by the fence [106]. However, this design feature in itself introduces added complexity in the setup of this assay whilst discrimination between net migration and proliferation can be difficult after 24 hours [97] but nevertheless can be

overcome in part with the use of mitomycin C which inhibits cellular proliferation [107].
For the direct measurement of cell motility which in turn can be an indication of angiogenesis, phagokinetic track methods are often used. These involve depositing a monolayer of polystyrene beads onto the base of a 96-well plate prior to seeding with ECs. The cells then generate tracks that can be measured for directional properties and total distance traversed [108]. This method allows for the accurate measurement of cell motility [109]. However, the analysis of such an assay can be time consuming to process, requiring complex software to track cell paths. In addition, only small numbers of cells can be tracked and there is debate over the use of an unnatural substrate to measure realistic cell motility [110].

The type of EC migration assay utilised depends upon the situation being investigated. Whilst the transfilter assays can quantify directional migration in response to a chemical stimuli (chemotaxis) and random motility (chemokinesis), the relatively simple scratch assay may be useful in measuring the response to wound healing since the cells at the border of the denuded area are likely to be damaged in the process. Alternatively for direct measurement of cell motility and directional effects on cell motion the phagokinetic track method may be the most appropriate [97].

### Endothelial cell differentiation assays

Cell differentiation assays aim to simulate the formation of capillary like tubes which are representative of the later stages of angiogenesis. These are widely used to assay the pro- and anti-angiogenic effects of various test substances. Basic 2D assays plate ECs onto or into a layer of gel matrix (i.e. collagen, fibrin or Matrigel) which stimulates attachment, migration and differentiation of ECs) into tubules. This process can be observed and monitored over a period of 4-24 hours via the use of a digital camera [109].

The type of matrix has proven to be important since different matrices can result in different rates of differentiation. For instance the use of collagen I and III (interstitial collagens) results in predominantly more cell proliferation than tubule formation whereas seeding cells onto a collagen

IV and V matrices (basement membrane collagens) results in more prevalent tubule formation with a reduced amount of cellular proliferation [111]. Matrigel, a complex gelatinous protein mixture derived from mouse sarcoma cells, has been found to be the most powerful matrix for tubule formation [112]. However there have been disputes over whether the tubules formed represent true capillaries due to their lack of lumen. In addition, human fibroblasts have also been shown to form tubules when seeded onto Matrigel [113–115]. As a result interpretation of the results obtained from using such a method should be made with caution.

Another tube formation assay involves the co-culture of ECs with stromal cells, either with or without the use of an ECM. The stromal cells can be fibroblasts, SMCs, or blood vessel explants containing an array of different cell types. Studies looking at the use of fibroblasts as the stromal cell type have found that these cells secrete matrix components that go on to act as the scaffold upon which ECs form tubules. These tubules were found to more closely resemble those found *in vivo*. However this assay is time consuming lasting between 12-14 days and also the matrix components secreted by the fibroblasts are not well defined and so this assay is less well characterised [97,113].

In addition 3D assays have been developed whereby ECs are sandwiched between layers of matrix (Matrigel, collagen or fibrin). In the initial 7 days post seeding tubule formation has been observed in the horizontal plane, but by day 15 tubules have been found to branch upwards penetrating the matrix and forming a 3D network. However assays such as this are difficult to analyse and the matrix must be relatively thin to allow for sufficient oxygen and nutrient diffusion to prevent excessive cell death [116].

Overall, there are a range of EC differentiation assays to choose from depending upon the type of angiogenesis being studied. Whilst 3D assays may be more representative of the *in vivo* environment there are technical challenges associated with their setup and analysis and so in reality many groups tend to use 2D assays [97]. Note that most of these measure either growth or migration. They do not measure vascularisation although it is one attribute that could be linked to the cell behaviour.

### Combinatorial cell assays

Once tubules form, mural cells are recruited in order to maintain stability of the vessel. As a result assays have been developed to investigate the interaction between ECs and mural cells. The simplest co-cultures involve either seeding both cell types at the same time or initially allowing one cell type to adhere followed by subsequent seeding of the other cell type. Assays of this type have been used to analyse the effects of ECs on mesenchymal cell differentiation and are both useful in obtaining information and easy to set up and analyse [117]. However, with assays of this nature it is not possible to assess the cell-cell interactions mediated by paracrine factors released by one cell type since all cells are evenly dispersed [97].

Alternatively, non-contact assays have been developed. One such method involves setting agarose in a well and punching two holes out of it before seeding the two cell types into each hole. The cells attach to the bottom of the well and over time the two cell types move towards one another under the agarose gel. Measurement of the soluble diffusible signals can be made and if cells are left for between 5-7 days the cell types can come into contact and it is possible to monitor the effects of cell-cell interactions on the cell phenotype [117].

As with tubule formation assays, 3D EC/mural cell co-culture assays have been developed. One such assay used initially was the spheroid method whereby ECs and mural cells are seeded together into non-adherent wells and after ˜1-4 days they will form spheroids. However, upon formation the mural cells are in the middle whilst the ECs do not form tubules [118]. An alternative method is similar to that of the 3D tubule formation assay where ECs and mural cells are sandwiched between layers of Matrigel and subsequently invade the matrix forming tubules resembling those found *in vivo* where the mural cells form a supporting layer [119]. Again, there are technical challenges involved in setting up such an assay and unlike the *in*

*vivo* situation there is no introduction of flow conditions which can alter cell phenotype [120].

Overall, direct cell contact assays can be useful in determining information regarding the direct effects of one cell type on another whilst non-contact assays can be useful in measuring the diffusible substances released by the different cell populations. Undoubtedly the 3D assay is most representative of the *in vivo* conditions however it can be difficult to both set up and analyse fully [97].

### 1.4.2. *Ex vivo* assays

Angiogenesis occurring *in vivo* involves a network of ECs and their surrounding cells in constant communication with the surrounding environment. This has led to the development of organ culture methods. In essence segments, discs or sections of specific tissue types are cultured in a 3D matrix *in vitro* and microvascular outgrowth is measured over a period of around 14 days. The aortic ring assay is a common method whereby a rat aorta is segmented into multiple rings which is then embedded in either a matrix of fibrin or collagen and analysed for vessel outgrowth. It has the advantage of including the effects of non-ECs (such as SMCs and pericytes) and a supporting matrix. However, the results are often hard to quantify and the model is not seen as wholly representative of the microvascular environment due to the use of a large vessel from which to observe microvascular outgrowth [121].

A modification of the rat aortic ring assay uses the chick aortic arch [122]. The ECs found here share characteristics of microvascular cells and this assay has the advantage of being rapid and relatively inexpensive. However since the explants are taken from growing embryos the ECs are proliferative and so are not truly representative of the non-proliferating cells that are stimulated to undergo angiogenic sprouting *in vivo* [97].

The main issue with assays of this type, other than the difficulty involved in analysing the results, is that the explants are taken from non-human tissue and results obtained may well be species specific.

### 1.4.3. *In vivo* assays

#### Chorioallantoic membrane (CAM) assay

The CAM assay is a well-established method that has been in use since the 1970's. Test substances or materials are implanted onto the chick membrane via a hole that is cut into the egg shell before covering the opening and incubating. The angiogenic response to the substance can then be quantified via image analysis techniques [109]. Overall the CAM assay is inexpensive and therefore provides the opportunity for relatively large scale screening of test substances. The ease of accessibility of the CAM also allows for repeated application of test substances which can be applied either directly or via intravenous or intra-allantoic injections. However, care must be taken when interpreting the results obtained from the CAM since chemical or physical irritation of the membrane can induce angiogenesis, disrupting identification of the response from the test substance [97,123]. The CAM is also well vascularised and so distinguishing between newly formed and existing capillaries can be difficult. In addition, angiogenesis occurs in the CAM up until day 11 post fertilisation, and so results obtained from younger embryos have the added complication of having unspecified interactions with endogenous factors affecting angiogenesis [97].

#### Corneal angiogenesis assay

The only avascular and transparent tissue in the body is the cornea. This means that any vessels that penetrate into the corneal stroma from the limbus are newly formed, which is why there has been development into using the cornea as a tool to observe angiogenesis [97,124]. Since almost all types of corneal injury can induce neovascularisation, many techniques have included either chemical cauterisation, mechanical scraping of the limbal epithelium or the implantation of slow release pellets from micropockets in the development of such assays [97]. The visualisation of vessels is usually achieved by the perfusion of the cornea using a fluorescent dye which are then removed from the host and flattened onto slides in order to image [125]. Although many of these methods are reliable and readily quantifiable, assays of this type are expensive and hard

to set up as the size of the eye decreases. In addition, different angiogenic responses have been found depending on the type of injury the cornea is subjected to and there is also dispute surrounding the relevance of using a naturally avascular tissue to investigate angiogenesis [97,126].

### Zebrafish assay

Zebrafish are tropical freshwater fish that can produce hundreds of embryos each time they mate. Since the embryos can be produced in large numbers, are optically transparent, share many genes and mechanisms as mammals and their development is very rapid, they make good organisms in which to observe the development and function of the vasculature [127]. To visualise the vessels several techniques are used, for instance injecting the embryo with dyes, alkaline phosphatase staining of the ECs and the use of confocal microangiography [128–130]. Recently transgenic zebrafish with green fluorescent protein (GFP) expressed under the control of promoters specific for the developing vasculature have been produced including Fli-eGFP [131], mTie-GFP [132] and Flk-GFP [133]. Such fluorescent zebrafish have the advantage of enabling high optical resolution imaging of the developing vasculature that can be clearly observed over time. This assay has the benefits of being inexpensive and easy to maintain. It is also possible to knockdown specific genes, enabling a quick evaluation of gene function in relation to angiogenesis [97,134]. Large screen studies can also be undertaken due to the large amounts of embryos produced whilst the experiments are relatively short meaning that only small amounts of a test substance are needed. However, as with all of these assay there are drawbacks. The main issue surrounding the use of this assay is the relevance of using fish ECs to study the response of human tumour xenografts [97].

### Chamber assay

Implantation of a transparent chamber *in vivo* enables the visualisation of new blood vessel formation over time [135]. A common example of this uses the dorsal skinfold as the chamber implantation site in mice, rats and hamsters [136–138]. This method uses two symmetrical frames which are implanted into the dorsal skinfold to sandwich an extended double layer of

skin. One layer of skin is then removed to expose the other, which is protected by covering with a glass cover slip incorporated into one of the frames [139]. It is possible to remove the cover slip for the implantation of tumour cells or transplants in order to observe neovascularisation [140]. The advantages of this assay are that it allows for the determination of 3D vessel growth in one animal usually whilst it is conscious over a period of 1-4 weeks [97]. This means that there is no need for multiple mice for each time point, therefore minimising the number of animals required [139]. It can also be used to simultaneously study cellular, molecular and functional parameters at each time point. However, the setup of this assay is technically demanding and quantification of functional parameters is often time consuming, requiring the use of sophisticated image analysis systems [97].

### Implantation of scaffolds and gels

A range of materials have been implanted into animals (mainly mice) to alter the environment in which angiogenesis occurs. These materials have included the use of stainless steel mesh chambers, hollow porous walled chambers, synthetic matrices and Matrigel plugs [97,141–143].

As mentioned previously, Matrigel is a complex protein mixture derived from mouse sarcoma cells that is a liquid at 4 °C but forms a solid gel at 37 °C. Test substances to be investigated can be encapsulated in Matrigel and subsequently injected subcutaneously into the animal to form a plug which slowly releases the test substance [144]. The angiogenic response can then be measured by retrieving and sectioning the gel and looking for CD31 positive vessel ingrowth or by measuring the haemoglobin content. However, sectioning and immunostaining of gels can be both time consuming and costly processes whilst haemorrhaging can lead to spurious haemoglobin measurements. In addition, Matrigel is costly and includes the presence of growth factors and cytokines which can have an effect on the angiogenic response and thus the results obtained must be interpreted with caution [97].

An alternative to using Matrigel is to load the test substance onto a sponge implant or polymer matrix and then implant this into the animal. Sponge implants have been used to observe the formation of fibrovascular tissue, neovascularisation, wound healing and cellular proliferation [145,146]. However, caution must be taken when drawing conclusions from such results since implants become encapsulated upon implantation and elicit an immune response which can lead to an angiogenic response in its own right thus interfering with the angiogenic response of the test substance [97].

Table 3 - Summary of current angiogenesis assays.

| | Assay Type | | Advantages | Disadvantages |
|---|---|---|---|---|
| *In vitro* | Cell migration | Transfilter assay | • High sensitivity to gradient changes<br>• Can distinguish between random and directional migration<br>• High reproducibility<br>• Short duration (4-6hrs) | • Difficult to set up<br>• Maintaining transfilter gradients for long periods of time is difficult<br>• Can't observe cell motion during experiment<br>• Cells migrate through unnatural filter material<br>• No flow conditions<br>• No ECM component |
| | | Scraping assay | • Good for wound healing studies<br>• Can estimate rate of migration | • Results may vary depending on size of wound<br>• Obtaining identical confluence between experiments difficult<br>• Exact denudation difficult<br>• No flow conditions<br>• No ECM component |
| | | Phagokinetic track method | • Can measure directional effects<br>• Accurate measurement of cell motility | • Cells migrating on unnatural substance<br>• Only small number of cells can be tracked<br>• Time consuming/complex analysis<br>• No flow conditions<br>• No ECM component |
| | Cell differentiation | Tube formation (2D) | • Short duration (4-24hrs)<br>• Relatively simple to analyse | • Lumen may not be formed<br>• Fibroblasts can also form tubes on Matrigel – interpret with caution<br>• No flow conditions |
| | | Tube formation (3D) | • More representative of *in vivo* environment | • Difficult to analyse<br>• Lengthy duration (˜15days)<br>• Matrices have to be thin to allow for adequate diffusion of nutrients/oxygen<br>• No flow conditions |
| | Combinatorial cell assay | Direct contact (2D) | • Easy to set up and analyse | • Not possible to assess cell-cell interactions mediated by factors released by each cell type<br>• No flow conditions |
| | | Non-contact (2D) | • Measurement of soluble factors can be made<br>• Possible to monitor effects of cell-cell interactions on phenotype | • Time consuming<br>• No flow conditions<br>• No ECM component |
| | | Spheroid method (3D) | • Simple to set up | • Mural cells form in centre of spheroid and ECs do not form tubules<br>• No flow conditions<br>• No ECM components |
| | | Matrigel (3D) | • More representative of *in vivo* environment | • Technically challenging<br>• No flow conditions |
| *Ex vivo* | Rat aortic ring | - | • Representative of general *in vivo* environment (inclusion of mural cells & ECM) | • Results hard to quantify<br>• Not truly representative of specific microenvironment since large vessel used to observe<br>• No flow conditions |
| | Chick aortic arch | - | • ECs similar to microvascular cells<br>• Rapid<br>• Inexpensive | • From growing embryos therefore proliferative – not representative of non-proliferative ECs found *in vivo*<br>• No flow conditions |
| *In vivo* | CAM | - | • Inexpensive<br>• Ease of accessibility allows for repeated administration of test substances | • Difficult to distinguish between existing and new capillaries<br>• Difficult to quantify<br>• Chemical/physical irritation of membrane can induce angiogenesis |
| | Corneal angiogenesis assay | - | • Reliable<br>• Readily quantifiable | • Expensive<br>• Difficult to set up as eye decreases in size<br>• Dispute over relevance of avascular tissue for angiogenesis studies |
| | Zebrafish assay | - | • Inexpensive<br>• Easy to maintain<br>• Large scale screening studies possible<br>• Quick<br>• Gene knockdown studies possible | • Dispute over relevance of fish EC angiogenesis in human tumour xenografts |
| | Implantation of sponges and polymers | Matrigel plug | • Not technically difficult<br>• Quantification by amount of haemoglobin in plug | • Time consuming analysis<br>• Costly analysis |
| | | Sponge implants | • Can be used to observe wound healing, cellular proliferation, fibrovascular tissue formation and neovascularisation | • Implant can become encapsulated inducing angiogenic response independently of test substance |

Although the development of angiogenesis assays has rapidly advanced over recent years, there is currently no 'gold standard' assay. Current *in vitro* models concentrate on EC migration, proliferation and differentiation in 2D with limited use of additional cell types. There are no standard assays that combine the use of supporting cells (e.g. fibroblasts, SMC, pericytes etc.), the ECM and/or basement membrane and fluid flow in 3D [97]. Although this complexity exists within *in vivo* models such assays are primarily limited by the species used (e.g. rat, chick etc.), organ sites available and complicated analysis techniques (Figure 6).

There is clearly a need for an *in vitro* model that has the capability of combining pro-angiogenic cells with an ECM component that can be monitored under flow conditions to learn more about the 'rules' of angiogenesis.

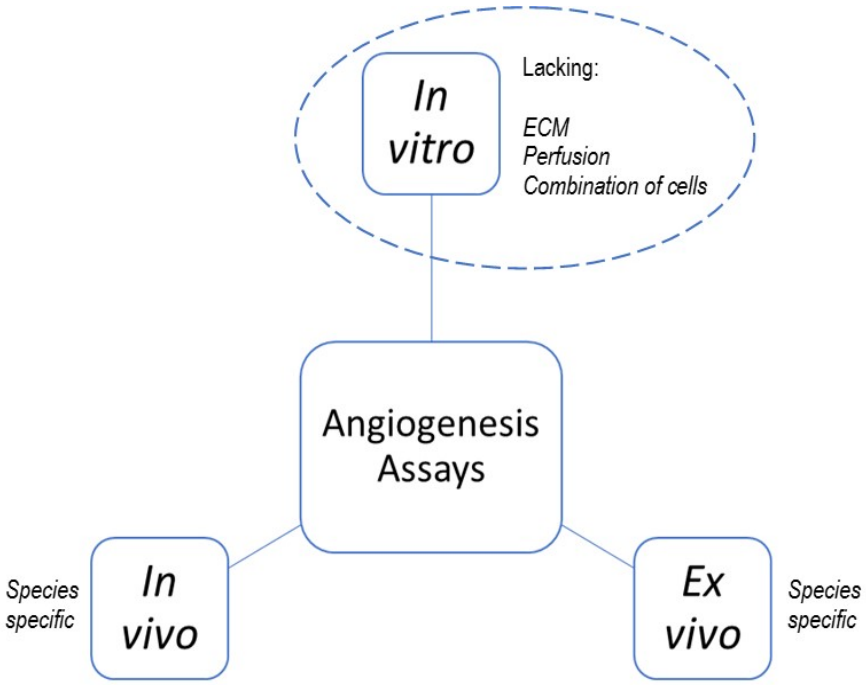


Figure 6 - Deficiencies in current angiogenesis assays

## 1.5. Natural vascular networks and their application as angiogenesis models

Several native tissues including; skin, bladder, small intestine, pericardium and heart valves have been used in the production of decellularised tissues and have been found to promote cell adhesion and migration as well as exhibiting low immunogenicity [79,147–149]. These characteristics have led to the clinical translation of such tissues with many being available commercially (as summarised in Table 4).

Table 4 - Examples of clinical products derived from decellularised tissues. Table reproduced from Crapo *et al.* [79].

| Product (Manufacturer) | Tissue Source | Application Focus |
|---|---|---|
| Alloderm® (Lifecell Corp.) | Human dermis | Soft tissue |
| AlloPatch HD™, FlexHD® (Musculoskeletal Transplant Foundation) | Human dermis | Tendon, breast |
| Neoform™ (Mentor Worldwide LLC) | Human dermis | Breast |
| GraftKacket (Wright Medical Technology Inc.) | Human dermis | Soft tissue, chronic wounds |
| Strattice (Lifecell Corp.) | Porcine dermis | Soft tissue |
| Zimmer Collagen Repair Patch (Zimmer Inc.) | Porcine dermis | Soft tissue |
| TissueMend (Stryker Corp.) | Bovine dermis | Soft tissue |
| MatriStem, Acell Vet (Acell Inc.) | Porcine urinary bladder | Soft tissue |
| Oasis, Surgisis (Cook Biotech Inc.) | Porcine small intestine | Soft tissue |
| Restore (DePuy Orthopaedics) | Porcine small intestine | Soft tissue |
| FortaFlex (Organogenesis Inc.) | Porcine small intestine | Soft tissue |
| CorMatrix ECM (CorMatrix Cardiovascular Inc.) | Porcine small intestine | Pericardium, cardiac tissue |
| Meso BioMatrix (Kensey Nash Corp.) | Porcine mesothelium | Soft tissue |
| IOPatch (IOP Inc.) | Human pericardium | Opthalmology |
| OrthAdapt, Unite (Synovis Orthopaedic and Woundcare Inc.) | Equine pericardium | Soft tissue, chronic counds |
| CopiOs (Zimmer Inc.) | Bovine pericardium | Dentistry |
| Lyoplant (B. Braun Melsungen AG) | Bovine pericardium | Dura mater |
| Perimount (Edwards Lifesciences LLC) | Bovine pericardium | Valve replacement |
| Hancock II, Mosaic, Freestyle (Medtronic Inc.) | Porcine heart valve | Valve replacement |
| Prima Plus (Edwards Lifesciences LLC) | Porcine heart valve | Valve replacement |
| Epic, SJM Biocor (St. Jude Medical Inc.) | Porcine heart valve | Valve replacement |

Small intestinal submucosa (SIS) is one of the most established and broadly used products available on the market [150]. It was first used over 40 years ago as a vascular substitute. It has developed over the years and nowadays is produced from decellularised small intestine segments applied as a sheet of roughly 100 μm thickness [150]. Beyond its use in reconstructive surgery in the form of SIS the decellularised small intestine has the potential to be used as a test system for both basic and applied research. In 2004 Schultheiss *et al.* [151] removed part of the small intestine whilst retaining the venous and arterial supplies allowing for the perfusion of the vascular bed. They then went on to decellularise the tissue producing a perfusable vascular bed that can be recellularised with appropriate cell types for a range of applications. This biological vascularised matrix, termed BioVaM, is still quite a new concept and therefore there are much fewer studies when compared to the work carried out for the SIS matrix. However studies that have been carried out have mainly looked into the following:

1. Re-endothelialising the vascular bed of the BioVaM
2. Using the BioVaM as a tissue model
3. Using the BioVaM to vascularise TE constructs *in vitro*

Initial work on the BioVaM seemed to concentrate on producing an endothelial cell lined vascular network. Different approaches were investigated with the first study introducing EPCs derived from peripheral blood into the vascular network [151]. This work seemed promising and a more detailed follow up study combined this network with SMCs and urothelial cells which were seeded into the intestinal lumen to model the bladder before implanting into a porcine model. No thrombosis was observed after 3 hours in comparison to that observed when no EC lining was present [72]. Another study by the same group looked at using human bone marrow derived MSCs, cutaneous microvascular ECs (mECs) and peripheral blood mononuclear cells (PBMCs) to repopulate the vascular network. These were shown to differentiate into endothelial like cells. A BioVaM scaffold with autologous PBMCs recellularised into the vascular networks and autologous SMCs and fibroblasts on the surface of the scaffold was then implanted into the upper arm of one patient for one week, forming anastomoses with the host vasculature. Upon explantation

occlusion was found in some microvessels but the main vessels showed little evidence of thrombosis [152]. Other studies carried have combined the BioVaM with porcine hepatic microvascular ECs and HCs to model the liver. The contruct is shown to be viable for 3 weeks and HCs maintained their morphology whilst showing stable metabolic activity. In contrast, HCs in monolayer showed morphological dedifferentiation and an unfavourable metabolic state [153]. The use of human mECs and HCs have also been used to produce a liver like tissue [154]. Modelling the intestine to observe cellular interactions and potential therapies has also been investigated. Human mECs seeded into the vascular bed and the cell line Caco-2 (derived from human coxlorectal adenocarcinoma) seeded into the lumen has been used to establish such a model [154]. Recently the development of an intestinal model based on a rat decellularised small intestine segment was reported [155]. The aim of this work was to produce an acellular intestinal matrix and only preliminary work regarding recellularisation was reported. This study showed that the ECM was preserved without disruption to the mechanical and structural properties that it endows. Amniotic fluid stem cells were repopulated into the lumen of the intestine and were shown to be viable. No re-endothelialisation of the vascular bed was undertaken. Another group has used the porcine BioVaM as an *in vitro* cancer model [156]. It is firstly decellularised and then the arterial and vascular pedicles are removed and the tubular SIS mucosa is seeded with primary fibroblasts, mECs and cells from the S462 tumour cell line. These recellularised flat sheets are then placed between metal rings and are cultured either statically or dynamically. This study states that the method is very promising to generate vascularised tumour tissues which will allow for the study of angiogenesis and other mechanisms relevant to tumour progression however surprisingly does not use the vasculature of the scaffold to form re-endothelialised vessels. Instead it seeds the mECs onto one side of the tubular SIS mucosa and the tumour cells onto the other. It could be argued that a more accurate model would indeed take advantage of this perfusable vascular bed to observe vascular sprouting into a tumour placed on top of the matrix. This is an approach that was harnessed in later studies in a bid to vascularise cardiac TE constructs *in vitro*. Nikolic *et al.* decellularised a porcine jejunum to produce the BioVaM before recellularising with a GFP and red fluorescent protein (RFP) labelled rat heart EC line (RHE-A) into

the venous and arterial pedicles, respectively [157]. A gel based cardiac construct (CC) prepared from rat tail type I collagen containing rat neonatal cardiomyocytes and ECs was then placed on top of the BioVaM. After 10 days under static culture results showed that the GFP and RFP labelled RHE-A cells had formed a dense network and were found in close proximity to the rat ECs seeded within the CC suggesting a connection between the two [157]. This proof of principle study aimed to prevascularise the construct in order to supply oxygen and nutrients whilst removing waste products from the 3D scaffold with a view to eventually translate such scaffolds to the clinic. This study and all previous work leading up to it (i.e. the decellularisation, recellularisation and different forms of analyses) has real potential to be used as a test system to investigate angiogenesis in more detail. Overall these approaches have utilised a scaffold that overcomes the main deficiencies of current angiogenesis models by:

1. Retaining native ECM components
2. Preserving a vascular architecture and the capacity to be perfused
3. Having the ability to be recellularised with a range of cell types

Table 5 to Table 7 summarise the studies mentioned above, providing more detail about the decellularisation, recellularisation and culture conditions. It can be seen that the majority of studies have used porcine jejunal segments with one study using rat. This has resulted in the need to repopulate the decellularised segments with a large number of endothelial and parenchymal (where used) cells. For translational use in the clinic this may be necessary but for use as a model the rat jejunum may be preferable. The decellularisation detergent used has been predominantly sodium deoxycholate, occasionally combined with sodium azide (for use as a lysis buffer) or sodium dodecyl sulphate (SDS). Detergents commonly used for decellularisation are either ionic or non-ionic. It has been found that in general ionic detergents (such as SDS, sodium deoxycholate etc.) are more effective in removing cell nuclei from dense tissues but have been found to disrupt the ultrastructure of the tissue whilst removing growth factors from the ECM [158–160]. In addition it has been shown that it is extremely important that tissues are washed thoroughly after decellularisation using ionic detergents, especially

SDS. Reports have indicated that even at low concentrations residual detergent has been found to have cytotoxic effects when it comes to repopulating the cell free scaffolds [79,161,162]. Conversely, non-ionic detergents (such as Triton-X 100) tend to have the opposite effects. They have been found to be less efficient at removing cell nuclei from dense, thick tissues but do tend to have less impact on the ultrastructure and growth factors contained within the tissues [79,163]. A recent paper that looked at detergents used for decellularisation of porcine jejunum for production of a BioVaM showed that the ionic detergent, SDS, bound to the matrix and even after repeated washing it remained present. This then had a subsequent detrimental effect on the survival rate of porcine primary ECs used to repopulate the BioVaM. In contrast when the milder non-ionic detergent, Triton-X 100 was used the same decellularisation efficacy was achieved but this time the long term survival and proliferation of the ECs was shown [164]. The method of decellularisation in the studies used either agitation or perfusion through the vascular bed to remove the cells from the tissue, with later studies preferring to use the latter method. The rate at which the vasculature was perfused with detergent seemed to be arbitrary with no justifications given in the literature. It varied from between 1.2-2.3 ml/min for porcine tissue and the sole study using rat tissue used a rate of 0.01 ml/min. Recellularisation of the vasculature used predominantly microvascular ECs with the occasional use of EPCs and cell lines whilst the lumen was recellularised with parenchymal cells determined by the tissue being mimicked. Culture conditions used in the studies varied. Some studies cultured the constructs under static conditions whilst others perfused the vasculature and lumen of the tissue simultaneously. Culture time ranged from 3 hours when implanted into a porcine model to 21 days when cultured *in vitro* and depended very much on the study.

Overall, the concept of using a decellularised vascular matrix derived from jejunal segments is relatively new and as a result the methodologies have yet to be standardised. Important questions relating to what decellularisation technique to use, what cells to use for recellularisation and how to return these cells to the appropriate locations within the decellularised tissue are still largely unanswered. Some view these broad issues as the main drawbacks of using such techniques to regenerate tissues

in general. However, initial results from the aforementioned studies indicate that the vascular matrix has real potential to be used as a test system to investigate a number areas, including angiogenesis.

Table 5 – Summary of studies re-endothelialising the vascular bed of the BioVam.

| Study | BioVaM Species | Decellularisation | | Sterilisation | Recellularisation | | Culture | Key Findings |
|---|---|---|---|---|---|---|---|---|
| | | *Detergent* | *Method* | | *Vasculature* | *Lumen* | | |
| Re-endothelialising vascular bed | Porcine | Sodium azide/sodium deoxycholate | Agitation | ? | $2.5\times10^7$ porcine peripheral blood EPCs | - | Static and *in vivo* (porcine model) | No thrombosis found after 3hrs *in vivo* [151]. |
| | Porcine | Sodium deoxycholate | Perfusion 2.3ml/min | γ irradiation 25kGy | $10.5\times10^6$ BM-MSCs or $4.5\times10^6$ mECs or $15\times10^6$ PBMCs (for HT) (all human) | $4\times10^5$ fibroblasts (for HT) | 1.26ml/min for 14 days *in vitro* or 1 week *in vivo* in human | Vascular endothelium formed *in vitro*. Clinical transplantation showed vessel patency & viability after 1 week [152]. |

Table 6 – Summary of studies using the BioVam to vascularise TE constructs *in vitro*.

| Study | Tissue | BioVaM Species | Decellularisation | | Sterilisation | Recellularisation | | Culture | Key Findings |
|---|---|---|---|---|---|---|---|---|---|
| | | | *Detergent* | *Method* | | Vasculature | Lumen | | |
| *In vitro* vascularisation | Cardiac patch | Porcine | Sodium deoxycholate/ SDS | Agitation | γ irradiation 150Gy | $6\times10^6$ GFP RHE-A cells venous supply; $6\times10^6$ RFP RHE-A cells arterial supply. | Rat CMs inside lumen; CC containing $4\times10^6$ rat neonatal heart cells seeded on top of lumen | Static *in vitro* | GFP & RFP labelled RHE-A cells found to have migrated to CC and connect with rat ECs [157]. |

Table 7 – Summary of studies using the BioVam as a tissue model.

| Study | Tissue | BioVaM Species | Decellularisation | | Sterilisation | Recelllularisation | | Culture | Key Findings |
|---|---|---|---|---|---|---|---|---|---|
| | | | *Detergent* | *Method* | | *Vasculature* | *Lumen* | | |
| Tissue Models | Intestine | Porcine | Sodium deoxycholate | Perfusion 2.3ml/min | γ irradiation 25kGy | $4.5\times10^6$ human mECs | Caco-2 cell line | 1.26ml/min (vasculature) 3.8ml/min (lumen); 14 days *in vitro* | Cell adhesion & 3D growth enhanced. HCs express important functional proteins compared to static culture in 2D [154]. |
| | | Rat | Sodium deoxycholate | Perfusion 0.01ml/min | | - | $1\times10^6$ AFSCs | Static 24hrs *in vitro* | Acelleular ECM with intact vascular net formed [155]. |
| | Liver | Porcine | Sodium deoxycholate | Perfusion 1.2ml/min | γ irradiation 25kGy | $8\text{-}15\times10^6$ porcine mECs | Porcine HCs (1 week after vascular seeding) | 0.8ml/min for 4 weeks *in vitro* | HCs maintained morphology & metabolic activity in BioVaM. HCs in monolayer showed dedifferentiation/unfavourable metabolic state [153]. |
| | | Porcine | Sodium deoxycholate | Perfusion 2.3ml/min | γ irradiation 25kGy | $4.5\times10^6$ human mECs | Human HCs | 1.26ml/min for 14 days *in vitro* | Cell adhesion & 3D growth enhanced. HCs express important functional proteins compared to static culture in 2D [154]. |
| | Bladder | Porcine | Sodium azide/sodium deoxycholate | Agitation | ? | $2.5\times10^7$ porcine peripheral blood EPCs | Porcine SMCs & UCs | Static 21 days; 3h *in vivo* porcine model | Re-endothelialisation of vessels after 21 days and no thrombosis after 3hr *in vivo* [72]. |
| | Tumour | Porcine | Sodium deoxycholate | Perfusion 80-100mmHg | γ irradiation 25kGy | - | Lumen cut open 8000cells/cm³ (mECs) seeded on one side; 8000cells/cm³ HDFs & 15000cells/cm³ S462 tumour cells on other | Static 14 days Dynamic 14 days 3.8ml/min (shear flow) *in vitro* | SIS like model leads to tumour like tissue formation of cells [156]. |

## 1.6. Synthetic vascular networks and their application as angiogenesis models

Approaches taken to model angiogenesis *in vitro* have mainly used natural materials, such as collagen I, in various configurations. Natural scaffolds have the advantage of containing intrinsic factors that allow for good cell attachment and survival rates as well as having the ability to stimulate cells to exhibit EC capillary morphogenesis and sprouting. However there is limited control over the degradation rates of such materials as well as their mechanical properties and batch-to-batch variability which could lead to irreproducible results [165]. Although the number of studies using synthetic materials to investigate angiogenesis is very limited, there has been increased interest into the use of synthetic materials. The benefits of using such materials include the ability to regulate the mechanical properties of the scaffold, the ease of chemical modification and the control of biochemical properties [166].

Chwalek *et al.* have recently reported the development of a 3D model for tumour angiogenesis from semi-synthetic hydrogels [167]. More specifically, hydrogels were prepared by cross linking star shaped poly(ethylene glycol) (PEG) and glycosaminoglycan heparin. This not only enabled cells to be embedded in 3D but it also provided the capability of binding multiple growth factors to the material, mimicking the ECM. By varying the ratio of PEG to heparin the mechanical properties of the material could be varied and enabling the identification of optimal matrix conditions to support vascular network formation. These matrix conditions were then used to determine the 3D interactions between ECs and mural cells. Network formation was observed and stable capillaries were maintained for up to 1 month *in vitro*. Although this model shows extremely promising results and offers a novel platform to test angiogenic factors it does not incorporate the ability to be perfused and thus observe the effects of fluid flow on vascular net formation.

Jeffries *et al.* later reported preliminary results using an alternative method to develop vascular networks by micropatterning electrospun scaffolds [168]. The ultimate goal of this work was to produce a re-

endothelialised TE vascular network that was capable of direct anastomosis to the host vasculature which could be perfused immediately. This approach used a combination of fused deposition modelling and electrospinning to create the networks. Fused deposition modelling is a rapid prototyping technique that deposits layers of thermoplastic material into a desired 3D geometry by extruding it through a heated nozzle [169]. In this study poly(vinyl alcohol) (PVA) was extruded into a predetermined geometry onto a layer of electrospun polydioxanone (PDO). Electrospinning is used to produce thin fibres (ranging from nm to μm diameters) with a large surface area by applying a potential difference between a polymer solution and collector. It has been used extensively in tissue engineering since the degradation rate, fibre diameter, porosity and mechanical properties can be easily varied depending on the application [170]. After deposition of the PVA onto the electrospun sheet of PDO a further layer of PDO was electrospun on top. The PVA was then removed by submerging the scaffold in water to leave a hollow electrospun scaffold which was then repopulated with HUVECs. These cells were shown to attach to the electrospun scaffold within the vascular channels, although the coverage was uneven. This represents a novel approach not only for the purpose of perfusing TE constructs *in vivo* (as was the intention of this study) but has the potential to be used as a model for angiogenesis, an application which has not been studied as yet. Scaffolds such as this offer the ability to be perfused, be recellularised with a variety of cells (either individually or in co-culture) and have ECM components placed onto them or deposited by the cells. This novel approach could offer not only the tissue engineering community but also those involved in cancer research an advanced 3D *in vitro* model to study angiogenesis.

## 1.7. Project aims and objectives

The aim of this project is to develop *in vitro* models for angiogenesis that have the capability of combining pro-angiogenic cells with an ECM component that can be monitored under flow conditions to learn more about the 'rules' of angiogenesis. In order to satisfy this aim, the objectives of the project are to:

1. Produce vascular networks for experimentation by decellularising animal tissue to retain the ECM components and vascular architecture.

2. Produce vascular networks for experimentation by electrospinning and robocasting to produce a synthetic vascular network.

3. Design a bioreactor for perfusion of vascular networks.

4. Investigate the optimal cell combinations to functionalise the vascular networks and recellularise these networks under both static and perfused culture.

5. Investigate the effect of flow rate on angiogenic sprouting.

6. Investigate the effect of pro-angiogenic stimuli on angiogenic sprouting.

7. Investigate the effects of pro-angiogenic stimuli and flow rate in combination to observe the collective effect on angiogenic sprouting.

# Chapter 2

# Materials and Methods

Please refer to Appendix A and B for a list of materials and preparation of general reagents, respectively.

## 2.1. Bioscaffold preparation

### Preparation of solutions

*Heparin solution*

Heparin solution was prepared to a final concentration of 100 U/ml by dissolving 153 mg of heparin sodium salt (from porcine intestinal mucosa) in 150 ml of PBS. The solution was then sterilised by passing it through a syringe filter into a sample container.

### Tissue retrieval

All surgical procedures and animal husbandry were carried out in accordance with the UK Home Office guidelines under the Animals (Scientific Procedures) Act 1986 and the local ethics committee. Fifteen adult DBIX rats were sacrificed by isoflurane inhalation and cervical dislocation. Once sacrificed a longitudinal abdominal incision was made to expose the abdominal cavity. The inferior vena cava was cannulated using a 24 G cannula and flushed with approximately 10 ml of heparin solution to prevent blood clot formation. An 8-10 cm long segment of jejunum was then isolated and ligations of vessels at the peripheries of the segment were made using suture thread before the intestinal lumen was transected at these locations and the jejunum was explanted. The intestinal lumen was flushed with supplemented PBS solution immediately after explantation.

The jejunum was then stored, submerged in supplemented PBS, in a container at -80 °C until required.

## 2.2. Decellularisation

### Preparation of solutions

*Non-ionic detergent*

To decellularise each jejunum 2 litres of detergent was required. The detergent was prepared by adding 1% (v/v) Triton-X 100 and 0.1% (v/v) ammonium hydroxide to distilled water in a 1L Duran® bottle. A magnetic stir bar was placed into the bottle and the solution was subsequently mixed on a magnetic stirrer until the Triton-X 100 had completely dissolved.

### Decellularisation

Decellularisation was performed to remove native cells and retain the ECM components. This method was adapted from work published by Baptista *et al.* [77]. Firstly, the jejunum was removed from the -80 °C freezer and thawed at 4 °C prior to transferring to a petri dish. This step contributes towards the decellularisation process since the freeze/thaw cycle assists in cell lysis. The superior mesenteric artery (SMA) was then cannulated using a 24 G cannula and suture thread under a dissection microscope. Approximately 1ml of blue food colouring was then perfused through the cannula to determine whether all of the jejunum would be equally supplied with detergent. Upon successful cannulation of the jejunum, the SMA was attached to a peristaltic pump via a luer barb adapter which in turn was attached to a 1 meter length of tubing. The tissue was then submerged completely in 2 L of distilled water (in a tall glass beaker), along with the opposite end of the tubing to form a closed circuit (Figure 7). Distilled water was then continuously perfused and recirculated through the vessels at a rate of 2.7 ml/min for 3 hours. Subsequently the jejunum was removed from the beaker and its contents was replaced with 2 L of non-

ionic detergent. The tissue was then re-submerged in the beaker and detergent was perfused and recirculated continuously overnight. Finally the beaker was filled with distilled water and this was circulated for a further 3 hours to remove any residual detergent from the tissue. Please note that buffers were not replenished/changed during the individual steps. Upon completion of the final distilled water wash the jejunum was transferred to a petri dish containing PBS and was stored at 4 °C until required. Please refer to Appendix C (Figure 72) for the calibration curve showing flow rate vs revolutions per minute (RPM) for this setup.

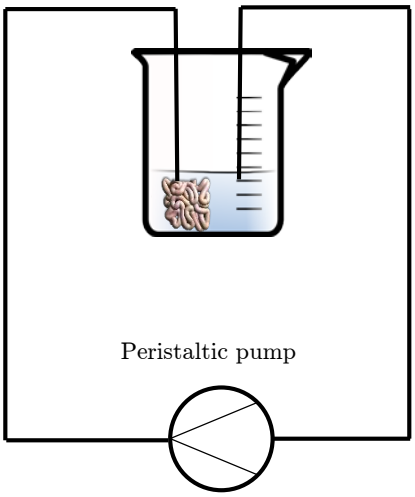


Figure 7 – Schematic outlining the decellularisation setup.

## 2.3. Bioscaffold sterilisation

To sterilise the decellularised jejunum approximately 5 ml of 0.1% (v/v) PA was flushed through the vasculature before being completely submerged in PA for 3 hours at 4°C. Sterile PBS was then flushed through the vasculature of the matrix three times to remove any residual acid. Once this process was complete the matrix was handled in sterile conditions in a class II laminar flow hood (Walker Safety Cabinets, Glossop, UK), unless otherwise stated.

## 2.4. Bioscaffold characterisation

Samples were fixed for 24 hours at 4 °C in 3.7% (w/v) neutral buffered formalin solution in PBS. They were dehydrated using graded alcohol washes before embedding in paraffin wax. Sections of 6 μm were taken for each sample using a microtome (Leica, Germany) and slides were stained appropriately as outlined.

### 2.4.1. Vascular patency

**Preparation of solutions**

*FITC-Dextran*

FITC-Dextran (250 kDa) was dissolved in PBS to a final concentration of 100 μg/ml.

**Vascular patency**

After decellularisation 1 ml of blue food colouring was injected through the SMA of the jejunum to determine the patency of the vessels. The vessels were macroscopically visualised and imaged under a dissection microscope.

To observe the patency of the vessels microscopically, approximately 1 ml FITC-Dextran was infused into the SMA of the jejunum and imaged immediately using a confocal microscope at wavelengths of between 492 nm $\lambda_{ex}$ and 520 nm $\lambda_{em}$.

### 2.4.2. Preparation of histological slides

Samples were washed with PBS and then fixed in 3.7% (w/v) formaldehyde for at least 24 hours at 4 °C. Samples were then processed

overnight in a benchtop tissue processor, undergoing the steps outlined in Table 8.

Table 8 – Summary of steps taken to prepare histology samples

| Step | Solution | Immersion Time (hours) |
|---|---|---|
| 1 | 70% IMS | 1 |
| 2 | 70% IMS | 1 |
| 3 | 80% IMS | 1.5 |
| 4 | 85% IMS | 1.5 |
| 5 | 90% IMS | 1.5 |
| 6 | 95% IMS | 1.5 |
| 7 | 100% IMS | 1.5 |
| 8 | 100% IMS | 1.5 |
| 9 | Xylene | 1.5 |
| 10 | Xylene | 1.5 |
| 11 | Paraffin wax | 2 |
| 12 | Paraffin wax | 2 |

Samples were then embedded in molten paraffin wax using the embedding centre, dispenser and hot plate. The wax blocks were then allowed to cool and solidify on ice blocks for at least 1 hour prior to sectioning using the microtome. Blocks were trimmed at an initial thickness of 15 μm until the surface of the sample within the block was reached. Sections were then sliced at 6 μm and immediately transferred to a water bath set to 38 °C. This allowed the sections to flatten out before being mounted onto the surface of the SuperFrost® Plus slides. Slides were then placed on top of the hot plate, set to 37 °C, to allow them to dry and stored at room temperature until required.

### 2.4.3. Hematoxylin and Eosin (H&E) staining

H&E staining was performed to compare samples and determine whether cells had been removed via the decellularisation process. Slides were placed into a holder and the following steps were carried out (Table 9). Using a pasteur pipette, DPX mountant was placed onto the samples

which were then covered with a coverslip and allowed to dry before imaging using a light microscope.

Table 9 – Summary of processing steps carried out for H&E staining.

| Step | Process | Solution | Immersion time (mins) |
|---|---|---|---|
| 1 | Dewaxing | Xylene | 3 |
| 2 | Dewaxing | Xylene | 3 |
| 3 | Re-hydration | 100% IMS | 1 |
| 4 | Re-hydration | 70% IMS | 0.5 |
| 5 | Re-hydration | Distilled water | 1 |
| 6 | Staining (cell nuclei) | Hematoxylin | 1.5 |
| 7 | Staining | Tap water (running) | 4 |
| 8 | Staining (intra/extracellular proteins) | Eosin | 5 |
| 9 | Staining | Tap water | 0.5 |
| 10 | Dehydration | 70% IMS | 0.5 |
| 11 | Dehydration | 100% IMS | 0.5 |
| 12 | Dehydration | Xylene | 0.5 |
| 13 | Mounting | DPX mountant | - |

### 2.4.4. Glycosaminoglycan (GAG) staining

#### Preparation of solutions

*Alcian blue solution*

Alcian blue solution was prepared by mixing 1 g of alcian blue 8GX into 100 ml of 3% (v/v) acetic acid solution in distilled water and adjusting the pH to 2.5 using acetic acid.

#### GAG Staining

GAGs are an important component of the ECM. They play key roles in binding growth factors, cytokines and water within the ECM [171]. To visually determine whether GAGs had been retained, staining using the

alcian blue stain was used. Freshly cut sections (within two days of sectioning) were placed into a holder and processed according to the processes in Table 10. It is important to use fresh sections as old slides can give inconsistent staining of GAGs with alcian blue. Using a pasteur pipette, DPX mountant was placed onto the samples which were then covered with a coverslip and allowed to dry before imaging using a light microscope.

Table 10 – Summary of processing steps for GAG staining of samples.

| Step | Process | Solution | Immersion time (mins) |
|---|---|---|---|
| 1 | Dewaxing | Xylene | 10 |
| 2 | Dewaxing | Xylene | 10 |
| 3 | Re-hydration | 100% IMS | 3 |
| 4 | Re-hydration | 100% IMS | 2 |
| 5 | Re-hydration | 100% IMS | 2 |
| 6 | Re-hydration | 70% ethanol | 2 |
| 7 | Re-hydration | Running tap water | 3 |
| 8 | Staining | 1% (w/v) Alcian blue | 15 |
| 9 | Staining | Running tap water | 1 |
| 10 | Staining | Distilled water | 0.5 |
| 11 | Staining | Periodic acid | 5 |
| 12 | Staining | Distilled water | 1 |
| 13 | Staining | Schiffs reagent | 15 |
| 14 | Staining | Running tap water | 5 |
| 15 | Staining | Gills no. 3 hematoxylin | 1.5 |
| 16 | Staining | Running tap water | Until water runs clear |
| 17 | Dehydration | 70% ethanol | 0.25 |
| 18 | Dehydration | 100% IMS | 1 |
| 19 | Dehydration | 100% IMS | 2 |
| 20 | Dehydration | 100% IMS | 3 |
| 21 | Dehydration | Xylene | 10 |
| 22 | Dehydration | Xylene | 10 |
| 23 | Mounting | DPX mountant | - |

### 2.4.5. Collagen staining

#### Preparation of solutions

*Picosirius red solution*

Picosirius red solution was prepared by adding 0.1 g of direct red 80 to 100 ml of saturated aqueous solution of picric acid (1.3% v/v in distilled water).

*Acidified water*

Acidified water was prepared by adding 5 ml of glacial acetic acid to 1 litre of distilled water.

#### Collagen Staining

Collagen is the main contributor to the mechanical and physical properties of the ECM, especially collagen type I. Sirius red staining was used to visualise the collagen content of the decellularised jejunum. Slides were placed into a holder and processed according to the steps in Table 11. Once stained DPX mountant was placed onto the samples and a coverslip was placed on top. Slides were allowed to dry before imaging using both light and polarised light microscopy.

Table 11 – Summary of steps taken for collagen staining of samples.

| Step | Process | Solution | Immersion time (mins) |
|---|---|---|---|
| 1 | Dewaxing | Xylene | 10 |
| 2 | Dewaxing | Xylene | 10 |
| 3 | Re-hydration | 100% IMS | 3 |
| 4 | Re-hydration | 100% IMS | 2 |
| 5 | Re-hydration | 100% IMS | 2 |
| 6 | Re-hydration | 70% ethanol | 2 |
| 7 | Re-hydration | Tap water | 1 |
| 8 | Staining | Weigert's hematoxylin | 5 |
| 9 | Staining | Running tap water | 4 |
| 10 | Staining | Picosirius red | 60 |
| 11 | Staining | Acidified water | 0.25 |
| 12 | Staining | Acidified water | 0.25 |
| 13 | Dehydration | 70% ethanol | 0.25 |
| 14 | Dehydration | 100% IMS | 1 |
| 15 | Dehydration | 100% IMS | 2 |
| 16 | Dehydration | 100% IMS | 3 |
| 17 | Dehydration | Xylene | 10 |
| 18 | Dehydration | Xylene | 10 |
| 19 | Mounting | DPX mountant | - |

### 2.4.6. Elastin staining

**Preparation of solutions**

*Working elastic stain solution*

The solution was prepared on the day of use by adding the following reagents, in the order indicated, into a glass container.

- Hematoxylin Solution 20 ml
- Ferric Chloride Solution 3 ml
- Weigert's Iodine Solution 8 ml
- Deionized Water 5 ml

*Working ferric chloride solution*

The working ferric chloride solution (for differentiation) was prepared on the day of use by adding 3 ml of ferric chloride solution and 37 ml deionized water to a glass container.

## Elastin staining

Elastin is a structural protein found in tissues that are required to stretch, such as skin, blood vessels etc. To determine whether elastin had been retained samples were stained with elastic stain and ferric chloride solution. Sections were placed into a slide holder and subjected to the protocol outlined in Table 12. Coverslips were then mounted to the slides by adding DPX mountant media and were allowed to dry before imaging using a light microscope.

Table 12 – Summary of processing steps taken to stain for elastin.

| Step | Process | Solution | Immersion time (mins) |
|---|---|---|---|
| 1 | Dewaxing | Xylene | 10 |
| 2 | Dewaxing | Xylene | 10 |
| 3 | Re-hydration | 100% IMS | 5 |
| 4 | Re-hydration | 100% IMS | 5 |
| 5 | Re-hydration | 95% IMS | 1 |
| 6 | Re-hydration | 70% ethanol | 1 |
| 7 | Re-hydration | Distilled water | 1 |
| 8 | Staining | Elastic stain | 10 |
| 9 | Staining | Distilled water | 1 |
| 10 | Staining | Ferric chloride | 1-2 |
| 11 | Staining | Tap water | 1 |
| 12 | Staining | 95% IMS | 0.5 |
| 13 | Dehydration | Distilled water | 0.5 |
| 14 | Dehydration | Van Gieson stain | 1-3 |
| 15 | Dehydration | 95% IMS | 0.5 |
| 16 | Dehydration | Xylene | 5 |
| 17 | Dehydration | DPX mountant | - |

### 2.4.7. Masson-Goldner trichrome staining

#### Preparation of solutions

*Glacial acetic acid*

A working solution of 1% (v/v) acetic acid was prepared by diluting the stock solution in the ratio of 1:100 in distilled water.

*Weigert's iron hematoxylin*

Weigert's solution A and Weigert's solution B (from catalogue number 115973) were mixed in the ratio 1:1 and used within one week of preparation.

#### Masson-Goldner trichrome staining

Masson-Goldner trichrome staining is a 3 colour staining protocol used in histology and is well suited for distinguishing cells from surrounding connective tissue. This stain was used for analysing CAM samples. Slides were placed into a holder and the steps were performed according to Table 13. Once stained DPX mountant was placed onto the samples and a coverslip was placed on top. Slides were allowed to dry before imaging using a light microscope.

Table 13 – Summary of processing steps to carry out Masson-Goldner trichrome staining.

| Step | Process | Solution | Immersion time (mins) |
|---|---|---|---|
| 1 | Dewaxing | Xylene | 5 |
| 2 | Dewaxing | Xylene | 5 |
| 3 | Re-hydration | 100% IMS | 1 |
| 4 | Re-hydration | 70% IMS | 0.5 |
| 5 | Rinse | Distilled water | 1 |
| 6 | Staining | Weigert's hematoxylin | 5 |
| 7 | Staining | Running tap water | 5 |
| 8 | Staining | 1% acetic acid | 0.5 |
| 9 | Staining | Azophloxine solution | 10 |
| 10 | Staining | 1% acetic acid | 0.5 |
| 11 | Staining | Tungstophosphoric acid orange G solution | 1 |
| 12 | Staining | 1% acetic acid | 0.5 |
| 13 | Staining | Light green SF solution | 2 |
| 14 | Staining | 1% acetic acid | 0.5 |
| 15 | Dehydration | 70% ethanol | 0.5 |
| 16 | Dehydration | 96% ethanol | 0.5 |
| 17 | Dehydration | 100% ethanol | 0.5 |
| 18 | Dehydration | 100% ethanol | 0.5 |
| 19 | Dehydration | 100% ethanol | 2 |
| 20 | Dehydration | Xylene | 5 |
| 21 | Dehydration | Xylene | 5 |
| 22 | Mounting | DPX mountant | - |

### 2.4.8. Staining of cell nuclei

**Preparation of solutions**

*DAPI*

A working DAPI solution containing 1 µg/ml was prepared by diluting DAPI in the ratio of 1:1000 in PBS.

### Staining of cell nuclei

DAPI is a fluorescent stain that binds strongly to A-T rich regions in DNA. It is used widely in fluorescence microscopy to determine the presence of cell nuclei. To determine the effectiveness of the decellularisation protocol in removing cells, samples were stained using DAPI to identify the presence of DNA. Slides were placed into a holder and de-waxed by submerging sequentially in xylene (2×3 minutes), 100% IMS (1×1.5 minutes), 70% IMS (1×1 minute) and distilled water (3×1 minute). A PAP pen was used to draw circles around each sample on the slide, forming a water repellent barrier that enabled staining reagents to remain localised on the tissue sections. The working DAPI solution was then pipetted over each sample before covering the samples with tin foil and leaving them at room temperature for 10 minutes. The samples were then washed three times with PBS and coverslips were affixed to the slides using DPX mountant media. The stained samples were imaged using a confocal microscope at a wavelength range of between 365 nm $\lambda_{ex}$ and 460 nm $\lambda_{em}$.

## 2.4.9. Immunolabeling of laminin and fibronectin

### Preparation of solutions

*BSA*

To prepare the blocking serum 0.75 g of BSA was measured and dissolved completely in 10 ml of PBS to give a final concentration of 7.5% (w/v).

Similarly 1% (w/v) BSA was produced by dissolving 0.1 g of BSA in 10 ml of PBS.

*Primary antibodies*

Polyclonal rabbit anti-fibronectin primary antibody was diluted in the ratio of 1:1500 in 1% (w/v) BSA.

Polyclonal rabbit anti-laminin primary antibody was diluted in the ratio of 1:100 in 1% (w/v) BSA.

*Secondary antibodies*

FITC anti-rabbit secondary antibody was diluted in the ratio of 1:500 in 1% (w/v) BSA.

*Triton-X 100*

Triton-X 100 was prepared to a final concentration of 0.1% (v/v) in PBS by dissolving 10 µl in 10 ml of PBS.

### Immunolabeling of laminin and fibronectin

Laminin is an adhesion protein found in the ECM, especially the basement membrane. It has been shown to play an important role in vascular formation and maintenance and is thought to be a key component to EC friendly scaffold materials [171]. Fibronectin is the next most abundant protein found in the ECM. It is a glycoprotein found in submucosal and basement membrane structures and is responsible for cell adhesion [172–174]. Immunolabeling of both proteins was performed to determine whether they had been retained post decellularisation. Slides were placed into holders, de-waxed and rehydrated by submerging sequentially in xylene (2×3 minutes), 100% IMS (1×1.5 minutes), 70% IMS (1×1 minute) and distilled water (3×1 minute). A PAP pen was used to draw circles around each sample on the slide, forming a water repellent barrier that enabled reagents to remain localised on the tissue sections. Cells were then permeabilised using 0.1% (v/v) Triton-X 100 for 20 minutes. Samples were subsequently incubated in 7.5% (w/v) BSA at room temperature for 60 minutes, followed by washing once with 1% (w/v) BSA in PBS. Samples were incubated with either anti-laminin primary antibody produced in rabbit or anti-fibronectin antibody produced in rabbit at 4 °C overnight. Samples were washed 3 times in PBS before incubating with FITC anti-rabbit secondary antibody at room temperature

for 60 minutes before washing a further 3 times with PBS. Nuclear counterstaining was then performed using DAPI by incubating at room temperature for 20 minutes and then washing a further three times with PBS. Coverslips were then fixed onto the slides using DPX mountant media. Samples were imaged using a confocal microscope set to 495 nm $\lambda_{ex}$, 515 nm $\lambda_{em}$ (FITC) and 358 nm $\lambda_{ex}$, 461 nm $\lambda_{em}$ (DAPI).

### 2.4.10. Contact cytotoxicity assay

#### Preparation of solutions

*Culture medium (DMEM, 10% FCS (v/v))*

Human dermal fibroblasts (HDFs and RN22 (rat Schwann cell line) cells were cultured in DMEM, 10% FCS (v/v) (Table 14).

Table 14 – Components of DMEM, 10% FCS (v/v) culture medium.

| Component | Volume (ml) | Final concentration |
|---|---|---|
| DMEM | 439 | 88% (v/v) |
| FCS | 50 | 10% (v/v) |
| Penicillin/streptomycin | 5 | 100 IU/ml / 0.1 mg/ml |
| Amphotericin B | 1.25 | 0.625 μg/ml |
| L-glutamine | 5 | 2 mM |

#### Contact cytotoxicity assay

To determine whether potentially cytotoxic detergents were effectively removed after decellularisation, a contact cytotoxicity assay was performed. Samples of sterile decellularised jejunum were cut into approximately 5 $mm^2$ sections. Cyanoacrylate contact adhesive (15 μl) was then placed into the centre of 1 well of a 6 well plate to serve as a positive control (i.e. cells will not grow on this). Subsequently 15 μl of type I rat tail collagen (handled on ice) was added to the centre of the adjacent well of the 6 well plate and was neutralised using 7.5 μl of sterile

1M sodium hydroxide. The pH of the collagen gel was tested using pH indicator test strips with the ideal pH being 7.4 upon neutralisation. The plate was placed in a 37 °C incubator for 15 minutes to allow the gel to set. This served as a negative control (i.e. cell will grow on this). Samples of decellularised jejunum (5 $mm^2$) were attached to the bottom of the remaining wells using collagen gel and sterile sodium hydroxide (again in the ratio 2:1) and were allowed to set in the incubator. The number of plates prepared corresponded to the number of cell types being tested (in this case two). Wells were washed three times with PBS for 10 minutes each. Whilst washing, HDFs and RN22 cells were passaged and counted (for more details on passaging and counting cells please see section 2.6). Please note that HDFs were used at passage 8 and RN22 cells were used at passage 12. Each cell type was resuspended in DMEM, 10% FCS (v/v) to a concentration of approximately 250,000 cells/ml. A total of 2 ml of cell suspension was added to each test and control well. Plates were incubated for 48 hours at 37 °C in a 5% $CO_2$ atmosphere. Media was then aspirated and the wells were washed gently with PBS. Samples were then fixed with 3.7% (w/v) formaldehyde for 10 minutes. After removing the formaldehyde, Giemsa stain was added to cover each cell layer and was incubated for 5 minutes. Each well was then rinsed using tap water until it ran clear and the plates were allowed to air dry. Plates were examined microscopically using bright field microscopy and changes in morphology, vacuolisation, detachment and cell lysis were recorded and imaged in order to determine whether cells had been adversely affected by the presence of the decellularised jejunum and potential residual cytotoxic detergents.

## 2.5. Quantitative analysis

### 2.5.1. DNA quantification

**Preparation of solutions**

*Buffer ATL & buffer AL*

Both of these buffers may form precipitates upon storage. When necessary, the buffered were warmed to 56 °C until the precipitates had fully dissolved.

*Buffer AW1 & buffer AW2*

Both of these buffers are supplied a concentrates. Prior to use, the appropriate amount of ethanol was added as indicated on the bottle to obtain the working solution.

*Digestion buffer*

This digestion buffer was prepared by adding the following reagents to a glass container, stirring continuously using a magnetic stirrer.

- L-Cysteine hydrochloride 0.394 g
- Di-sodium ethylenediaminetetraacetic acid 0.931 g
- PBS containing calcium and magnesium 500 ml

The pH was then adjusted to 6.0 ± 0.1 by adding 6 M hydrochloric acid or 6 M sodium hydroxide. This solution was stored at room temperature for a maximum of 6 months.

*DNA standard solutions*

Stock solution was prepared by adding 5ml of nuclease free water to 5 mg of calf thymus DNA and dissolving by inversion. This was stored at -20 °C for a maximum of 6 months.

A primary standard was prepared by adding 200 µl of DNA stock solution to 1.8 ml of digestion buffer (100 µg/ml).

To prepare the DNA standard, reagents were combined according to Table 15.

Table 15 – Summary of DNA standard preparation.

| Standard concentration (µg/ml) | Volume of primary standard (µl) | Volume of digestion buffer (µl) |
|---|---|---|
| 50 | 200 | 200 |
| 45 | 180 | 220 |
| 40 | 160 | 240 |
| 35 | 140 | 260 |
| 30 | 120 | 280 |
| 25 | 100 | 300 |
| 20 | 80 | 320 |
| 15 | 60 | 340 |
| 10 | 40 | 360 |
| 5 | 20 | 380 |
| 0 | 0 | 400 |

## DNA quantification

In order to determine the effectiveness of the decellularisation protocol, quantification of the DNA present in samples pre- and post-decellularisation was performed. DNA was isolated and quantified from fresh (n=3) and decellularised (n=3) rat jejunums using the DNeasy Blood and Tissue kit according to the manufacturer's (Qiagen) instructions. Firstly, around 100 mg of fresh and decellularised tissue was macerated, placed in a sterile 1.5 ml micro centrifuge tube and lyophilised to a constant weight. Samples were digested by adding 360 µl of buffer ATL and 40 µl of proteinase K which was mixed thoroughly by vortexing and then samples were incubated overnight at 56 °C. After this 400 µl of buffer AL and 400 µl ethanol were added to each digest and mixed thoroughly by vortexing. Each sample was transferred to a DNeasy mini spin column placed in a collection tube and centrifuged at 6000 g for one minute before discarding the flow-through. Buffer AW1 (500 µl) was added and centrifuged again for one minute at 6000 g discarding any flow-through. To dry the DNeasy membrane 500 µl of buffer AW2 was added and centrifuged for three minutes at 20,000 g. This stage is important

since any residual ethanol can potentially interfere with subsequent reactions. The DNeasy mini spin columns were then transferred to 1.5 ml centrifuge tubes before adding 200 µl of buffer AE to the DNeasy membrane and incubating for 1 minute at room temperature. DNA was then eluted by centrifuging for one minute at 6000 g. For maximum DNA yield this step was repeated (i.e. adding buffer AE). The amount of DNA present in each sample was measured by determining the absorbance at 260 nm through the use of a NanoDrop 1000 (Thermo Scientific). A DNA standard was also tested to ensure the accuracy of the readings. Samples were stored at 4 °C for short periods or -20 °C for long term storage.

### 2.5.2. Collagen quantification

**Preparation of solutions**

*Assay buffer*

The assay buffer was prepared by adding the following reagents, in the order indicated, into a glass container.

- Citric acid (monohydrate) 6.65 g
- Glacial acetic acid 1.6 ml
- Sodium acetate (trihydrate) 16 g
- Sodium hydroxide 4.55 g
- Propan-1-ol 40 ml

The volume of solution was then made up to 150 ml using distilled water. The pH was adjusted to 6.0-6.5 using 6 M hydrochloric acid whilst stirring using a magnetic stirrer. The volume was then adjusted to 200 ml using distilled water. This solution will remain stable for up to 2 months if kept in a dark bottle at 4 °C.

*Chloramine T*

Chloramine T (1.41 g) was dissolved in 100 ml of distilled water using a magnetic stirrer. This was prepared fresh immediately prior to use.

*Ehrlich's reagent*

This solution was prepared by adding the following reagents to a glass container, stirring continuously using a magnetic stirrer.

- P-dimethylaminobenzaldehyde 1.88 g
- Propan-1-ol 7.5 ml
- Perchloric acid 3.35 ml
- Distilled water 1.65 ml

Once prepared the solution was used within 1 hour.

*Assay standards*

To make the primary standard the following reagents were combined.

- Trans-4-hydroxy-L-proline 25 mg
- Assay buffer 25 ml

To make the secondary standard the following reagents were combined and then prepared as outlined in Table 16.

- Primary standard 1 ml
- Assay buffer 9 ml

Table 16 – Secondary standard preparation for collagen quantification.

| Standard concentration ($\mu g.ml^{-1}$) | Volume of secondary standard (µl) | Volume of buffer (µl) |
|---|---|---|
| 30 | 750 | 1750 |
| 25 | 625 | 1875 |
| 20 | 500 | 2000 |
| 15 | 375 | 2125 |
| 10 | 250 | 2250 |
| 8 | 200 | 2300 |
| 6 | 150 | 2350 |
| 4 | 100 | 2400 |
| 2 | 50 | 2450 |
| 0 | 0 | 2500 |

## Collagen quantification

To determine whether collagen had been retained post-decellularisation a quantitative analysis was performed. Hydroxyproline is an amino acid found almost exclusively in the protein collagen. This assay uses a chloramine T mixture to convert hydroxyproline in the digested samples to a pyrrole. Ehrlich's reagent is then added to react with the pyrrole to produce a chromophore and the absorbance of the plate is read. The content of hydroxyproline in the unknown samples is determined by comparison with a predetermined hydroxyproline standard curve.

To perform the assay approximately 100 mg of fresh and decellularised tissue was macerated and placed into 1.5 ml micro-centrifuge tubes. The mass of the centrifuge tubes was measured before and after the addition of tissue samples to determine the mass of tissue. The samples were then transferred to a freeze dryer and were lyophilised at -50 °C to a constant mass. The mass of the tubes was measured after 12 hr of lyophilisation and again at intervals of 4 hr or until the mass of the tubes was constant. Lyophilised tissue samples were then digested using 6 M hydrochloric acid to break down proteins to their component amino acids at 121 °C in an oven overnight in polypropylene universal containers. Sodium hydroxide

(6 M) was added to neutralise each sample and the final volume was noted. Collagen content was measured indirectly through measurement of the hydroxyproline content according to Reddy *et al.* [175]. Briefly, 50 µl of each sample was added to a clear flat bottomed 96 well plate and oxidised by adding 100 µl of chloramine T solution. The plate was gently shaken at 60 rpm for 5 minutes using a table shaker before adding 100 µl of Ehrlich's reagent to each well. The plate was then incubated at 60 °C for 45 minutes. Absorbance was read at 562 nm. Blank values (i.e. assay buffer) were then subtracted from all of the standards and unknown samples. A standard curve of hydroxyproline concentration against absorbance was plotted (Appendix C, Figure 68) and unknown values were interpolated using a linear regression of the standard curve.

### 2.5.3. GAG quantification

#### Preparation of solutions

*Papain digestion solution*

1250 units of papain were dissolved in 25 ml of digestion buffer using a magnetic stirrer to give a final concentration of 50 U/ml. This solution was used immediately.

*0.1 M sodium di-hydrogen orthophosphate*

3.45 g of sodium di-hydrogen orthophosphate was added to 250 ml of distilled water and mixed thoroughly using a magnetic stirrer. This solution was stored for up to 3 months at room temperature.

*0.1 M di-sodium hydrogen orthophosphate*

3.55 g of di-sodium hydrogen orthophosphate was added to 250 ml of distilled water and mixed thoroughly using a magnetic stirrer. This solution was stored for up to 3 months at room temperature.

*Assay buffer*

The assay buffer was prepared by adding the following reagents to a glass container and stirring continuously using a magnetic stirrer.

- 0.1M sodium di-hydrogen orthophosphate 137 ml
- 0.1M di-sodium hydrogen orthophosphate 63 ml

The pH was adjusted to 6.8 using 6 M hydrochloric acid or 6 M sodium hydroxide. The assay was stored for a maximum of 3 months at room temperature.

*1,9 Dimethylmethylene blue (DMB) dye solution*

The DMB dye solution was prepared by adding the following reagents to a glass container and stirring continuously using a magnetic stirrer.

- 1,9 dimethylene blue 8 mg
- Ethanol 2.5 ml
- Formic acid 1 ml
- Sodium formate 1 g

The volume was then increased to 500 ml using distilled water and the pH was adjusted to 3.0 using formic acid. The dye was stored for a maximum of 3 months at room temperature.

*Assay standards*

To make the primary standard the following reagents were combined and then prepared according to Table 17.

- Chondroitin sulphate B 10 mg
- Assay buffer 10 ml

Table 17 – Preparation of the GAG assay standard.

| Standard concentration ($\mu g.ml^{-1}$) | Volume of primary standard (µl) | Volume of buffer (µl) |
|---|---|---|
| 200 | 40 | 160 |
| 150 | 30 | 170 |
| 100 | 20 | 180 |
| 50 | 10 | 190 |
| 25 | 5 | 195 |
| 12.5 | 5 | 395 |
| 6.25 | 5 | 795 |
| 3.125 | 5 | 1595 |
| 0 | 0 | 250 |

## GAG quantification

GAG content was analysed to determine quantitatively how much had been preserved post decellularisation using the dimethylmethylene blue (DMB) assay first described by Farndale *et al.* [176]. The assay uses the metachromatic dye 1,9 dimethylmethylene blue to quantify the amount of GAGs in the standard and test samples. The binding of the GAGs to the dye induces a shift in the absorption spectrum which is directly proportional to the amount of GAGs. The sample values of GAGs are determined by the standard curve.

Briefly, fresh and decellularised tissues (100 mg) were macerated and lyophilised. Samples were digested by adding 5 ml of papain digestion solution and incubating for 48 hours at 60 °C before transferring 40 µl of each test solution into a clear flat bottomed 96 well plate. DMB dye solution (250 µl) was added to each well and the plate was shaken for two minutes on a plate shaker. The optical densities were measured using a micro plate spectrophotometer at 520 nm. Blank values (i.e. assay buffer) were subtracted from all of the standards and unknown samples. A standard curve of chondroitin sulphate B concentration *vs* absorbance (Appendix C, Figure 67) was plotted and unknown values were interpolated using a linear regression of the standard curve.

## 2.6. General cell culture

All cell culture work was carried out in a class II biological safety cabinet (Walker Safety Cabinets, Derbyshire, UK). Prior to commencing work the safety cabinet was sterilised using 70% IMS (Fisher Scientific UK, Loghborough, UK) and all equipment to be used within it was either sterilised using 70% IMS or autoclaved. Sterile cell culture plasticware (Costar, Buckinghamshire, UK) was used and liquids were either purchased sterile or were filter sterilised. All cells were incubated under humidified conditions at 37 °C containing 5% $CO_2$.

### 2.6.1. Human dermal fibroblast culture

**Preparation of solutions**

*'Difco-trypsin'*

'Difco-trypsin' was prepared to a final concentration of 0.1% (w/v) by combining the following reagents.

- Difco-trypsin powder 0.5 g
- D-glucose 0.5 g
- Phenol red 0.5 ml
- PBS 500 ml

The pH was adjusted to 7.4 using 2 M sodium hydroxide solution and was filter sterilised. Aliquots were prepared (10 ml) and frozen at -20 °C until required.

*Collagenase A solution*

Collagenase A powder was dissolved in serum free culture media (see above) to a final concentration of 0.05% (w/v). The solution was filter sterilised and stored in 10 ml aliquots at -20 °C until required.

*Cryopreservation medium*

Cryopreservation medium was prepared to the required volume by using 90% (v/v) FCS and 10% (v/v) DMSO.

## Cell isolation

Skin samples were taken from consenting patients undergoing elective abdominoplasty or breast reduction surgery. Tissues were collected and used under the requirements stipulated by Research Tissue Bank Licence 12179. Tissue samples (0.5 x 0.5 cm) were incubated in 10 ml of 'Difco-trypsin' for between 12-18 hours at 4 °C. Enzymatic action was stopped by adding 5 ml of FCS. The epidermis was separated from the dermis using sterile forceps before mincing the dermis finely and incubating with 10ml of collagenase solution at 37 °C overnight. The action of the collagenase solution was stopped with the addition of 10 ml of culture medium (DMEM, 10% FCS (v/v)). Following centrifugation of the resulting cell suspension (400 g for 10 minutes), pelleted cells were cultured in a T25 flask containing DMEM, 10% FCS (v/v). The medium was changed after 24 hours and then every 3-4 days until ˜80% confluent.

## Passaging cells

Once cells had reached ˜80% confluence they were transferred into new flasks in order to continue cellular proliferation and ultimately increase the total number of cells available for experiments. To passage cells, cell culture medium in the flask was removed and the cell layer was washed with 10ml PBS to remove any excess serum proteins left from the medium (this would inhibit subsequent enzyme action). The cells were then incubated with 2.5 ml trypsin/EDTA solution and incubated at 37 °C for 5 minutes or until the cells had detached from the flask (this was confirmed using phase microscopy). The trypsin/EDTA was then neutralised using 7.5 ml of culture medium and the cell suspension was transferred to a universal container before centrifuging at 200 g for 5 minutes. The supernatant was then removed before gently tapping the

cell pellet to break it up. The cells were then resuspended in culture medium and approximately $1 \times 10^5$ cells were seeded into each T75 flask before incubating at 37 °C in a 5% $CO_2$ environment. Again, the medium was changed after 24 hours and then every 3 days until ~80% confluent.

## Counting cells

In order to count the number of cells in a cell suspension, a haemocytometer was used. After thoroughly resuspending cells in a known volume of culture medium 10 µl of the suspension was pipetted into the haemocytometer by placing the pipette tip at the edge of the chambers and allowing capillary action to draw the suspension from the pipette. Care was taken not to overfill the chamber. The grid lines of the haemocytometer were focussed upon using the 10x objective of an inverted microscope and phase contrast was used to visualise cells. A hand tally counter was then used to count the total number of cells present in a set of 16 squares (as indicated in Figure 8) which occupies a volume of $1 \times 10^{-4}$ ml. At least 2 sets of 16 squares were counted to obtain an average number of cells. The calculation below was used to calculate the total number of cells present per milliliter of cell suspension.

$$Cell\ concentration\ per\ ml\ = \frac{Average\ no.of\ cells\ counted\ \ x\ \ dilution\ factor}{1\ x\ 10^{-4}}$$

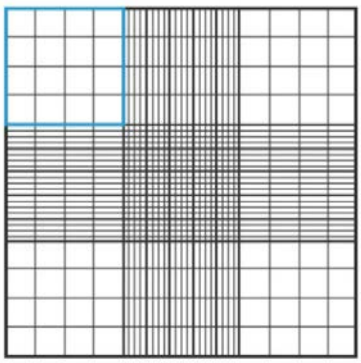

Figure 8 – Haemocytometer showing 9 squares comprised of 16 individual squares each (blue).

### Cryopreservation of cells

Cells were treated as if passaging but instead of resuspending in DMEM, 10% FCS (v/v) culture medium after centrifuging, cells were instead resuspended in cryopreservation medium to a concentration of $1 \times 10^6$ cells/ml. This cell suspension was then added to 1 ml cryovials which were transferred to a Mr Frosty™ freezing container that enables cells to be cooled at a rate of -1 °C per minute. The container was placed into a -80 °C freezer for at least 4 hours before transferring the cryovials to a liquid nitrogen dewar (~ -196 °C).

### Thawing cells

Cryovials were removed from the liquid nitrogen Dewar using necessary safety precautions and were immediately thawed in a water bath set to 37 °C. When the cell suspension had just thawed it was transferred to a universal container filled with 10 ml of culture medium before centrifuging at 200 g for 5 minutes. The cell pellet was then resuspended in culture medium, transferred to a T75 flask and incubated at 37 °C in a 5% $CO_2$ environment. The culture medium was replaced after 24 hours and then every 3 days thereafter until ˜80% confluent.

## 2.6.2. Human dermal microvascular endothelial cell culture

### Preparation of solutions

*Pig skin gelatin (0.1%) solution*

Pig skin gelatin solution was prepared by dissolving 0.1 g of pig skin gelatin in 100 ml of PBS. The solution was then sterile filter, aliquoted and stored at -20 °C until required.

*HDMEC growth medium*

HDMEC growth medium was bought from PromoCell as a kit, containing the basal medium and supplement mix. To prepare the culture medium the contents of the supplement mix was added to 500 ml of basal medium in a class II cell culture cabinet. In addition, 5 ml of penicillin/streptomycin and 1.25 ml of amphotericin B were added. The final concentrations of the components used in the HDMEC growth medium are shown in Table 18.

Table 18 – Summary of the composition of HDMEC growth medium.

| Component | Final concentration |
|---|---|
| FCS | 0.05 ml/ml |
| EC growth supplement | 0.004 ml/ml |
| Epidermal growth factor (recombinant human) | 10 ng/ml |
| Heparin | 90 µg/ml |
| Hydrocortisone | 1 µg/ml |
| Penicillin | 100 U/ml |
| Streptomycin | 0.1 mg/ml |
| Amphotericin B | 0.25 µg/ml |

**Passaging cells**

Proliferating HDMECs derived from human juvenile foreskin were purchased from PromoCell. Prior to passaging cells T25 flasks were coated with 5 ml pig skin gelatin solution and incubated at 37 °C in a 5% $CO_2$ atmosphere overnight. The gelatin solution was then aspirated off and the flask was washed 3 times with sterile PBS. To passage cells, media was first aspirated from the T25 flask before washing with 2.5mls of hepesBSS to remove any residual serum proteins. After removal of the hepesBSS solution, pre-warmed trypsin EDTA (2.5 ml) was then added and flasks were incubated at room temperature for 2-3 minutes, monitoring cell detachment continuously using phase contrast microscopy. To quench the action of the trypsin EDTA, 2.5 ml of trypsin neutralising solution was added and the cell suspension was collected in a sterile

universal container. Cells were centrifuged at 200 g for 5 minutes before resuspending in culture medium and splitting in the ratio 1:3 into T25 flasks. HDMECs were used at passage 5 in this study.

### Cryopreservation of cells

Please refer to section 2.6.1. Please note that cells were resuspended in Cryo-SFM bought from PromoCell instead of cryopreservation medium (90% FCS/10% DMSO).

### Thawing cells

Please refer to section 2.6.1. Note that cells were transferred to a T25 flask.

## 2.7. Melanin infusion of dermal fibroblasts

### Preparation of solutions

*Melanin supplemented culture medium*

Culture medium was prepared as outlined in section 2.6.1. To 10 ml of culture medium, 10 mg of melanin was added to give a concentration of 1 mg/ml. This was then sonicated for 15 minutes.

### Melanin infusion of dermal fibroblasts

To macroscopically determine the distribution of cells when infused into the decellularised jejunum, fibroblasts were infused with melanin so that they were visible. To do this 5 ml of melanin supplemented culture medium was added to T75 flasks containing HDF cells that were at least 70% confluent. Cells were incubated for 24 hours before removing the melanin solution and were then used for recellularisation.

## 2.8. Bioscaffold recellularisation

### Bioscaffold recellularisation

*HDMECs inside vascular channels only*

Re-endothelialisation of the jejunum was performed by perfusing HDMECs into the vascular channels. A sterile decellularised jejunum was placed into a sterile petri dish in a class II biological safety cabinet. Using a 5 ml syringe and forceps, HDMEC culture medium was perfused through the cannula and thus the bioscaffold. The jejunum was then immersed in culture medium and placed in an incubator set at 37 °C in a 5% $CO_2$ atmosphere. HDMECs were then passaged and counted as described in section 2.6.1 and 2.6.2. $1.5 \times 10^6$ cells were resuspended in 1ml of HDMEC growth medium and then perfused through the vasculature of the pre-warmed decellularised jejunum using a 1 ml syringe. This was incubated at 37 °C in a 5% $CO_2$ atmosphere overnight.

*HDMECs and HDFs inside vascular channels*

HDMECs were recellularised into the decellularised jejunum as described above. This was incubated for at least 3 hours at 37°C in a 5% $CO_2$ atmosphere. HDFs were then passaged and counted as described in section 2.6.1. $1.5 \times 10^6$ HDFs were then resuspended in 1ml of HDMEC medium and perfused through the vasculature of the decellularised jejunum using a 1ml syringe. This was incubated at 37°C in a 5% $CO_2$ atmosphere overnight.

*HDMECs inside vascular channels and HDFs inside lumen*

A sterile decellularised jejunum was preconditioned with media and warmed as described above. HDFs were passaged and counted as described in section 2.6.1. $0.75 \times 10^6$ HDFs were resuspended in 5 ml of HDMEC medium and perfused through the lumen of the intestine. This was incubated (fully submerged in HDMEC medium) for at least 3 hours

at 37 °C in a 5% $CO_2$ atmosphere. This process was repeated but this time the jejunum was flipped onto the reverse side so that the HDFs were perfused onto the opposite surface of the lumen. Again the jejunum was incubated for at least 3 hours at 37 °C in a 5% $CO_2$ atmosphere. HDMECs were then passaged and counted as described in section 2.6.1 and 2.6.2. $1.5 \times 10^6$ cells were resuspended in 1 ml of HDMEC growth medium and then perfused through the vasculature of the decellularised jejunum using a 1 ml syringe. This was then incubated at 37 °C in a 5% $CO_2$ atmosphere overnight.

## 2.9. Bioreactor design and preparation

### Bioreactor design and production

The bioreactor was designed using the 3D CAD design software, SolidWorks. The drawings produced by this program are provided in Appendix C (Figure 69 - Figure 71). The base and lid of the bioreactor chamber were made from Lexan medical grade polycarbonate due to its optical clarity, durability and known biocompatibility [177].

### Gasket production

Gaskets were manufactured to produce a seal between the lid and base of the bioreactor. Silicon gaskets were produced by adding 50 ml of silicone elastomer and 5 ml of curing agent to a straight sample container and stirring thoroughly. This was then transferred to a square petri dish and baked in an oven for 60 minutes at 60 °C. The flat silicon sheet was then cooled and transferred to a laser cutter. The silicon gasket was drawn on the package Inkscape and this file was loaded onto the laser cutting software. The gaskets were then cut out of the silicon.

### Bioreactor preparation

*Base and lid*

Prior to use, the base of the bioreactor had a barbed to threaded adapter screwed into the inner aspect of inlet port. A 2 cm long piece of tubing was then attached to the adapter which in turn had a male luer lock adapter attached to the end as illustrated in Figure 9.

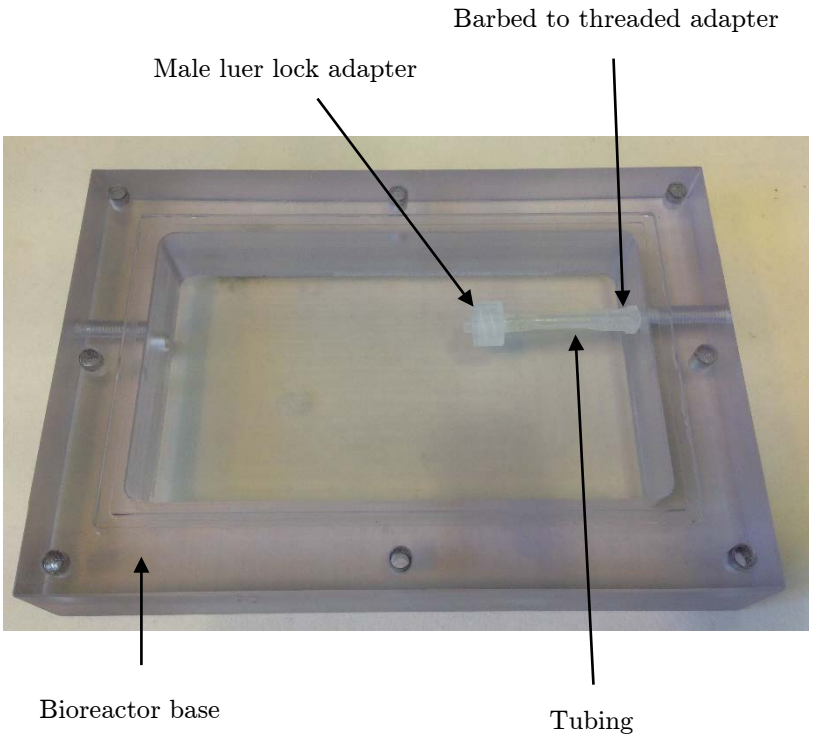


Figure 9 – Image showing the configuration of the base of the bioreactor prior to sterilisation

The lid of the bioreactor had barded to threaded adapters screwed into one pair of adjacent holes with 1 cm long tubing attached whilst the other pair of holes were blocked by screwing in plugs (Figure 10).

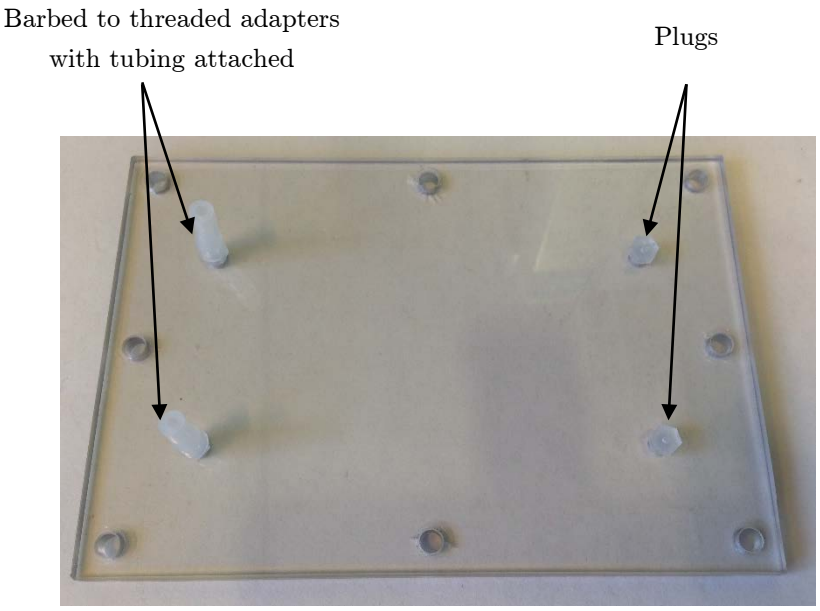


Figure 10 – Image showing the configuration of the lid of the bioreactor prior to sterilisation

Both the base and lid of the bioreactor were placed into a tall 2 L capacity glass beaker inside a class II biological safety cabinet. This was then filled with 2 L of 0.1% PA and incubated at room temperature for up to 5 hours. The PA was then removed and replaced with sterile distilled water. This was then left overnight to wash the bioreactor base and lid to remove any residual acid.

*Tubing*

Pharmed BPT was used for the section of tubing to be placed over the peristaltic pump rollers since it is more durable than conventional silicon tubing when used in such circumstances. Due to the increased cost of such tubing the rest of the system consisted of cheaper Versilic silicon tubing. Both types of tubing were connected to one another using straight barbed tubing connectors (Figure 11).

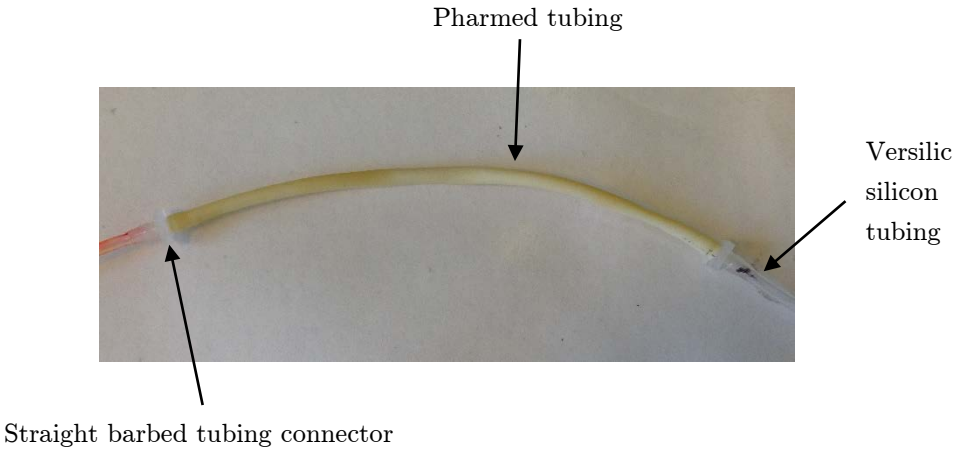


Figure 11 – Image showing the configuration of the central section of the tubing

Barbed to threaded adapters were placed at the ends of the lengths of Versilic silicon tubing (so that it could be connected to the base of the bioreactor – Figure 12).

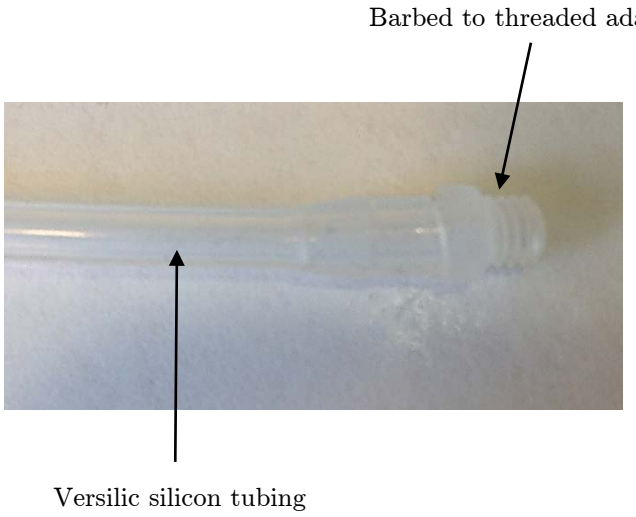


Figure 12 - Image showing the configuration of the end section of the tubing

Prior to use the tubing was sterilised by autoclaving.

*Gasket, stainless steel grid and screws*

Prior to use, the gasket, stainless steel grid and screws were all sterilised by autoclaving.

## 2.10. Perfusion of recellularised bioscaffold

**Perfusion of recellularised bioscaffold**

Assembly of the bioreactor took place in a sterile class II biological safety cabinet. The base was firstly removed and the barbed to threaded adapters at the end of the tubing were screwed into the inlet and outlet ports using sterile forceps. The silicon gasket was then positioned in place before placing the stainless steel grid into the base chamber (Figure 13). The chamber was then filled with ˜70 ml of HDMEC growth medium. The tubing was attached to the peristaltic pump and the medium was perfused through the tubing. The recellularised jejunum was then

removed from the incubator and the cannula was attached to the male luer lock adapter. The lid was placed on top of the base and secured into place using 8 socket head cap screws. Sterile syringe filters were then attached to the tubing on the lid to allow for gas exchange (Figure 14). The bioreactor was then transferred to an incubator with the peristaltic pump positioned outside and perfused continuously with medium (Figure 15).

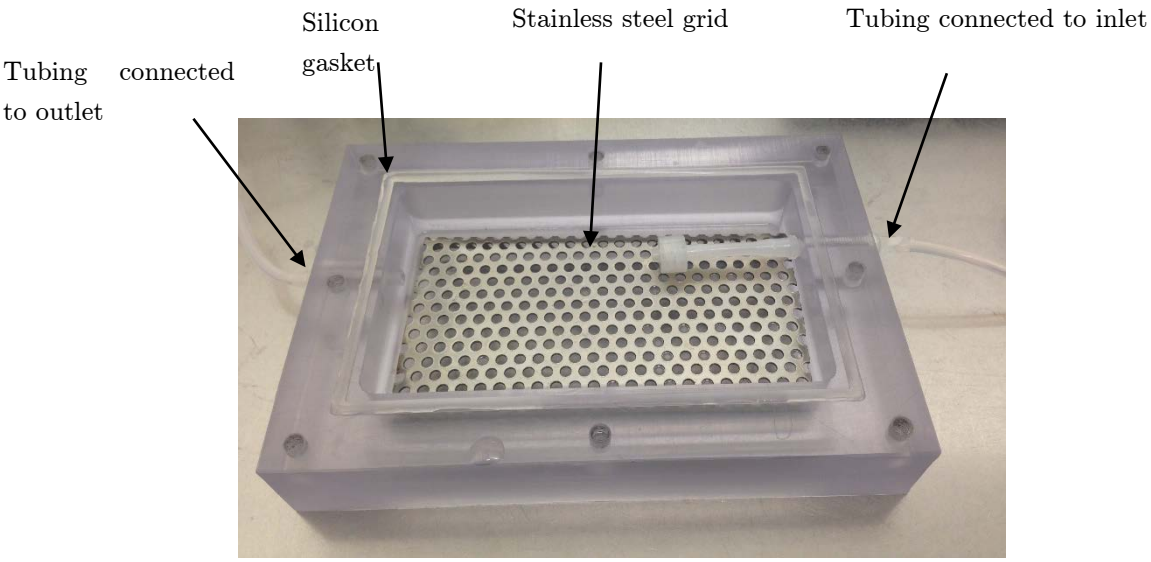


Figure 13 - Image showing the configuration of the base of the bioreactor for perfusion of the recellularised jejunum

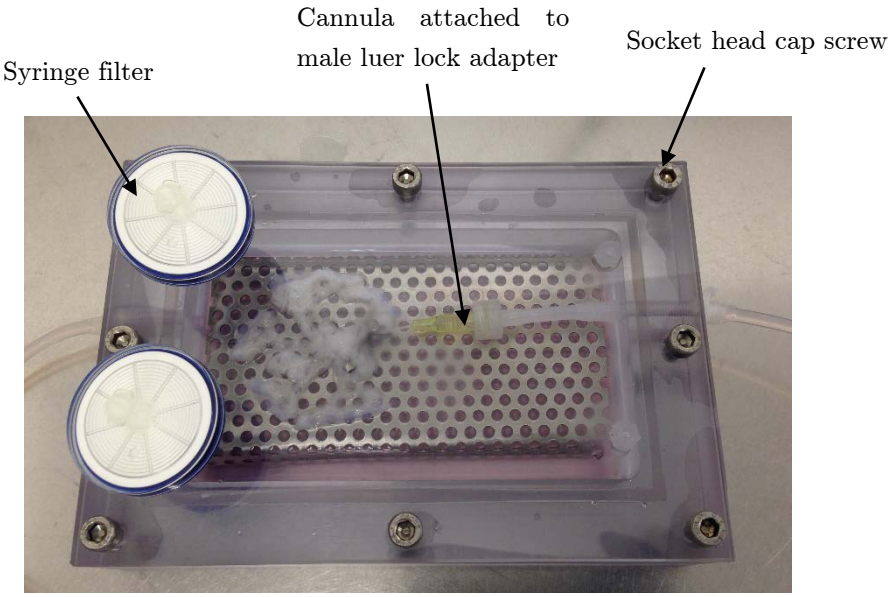


Figure 14 – Image showing the assembled bioreactor used to perfuse the recellularised jejunum

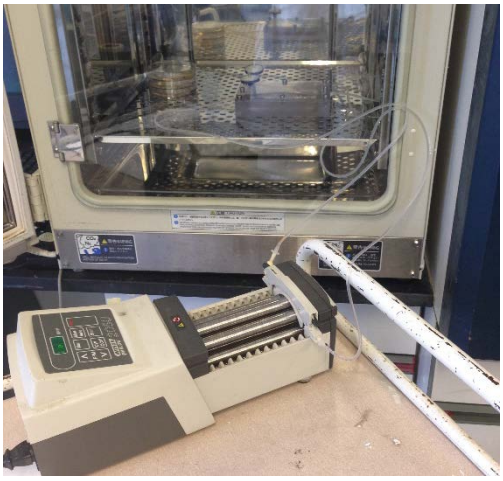

Figure 15 – Image showing the bioreactor perfusion setup

## 2.11. LIVE/DEAD® Cell Staining

### Preparation of solutions

*LIVE/DEAD® cell staining solution*

Propidium iodide and Syto® 9 were diluted in pre-warmed DMEM in the ratio 1:3000 under sterile conditions.

### LIVE/DEAD® cell staining

LIVE/DEAD staining was performed to determine whether cells perfused throughout the samples had survived. The staining procedure employs two nucleic acid stains — the green-fluorescent Syto® 9 stain and the red-fluorescent propidium iodide stain. These stains differ in their ability to penetrate healthy cells. When used alone, Syto® 9 stain labels both live and dead cells. In contrast, propidium iodide penetrates only cells with damaged membranes, reducing Syto® 9 fluorescence when both dyes are present. Thus, live cells with intact membranes fluoresce green, while dead cells with damaged membranes fluoresce red. Sections were taken, transferred to a 6 well plate and incubated at 37 °C at 5% $CO_2$ for 20 minutes. Samples were then imaged using a confocal microscope.

## 2.12. Collagen gel preparation

### Preparation of solutions

*VEGF 165 solution*

A stock solution of VEGF 165 (10 ng/µl) was diluted to a concentration of 1 ng/µl by adding sterile PBS.

### Collagen gel preparation

Working on ice, VEGF loaded and 'plain' collagen gels were prepared using the reagents outlined in Table 19.

Table 19 – Components of the plain and VEGF loaded collagen type I gels.

| Component | 'Plain' gel | VEGF loaded gel |
|---|---|---|
| Rat tail collagen type I | 0.2 ml | 0.2 ml |
| HDMEC culture medium | 0.1 ml | 0.1 ml |
| VEGF | - | 3 µl |
| Sodium hydroxide | Added drop-wise | Added drop-wise |

Firstly the rat tail collagen (type I) and HDMEC culture medium were combined with or without the addition of VEGF 165. The final concentration of VEGF 165 within the gels was 10 ng/ml. Sterile 1 M sodium hydroxide was added drop-wise to neutralise the pH before allowing to set in a 37 °C incubator for 15 min.

## 2.13. Production of natural angiogenesis model

Angiogenesis models consisted of the recellularised jejunum containing varying cell combinations with VEGF loaded gels placed on top. The aim of such combinations was to induce EC outgrowth into the gels.

Recellularised natural scaffolds were placed into the bioreactor as explained in section 2.10. Stainless steel rings were then placed on top of the recellularised jejunum as shown in Figure 16. Collagen was prepared as described in section 2.12 and 100 µl was pipetted into each metal ring. The bioreactor was then sealed and transferred to an incubator where the gels were allowed to set at 37 °C for 15 min. The scaffold was then perfused.

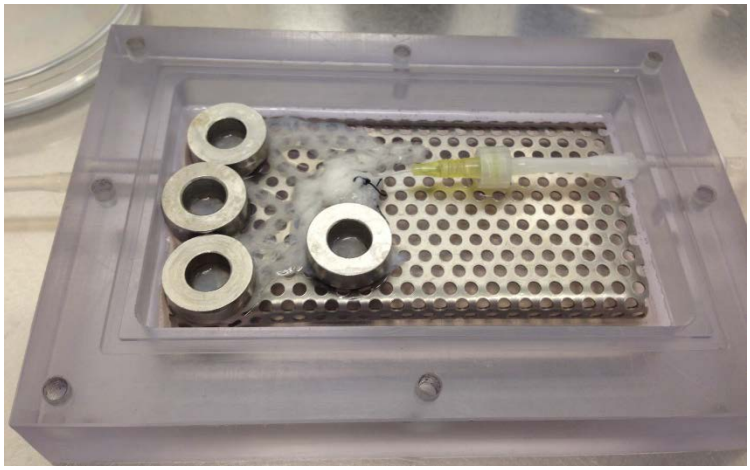

Figure 16 – Image showing the placement of collagen gels onto the recellularised jejunum

## 2.14. Chick CAM assay

To assess the angiogenic properties of decellularised jejunum *in vivo* the CAM assay was used. Fertilised chick eggs were incubated at a constant temperature of 37 °C and humidity of 40% in a chick egg incubator. Seven days post fertilisation, a small window was dissected into the chick egg using a sterile blade and forceps. Small segments (~1 cm in length) of sterilised decellularised jejunum were placed onto the CAM. This was repeated with a collagen gel (please refer to section 2.12 for preparation details) as a negative control. The window was sealed by covering with parafilm (sterilised by submerging in 70% IMS) and securing with masking tape and returned to the incubator for a further 7 days. Samples were then exposed by removing the surrounding egg shell and imaged using a digital microscope.

## 2.15. Synthetic scaffold production

Synthetic vascular nets were made via a multi-step process as illustrated by Figure 17. Firstly a thin layer of poly(3-hydroxybutyrate-co-3-hydroxyvalerate) (PHBV) was electrospun onto a flat metal sheet

collector. Alginate was then printed onto the electrospun sheet before spinning another layer of PHBV on top. Alginate was then removed using ethylenediaminetetraacetic acid (EDTA) solution. Each step is described below.

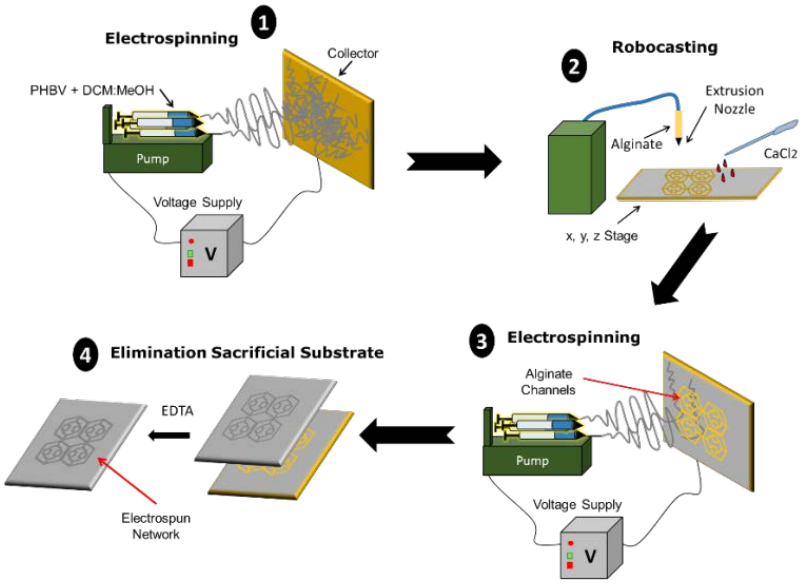


Figure 17 – Schematic showing the production of the synthetic vascular networks

### 2.15.1. Electrospinning PHBV

#### Preparation of solutions

*PHBV polymer solution*

Working in a fume hood, 3 g of PHBV pellets, 3 g methanol and 24 g of DCM were added to a clean 30 ml glass container. This mixture was magnetically stirred overnight to dissolve the bulk polymer.

#### Electrospinning PHBV

Once fully dissolved, 2.2 ml of the polymer solution was transferred into 4x5ml syringes with 0.6 mm ID blunt tip needles placed onto the ends. These were then placed onto a single syringe pump, set to deliver 40 µl/min per syringe. A flat metal sheet was placed onto a mandrel at a distance of 17 cm from the needle tip. A potential difference of 17 kV was applied to the needles using a high voltage power pack until all of the polymer had been electrospun.

### 2.15.2. Alginate printing

#### Preparation of solutions

*Alginate paste*

Alginate paste was produced by firstly adding 36.35 g of distilled water and 0.1 g of calcium chloride dihydrate to a glass beaker and stirring magnetically until dissolved. The solution was heated to approximately 60 °C before adding 0.75 g of alginic acid sodium salt from brown algae whilst constantly stirring. Finally, 12.125 g of glycerol was added and stirred until the alginic acid sodium salt was homogeneously distributed and resembled a smooth paste. To test the ultimate removal of alginate the paste was supplemented with 0.25 g of fluorescent Eosin Y.

#### Alginate printing

Once cool, the alginate paste was transferred into a 3 $cm^3$ syringe barrel with a 0.6 mm ID blunt dispensing tip attached. The syringe barrel was attached to a positive displacement dispensing system that controlled the extrusion rate of the alginate. A 3D printer was used to hold the positive displacement dispensing arm and thus print the alginate. The design to be printed was controlled through the use of custom built g-code software (Vascular Pattern Path Generator (VPPG)) where the geometry, feed rate of the printer and number of iterations could all be controlled. For each design a separate g-code file was produced with the given parameters and then loaded into the Pronterface software used to control the printer. The

flat metal sheet containing the electrospun layer was placed onto the RepRap stage and the blunt dispensing tip attached to the syringe barrel was positioned just above it. To print the design alginate was discharged from the syringe barrel by pressing down the foot pedal that controls the positive displacement dispensing system whilst simultaneously pressing the 'print' button on the Pronterface software. Previous work carried out by Adam Kelly had determined that the optimum extrusion rate of alginate was 0.025 $cm^3$/min and feed rate of the printer is 5000 mm/min and these values were used for all printed designs. Once the alginate design had been printed onto the electrospun mat, the electropinning process was repeated in order to cover the alginate with a further layer of electrospun PHBV.

### 2.15.3. Alginate removal

#### Preparation of solutions

*EDTA (0.5 M) solution*

EDTA (0.5 M) was prepared by adding 73.02 g of anhydrous acid free EDTA (MW 292.24) to 400 ml of distilled water and stirring continuously. The pH was adjusted to 8.0 by adding sodium hydroxide pellets (approximately 32.5 g) to ensure that the EDTA would dissolve. The final volume was then adjusted to 500 ml by adding distilled water.

#### Alginate removal

To remove the alginate and leave a hollow void between the two electrospun sheets, the vascular nets were removed from the flat sheet using a scalpel blade and placed into a 100 ml plastic tub and submerged in 0.5 M EDTA solution overnight on a see-saw rocker set to 70 oscillations/min.

## 2.16. Scanning electron microscopy (SEM)

### Preparation of solutions

*Ethanol solutions*

Graded ethanol solutions were prepared as indicated in Table 20.

Table 20 – Preparation of graded ethanol solutions for preparation of samples for SEM.

| Absolute ethanol (ml) | Distilled water (ml) | Final volume (ml) | Final concentration (%) |
|---|---|---|---|
| 9 | 1 | 10 | 90 |
| 8 | 2 | 10 | 80 |
| 6 | 4 | 10 | 60 |
| 3.5 | 6.5 | 10 | 35 |

*Ethanol/HMDS solution*

Ethanol and HMDS were combined in the ratio 1:1 to give 10 ml of solution.

### SEM – Samples with cells

To image samples containing cells the steps indicated in Table 21 were carried out.

Table 21 – Preparation of samples containing cells for SEM.

| Step | Solution | Immersion time (mins) |
|---|---|---|
| 1 | 2.5% gluteraldehyde | 60 mins |
| 2 | PBS | 15 |
| 3 | PBS | 15 |
| 4 | PBS | 15 |
| 5 | Distilled water | 5 |
| 6 | 35% ethanol | 15 |
| 7 | 60% ethanol | 15 |
| 8 | 80% ethanol | 15 |
| 9 | 90% ethanol | 15 |
| 10 | 100% ethanol | 15 |
| 11 | Ethanol/HMDS (1:1) | 60 |
| 12 | 100% HMDS | 5 |

Samples were then allowed to dry completely in air. Samples were then covered in a thin layer of gold coating using a sputter coater and imaged using a SEM with an accelerating voltage of 10 kV and a spot size of 3.

**SEM – Samples without cells**

Samples were covered in a thin layer of gold coating using an Emscope SC500 sputter coater and then imaged using an Inspect F SEM with an accelerating voltage of 10 kV and a spot size of 3.

## 2.17. Synthetic scaffold sterilisation

Prior to sterilisation each scaffold was cannulated with a 24 G cannula under a dissection microscope. Scaffolds were then transferred to a petri dish and sterilised by submerging in 30 ml of 70% ethanol for 45 minutes. Scaffolds were then washed 3 times with sterile PBS.

## 2.18. Mechanical testing

Tensile mechanical testing was conducted for the synthetic scaffolds using a uniaxial load test machine fitted with a 4.5 N load cell. To test the bulk material the dimensions of strips of scaffold sheets were measured using a pair of digital callipers before being fixed to the clamps of the machine positioned 10 mm apart. Each sample was then pulled at a rate of 0.1 mm per minute and elongated to failure (n = 4). Data of the force and extension were logged before being converted into stress-strain curves using the following equations:

$$Stress = \frac{Force}{Area}$$

$$Strain = \frac{Extension}{Original\ length}$$

The following parameters were calculated using the stress-strain curve (as indicated in Figure 18):

1. ***Ultimate tensile stress*** (UTS) – this is the maximum stress that a material can withstand prior to failure and is the maximum stress on the stress vs. strain curve.
2. ***Yield stress*** – this is the point at which a material deforms plastically i.e. it will not return to its original shape.
3. ***Young's modulus*** – this is a measure of the stiffness of a material and is the gradient of the stress vs. strain curve within the elastic region.
4. ***Ultimate strain*** – this is the strain measured at the point of failure.

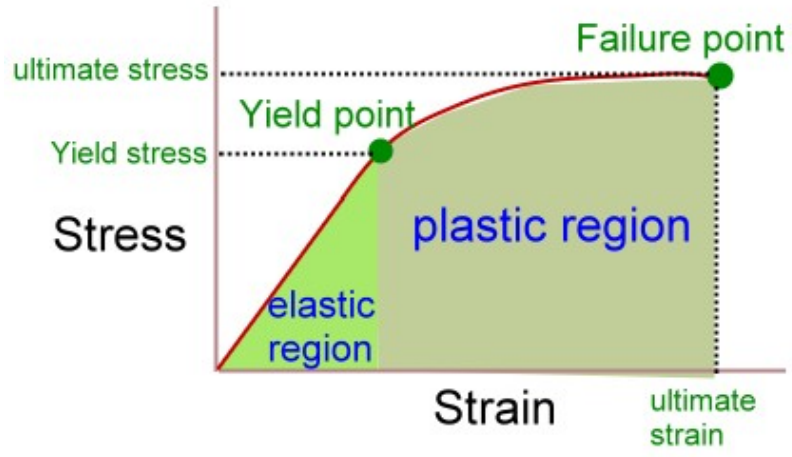


Figure 18 – Stress vs strain curve showing relevant parameters

To obtain the suture retention strength both ends of the scaffold sheet were sutured 3 mm from the end of the sample before being clamped in place within the uniaxial load test machine (as shown in Figure 19). The distance between the clamps was measured and each sample was then pulled at a rate of 0.1 mm per minute and elongated to failure (n = 6). Suture retention strength was calculated as the following equation:

$$Suture\ retention\ strength = \frac{Load}{Suture\ diameter\ x\ material\ thickness}$$

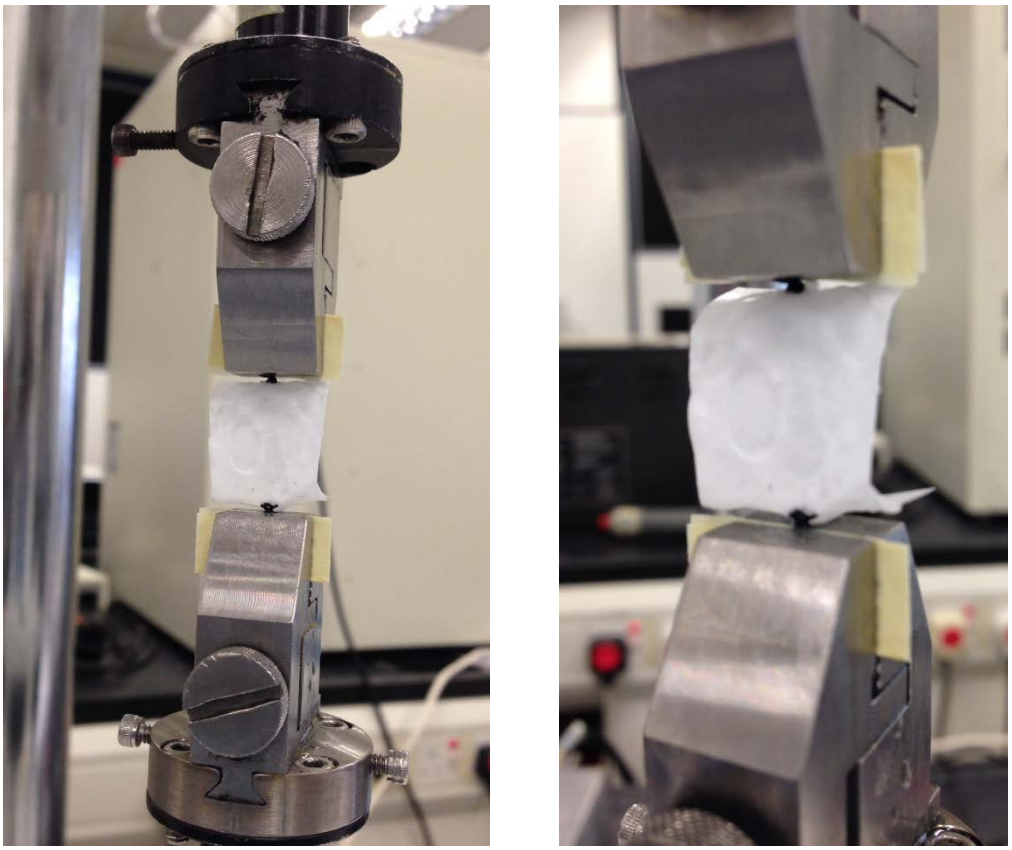

Figure 19 – Images showing the placement of scaffolds in the tensile test machine for determination of the suture retention strength

## 2.19. Synthetic scaffold recellularisation

*HDMECs only*

To endothelialise the synthetic vascular channels HDMECs were perfused into the scaffolds. A sterile synthetic scaffold was placed into a sterile petri dish in a class II biological safety cabinet. HDMECs were passaged and counted as described in section 2.6.1 and 2.6.2. $0.5 \times 10^6$ cells were resuspended in 1 ml of HDMEC growth medium and then perfused through the synthetic net using a 1 ml syringe. This was incubated at 37 °C in a 5% $CO_2$ atmosphere overnight (Figure 20). The following day the synthetic scaffold was flipped over and the same process was repeated.

*HDMECs and HDFs inside vascular channels*

A sterile synthetic scaffold was placed into a sterile petri dish in a class II biological safety cabinet. HDMECs were passaged and counted as described in section 2.6.1 and 2.6.2. $0.5 \times 10^6$ cells were resuspended in 1ml of HDMEC growth medium and perfused through the synthetic net using a 1ml syringe. This was incubated for at least 3 hours at 37 °C in a 5% $CO_2$ atmosphere. HDFs were then passaged and counted as described in section 2.6.1. 0.5 x $10^6$ HDFs were resuspended in 1 ml of HDMEC growth medium and perfused through the synthetic net. This was incubated at 37 °C in a 5% $CO_2$ atmosphere overnight (Figure 21). The following day the synthetic scaffold was flipped over and the same process was repeated.

*HDMECs inside vascular channels and HDFs on outer surface of scaffold*

A sterile synthetic net was placed into a sterile petri dish in a class II biological safety cabinet. HDMECs were passaged and counted as described in section 2.6.1 and 2.6.2. $0.5 \times 10^6$ cells were resuspended in 1 ml of HDMEC growth medium and perfused through the synthetic net using a 1 ml syringe. This was submerged in HDMEC medium and incubated at 37 °C in a 5% $CO_2$ atmosphere. HDFs were then passaged and counted as described in section 2.6.1. The scaffold was removed from the incubator and placed in a sterile petri dish. 0.5 x $10^6$ HDFs were resuspended in 200 µl of HDMEC growth medium and pipetted over the outer surface of the scaffold. This was then returned to the incubator for up to 2 hours to allow the HDFs to attach to the surface. The scaffold was then submerged in HDMEC growth medium and incubated overnight (Figure 22). The following day the synthetic scaffold was flipped over and the same process was repeated.

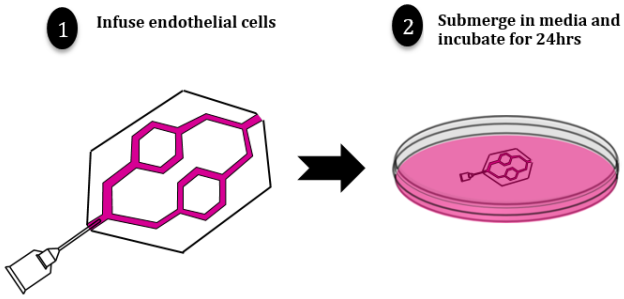


Figure 20 – Schematic showing the steps taken to recellularise the synthetic scaffolds with HDMECs only

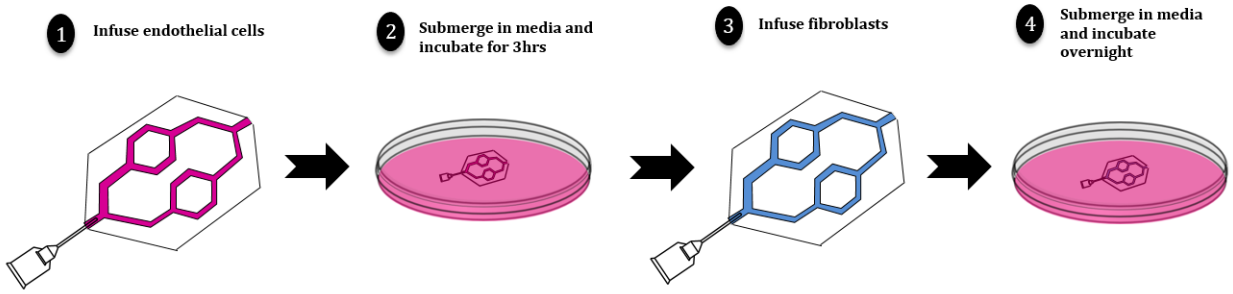


Figure 21 – Schematic showing the steps taken to recellularise the synthetic scaffolds with HDMECs and HDFs within the channels

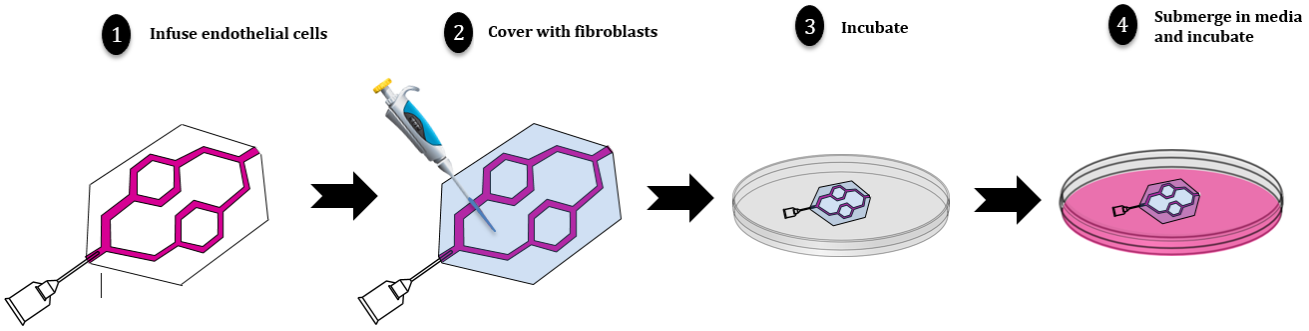


Figure 22 - Schematic showing the steps taken to recellularise the synthetic scaffolds with HDMECs within the channels and HDFs on the outer surface of the scaffolds

## 2.20. Production of synthetic angiogenesis model

Synthetic angiogenesis models consisted of the recellularised synthetic scaffolds combined with VEGF loaded collagen gels. The aim of the models was to observe the outgrowth of ECs into gels.

Recellularised synthetic scaffolds were incubated for 7 days and then placed in a sterile petri dish in a class II biological safety cabinet. Using the sterile needle from a 24 G cannula, holes were pierced in the channels of the synthetic scaffolds. Collagen was then prepared as described in section 2.12 and 100 µl was pipetted into each hexagonal well formed by the channels. The gels were allowed to set in a 37 °C incubator for 15 min. The scaffolds were then re-submerged in HDMEC growth medium (Figure 23) and cultured for 7 days.

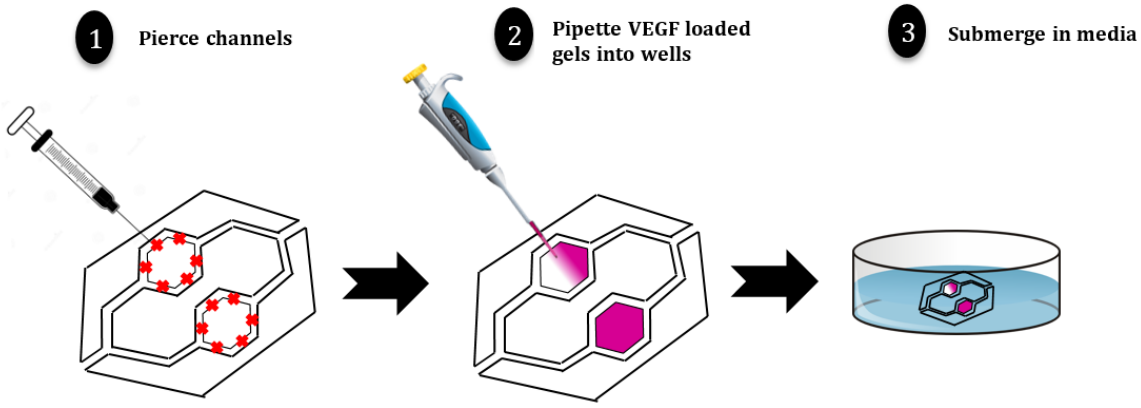


Figure 23 – Schematic showing the production of the angiogenesis model using the synthetic pseudo-vascular networks.

## 2.21. Immunohistochemistry

**Preparation of solutions**

*BSA*

To prepare the blocking serum 0.75 g of BSA was measured and dissolved completely in 10 ml of PBS to give a final concentration of 7.5% (w/v).

Similarly 1% (w/v) BSA was produced by dissolving 0.1 g of BSA in 10 ml of PBS.

*Primary antibodies*

| Antigen | Host | Dilution |
|---|---|---|
| Fibronectin | Rabbit | 1:1500 |
| Laminin | Rabbit | 1:100 |
| CD31 | Mouse | 1:20 |
| CD144 | Mouse | 1:50 |
| αSMA | Rabbit | 1:200 |
| DLL4 | Rabbit | 1:200 |
| Collagen IV | Goat | 1:100 |

*Secondary antibodies*

All secondary antibodies were diluted in the ratio 1:500 in 1% BSA.

*Triton-X 100*

Triton-X 100 was prepared to a final concentration of 0.1% (v/v) in PBS by dissolving 10 µl in 10 ml of PBS.

*PFA (4%)*

20 g of PFA was added to 500 ml of HBSS containing calcium and magnesium (in a fumehood). The solution was then heated to 60 °C

before adding 1 M sodium hydroxide solution drop-wise until the PFA had gone into solution. This was then cooled to room temperature before use.

*BSA/Tween® 20 solution*

100µl of Tween®20 was pipetted into 10 ml 1% (v/v) BSA to produce a 1% BSA/1% Tween® 20 (v/v).

10µl of Tween®20 was pipetted into 10 ml 1% (v/v) BSA to produce a 1% BSA/0.1% Tween® 20 (v/v).

*Glycine (100mM) solution*

0.75 g of glycine was dissolved to 100 ml of PBS to give a 100 mM solution.

**Immunohistochemistry (slides)**

Slides were prepared as described in section 2.4.2. They were then placed into a holder and were processed using the steps outlined in Table 22 below.

Table 22 – Outline of immunohistochemistry steps.

| Step | Process | Solution | Immersion time (mins) |
|---|---|---|---|
| 1 | Dewaxing | Xylene | 3 |
| 2 | Dewaxing | Xylene | 3 |
| 3 | Re-hydration | 100% IMS | 1 |
| 4 | Re-hydration | 70% IMS | 0.5 |
| 5 | Re-hydration | Distilled water | 1 |

A PAP pen was used to draw circles around each sample on the slide, forming a water repellent barrier that enabled staining reagents to remain localised on the tissue sections. Cells were then permeabilised by submerging in 0.1% Triton-X 100 for 20 minutes. Samples were incubated

in 7.5% BSA at room temperature for 1 hour, followed by washing once with 1% BSA. Samples were incubated with the appropriate primary antibodies diluted in 1% BSA at 4 °C overnight. Samples were washed 3 times in PBS before incubating with the appropriate secondary antibodies diluted in 1% BSA at RT for 1 hour and washing a further 3 times with PBS. Samples were counterstained with DAPI solution by incubating at RT for 20 minutes and washing a further three times with PBS. Slides were imaged using a confocal microscope.

### Immunohistochemistry (3D cultures)

Many of the synthetic and bioscaffold samples were immunostained intact (i.e. without processing and producing slides) since many structures and cell distribution patterns are not readily appreciated in 2D. Samples were fixed in 4% PFA for 20 minutes at RT. Samples were then quenched with 100 mM glycine, followed by one wash with PBS, and were then blocked for 1 hour with 1% BSA at RT. Primary antibodies were added at the appropriate dilutions in 1% BSA and incubated at RT overnight. The samples were subsequently washed for 2 hours in 1% BSA/0.1% Tween® 20 (v/v), followed by incubation with the appropriate secondary antibodies for 2 hours at RT. Once the secondary antibody had been added all subsequent processes were carried out in the dark (by covering in aluminium foil). Finally the samples were washed again with 1% BSA/1% Tween20 for at least 8 hours with hourly changes of the BSA/Tween20 solution, after which the samples were stored in PBS at 4 °C in the dark before imaging using a confocal microscope.

## 2.22. FITC-lectin perfusion

### Preparation of solutions

*FITC-lectin solution*

FITC conjugated lectin from Lycopersicon esculentum was diluted in HBSS with calcium and magnesium in the ratio 1:20 under sterile conditions.

**FITC-lectin perfusion**

Lectins are proteins that have been found to specifically bind to sugar complexes attached to lipids and proteins [178,179] and have been found to be extremely useful for microvascular labelling [180–182]. When conjugated with a fluorescent dye (FITC), any lectin that binds to the vascular endothelium can be visualised using fluorescence microscopy. To visualise potential vessel formation in the synthetic angiogenesis model, the scaffolds were perfused with 100 µl of FITC-lectin solution at a rate of 40 µl/min, controlled using a syringe pump. The scaffolds were then fixed in 4% PFA in HBSS with $Ca^{2+}$ and $Mg^{2+}$ for 30 minutes and subsequently immunostained for CD31 as described above.

## 2.23. Statistical analysis

Statistics were performed using an unpaired Student's t-test. The significance of the results are denoted by a * symbol (* $p < 0.05$, **** $p < 0.0001$).

# Chapter 3

# Use of natural vasculature to study angiogenesis

## 3.1. Aims and objectives

The aim of this chapter is to develop a naturally derived *in vitro* model for studying angiogenesis by:

1. Producing vascular networks via decellularising animal tissue to retain the ECM components and vascular architecture.

2. Designing a bioreactor for perfusion of these vascular networks.

3. Investigating the optimal cell combinations to functionalise the vascular networks and recellularise these networks.

4. Investigate the effects of pro-angiogenic stimuli on angiogenic sprouting.

## 3.2. Introduction

Vascularisation plays a vital role in the survival of TE constructs. Several groups have investigated different methods to overcome the issue of constructs failing because of slow neovascularisation but as yet none have succeeded in developing an adaptable solution. Although it is recognised that:

- Perfusion conditions
- The cell type
- Scaffold architecture

are all important with respect to vascularisation strategies many of the studies used fail to consider them in combination. It is therefore important to take a step back and understand how these factors work together to promote angiogenesis in order to advance this crucial area. This lack of understanding may be due to the deficiencies of current angiogenesis models which in turn fail to combine:

- Supporting cells
- An ECM and/or basement membrane and
- Perfusion in 3D

Recently, in an attempt to vascularise TE constructs *in vitro* for subsequent translation to the clinic, Schultheiss *et al.* developed a perfusable 3D vascular net by decellularising porcine jejunum [151]. Not only can this construct be recellularised with porcine peripheral blood EPCs but it is also composed of predominantly ECM components and can be perfused through the arterial and venous pedicles. This technique therefore offers real potential for use as a model to investigate angiogenesis *in vitro*.

In this chapter an angiogenesis model derived from a decellularised rat jejunum is presented. It is characterised to determine the ECM components present after decellularisation prior to recellularising with a combination of HDMECs and HDFs. A custom built bioreactor is then used to perfuse the vascular network to establish the effects of perfusion on re-endothelialisation. A VEGF loaded gel is then placed onto the scaffold to observe the effects of this pro-angiogenic stimulator.

## 3.3. Results

### 3.3.1. Decellularisation

To decellularise the jejunum the vasculature was used as a transport network to continuously perfuse the non-ionic detergent solution containing Triton-X 100 and ammonium hydroxide for ~16 hours. Macroscopically, decellularisation appeared to have occurred since the intestine turned increasingly translucent compared to its intact counterpart as indicated in Figure 24 (A&B). Histological staining was carried out to characterise the microscopic composition of the intact and decellularised jejunum. H&E staining (Figure 24 (C&D)) showed that the process removed almost all cells since there is little to no basophilic staining typical of nuclear material. It also showed the retention of the pink eosinophilic staining associated with collagen suggesting that this is retained post decellularisation.

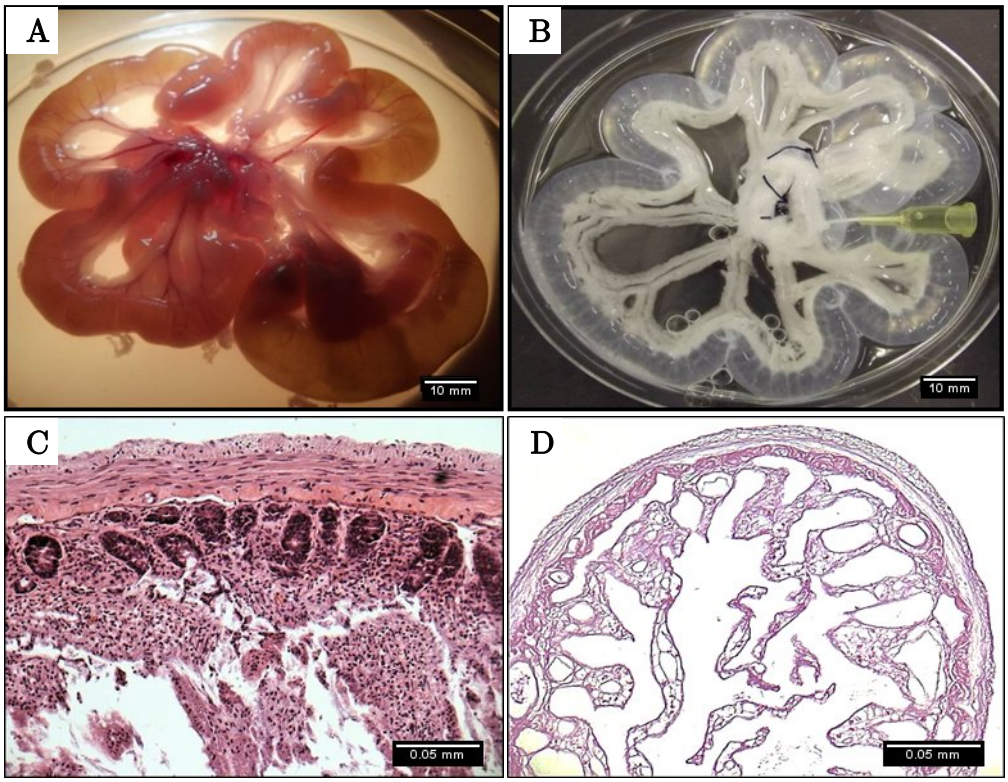


Figure 24 - Macroscopic view of intact jejunum (A) and translucent decellularised jejunum after treatment with detergent (B). H&E staining of the intact jejunum shows the presence of cells (C) but the almost complete removal of cells post decellularisation (D).

### 3.3.2. Bioscaffold characterisation

Once decellularised, it was important to characterise the jejunum in order to determine whether this would be a suitable biomaterial to use as a potential vascular network for subsequent use as an angiogenesis model. Key questions to answer included:

1. Are the decellularised vessels patent?
2. What are the components of the ECM and how do these compare to the fresh jejunum?
3. Is the resultant biomaterial cytotoxic?
4. Is the bioscaffold inherently angiogenic?

This section outlines the key findings to the questions listed above.

#### 3.3.2.1 Vascular patency

The vessels of the decellularised jejunum were easily seen macroscopically (greater than ˜300 μm) by placing the sample above a light source (Figure 25A). To test the patency of the vessels blue dye was injected into the scaffold, highlighting the intact vascular structures (Figure 25B). To further confirm vascular patency, FITC-Dextran (250 kDa) containing solution was injected via the SMA and viewed using a confocal microscope. Fine branching of the vasculature was observed (Figure 25C) however after ~5-10 minutes the fluorescent dye had leaked into the tissue parenchyma.

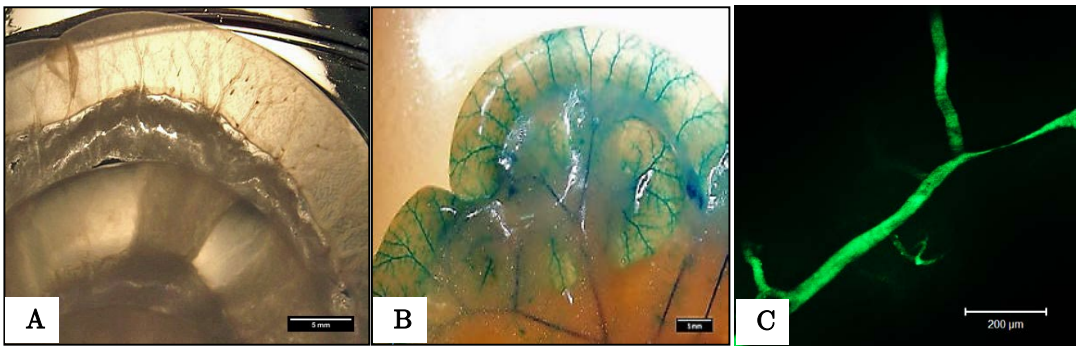


Figure 25 – Macrocopic view of the vessels of the decellularised jejunum placed over a light source (A) and via the injection of blue dye (B). FITC-Dextran injection shows microscopic patency (C).

#### 3.3.2.2 DNA content

To investigate whether nuclear material had been retained after decellularisation, DAPI staining was carried out. Figure 26A shows the presence of DNA in the intact jejunum section but very little in the decellularised section (Figure 26B). Quantification of DNA (n=3) found that ~97% of DNA is removed after the decellularisation process, illustrating its efficacy (Figure 26C).

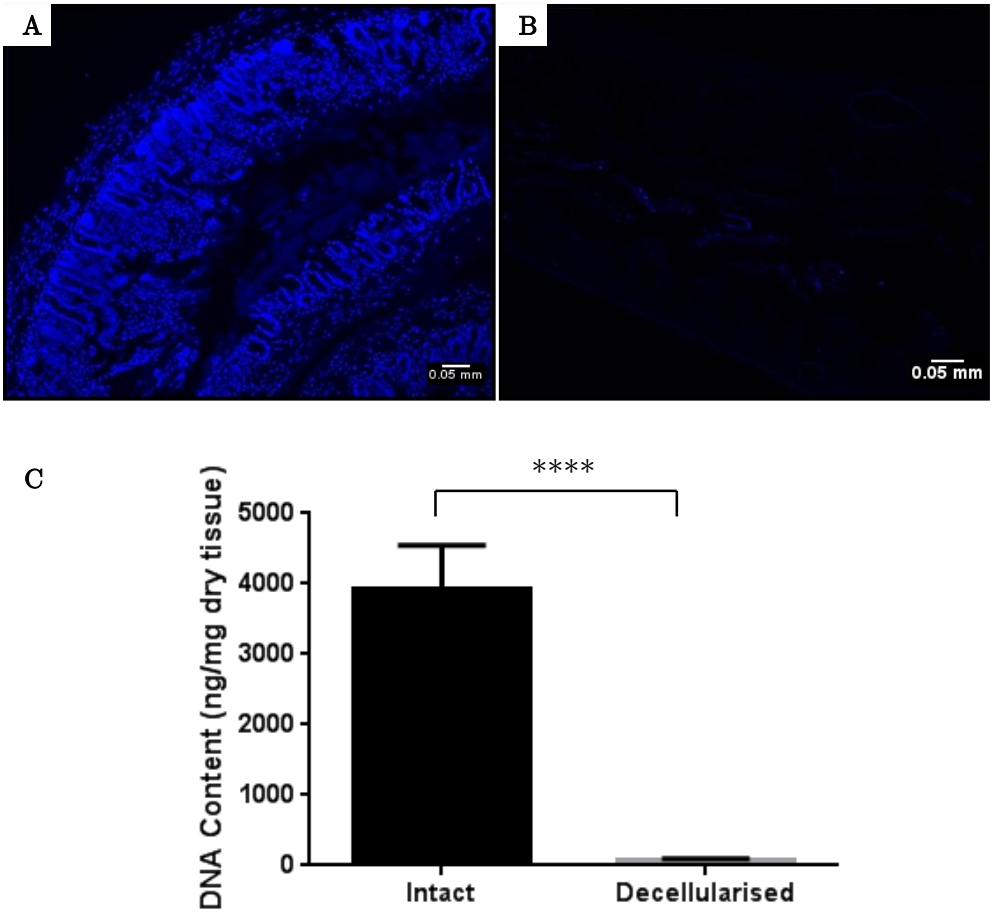


Figure 26 – DAPI staining of intact jejunum (A) and decellularised jejunum (B). Quantitative analysis of the DNA content shows a 97% reduction post decellularisation n=3 ($P < 0.0001$) (C).

#### 3.3.2.3 Collagen content

Collagen content was investigated by firstly staining with Picosirius red and imaging the samples using bright field microscopy. Using this method collagen is stained red and appears to be retained when comparing the intact (Figure 27A) and decellularised (Figure 27B) jejunum. When examined under circularly polarised light, larger collagen fibres tend to appear bright orange or red whilst smaller reticular fibres appear green in colour [183,184]. From Figure 27 (C&D) it can be seen that the majority of fibres appear to be bright orange/red indicating the presence and retention of larger collagen fibres after decellularisation. Quantification of collagen (n=3) measured per mg of dry tissue mass indicates a 30% increase in its proportion of the total mass of tissue after decellularisation

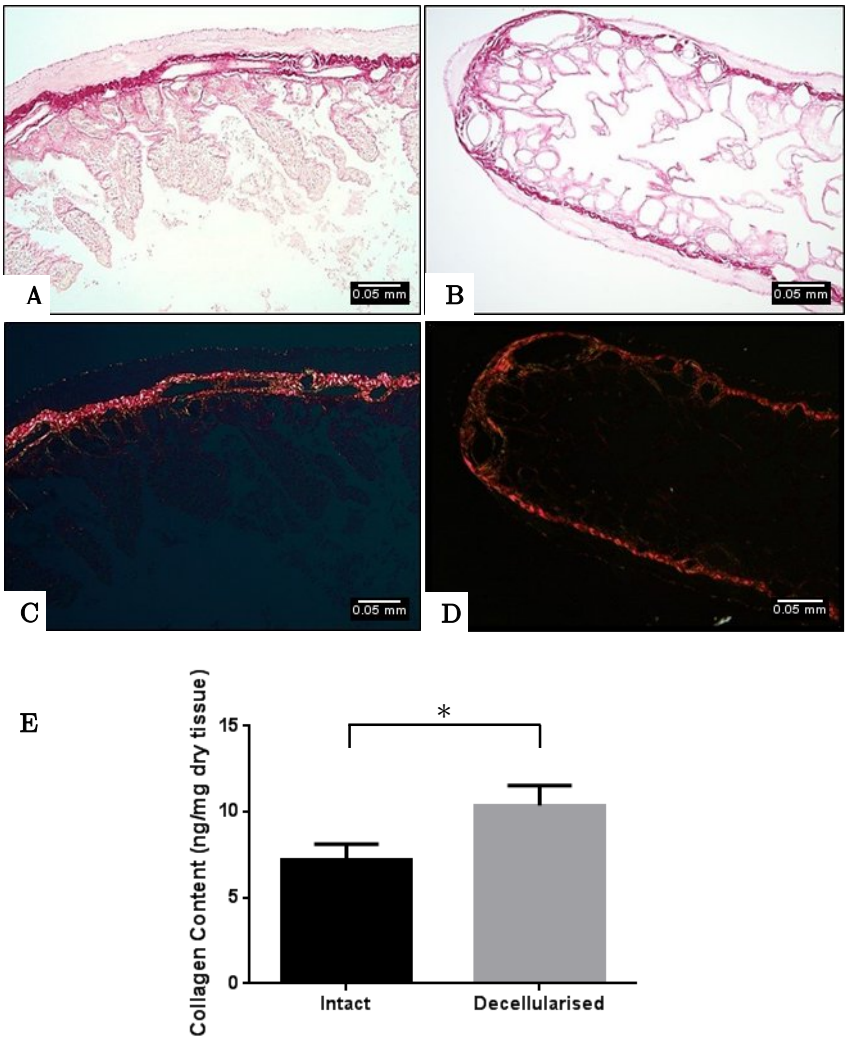


Figure 27 – Bright field microscopy images of Pico-Sirius red staining of intact (A) and decellularised jejunum (B). Circularly polarised light microscopy images of intact (C) and decellularised jejunum (D) showing larger collagen fibers (bright orange/red) and smaller reticular fibers (green). Quantification of collagen content shows a 30% increase post decellularisation n=3 ($P < 0.05$) (E).

(Figure 27E) and may be explained by the removal of other components such as cellular proteins.

#### 3.3.2.4 GAG content

Alcian blue staining of the fresh and decellularised jejunum (Figure 28 (A&B)) shows little difference in terms of colouration. Further analysis via GAG quantification (n=3) showed that there was no significant difference in GAG content before and after the decellularisation process (Figure 28C).

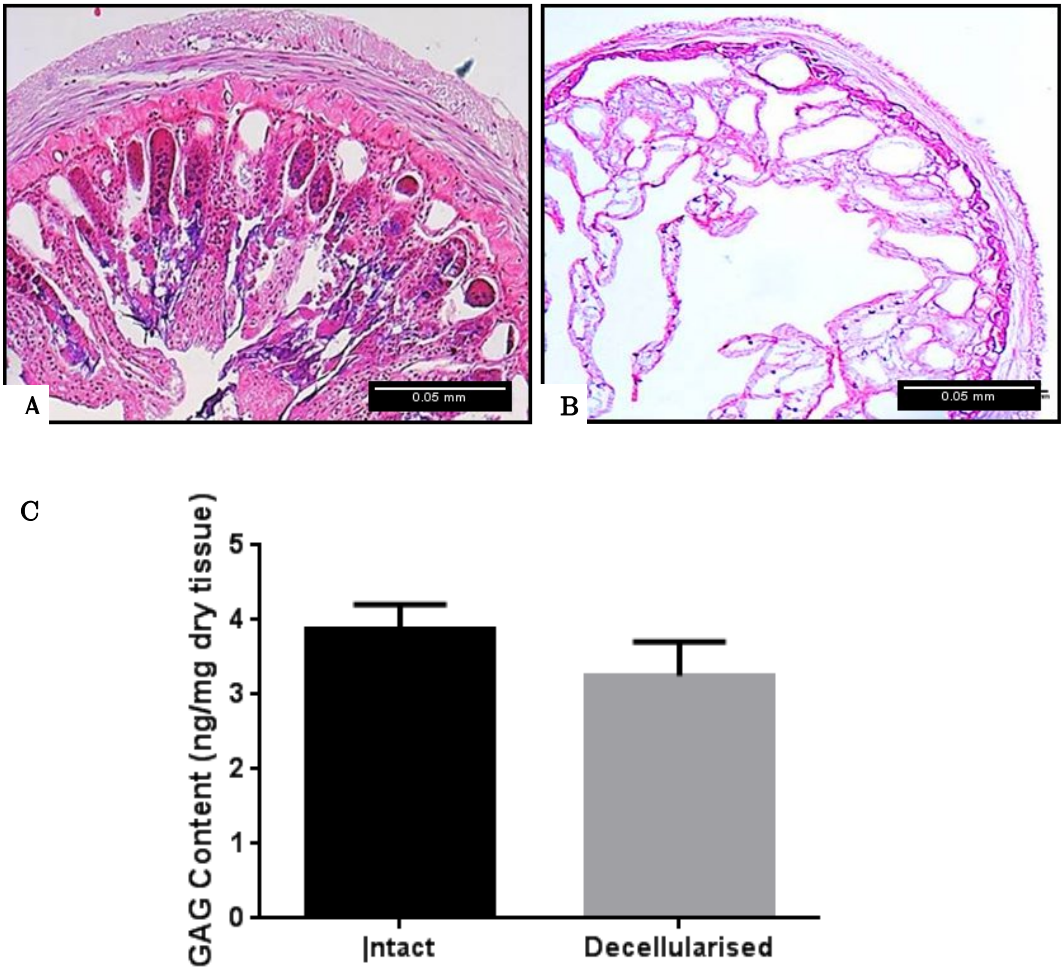


Figure 28 – Alcian blue staining for GAGs shows little difference in colouration between the intact (A) and decellularised jejunum (B). Quantification confirms that there is no significant difference between GAG content before or after decellularisation n=3 (C).

#### 3.3.2.5 Elastin content

The Accustain elastic staining protocol was carried out on both intact and decellularised jejunum sections. The presence of elastic fibres is indicated by the presence of a blue black to black colour, collagen by a red colour and muscle or other tissue elements by a yellow colour. Figure 29 shows the complete removal of any blue black to black staining and hence elastic fibres after decellularisation but does show the retention of collagen confirming previous results. As a result of this staining, quantification of elastin was deemed unnecessary. Elastin content is important in larger vessels that require elastic recoil but less important in smaller vessels such as capillaries which consist of only the tunica intima [1]. Since this study aims to induce angiogenic sprouting from microvasculature, the loss of elastin was not deemed a significant enough reason to optimise the decellularisation protocol in an attempt to retain this protein.

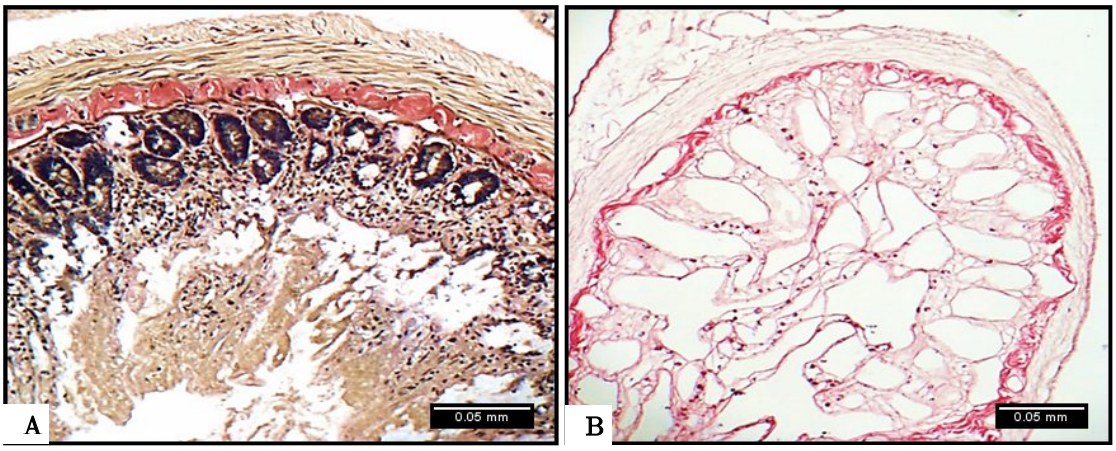


Figure 29 – Elastic staining of the intact (A) and decellularised (B) jejunum shows almost complete removal of any elastic fibers indicated by the blue/black to black colour. Collagen fibers are shown in red confirming the retention of collagen post decellularisation.

#### 3.3.2.6 Laminin and Fibronectin content

Immunostaining for the ECM proteins laminin and fibronectin was undertaken for sections of intact and decellularised jejunum. Figure 30A

and Figure 30B show sections of intact and decellularised jejunum immunostained for laminin (red) and counterstained with the nuclear stain DAPI (blue), respectively. These images show that laminin is preserved after the decellularisation process whilst removing the majority of the nuclear material. Immunostaining for fibronectin on sections of both intact (Figure 30C) and decellularised (Figure 30D) jejunum shows the almost complete removal of the protein and nuclear material after the decellularisation process.

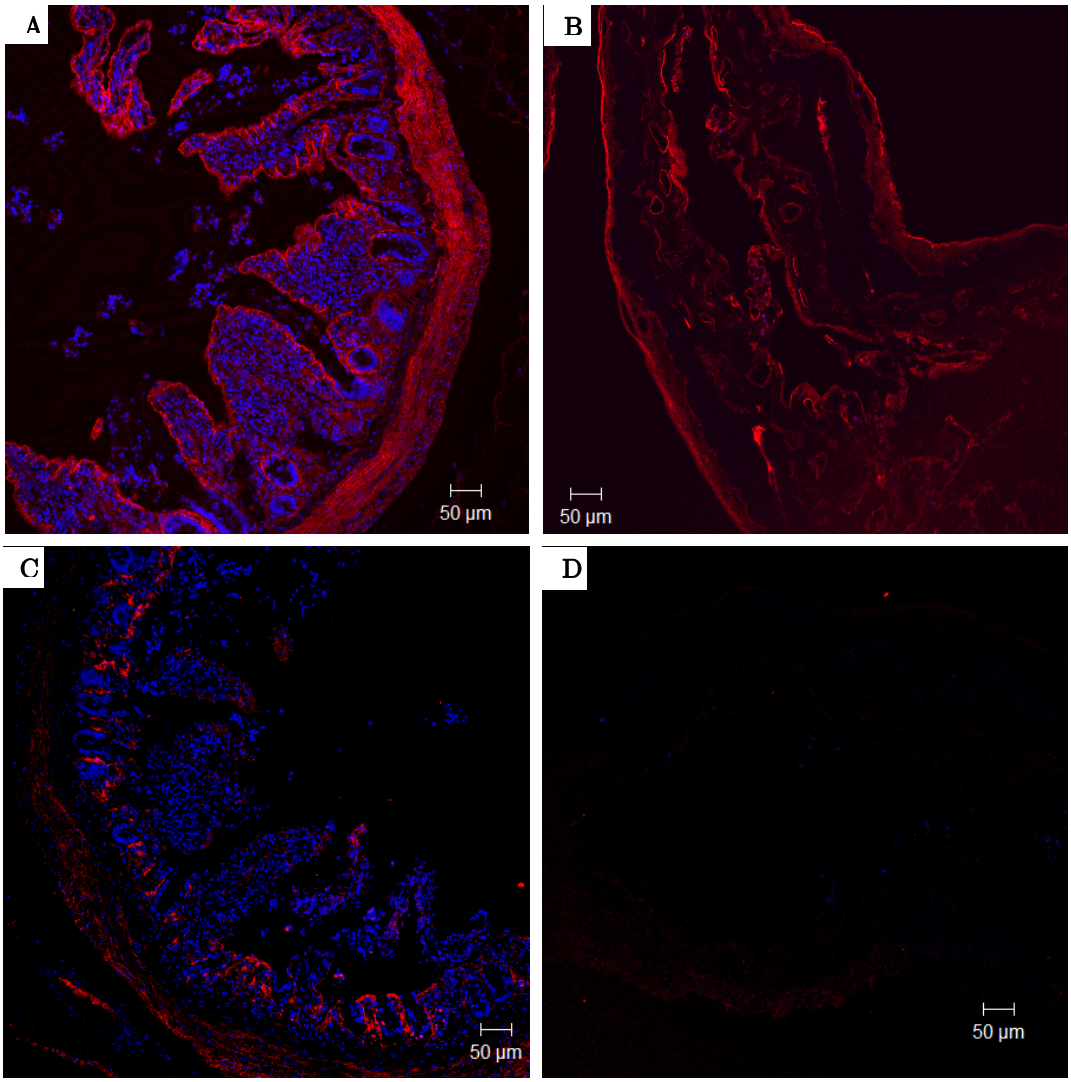


Figure 30 – Immunostaining for laminin (red) on intact (A) and decellularised (B) sections of jejunum shows the retention of the ECM protein post decellularisation. Immunostaining for fibronectin (red) on intact (C) and decellularised (D) sections of jejunum shows the complete removal of the protein post decellularisation. Counterstaining with DAPI (blue) shows the almost complete removal of nuclear material post decellularisation in both instances.

#### 3.3.2.7 Cytotoxicity

To determine whether the decellularised jejunum would be cytotoxic to cells, rat Schwann cells (derived from the RN22 cell line) and HDFs were cultured in the presence of decellularised jejunum segments and then stained using the Giemsa stain. Rat tail collagen type I was used as a negative control since it is well know that cells will grow in its presence

[185,186] whilst cyanoacrylate glue was used as a positive control due to its potent cytotoxic nature [187,188]. Figure 31 (A-E) and Figure 32 (A-E) shows macroscopically that both cell types grow up to and around the decellularised jejunal segments and the collagen type I gels, whilst almost all cells died in the presence of cyanoacrylate (Figure 31F and Figure 32F). This is confirmed microscopically as shown in Figure 33. This illustrated that the decellularised jejunum is not cytotoxic to cells. This assay could have also been used to determine the quantitative viability of cells in the presence of the jejunum samples and would have given more definitive results but as a crude assay to determine cytotoxicity, this assay was deemed sufficient.

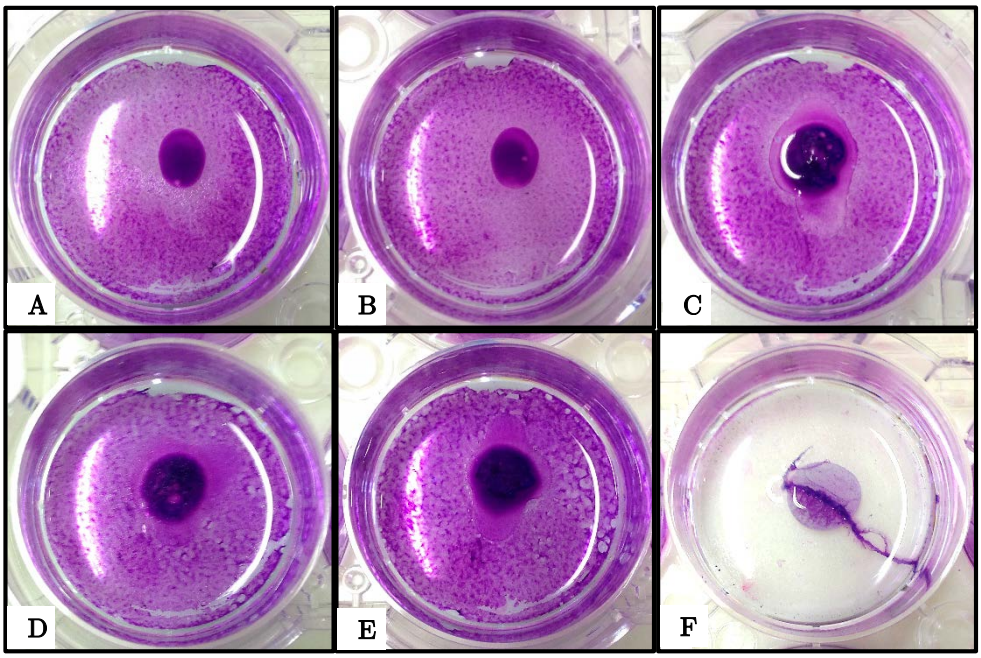


Figure 31 – HDF cytotoxicity tests using Giemsa staining. HDFs were cultured in the presence of type I rat tail collagen as a negative control (A-B) and decellularised jejunum (C-E) and show growth up to and in contact with the biomaterials. HDFs cultured in the presence of cyanoacrylate glue did not survive due to its cytotoxic nature (F).

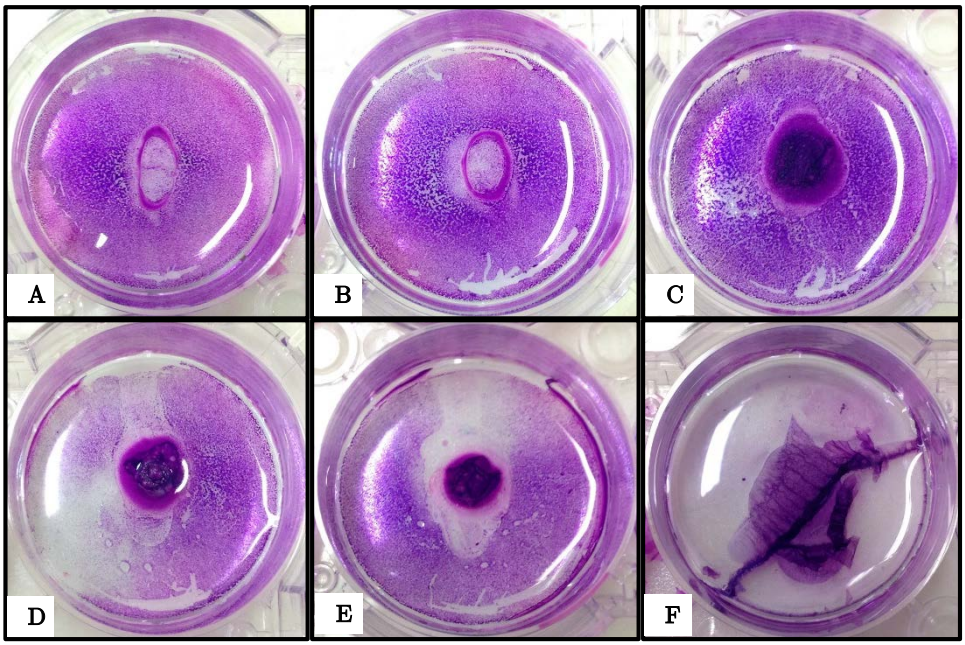


Figure 32 – RN22 cytotoxicity tests using Giemsa staining. RN22 cells were cultured in the presence of type I rat tail collagen as a negative control (A-B) and decellularised jejunum (C-E) and show growth up to and in contact with the biomaterials. RN22 cells cultured in the presence of cyanoacrylate glue did not survive due to its cytotoxic nature (F).

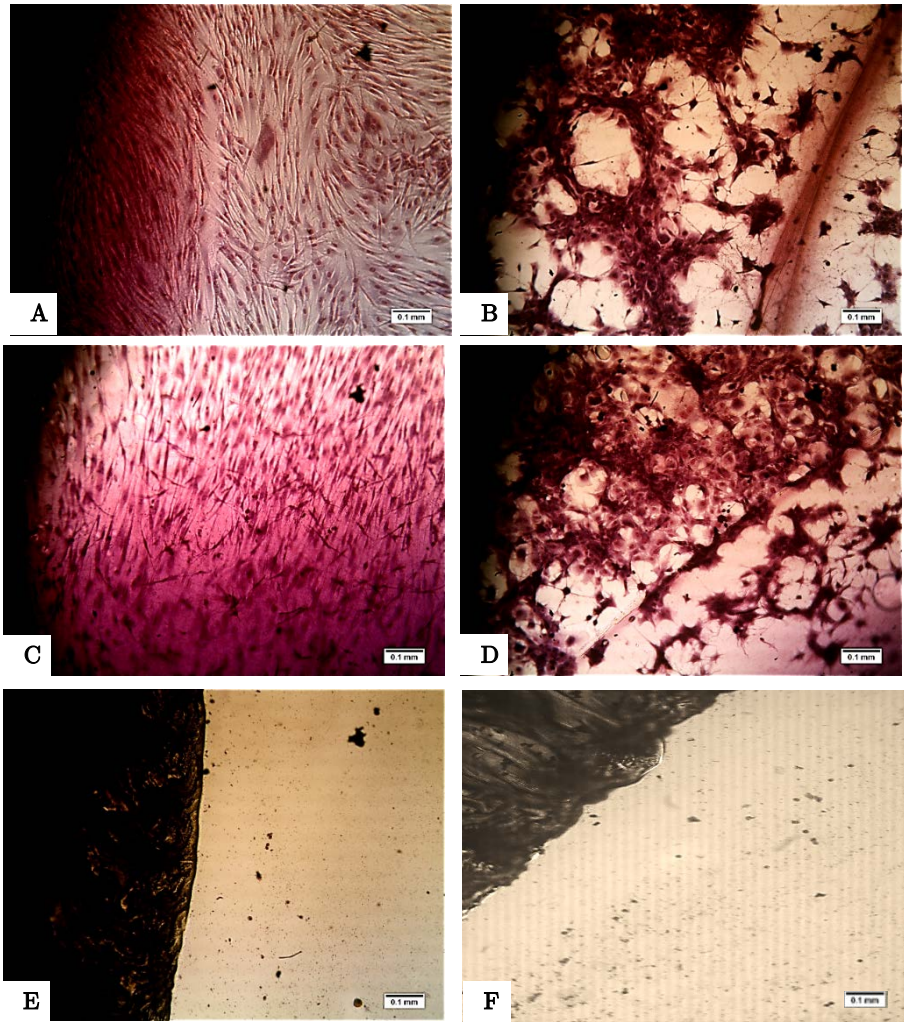


Figure 33 – Light microscopy images of HDF and RN22 cell cytotoxicity tests using Giemsa stain. HDFs and RN22 cells cultured in the presence of type I rat tail collagen as a negative control (A&B respectively) and decellularised jejunum (C&D respectively) show growth up to and in contact with the biomaterials. HDFs and RN22 cells cultured in the presence of cyanoacrylate glue did not survive due to its cytotoxic nature (E&F respectively).

#### 3.3.2.8 Angiogenic potential

To assess the inherent angiogenic properties of the decellularised scaffold via the presence of growth factors, the CAM assay was used. Sections of decellularised intestine were placed onto chick membranes along with negative collagen gel controls at seven days post fertilisation and incubated in place for a further 7 days. Samples were then exposed by removing the surrounding egg shell and imaged using a digital microscope. A 15mm diameter circle was then drawn around each sample and vessels crossing the circle were counted as indicated in Figure 34. If vessels entered and exited the circle without branching they were counted only once (Figure 34 (left)). However if vessels entered the circle and then branched before exiting, they were counted as separate vessels (Figure 34 (right)). Only vessels of approximately 50μm in diameter (Figure 35) or greater were counted. Figure 36(A,C,E) and Figure 36(B,D,F) show representative images of blood vessel development around and towards the decellularised jejunum sections and negative collagen gel control, respectively. Macroscopic quantification (n=3) measured blindly by assessors showed a significant increase ($P < 0.0001$) in the number of vessels growing towards the decellularised intestine sections compared to the collagen gel control (Figure 36G). This suggests that the decellularised scaffold has a certain degree of angiogenic capability. However caution should be taken when interpreting results from the CAM assay since chemical or physical irritation of the membrane can induce angiogenesis, disrupting identification of the response from the test substance, as discussed in section 1.4.3 [97,123]. Staining sections of the samples using the Masson-Goldner trichrome stain showed that blood vessels infiltrated the decellularised scaffolds as indicated by the black arrows (Figure 37(A-B)). Red blood cells are highlighted by the orange/red colour whilst the collagen component of the ECM is shown by the green/blue colour. Staining of the collagen gel controls (Figure 37(C-D)) showed a lack of cellular and blood vessel infiltration. This further indicates the angiogenic nature of the decellularised intestinal scaffolds. It would be interesting to identify and quantify the growth factors that may be present within the scaffolds. To do so a commercial multiplex angiogenesis ELISA could be used.

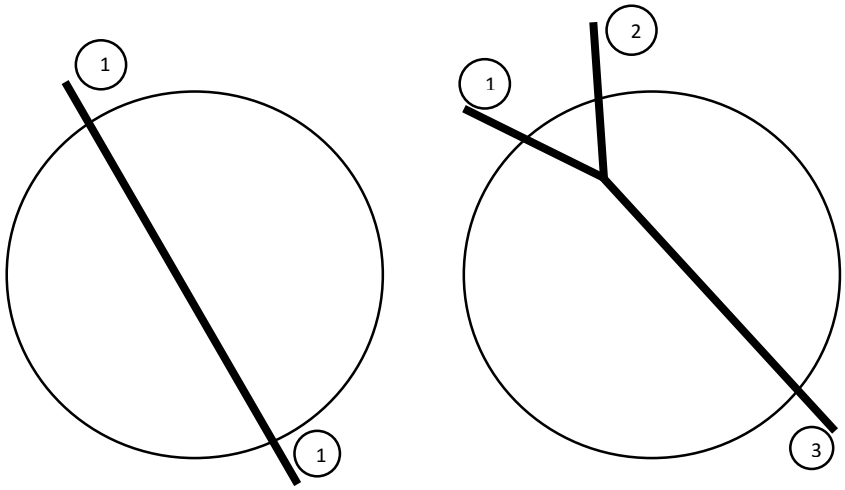


Figure 34 – Schematic illustrating how the blood vessels were counted for each sample. If vessels entered and exited the circle without branching they were counted only once (left). However if vessels entered the circle and then branched before exiting, they were counted as separate vessels (right).

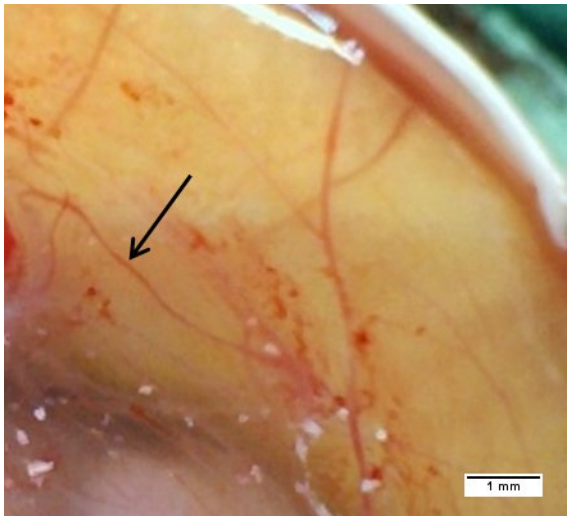


Figure 35 – CAM assay image showing representative minimum vessel size. Only vessels of approximately 50 μm or above (arrow) were counted.

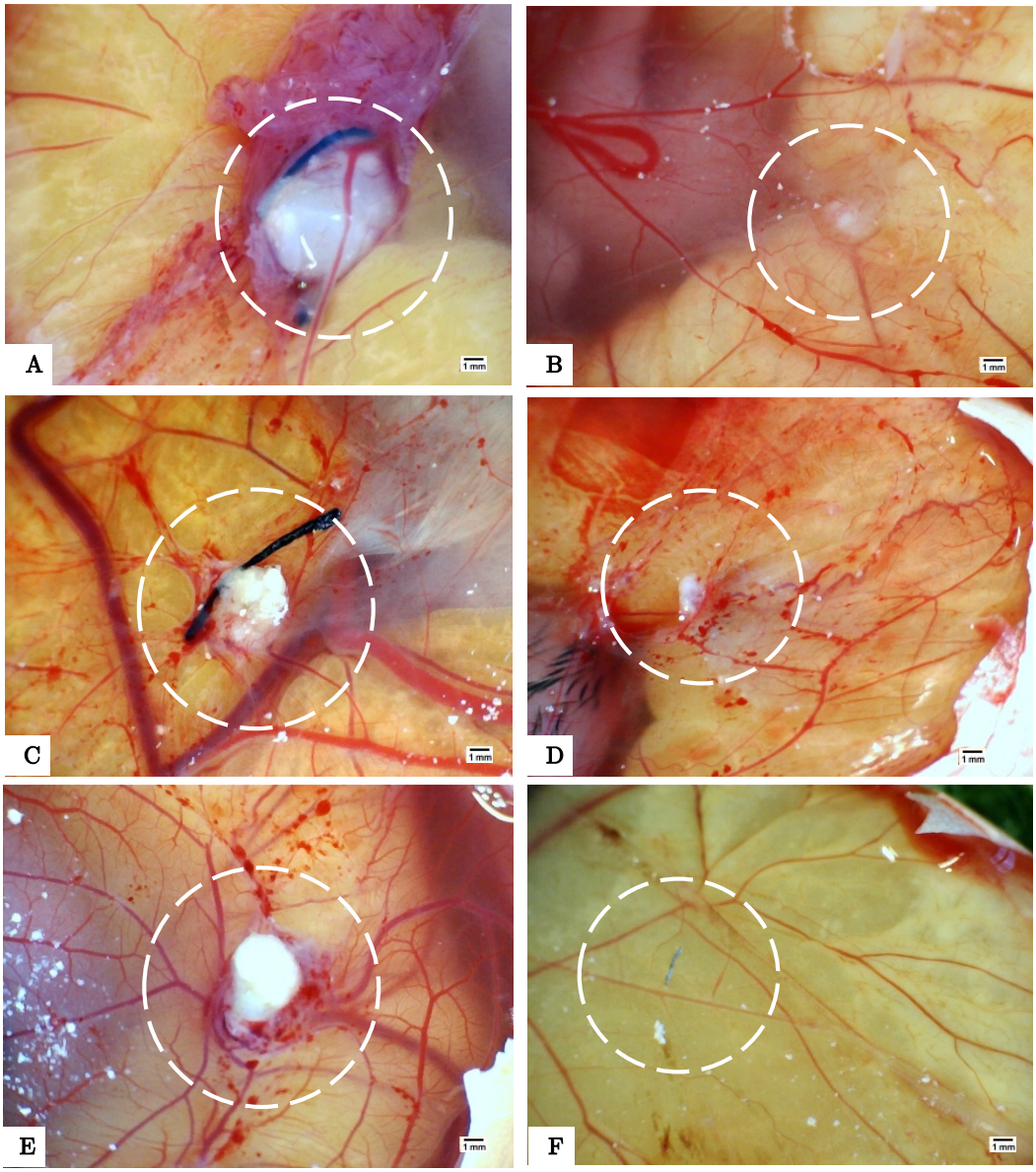


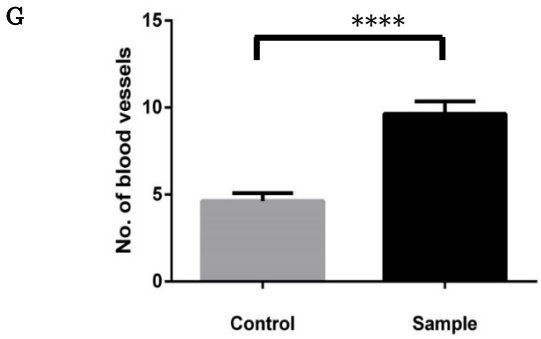


Figure 36 – Representative CAM assay images of blood vessel development around and towards the decellularised jejunum sections (A, C, E) and negative collagen gel control (B, D, F). Macroscopic quantification measured blindly by assessors showed a significant increase ($P < 0.0001$) in the number of vessels growing towards the decellularised intestine sections compared to the collagen gel control n=3 (G).

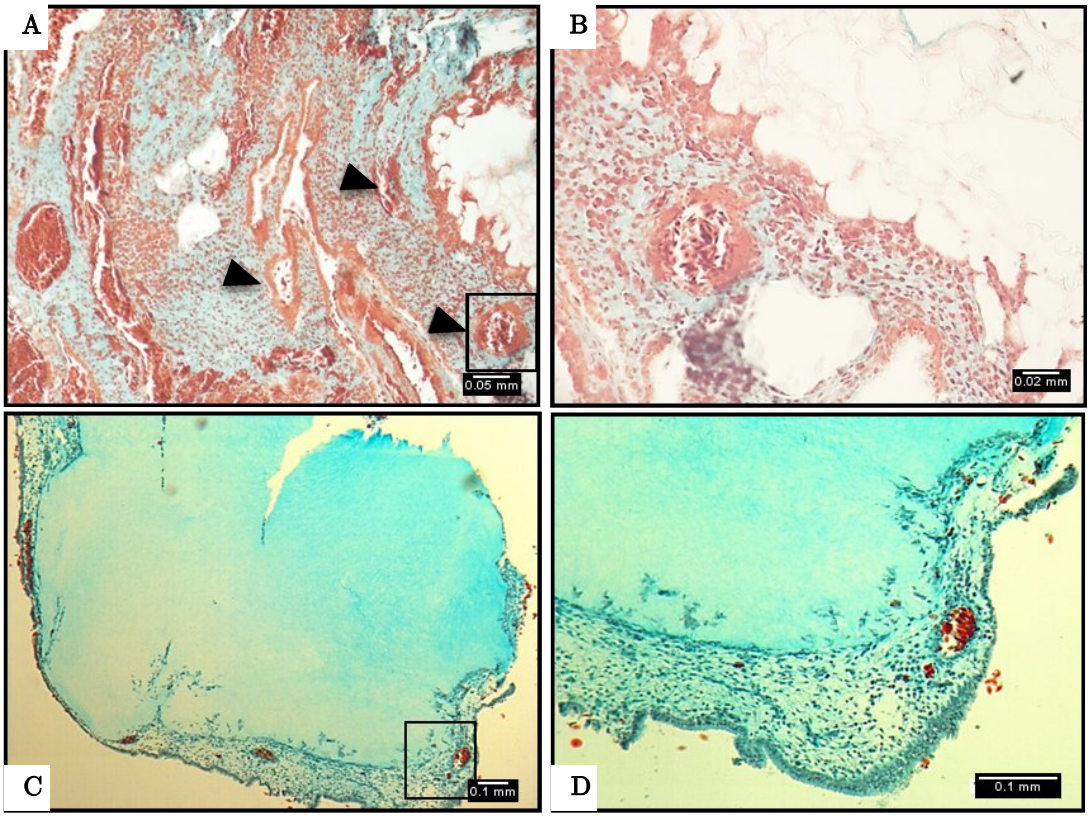


Figure 37 – Images showing sections of decellularised jejunum and collagen gels placed on the CAM assay and subsequently stained using Masson-Goldner trichrome stain. Images showed that blood vessels infiltrated the decellularised scaffolds as indicated by the black arrows (A). A magnified view of the area indicated by the black box in (B) shows cellular infiltration and blood vessels occupied by RBCs. The same staining of the collagen gel controls shows a distinct lack of cellular and blood vessel infiltration (C, D). Please note that RBCs are highlighted by the orange/red colour whilst the collagen component of the ECM is shown by the green/blue colour.

### 3.3.3. Recellularisation

#### 3.3.2.9 Distribution of cells

To determine the macroscopic distribution of cells throughout the decellularised jejunum once recellularised, HDFs were cultured in the presence of melanin to allow for its endocytosis and subsequent visualisation of the cells. Viability of the melanin infused HDFs was assessed visually by inspecting the morphology of the cells under a light microscope. Inspection showed the typical elongated shape associated with HDFs with attachment to the T75 plastic substrate. Figure 38A shows

the visible monolayer of HDFs on the surface of a T75 flask after a 24 hour incubation with melanin. When centrifuged a dark brown cell pellet could also be seen (Figure 38B) showing that melanin had been endocytosed. Bright field microscopy images show that HDFs appear brown after incubation with melanin after 24 hours (Figure 38 (C, D)). After cells were infused into the decellularised jejunum it could be seen that they had distributed evenly throughout the entire vascular network (Figure 39 (A, B)). As a result, sections of jejunum could subsequently be taken and analysed with increased confidence that they would be representative of the entire jejunum.

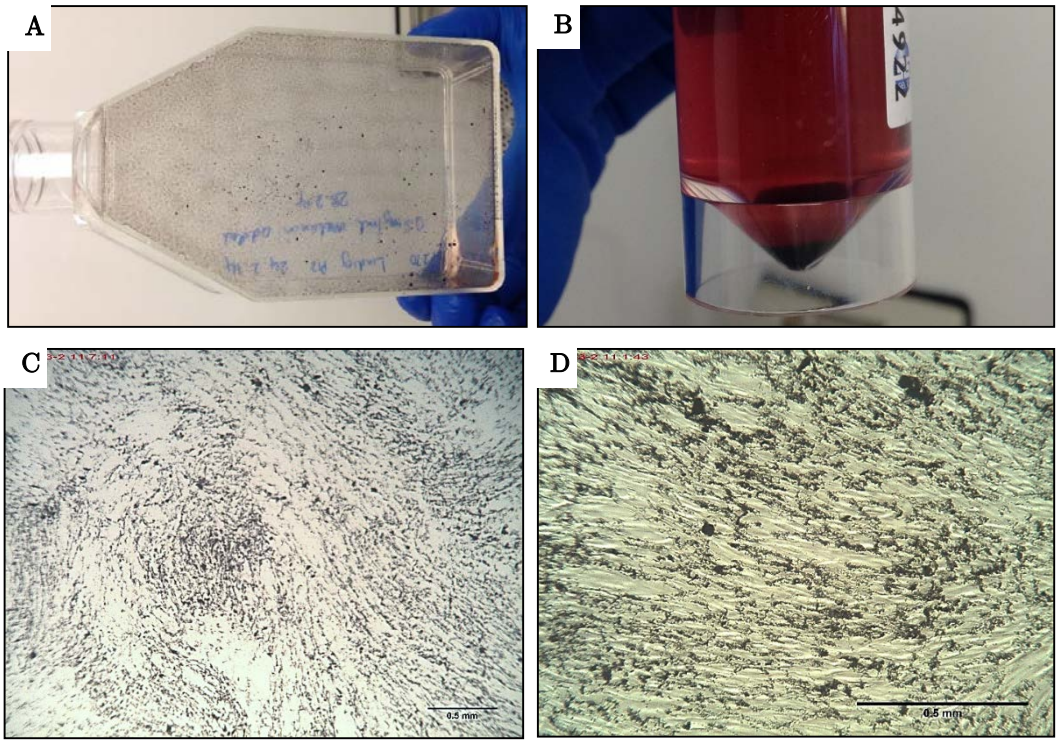


Figure 38 – Melanin endocytosis in HDFs. A macroscopically visible cell monolayer can be seen in a T75 flask after 24 hours of incubation with melanin (A) and a brown cell pellet is visible after centrifugation (B). Bright field microscopy images show the uptake of melanin into HDFs (C, D).

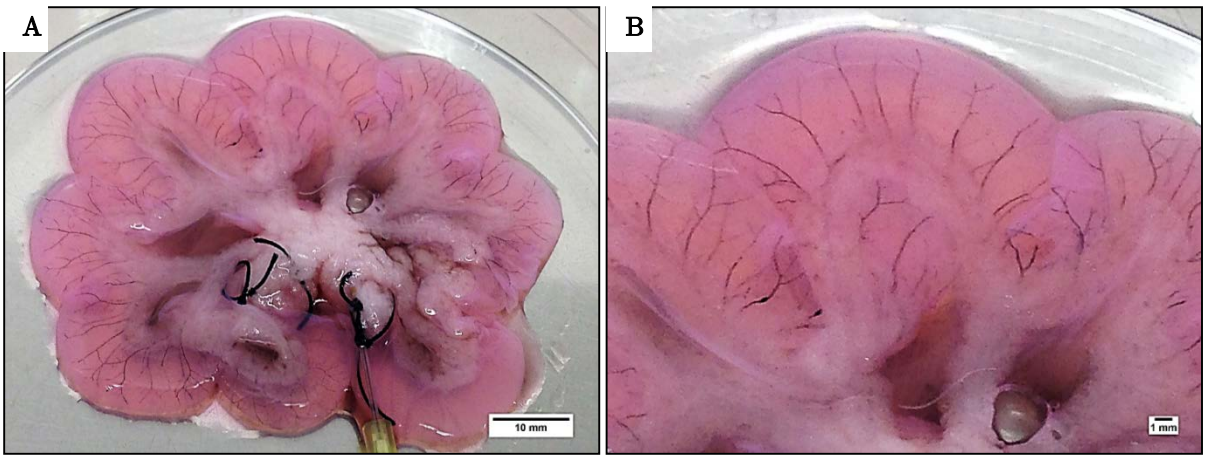


Figure 39 – Recellularisation of jejunum with HDFs containing melanin. An even distribution of cells can be seen throughout the jejunum (A). A magnified section shows that the HDFs occupy the vessels within the jejunum (B).

#### 3.3.2.10 Re-endothelialisation of vessels

To assess the ability of the decellularised jejunum to act as a scaffold for vessel reconstruction and development, HDMECs were infused and allowed to attach to the matrix for at least 24 hours. After this time LIVE/DEAD® staining was performed on segments of the jejunum and imaged using confocal microscopy to assess whether the HDMECs were able to attach and survive. Figure 40A shows that the majority of cells are live (green) with a very small proportion of dead (red) cells. Immunostaining of the samples to detect CD31+ cells shows that the ECs had attached to the vessels seemingly forming an interconnected layer (Figure 40B).

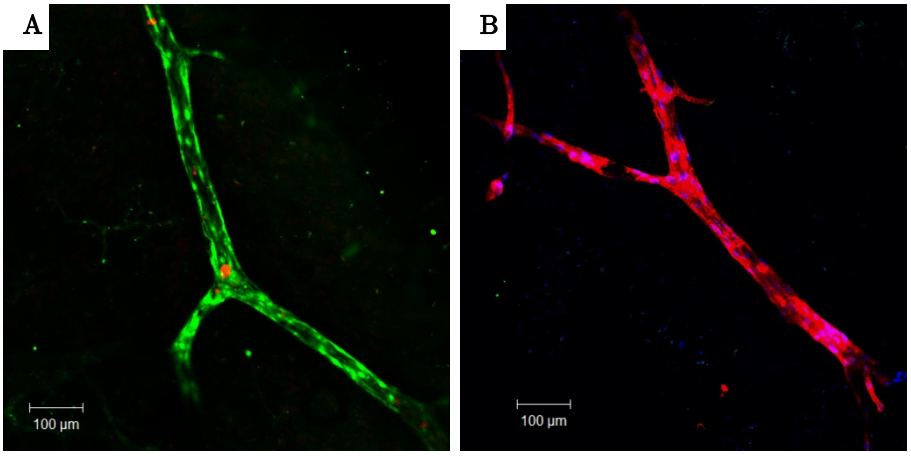


Figure 40 – Images of representative jejunum segments after recellularisation with HDMECs after 24 hours. LIVE/DEAD® staining shows mostly live cells (green) with a small proportion of dead (red) cells occupying the vessels (A). CD31+ staining (red) shows the HDMECs lining the vessels with DAPI counterstaining highlighting the cell nuclei (blue) (B).

### 3.3.4. Perfusion flow vs. static culture

Static culture of HDMECs within the decellularised jejunum for 24 hours showed that the cells were alive and seemed to occupy the vascular spaces (Figure 40). For longer periods of culture samples were either perfused using a bioreactor or cultured under static conditions. Previous research by other groups has shown that perfusion allows for nutrient supply to the ECs whilst the shear stress on the cells lining the vessels can stimulate EC differentiation and function, suggesting that perfusion is better than static culture [154]. However there is very little, if any, literature looking at which flow rates are best to use to promote differentiation and function of HDMECs when recellularised in a rat jejunum. Several flow rates were therefore investigated when perfusing the bioscaffolds. Recellularised jejunum sections were cultured and sections were taken after 24 hours of static culture and 3 days of either static or perfused culture to be analysed using the LIVE/DEAD® stain and for immunohistochemical analysis. Figure 41 shows the results of the LIVE/DEAD® staining. After 24 hours in static culture cells appear to be alive with the majority staining green (Figure 41 (A, D, G)), as shown previously. Sections were then taken and cultured under static conditions whilst the rest of the bioscaffold was

attached to the bioreactor and perfused. Figure 41 (B, E, H) shows the LIVE/DEAD staining of the sections cultured for 3 days under static conditions. In all cases there are few cells and those that are present in the vasculature appear to be dead (red). Figure 41 (C, F, I) shows LIVE/DEAD staining of the sections cultured for 3 days at 2.7 ml/min, 0.5 ml/min and 0.025 ml/min respectively. The initial flow rate of 2.7 ml/min was determined by researching the physiological measurements of blood flow through first order mesenteric artery branches of rats which has been shown to be 0.3 ml/min [189]. To determine the flow to be applied through the SMA the number of branches for each jejunal segment (in this study, 9) was multiplied by this flow rate since the total flow rate through the SMA is equal to the sum of the flow rates through the first order branches. Using this physical law of continuity the flow rate of detergent perfused through the vasculature was 2.7 ml/min. Values of 0.5 ml/min and 0.025 ml/min were chosen arbitrarily to be one and two orders of magnitude smaller than the initial 2.7 ml/min flow rate. Results showed that at the higher flow rate there are fewer cells present occupying the vessels suggesting that this flow rate is too high and may be detaching the cells from the vessel wall. At the lower flow rates more cells appear to be present and in addition these cells are alive.

Figure 42 shows the results of immunostaining for the endothelial cell marker CD31 (red). After 24 hours in static culture the vessels were occupied with HDMECs that appeared to have formed a uniform layer (Figure 42 (A, D, G)). Immunostaining of sections cultured for 3 days under static conditions confirmed what was seen using the LIVE/DEAD stain as HDMEC coverage was sparse (Figure 42 (B, E, H)). Figure 42 (C, F, I) shows immunostaining of the sections cultured for 3 days at 2.7 ml/min, 0.5 ml/min and 0.025 ml/min respectively. Again, at the highest flow rate CD31+ staining showed an uneven coverage of HDMEC cells throughout the vascular spaces. At 0.5 ml/min HDMECs were present in the vessels which appeared to be more populated when comparing to the sections that were perfused at 2.7 ml/min. However the coverage was still discontinuous in parts. At the lowest flow rate (0.025 ml/min) there appeared to be more HDMEC cells present in the vessels that showed a more uniform coverage. All of these experiments were repeated twice and at least three sections of recellularised jejunum were analysed per

experiment. At least 5 images of each section were taken. Future analysis should aim to quantify the differences in cell distribution, survival etc. between each flow rate. This could be achieved by quantifying the level of fluorescence in each image taken from the samples.

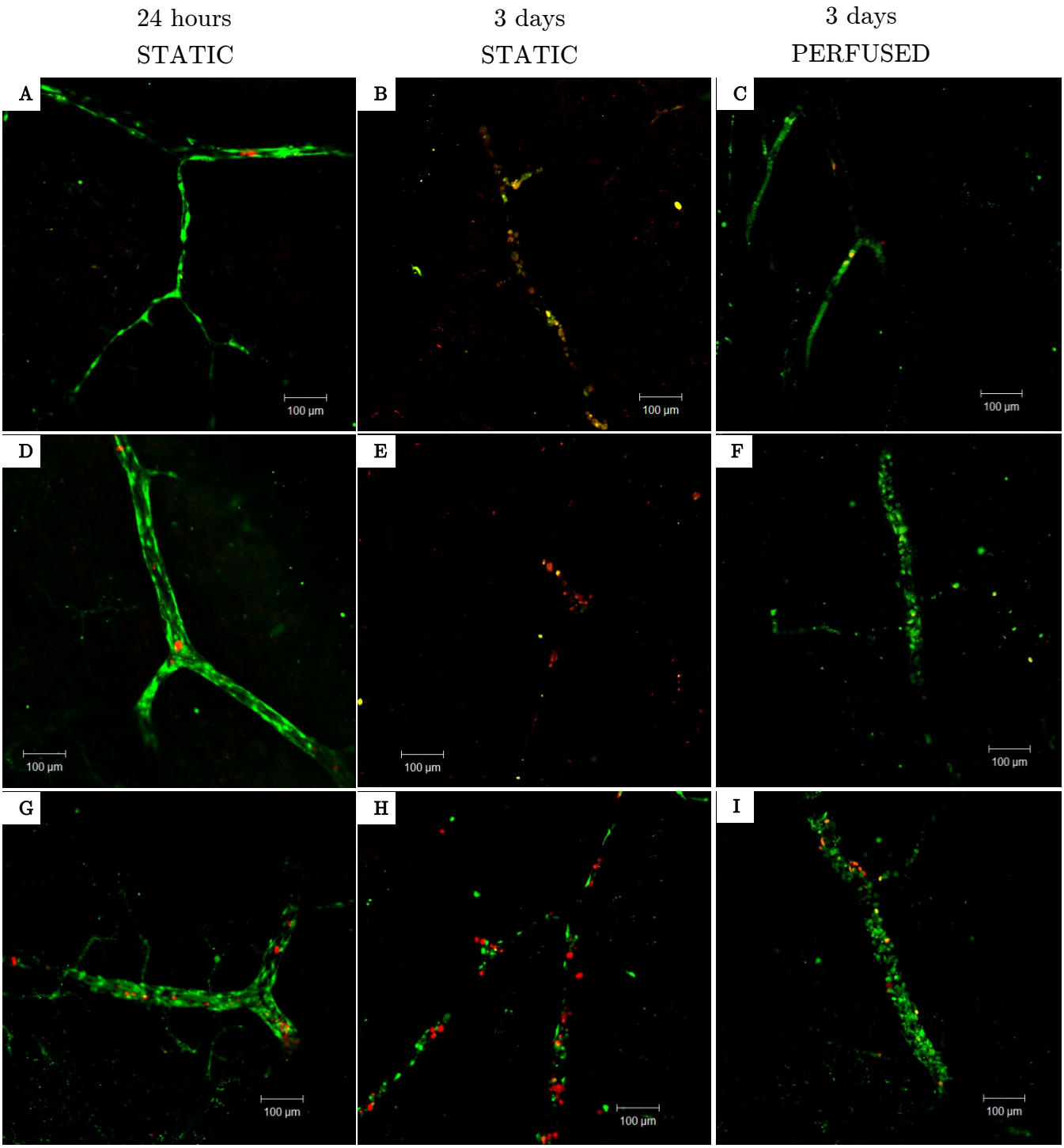


Figure 41 – LIVE/DEAD® staining of sections of jejunum recellularised with HDMECs and cultured under static and perfused conditions. Staining after 24 hours in static culture showed well populated vascular spaces with live cells (A, D, G). After 3 days in static culture sections show the presence of very few live cells (B, E, H). Staining of sections perfused for 3 days at 2.7 ml/min (C) shows few HDMECs occupying the vessels suggesting that this flow rate is too high and may be detaching the cells from the vessel wall. Lowering the flow rate to 0.5 ml/min (F) and 0.025 ml/min (I) shows an increased number of HDMECs present.

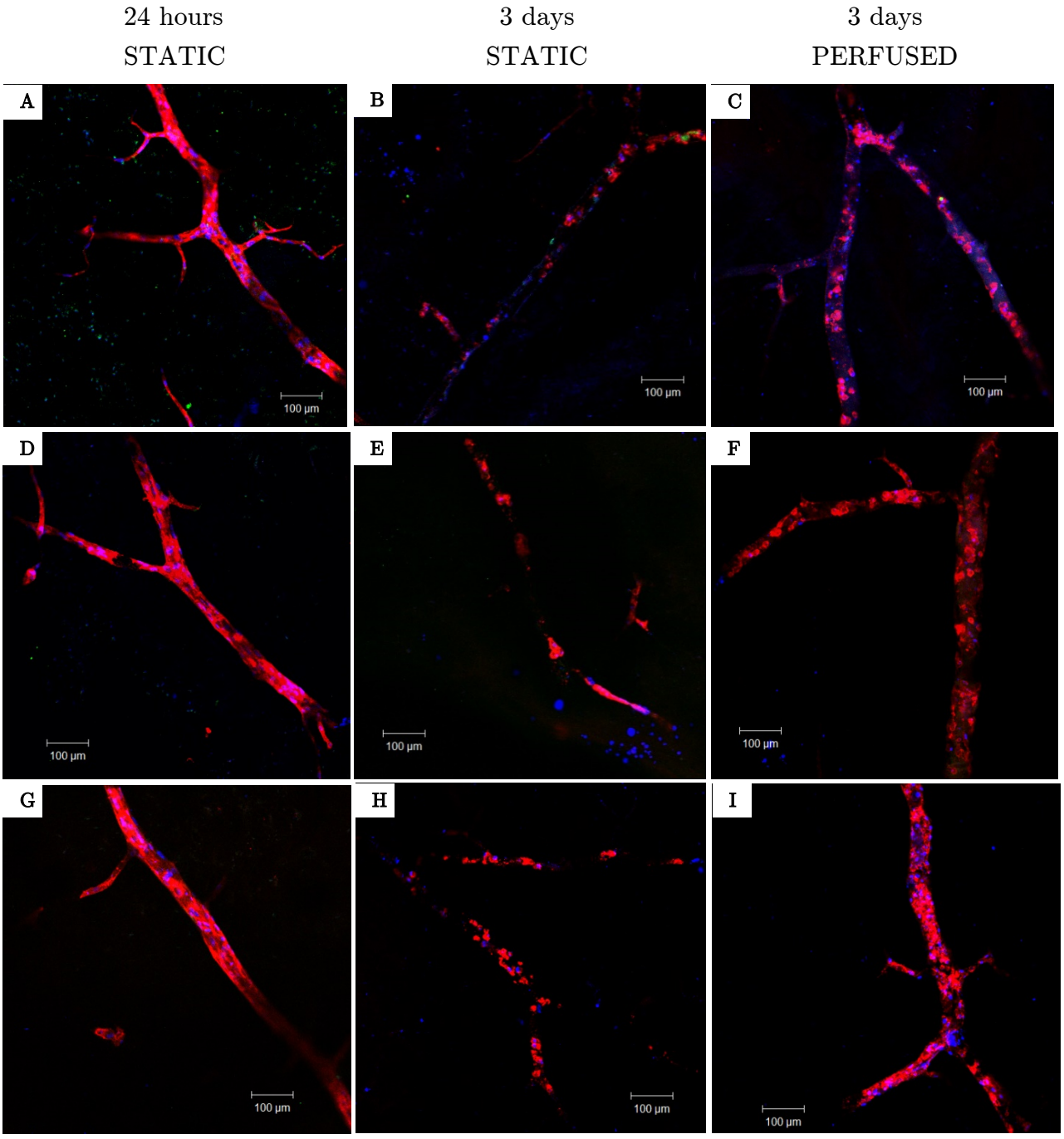


Figure 42 - Immunostaining of sections of recellularised jejunum cultured under static and perfused conditions. CD31+ staining (red) and counterstaining with DAPI (blue) shows well distributed HDMECs throughout the vascular spaces after 24 hours in static culture (A, D, G). After 3 days in static culture sections showed sparse population with HDMECs (B, E, H). Staining of sections perfused for 3 days at 2.7 ml/min (C) shows few HDMECs occupying the vessels suggesting that this flow rate is too high and may be detaching the cells from the vessel wall. Lowering the flow rate to 0.5 ml/min (F) showed an increased number of HDMECs, although the coverage was discontinuous in parts. At the lowest flow rate (0.025 ml/min) there appeared to be more HDMEC cells present in the vessels that showed a more uniform coverage (I).

### 3.3.5. Incorporation of HDFs and their effects on re-endothelialisation

Interactions between endothelial and stromal cells are important for vascularisation of regenerating tissue and it has been shown that fibroblasts play a key role by acting as a 'helper' cell modulating EC migration, viability and network formation in a 3D tissue like environment and also during the angiogenic process [88,190–192]. HDFs were therefore co-cultured with HDMECs to investigate whether they had an effect on the re-endothelialisation of the jejunum vessels.

HDFs were perfused:-

1. Into the vessels along with HDMECs
2. Into the lumen of the intestine to surround the vessels

The recellularised jejunum was then cultured under either static conditions or perfused at a rate of 0.025 ml/min.

Figure 43 shows LIVE/DEAD® staining and immunostaining of sections that had HDFs perfused into the vessels along with the HDMECs. After 24 hours in static culture the majority of the cells were alive (Figure 43A). Immunostaining for CD31 after 24 hours showed the presence of HDMECs in what appeared to be distinct locations throughout the vessels with other areas stained only with DAPI, showing the locations of the HDFs (Figure 43D). After 3 days in static culture LIVE/DEAD® staining (Figure 43B) shows a lack of cells which was confirmed by immunostaining (Figure 43E). Perfusion of the bioscaffold at a rate of 0.025 ml/min shows an improvement in the presence of cells after 3 days when compared to static culture. LIVE/DEAD® staining (Figure 43C) shows that the cells are alive but does not distinguish between HDFs and HDMECs. Immunostaining for CD31 (Figure 43F) shows distinct areas occupied by HDMECs (red/blue) and HDFs (blue). This suggests that the different cell types are competing for space within the vascular channels and which actually inhibits HDMECs from forming a continuous monolayer.

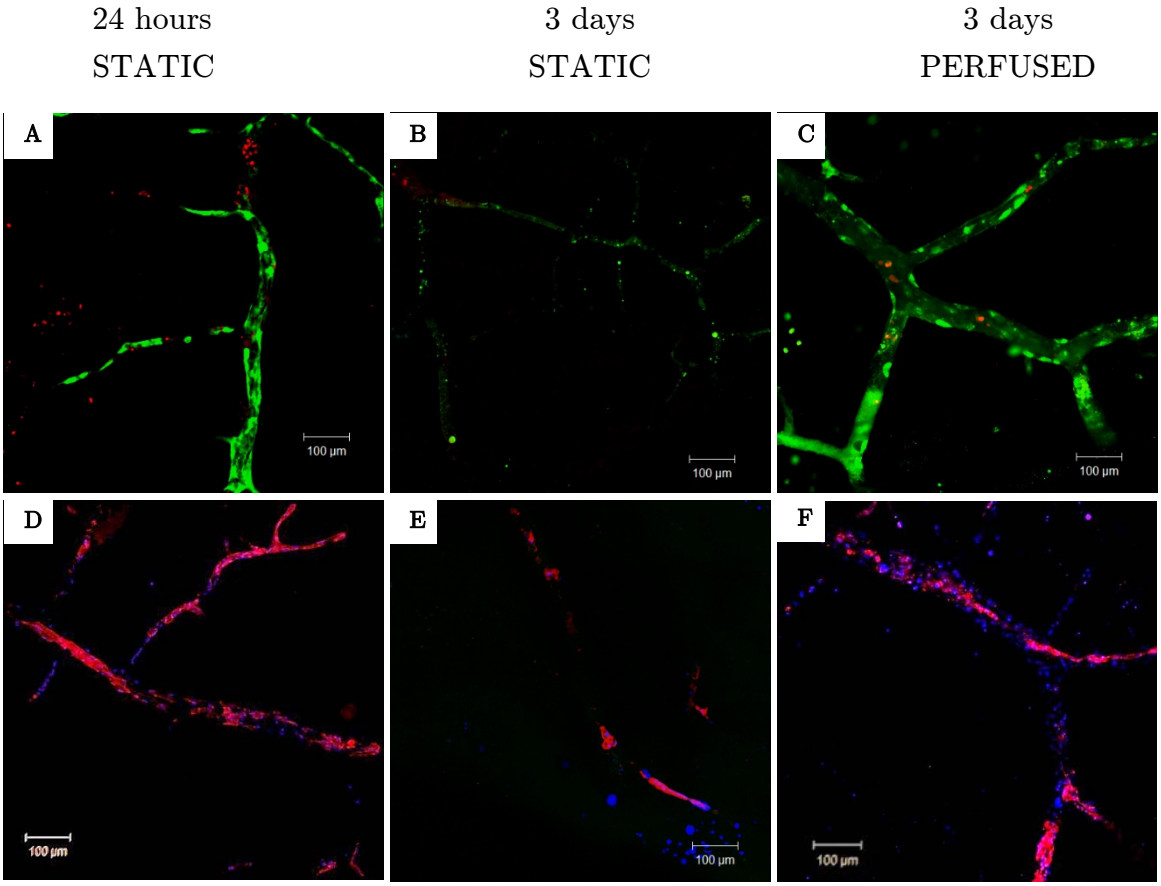


Figure 43 - LIVE/DEAD® staining and immunostaining of sections that had HDFs perfused into the vessels along with the HDMECs. LIVE/DEAD® staining after 24 hours (A) shows the presence of mainly live cells. After 3 days of static culture (B) there are very few cells when compared to those present after 3 days of perfused culture at 0.025 ml/min (C). Immunostaining for CD31 (red) and counterstaining with DAPI (blue) shows the presence of HDMECs in distinct locations throughout the vessels with other areas stained only with DAPI, showing the locations of the HDFs after 24 hours in static culture (D). After 3 days in static culture there are very few cells (E). Perfusion of the bioscaffold at a rate of 0.025 ml/min shows an improvement in the presence of cells after 3 days when compared to static culture whilst showing distinct areas occupied by HDMECs and HDFs (F).

Figure 44 shows LIVE/DEAD® staining and immunostaining of sections that had HDFs perfused into the lumen of the jejunum and HDMECs perfused into the vasculature. After 24 hours in static culture the majority of the cells were alive (Figure 44A). Immunostaining for CD31 after 24 hours showed the presence of HDMECs in what appeared to be a uniform distribution throughout the vessels (Figure 44D). After 3 days in static

culture LIVE/DEAD® staining (Figure 44B) shows a lack of cells which was confirmed by immunostaining (Figure 44E). Perfusion of the bioscaffold at a rate of 0.025 ml/min showed an improvement in the presence of cells after 3 days when compared to static culture. LIVE/DEAD® staining (Figure 44C) shows that the cells are alive within the vessels. Immunostaining for CD31 and counterstaining with DAPI (Figure 44F) shows an almost uniform distribution of HDMECs within the vascular channels with the presence of HDFs (only stained with DAPI) outside the channels. In all cases it has been shown that perfusion at a low flow rate is better than static culture. Figure 45 shows a comparison

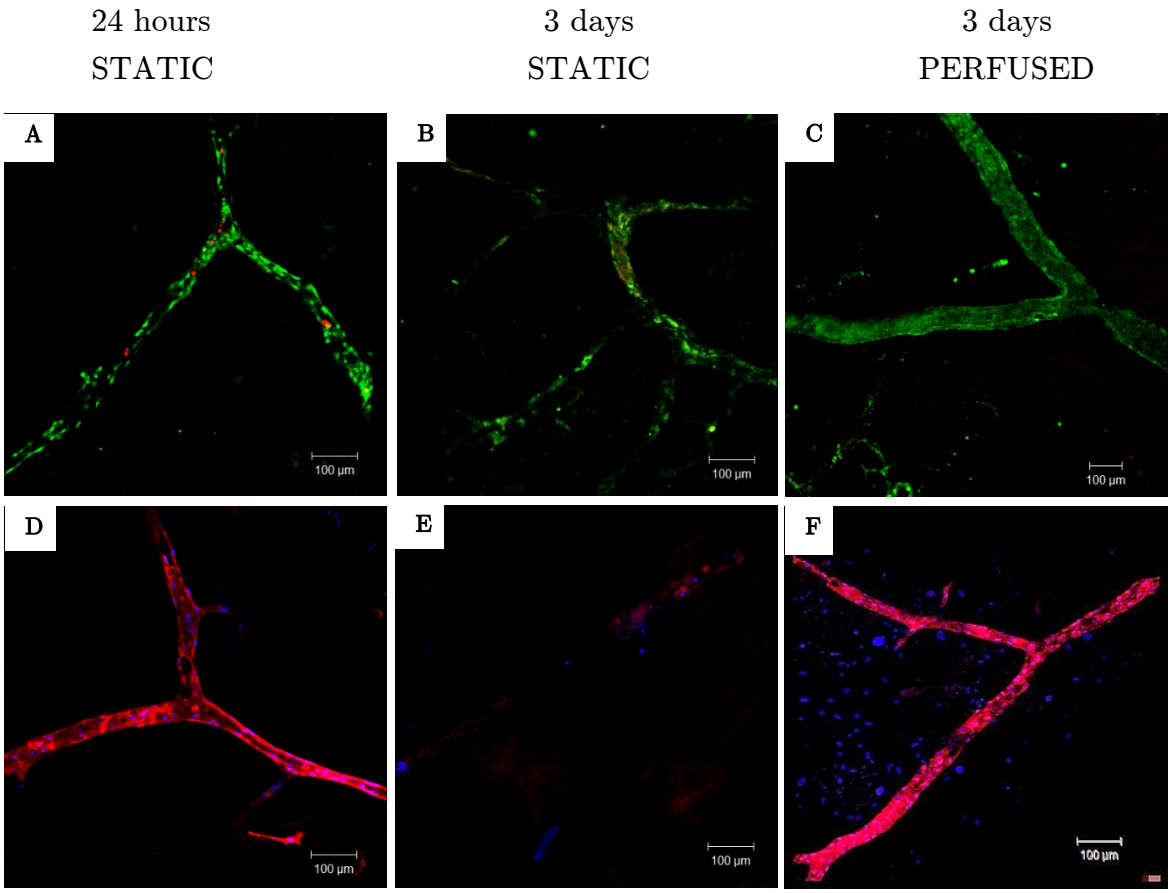


Figure 44 - LIVE/DEAD® staining and immunostaining of sections that had HDFs perfused into the lumen of the jejunum and HDMECs perfused into the vasculature. LIVE/DEAD® staining after 24 hours (A) shows the presence of mainly live cells. After 3 days of static culture (B) there are very few cells when compared to those present after 3 days of perfused culture at 0.025 ml/min (C). Immunostaining for CD31 (red) and counterstaining with DAPI (blue) shows the uniform distribution of HDMECs throughout the vascular channels (D). After 3 days in static culture there are very few cells (E). Perfusion of the bioscaffold at a rate of 0.025 ml/min shows an improvement in the presence of cells after 3 days when compared to static culture whilst showing an almost uniform distribution of HDMECs (F).

between the three perfused (0.025ml/min) cell combinations:

1. HDMECs only (Figure 45A)
2. HDMECs and HDFs inside the vessels (Figure 45B)
3. HDMECs within the vessels and HDFs within the intestinal lumen (Figure 45C)

Perfusing HDMECs within the vessels and HDFs within the intestinal lumen appears to give the most uniform distribution of HDMECs within the vascular channels after 3 days in culture. Figure 46 shows a higher magnification view of the immunostained segment of jejunum infused with HDMECs within the vessels and HDFs within the intestinal lumen. It shows a continuous layer of HDMECs within the vascular structures. All of these experiments were repeated twice and at least three sections of recellularised jejunum were analysed per experiment.

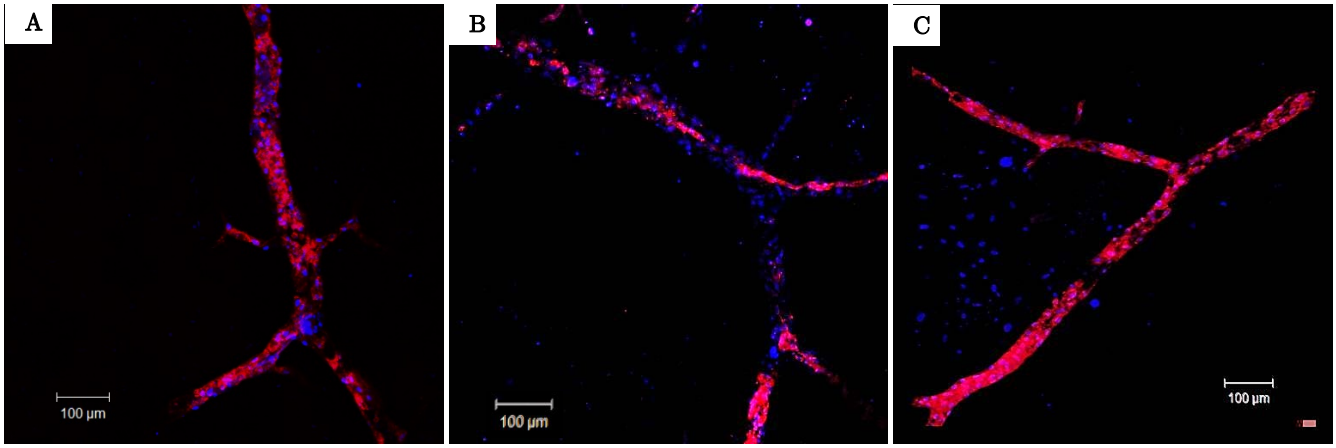


Figure 45 – Immunostained sections of perfused jejunum (0.025 ml/min) which had HDMECs infused through the vasculature only (A), HDMECs and HDFs infused through the vasculature (B) and HDMECs infused through the vasculature with HDFs infused through the intestinal lumen (C). CD31 staining is shown in red and nuclear staining is shown in blue.

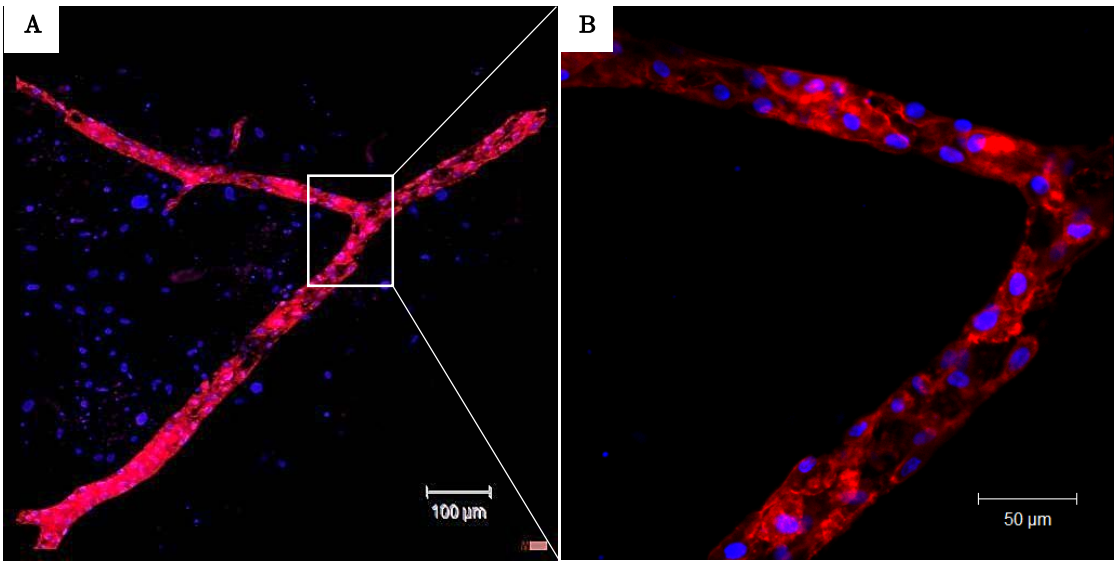


Figure 46 – Immunostained section of jejunum with HDMECs infused through the vasculature and HDFs infused through the intestinal lumen (A). A magnified view of the sample indicated by the white box shows a uniform and continuous distribution of HDMECs within the vascular channels (B). CD31 staining is shown in red and nuclear staining is shown in blue.

### 3.3.6. Use of the recellularised natural vascular net as an angiogenesis model

Experiments showed that infusing HDMECs within the vascular channels with HDFs infused through the intestinal lumen and then perfusing this at a rate of 0.025 ml/min for 3 days gave the most uniform distribution of HDMECs within the vascular channels. This cell combination and flow rate were therefore taken forward and used in the development of the angiogenesis model.

VEGF is a potent and well known stimulator of angiogenesis. To test whether HDMECs could be stimulated into sprouting, VEGF (10 ng/ml) and non-VEGF loaded collagen gels were placed on top of the recellularised intestine and the intestines perfused for 3 days. Gels and segments of recellularised jejunum were then immunostained for CD31 (HDMEC marker) and delta like ligand 4 (DLL4) (tip cell marker) and are shown in Figure 47. HDMECs present in the sections of jejunum that had VEGF loaded gels placed on top expressed DLL4 (shown in green)

indicating that HDMECs had become specialised endothelial tip cells capable of leading the outgrowth of blood vessel sprouts towards gradients of VEGF (Figure 47 (A-C)). Analysis of the VEGF loaded collagen gel shows that HDMECs had migrated into the gel and some expressed DLL4 but they had not organised themselves into vessel like structures (Figure 47D). Analysis of sections of jejunum that had non-VEGF loaded gels placed onto them showed the presence of HDMECs within the vessels but did not show expression of the DLL4 marker (Figure 47 (E, F)). This experiment was repeated twice and at least three sections of recellularised jejunum were analysed per experiment.

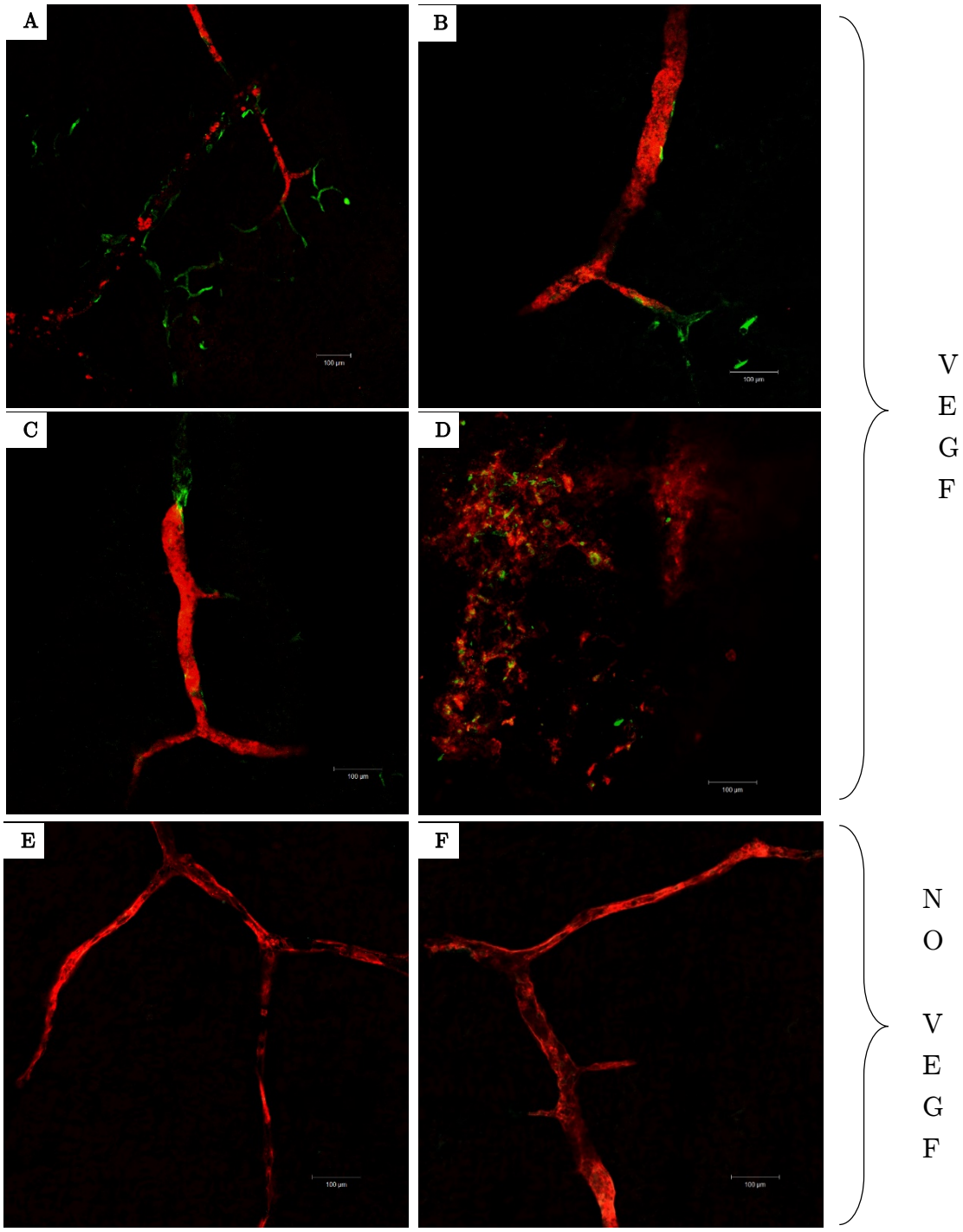


Figure 47 – Immunostained segments of recellularised jejunum (HDMECs within the vascular channels and HDFs within the intestinal lumen) and VEGF/non-VEGF loaded gels for CD31 (red) and DLL4 (green). HDMECs present in the sections of jejunum that had VEGF loaded gels placed on top expressed DLL4 indicating that they had become specialised endothelial tip cells (A-C). VEGF loaded collagen gel sections showed that HDMECs had migrated into the gel and some expressed DLL4 but they had not organised themselves into vessel like structures (D). Sections of jejunum that had non-VEGF loaded gels placed onto them showed the presence of HDMECs within the vessels but did not show expression of the DLL4 marker (E, F).

## 3.4. Discussion

Advances in the field of tissue engineering have shown promising steps towards the regeneration of vital tissues and organs including skin [193], bladder [54], urethra [194] and trachea [195]. However one of the main challenges in almost all cases is the lack of rapid vascularisation upon transplantation which leads to early graft failure. Without an understanding of the factors that affect blood vessel formation and sprouting it is unlikely that this problem will be solved. Many *in vitro* angiogenesis assays are available but none combine the ability to include supporting cells (e.g. SMCs, pericytes or fibroblasts or other stromal cells), the ECM and perfusion [97]. In the present study we aimed to develop a model that will allow all three components to be combined for investigation of the sprouting angiogenesis process.

### 3.4.1.Bioscaffold characterisation

As discussed in Chapter 1 (section 1.5), using rat jejunal segments reduces the number of cells required to repopulate the scaffold and is the reason for the use of this species in this study. Since the rat jejunum is relatively thin it was decided to use Triton-X 100 as the decellularisation detergent because it has been shown to cause less damage to the ultrastructure of the tissue when compared to ionic detergents [79,163]. The protocol was modified from that published by Baptista *et al.* [77]. Physiological measurements of blood flow through first order mesenteric artery branches (indicated in Figure 48) has been shown to be 0.3 ml/min [189]. To determine the flow to be applied through the SMA the number of branches for each jejunal segment (in this study, 9) was multiplied by this flow rate since the total flow rate through the SMA is equal to the sum of the flow rates through the first order branches. Using this physical law of continuity the flow rate of detergent perfused through the vasculature was 2.7 ml/min.

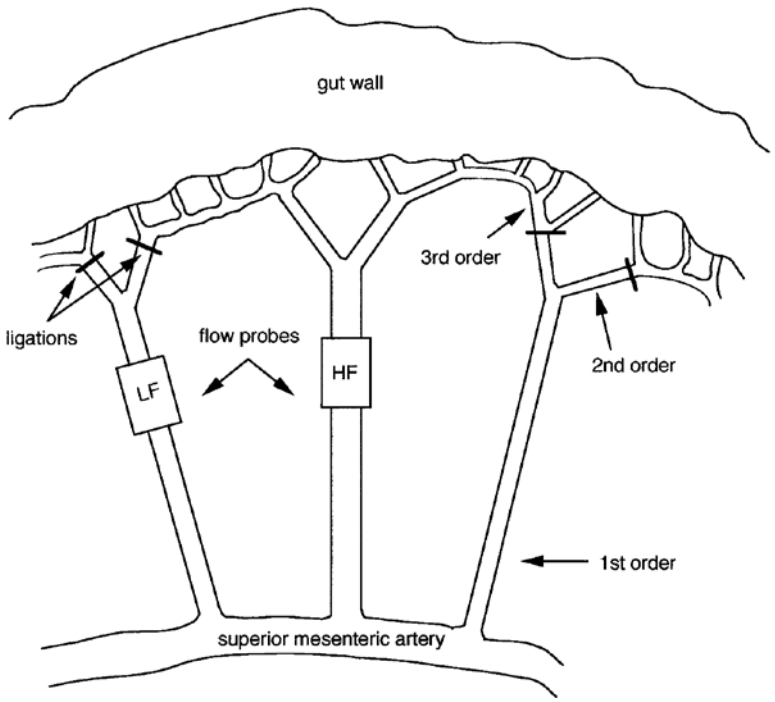


Figure 48 – Schematic showing the mesenteric branched circulation of a rat. Reproduced from the study by Pourageaud et al. [189]

Continuous perfusion of detergent via the vascular tree of the rat intestine allowed for the production of a natural acellular matrix after ˜18 hours. Initial H&E staining showed the removal of the majority of cellular material from the fresh jejunum after which was further confirmed via DAPI staining which highlighted the almost complete removal of cellular material from the jejunum. Quantification of the DNA in both the intact and decellularised samples showed a 97% removal of cellular material. Vascular patency was then tested by infusing blue food dye through the vascular net. This was shown to fill acellular vascular architecture showing the preservation of the native vascular network after decellularisation. Further confirmation was made by injecting FITC-Dextran into the vasculature, and again this filled the acellular vascular architecture. However in both instances the injected liquid diffused into the tissue parenchyma after a period of around 5-10 minutes and is most likely due to the leakiness of the acellular vascular structures as a result of the removal of the EC lining.

Histology and quantitative assays were then used to investigate the composition of the ECM after decellularisation. The ECM has been shown to be a collection of proteins, glycoproteins and proteoglycans produced by cells not only to structurally support the surrounding tissue but also to provide important functional biochemical cues. It has been shown to be responsible for a range of processes such as angiogenesis, vasculogenesis, inflammation, cell proliferation, migration and more [171]. The main component of the ECM is the protein, collagen with more than 20 different types identified. Collagen is the main contributor to the mechanical and physical properties of the ECM, especially collagen type I. Sirius red staining was used to visualise the collagen content of the decellularised jejunum. Staining showed little difference in the presence of collagen (stained red) when comparing the intact and decellularised jejunum sections. When Sirius red stained sections are examined under circularly polarised light, larger collagen fibres (indicative of type I collagen) tend to appear bright orange or red whilst smaller reticular fibres (indicative of type III collagen) appear green in colour [183,184]. Comparing the intact and decellularised sections it can be seen that the majority of fibres appear to be bright orange/red indicating the presence and retention of larger collagen type I fibres. Quantification showed that the proportion of collagen increased by 30% after the process and could be as a result of the removal of other cellular proteins within the matrix increasing the proportion of collagen with respect to the dry weight after processing. Fibronectin is the next most abundant protein found in the ECM. It is a glycoprotein found in submucosal and basement membrane structures and is responsible for cell adhesion [173,174,196]. Immunostaining for this protein showed that it was almost completely removed after decellularisation. To discover the affect that this has on recellularisation experiments, the bioscaffold could be perfused with fibronectin prior to reseeding the vascular structures with cells in future experiments. Laminin is another adhesion protein found in the ECM, especially the basement membrane [173]. It has been show to play an important role in vascular formation and maintenance and is thought to be a key component to EC friendly scaffold materials [171]. Fortunately laminin was found to be preserved after the decellularisation process as identified through the use of immunohistochemistry. GAGs are another important component of the ECM. They play key roles in binding growth factors, cytokines and water

within the ECM. The heparin rich GAGs do this by taking advantage of the heparin binding capabilities of many cell surface receptors and growth factors such as VEGF [171]. This makes their presence desirable in tissue engineering scaffolds due to their angiogenic potential. The presence of GAGs was visualised by using the alcian blue stain. This showed little difference between the intact and decellularised samples. Quantification confirmed that there was no significant difference between the two samples. Finally the Accustain elastic staining kit was used to stain for the presence of elastin (black colour). Elastin is another structural protein found in tissues that are required to stretch, such as skin, blood vessels etc. This was found to be completely removed in sections of decellularised jejunum and so no formal quantification was performed. These findings are similar to those published in related literature [77,155]. Baptista *et al.* report findings from the decellularisation of rat livers using the same detergents as used in this study (the decellularisation protocol in this study was derived from this paper). They report similar trends as found in this study with the removal of 97% of DNA, an increase in the proportion of collagen (10%) in relation to the dry weight of tissue, the retention of GAGs, slight reduction in elastin but they do show the retention of both laminin and fibronectin [77]. This slight difference may be due to difference in the tissue that was being decellularised. To the best of my knowledge Totonelli *et al.* are the only group that have reported on the decellularisation of rat jejunum. They use the detergent sodium deoxycholate and again report similar trends to those observed in this study. They showed the removal of 99% of DNA, the retention of GAGs, removal of elastin and an increased proportion of collagen [155].

To investigate whether or not the scaffold would be cytotoxic to cells after the decellularisation process, RN22 cells and HDFs were cultured in the presence of decellularised jejunum segments. Rat tail collagen type I was used as a negative control since it is well know that cells will grow in its presence [185,186] whilst cyanoacrylate glue was used as a positive control due to its potent cytotoxic nature [187,188]. Giemsa staining, used to impart colour to cells to aid microscopic identification, showed that cells grew up to and around the decellularised jejunum segments in the same way as they did in the presence of the collagen gel. However all cells died

in the presence of the cyanoacrylate glue. This confirmed that the decellularised jejunum was not cytotoxic to cells.

To examine the retention of angiogenic growth factors by the presence of GAGs, sections of decellularised jejunum were loaded onto the CAM assay. As a control, collagen I gels were used containing no growth factors. Macroscopic quantification measured blindly by assessors showed a significant increase ($P < 0.0001$) in the number of vessels growing towards the decellularised intestine sections compared to the collagen gel control showing the inherent angiogenic effect of the decellularised jejunum. This response argues for the preservation of key growth factors or GAGs that have bound chick growth factors that will ultimately affect cell response upon reseeding. Masson-Goldner trichrome staining showed that there had been a high level of cellular infiltration into the decellularised jejunum segments in comparison to the collagen gel control. This confirms the cytotoxicity results that showed that the scaffold is cell friendly. In addition blood vessels had infiltrated the decellularised jejunum further confirming its angiogenic potential.

### 3.4.2. Recellularisation of the vascular network

In order to produce a model to investigate angiogenesis, cells were infused through the vasculature to repopulate the acellular matrix. To macroscopically observe the distribution of cells within the matrix to ensure even dispersal, advantage was taken of the process of phagocytosis of synthetic melanin by HDFs to allow for their pigmentation and visualisation. HDFs were used not only for their ability to phagocytose melanin but also because fibroblasts have been reported to act as helper cells in neovascularisation [192,197,198] and were investigated for this purpose in this study. The results highlighted that the cells could indeed phagocytose melanin and appeared as a brown sheet in a T75 flask. After infusion into the decellularised jejunum they had distributed evenly throughout the bioscaffold, occupying the vascular structures. This gave confidence that when a section was taken from the recellularised jejunum it would be representative of the whole sample.

Delivering cells of endothelial origin has been the focus of many studies aimed at investigating angiogenesis since they are directly associated with contributing to vessel formation. Until recently the most commonly used human ECs used for *in vitro* angiogenesis assays have been HUVECs. However since angiogenesis involves the microvasculature there has now been a shift towards the use of microvascular ECs [97] with many studies using HDMECs to study angiogenesis [199–203]. HDMECs were therefore used initially to recellularise the decelluarised jejunum. After 24 hours in static culture LIVE/DEAD® staining showed that the cells had occupied the vascular structures and the majority were live. Immunostaining for the EC marker CD31 confirmed that the cells had attached to the vascular channels and they had formed an evenly distributed layer.

Although the recellularised jejunal segments were cultured under static conditions it is widely acknowledged that fluid flow and shear stress associated with it plays a role in determining the structure and function of ECs *in vivo* [204]. The exact mechanism by which the endothelium experiences shear stress remains unclear since every mechanosensing molecule in the process is not known [205]. However the activation of ion [206–208], cation [209] and stretch sensitive channels [210] have been observed immediately after exposure to shear stress. An increase in intracellular calcium and a considerable increase in NO production has also been noted. An increase in the levels of NO due to the action of shear stress is known to be caused by the activation of the enzyme eNOS. Upon activation eNOS catalyses L-arginine to L-citrulline and nitric oxide (NO) [15]. These factors play a key role in signalling to the EC that it is under shear, which in turn elicits an angiogenic response depending on the level of shear stress encountered [205]. NO has also been shown to play a key role in regulating vessel tone (vessel wall tension), acting as a powerful vasodilator. Briefly, it stimulates soluble guanylyl cyclase in the vascular SMCs to induce formation of cyclic guanosine monophosphate. This in turn activates protein kinase G which promotes the reuptake of cytosolic calcium into the sarcoplasmic reticulum, the expulsion of calcium out of the cell and the opening of calcium activated potassium channels. The calcium concentration then decreases in the cell and SMC relaxation ensues [211]. Due to the link between behaviour of the endothelium and fluid forces it was decided to investigate the effects of perfusion on the re-

endothelialisation of the vascular structures. Previous studies (summarised in Table 5 and Table 7 in Chapter 1) that have perfused the recellularised jejunum have used flow rates ranging from 0.8 ml/min to 3.8 ml/min. None of the studies have provided justification for this choice or observations using different flow rates. It was therefore decided to trial several flow rates to see what effects this would have on the re-endothialisation of the vessels. An initial flow rate of 2.7 ml/min was used to perfuse the network. This was the same flow rate used to decellularise the jejunum and was chosen due to its relation to the physiological fluid flow found in the small jejunum of rats [189]. After 24 hours after the infusion of HDMECs the scaffold was constantly perfused at this rate for 3 days.

LIVE/DEAD® analysis and immunostaining for CD31 showed the presence of very few cells suggesting that this flow rate is too high and may be detaching the cells from the vessel wall. Flow rates of approximately one and two orders of magnitude smaller were then used (0.5 ml/min and 0.025 ml/min respectively). In both instances there were more live HDMECs present after 3 days under constant perfusion than when cultured under static conditions. Also when the lower flow rate of 0.025 ml/min was used there appeared to be more live cells occupying the vascular channels with a more uniform distribution when compared to using a flow rate of 0.5 ml/min. This suggests that HDMECs need a low flow rate (but not static) to attach and distribute throughout the vascular network.

Having identified a suitable flow rate, the HDMECs were then co-cultured with HDFs in an attempt to improve the re-endothelialisation of the vessels. Studies have shown that using mature HDMECs in a monoclonal culture have shown relatively poor results when seeded onto biomaterial scaffolds due to their inability to survive, proliferate over long periods and most importantly to self-assemble into tube like structures [192]. However, improved results have been noted by using a co-culture of HDMECs and fibroblasts [192,197,198]. Cell proliferation and cell signalling have been improved through the use of such co-cultures and it is believed that this is as a result of paracrine signalling mechanisms that promote production of VEGF from fibroblasts and the upregulation of VEGF receptors on

HDMECs [192]. To determine whether the HDFs had to be in direct contact with the HDMECs to could accomplish this 'helper' cell status, they were either seeded within the vascular channels along with the HDMECs or they were seeded into the lumen of the jejunum so that they were not in direct contact with the HDMECs. The co-culture of cells into the decellularised intestinal scaffold was again maintained under both static and perfusion cultures to determine whether perfusion enhanced re-endothelialisation with the inclusion of HDFs. Results clearly indicated the necessity for a low rate of perfusion since there were very few cells present in both instances when the scaffolds were cultured statically. When perfused different results were obtained when HDFs were infused into the vasculature of the jejunum along with the HDMECs compared to when they were seeded within the lumen. Immunostaining for CD31 showed distinct areas occupied by HDMECs and HDFs when they were both infused into the vascular channels. This suggests that the different cell types are competing for space within the vascular channels which actually inhibits HDMECs from forming a continuous monolayer. However, when the HDFs were seeded within the lumen results showed an almost uniform distribution of HDMECs within the vascular channels, showing a similar distribution to that obtained after 24 hours in static culture. This implies that HDFs and HDMECs do not need to be in direct contact for the HDFs to act as 'helper' cells and that they communicate via soluble mediators that can penetrate through the bioscaffold. These could be cytokines such as VEGF, FGF etc. The most uniform distribution of HDMECs was therefore obtained by infusing HDMECs into the vascular channels and seeding HDFs into the lumen of the jejunum and then perfusing continuously for 3 days at a rate of 0.025 ml/min.

### 3.4.3.The use of the recellularised vascular network as an angiogenesis model

The aforementioned cell combination and flow rate that gave the most uniform distribution of HDMECs within the vascular channels was taken forward and used in the development of the angiogenesis model, with particular focus placed on investigating sprouting angiogenesis.

It is well documented that VEGF is a potent pro-angiogenic molecule [22,212–214]. As discussed in Chapter 1 it is not the only pro-angiogenic growth factor associated with angiogenesis and in fact it is the interplay between a variety of factors (chemical and mechanical) that ultimately promotes angiogenesis [4]. However, for the preliminary development of the angiogenesis model it was decided to initially focus solely on the use of VEGF before adding other growth factors which could potentially complicate the analysis and potential troubleshooting. The concentration of VEGF to use in angiogenesis assay has been investigated by many groups. In many instances a concentration of 10 ng/ml was found to be optimal [215–218] and so was used in this study. In order to immobilise and set up a VEGF concentration gradient the growth factor was added to a collagen gel. Type I collagen from rat tails has also been used widely in angiogenesis assays since ECs have been shown to penetrate into the collagen gels to a depth of ˜200 μm in a 24 h period [219–221]. It was decided not to use matrices such as Matrigel since this is not completely defined, containing multiple ECM proteins and growth factors [222]. Furthermore, fibroblasts have been shown to act like ECs when seeded onto Matrigel [113–115] and this could have potentially interfered with the interpretation of results obtained when using HDFs. Collagen was therefore used in order to immobilise the VEGF. The final concentration of the VEGF in the gels was 10 ng/ml since this had been used in previous studies whereby ECs had been found to infiltrate and form capillary like structures [44,223–225]. The collagen gels (with and without VEGF) were loaded into metal rings that had been placed onto the recellularised jejunum in order to fix the gel in place and identify their location at the end of the experiments since both the recellularised jejunum and gels were translucent. The recellularised jejunum was then continuously perfused for 3 days before staining sections for the CD31 and DLL4 markers. A period of 3 days was chosen to reduce the likelihood of infections whilst using the bioreactor system, however it would be possible to run the system for longer (order of weeks) if the system was housed in a clean room. Results showed that HDMECs present in the sections of jejunum that had VEGF loaded gels placed on top expressed DLL4 indicating that HDMECs had become specialised endothelial tip cells capable of leading the outgrowth of blood vessel sprouts towards a VEGF signal. Analysis of the VEGF

loaded collagen gel showed that HDMECs had migrated into the gel and some expressed DLL4 but they had not organised themselves into vessel like structures. Future experiments would aim to extend the culture time to see if the ECs reorganised into capillary like structures with further perfusion. Analysis of sections of jejunum that had non-VEGF loaded gels placed onto them showed the presence of HDMECs within the vessels but did not show expression of the DLL4 marker. These observations are validated by what has been reported in the literature where VEGF has been shown to regulate tip cell migration [226–228]. These preliminary results indicate that this technique offers real potential for use as a model to investigate angiogenesis *in vitro*.

### 3.4.4.Limitations

Although this technique combines an ECM component, the ability to add a variety of supporting cells and the capacity to be perfused there are some limitations. Firstly, since it is a natural scaffold there is inevitable batch-to-batch variability amongst the resected jejunal sections. In addition the process of cannulating the SMA, recellularising the jejunum and setting up the bioreactor system is quite intricate and therefore requires a lot of practise to become efficient and so it is difficult to efficiently scale up experiments to gain rapid outputs.

## 3.5. Summary

In this chapter an angiogenesis model derived from a decellularised rat jejunum was presented. After decellularisation ˜97% of the DNA content was removed whilst preserving the vascular network. Analysis of the ECM components showed an increase in the proportion of collagen with respect to the dry weight (˜30%), the retention of GAGs and laminin but did show the removal of elastin and fibronectin. Recellularisation showed that the vascular network could be evenly re-endothelialised with HDMECs when HDFs were seeded into the lumen and the jejunum was perfused at a

rate of 0.025 ml/min for 3 days, continuously recirculating the medium (without replenishment). Higher flow rates resulted in the loss and subsequent uneven coverage of HDMECs within the channels. Placing VEGF loaded gels onto the recellularised jejunum led to the expression of DLL4 by HDMECs indicating their transformation into tip cells. Tip cells are synonymous with sprouting angiogenesis since they allow for the exploration of the surrounding environment to sense chemoattractants, such as VEGF, emitted as a result of hypoxia. Please note that the culture medium was not supplemented with VEGF. These results indicate the potential of this technique to model angiogenesis and overcome the shortcomings of current angiogenesis assays by allowing the inclusion of supporting cells, an ECM component and the ability to perfuse the whole scaffold.

# Chapter 4

# Synthetic vasculature to study angiogenesis

## 4.1. Aims

The aim of this chapter is to develop a synthetically derived *in vitro* model in which to study angiogenesis by:

1. Producing vascular networks for experimentation by electrospinning and robocasting to produce a synthetic vascular network.

2. Investigating the optimal cell combinations to functionalise the vascular networks and recellularise these networks.

3. Investigating the effects of pro-angiogenic stimuli on angiogenic sprouting.

## 4.2. Introduction

Over the years many assays have been developed and are now used extensively to investigate the process of angiogenesis, as discussed in Chapter 1. The vast majority of the knowledge gained about angiogenesis has been gained from the use of static 2D cell culture systems. Although helpful, the use of very simplified systems using flat, stiff substrates to culture cells does not capture the highly complex tissue environment in which angiogenesis naturally takes place. It is therefore suspected that cells will behave differently in such simple systems and are misrepresentative, potentially giving erroneous results. The development

of 3D assays has therefore been undertaken by various groups [165]. These have mostly used natural materials such as collagen I, fibrin or Matrigel because they have intrinsic properties that enable good cell attachment, proliferation and EC sprouting [165]. However it has been identified that when using natural materials there is limited control over degradability and mechanical properties whilst batch-to-batch variability has been identified. Groups have therefore started to look into using synthetic materials to model angiogenesis since they can be easily modified both chemically and biochemically whilst their mechanical properties can be tightly controlled.

As discussed in Chapter 1, Jeffries *et al.* reported the use of a novel technique combining fused deposition modelling and electrospinning to form synthetic vascular networks that were then capable of being perfused and recellularised with ECs [168]. The purpose of this study was to produce a synthetic scaffold to act as a vascular bed to support TE constructs. In this chapter the aforementioned approach is modified and used to produce perfusable synthetic networks for use as an angiogenesis model. Instead of using fused deposition modelling of PVA, robocasting of alginate is used instead. Robocasting is also an extrusion based technique but unlike fused deposition modelling it does not require a heated nozzle to extrude the material [229]. This means that it potentially allows for the introduction of biomolecules within the fabrication process increasing the functionality without facing the loss of activity or denaturation of proteins and it also enables the retention of microstructural integrity of the electrospun mats as they will not be altered by the high temperatures. The use of alginate is also easy to remove and cell friendly. Electrospinning of the vascular network uses the polymer, PHBV since previous work carried out in our group has found it to be biocompatible and biodegradable [230]. The pseudo-vascular synthetic networks are then recellularised with a combination of HDFs and HDMECs and analysed to determine the extent of cell attachment. A VEGF loaded gel is then placed onto the scaffold to observe the effects of this pro-angiogenic stimulator on blood vessel sprouting.

## 4.3. Results

### 4.3.1. Synthetic vascular net production

Through the combination of alginate printing (via the use of a 3D printer) and electrospinning it was possible to rapidly produce a number of replicate scaffolds. The geometry of the scaffolds was controlled through the use of custom built g-code software, VPPG, and varying sizes of scaffolds (Figure 49 (A, B)) made from randomly aligned fibres (Figure 49C) could be produced. Removal of the alginate was studied though the use of SEM and fluorescence microscopy (Figure 50). SEM microscopy showed that by removing the alginate (Figure 50A) after electrospinning it was possible to produce a hollow, interconnected structure (Figure 50B). The complete removal of alginate was confirmed using fluorescence microscopy by loading Eosin Y into the alginate mixture. Figure 50C shows alginate printed on top of the electrospun mat and Figure 50D shows the presence of alginate after electrospinning a further layer on top. No fluorescence was visible after adding the electrospun networks into a 0.5 M solution of EDTA overnight (Figure 50E).

The scaffolds used throughout this study had geometries indicated by Figure 49A and Figure 50 (A&B). These were ~30 mm in length and ~17 mm wide with the elongated hexagonal shapes in the centre measuring ~7mm in length and ~4 mm in width. For each 'production run' 36 scaffolds were produced and around 70% of these were used. There were several reasons for the 30% wastage but the main one was due to the printing of the alginate. Figure 51(A&B) (left) show examples of 'good' prints where there is not overlap of the alginate but in some cases the alginate was completely misprinted as a result of a printer error as indicated by Figure 51A (right) and in some cases the alginate would merge meaning that the channels were not separate (Figure 51B (right)). In these instances the scaffolds were discarded as they were deemed not fit for purpose. Since this was a preliminary study of whether these scaffolds would support cell growth and have the potential to be used as an angiogenic model, increasing the printing efficiency was not a key focus of

the project since enough scaffolds were produced for these purposes via this setup.

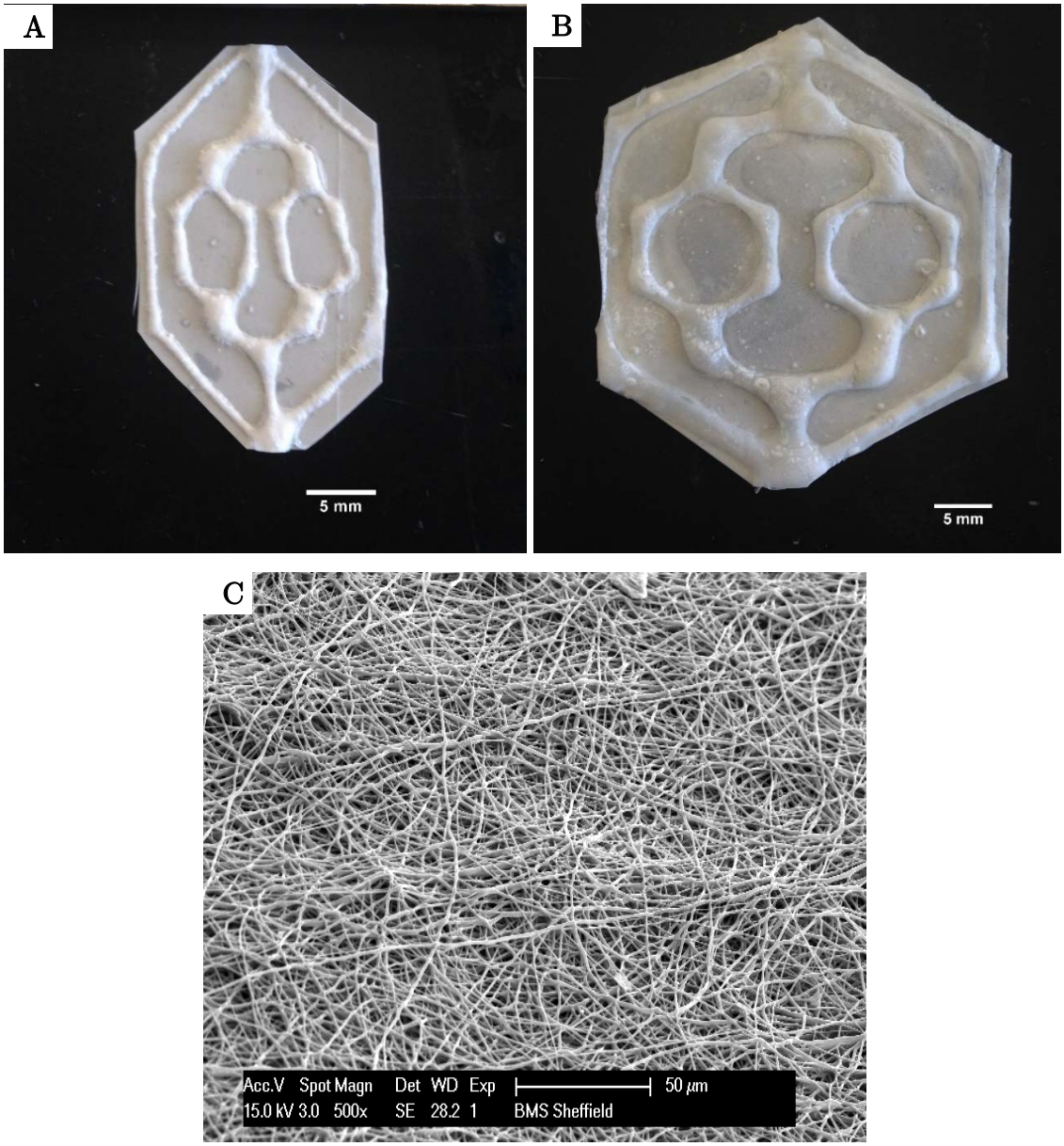


Figure 49 – Synthetic pseudo-vascular nets were produced through a combination of robocasting and electrospinning. The size of the scaffolds could be varied (A, B) and SEM imaging showed that they were comprised of randomly aligned fibres (C).

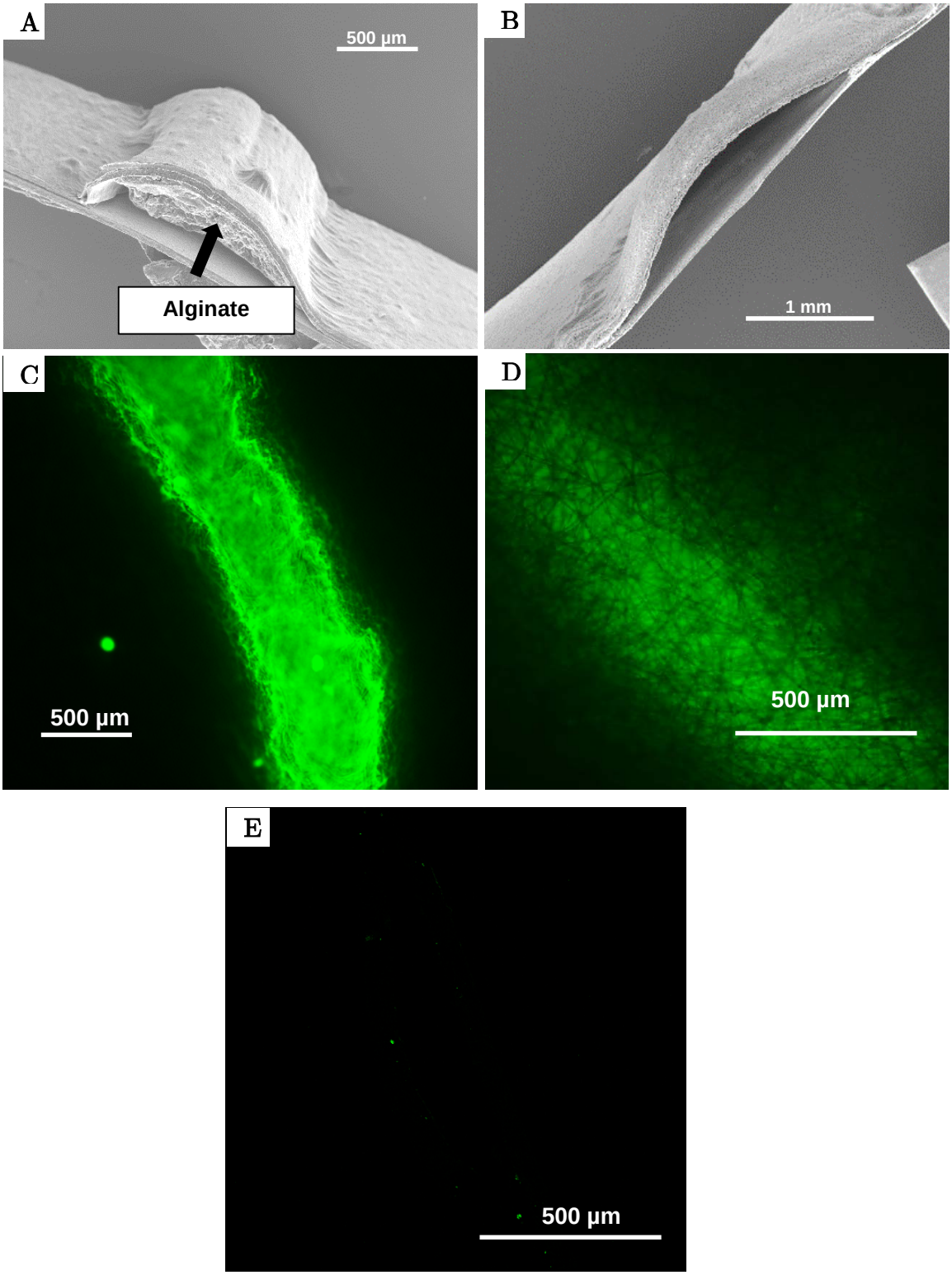


Figure 50 – Synthetic pseudo-vascular scaffold prior to the removal of alginate (A) and after removal of this sacrificial substrate by submerging in EDTA solution overnight (B) shown by SEM microscopy. The complete removal of alginate was confirmed through the use of fluorescence microscopy. Alginate loaded with Eosin-Y after printing on top of the electrospun mat (C) and after electrospinning on top of the alginate (D). After submerging the sscaffold in 0.5M EDTA overnight the alginate was completely removed (E).

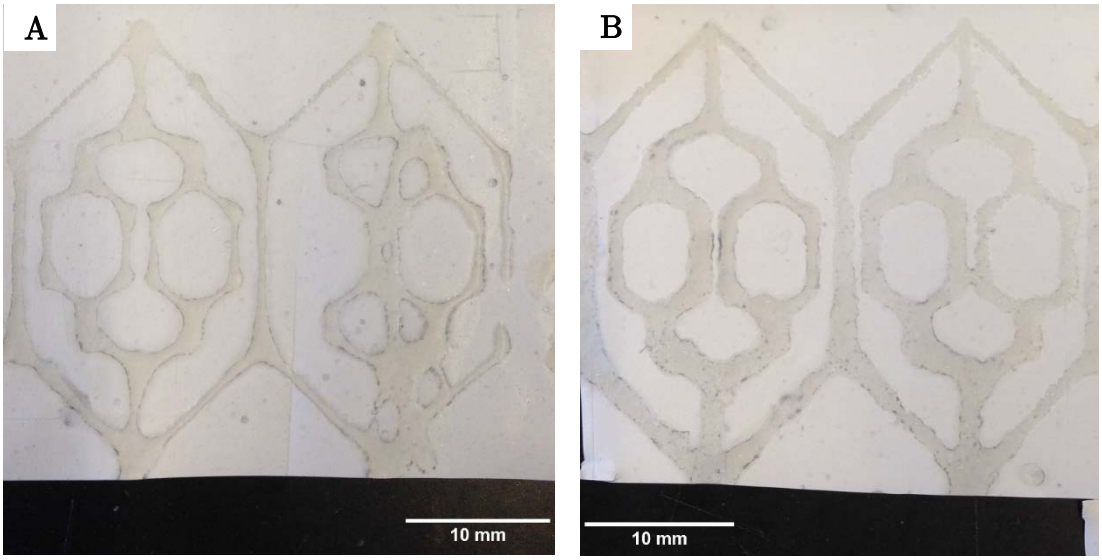


Figure 51 – Images of alginate printing onto the electrospun mat. Examples of good printing are shown in (A) and (B) (left). Examples of alginate printing errors are shown where the printer has malfunctioned (A) (right) and where the alginate has merged meaning that the channels are not separate (B) (right). In cases where the alginate had not been printed correctly, the scaffolds were discarded.

### 4.3.2. Characterisation of synthetic vascular nets

Prior to cell culture, the fibre diameter and mechanical properties of the PHBV scaffolds were tested. Measurements using Image J software showed that the diameter of the fibres was 0.70 ± 0.05 μm. Previous work from our group has shown that PHBV nanofibers such as this are capable of allowing the passage of nutrients through the fibres but prevent cells from passing through them for a period of up to 6 weeks [230,231]. Mechanical testing of the bulk PHBV scaffold enabled the UTS, Young's Modulus (E), yield strength and elongation at break to be determined. A typical stress vs. strain graph for such samples is shown in Figure 52. Analysis of data from 4 different samples allowed for the average properties of the bulk PHBV material to be determined, as summarised in Table 23. The results show that the bulk material has an average UTS of 0.6 MPa, similar to poly(ether urethane urea) (PEUU) vascular graft scaffolds that have been used previously *in vivo* [232]. Mechanical testing of the pseudo-vascular PHBV scaffolds enabled the suture retention strength to be determined. A typical stress vs. strain curve for such

samples is shown in Figure 53. The suture retention strength of this material is also similar to scaffolds that have been used *in vivo* which have a typical range of between 35–59 MPa [233].

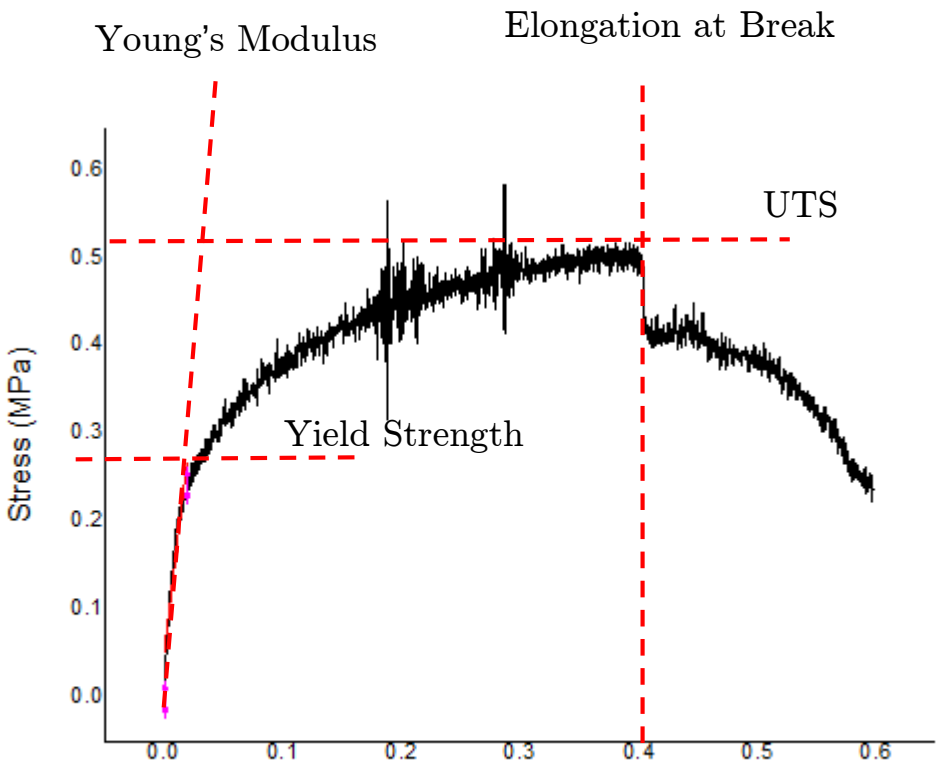


Figure 52 – Representative stress vs strain curve for the bulk PHBV material.

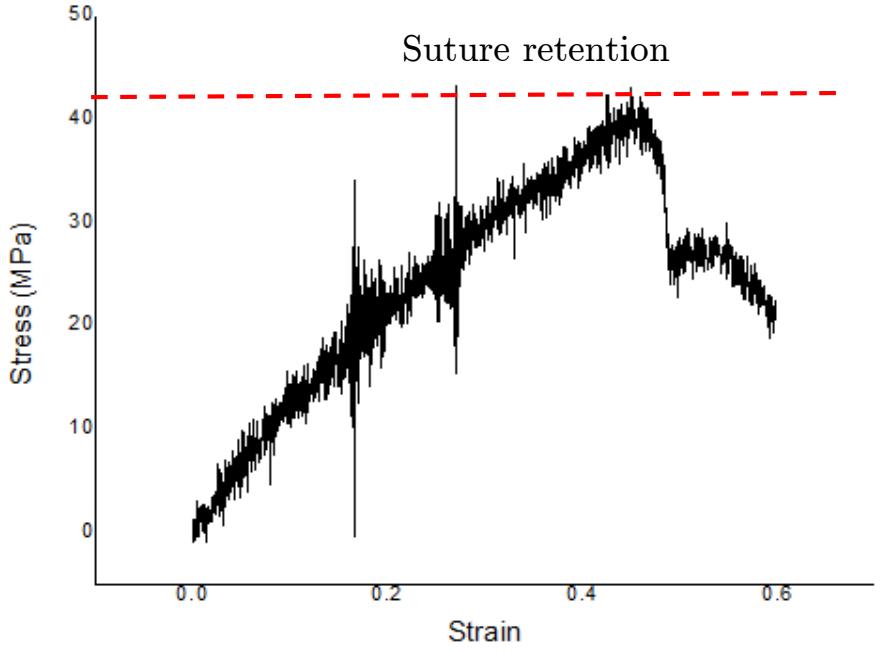


Figure 53 - Representative stress vs strain curve of the pseudo-vascular scaffolds to calculate the suture retention strength.

Table 23 – Summary of the mechanical properties of the bulk PHBV material and pseudo-vascular scaffold suture retention strength.

| | Tensile testing (n=4) | | | | |
|---|---|---|---|---|---|
| ***Fibre diameter (μm)*** | *UTS (MPa)* | *Yield Strength (MPa)* | *Young□s Modulus (MPa)* | *Elongation at Break (%)* | *Suture Retention Strength (MPa) (n=6)* |
| **0.70 ± 0.05** | 0.60 ± 0.08 | 0.29 ± 0.05 | 15.00 ± 2.60 | 36.47 ± 5.03 | 41.67 ± 5.85 |

### 4.3.3. Re-endothelialisation of synthetic pseudo-vessels

To determine whether the scaffolds could support cellular attachment, growth and survival to form a pseudo-vascular network, HDMECs were infused into the scaffolds and cultured under static conditions for 7 days. Samples were then analysed for the presence and distribution of cells. Figure 54 shows various magnification H&E sections of the scaffolds after 7 days and shows the distinct lack of HDMEC cells. SEM analysis of both the curved (Figure 55A) and flat (Figure 55B) surfaces shows some cell attachment and spreading but it is sporadic. This was further confirmed by immunostaining for CD31 and counterstaining with the nuclear stain DAPI on the curved (Figure 55C) and flat (Figure 55D) surfaces where HDMEC distribution is patchy.

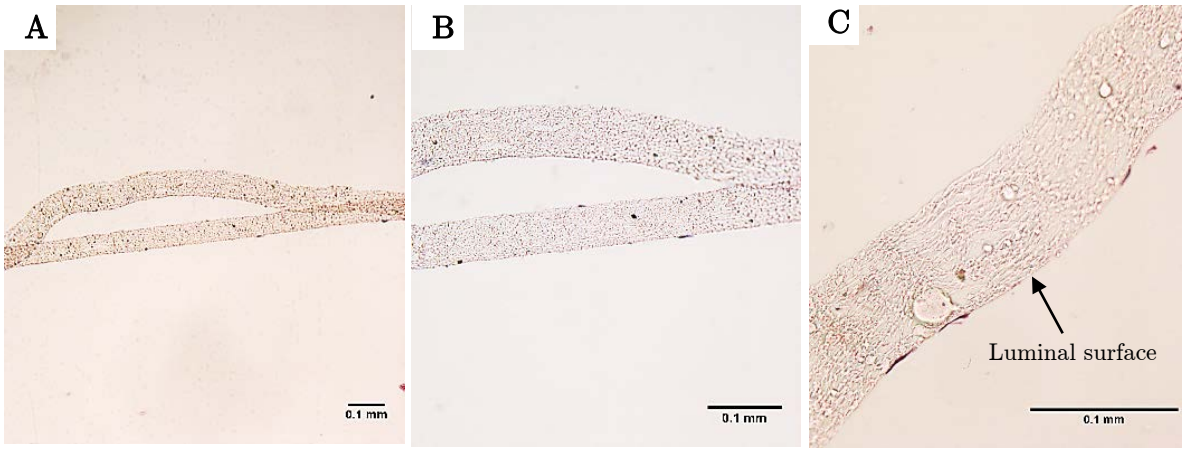


Figure 54 – H&E staining of sections of scaffolds recellularised with HDMECs and cultured under static conditions for 7 days. Varying magnifications at 10x (A), 20x (B) and 40x (C) show a lack HDMECs present.

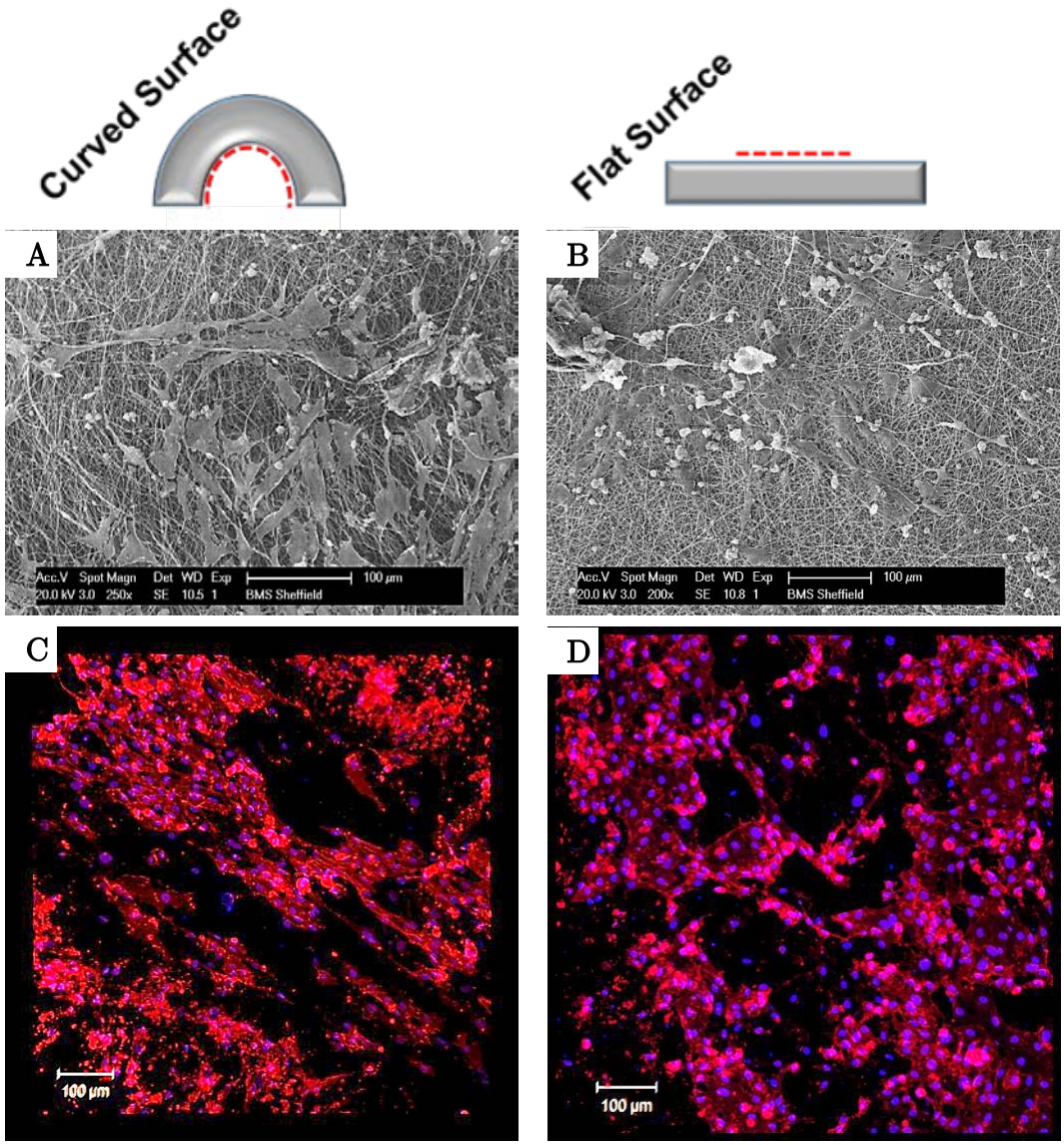


Figure 55 – Distribution of HDMECs within the PHBV pseudo-vascular scaffold. SEM images of the curved (A) and flat surface (B) shows the attachment of HDMECs onto the scaffold albeit with a sparse distribution. Fluorescence images stained for CD31+ (red) and DAPI (blue) of the curved (C) and flat (D) surfaces again shows the presence of HDMECs (red) but with an irregular coverage throughout the scaffold.

### 4.3.4. Incorporation of HDFs and their effects on re-endothelialisation

As mentioned in the previous chapter interactions between endothelial and stromal cells are important for vascularisation of regenerating tissue and it has been shown that fibroblasts play a key role as acting as a 'helper' cell modulating EC migration, viability and network formation in a 3D tissue like environment and also during the angiogenic process [88,190–192]. As with the natural vascular net HDFs were therefore co-cultured with HDMECs to investigate whether they had an effect on the re-endothlialisation of the jejunum vessels. In the case of the synthetic pseudo-vascular scaffolds HDFs were infused either:

3. Into the scaffold along with HDMECs or
4. Pipetted onto the outer surfaces of the scaffold

Figure 56 shows H&E stained sections of scaffolds recellularised with:

1. HDMECs only (A-C)
2. HDMECs and HDFs inside the channels (D-F)
3. HDMECs within the channels and HDFs on the outer surfaces (G-I)

In both cases where HDFs had been co-cultured with HDMECs there appeared to be more cells present on the scaffolds. Comparing SEM images of the different scaffolds shows a uniform coverage of cells when HDMECs and HDFs were both seeded inside the channels (Figure 57(C, D)) and when HDMECs were within the channels and HDFs were seeded on the outer surfaces (Figure 57(E, F)) when compared to recellularising with HDMECs alone ((Figure 57(A,B)). To distinguish between HDMECs and HDFs immunohistochemistry was used, where the CD31 marker was used to determine the presence of HDMECs and counterstaining with the nuclear stain DAPI was used to identify HDFs. Figure 58(A, B) shows the results of recellularising with HDMECs alone where the distribution of cells is sporadic. When adding HDFs into the channels along with HDMECs there are distinct areas occupied by both cell type on the curved

and flat surfaces (Figure 58(C, D)) although in this case the HDMECs seem to attempt to form an interconnected layer. This suggests that both cell types compete for space within the channels preventing a uniform monolayer of HDMECs from forming. However, by adding HDFs to the outer surfaces of the channels whilst recellularing the inner surfaces of the channels with HDMECs shows a very different result. Here both the curved and flat surfaces show a uniform monolayer of HDMECs (Figure 58(E, F)). To confirm that the HDMECs had formed cell-cell junctions samples were immunostained for endothelial adherens junction protein VE-Cadherin (vascular endotheial) also known as CD144. HDMECs that had been seeded into the channels with HDFs on the outer surface of the scaffolds exhibited CD144 (Figure 59) indicating that they had formed functional intercellular junctions which are a key determinant in the cellular permeability and therefore functionality of an endothelium. To test for cellular permeability FITC-Dextran could be perfused through the re-endothelialised scaffold and imaged to determine whether the HDMECs act as a functional endothelium.

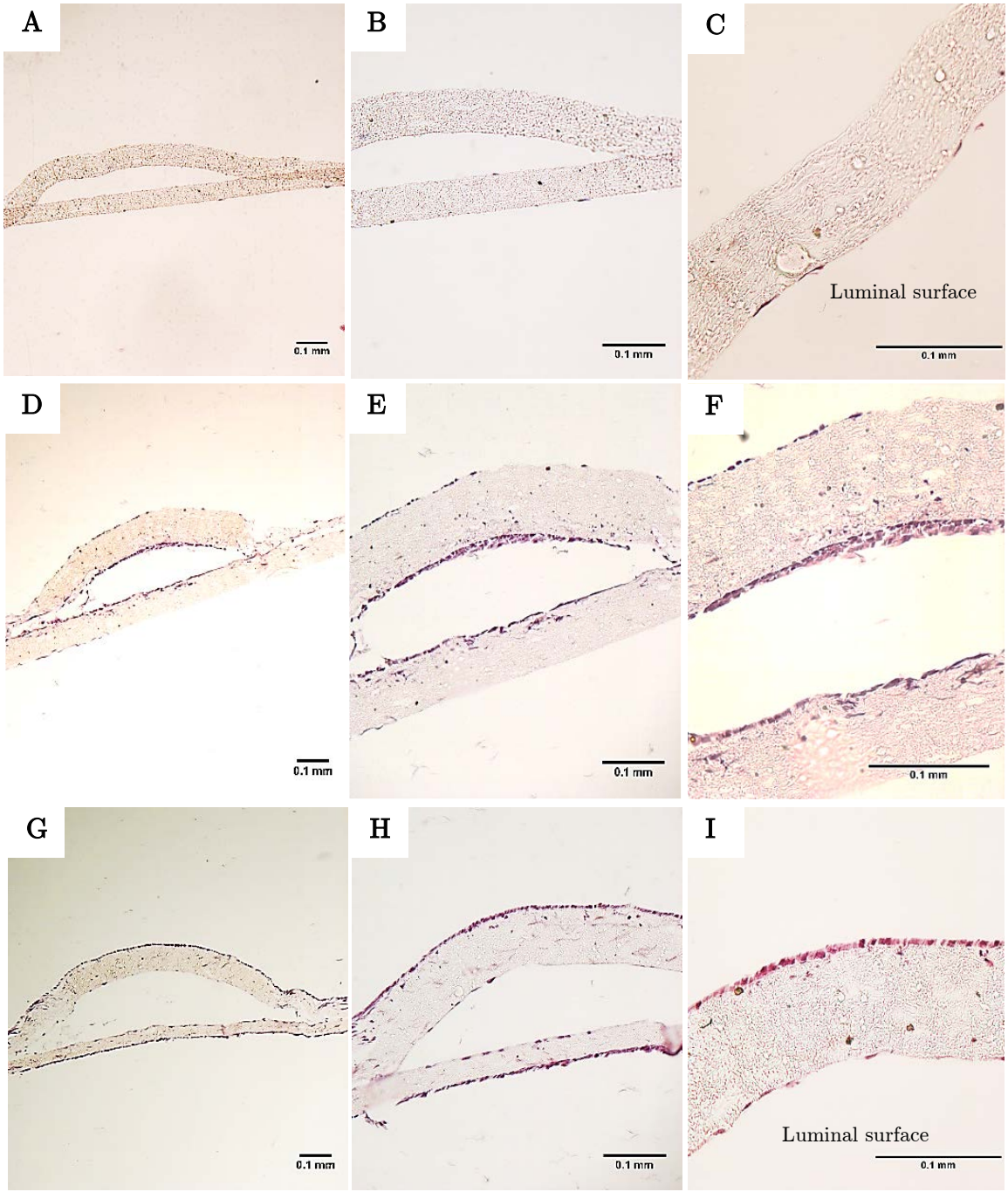


Figure 56 - H&E staining of sections of scaffolds recellularised with HDMECs only (A-C), HDMECs and HDFs both inside the channels (D-F) and HDMECs within the channels and HDFs on the outer surfaces (G-I). All samples were cultured under static conditions for 7 days. Note the presence of artefacts on the outer surface of the scaffolds shown in D-F, this could be remnants from the H&E sectioning or residual cells that had attached during the scaffold seeding process.

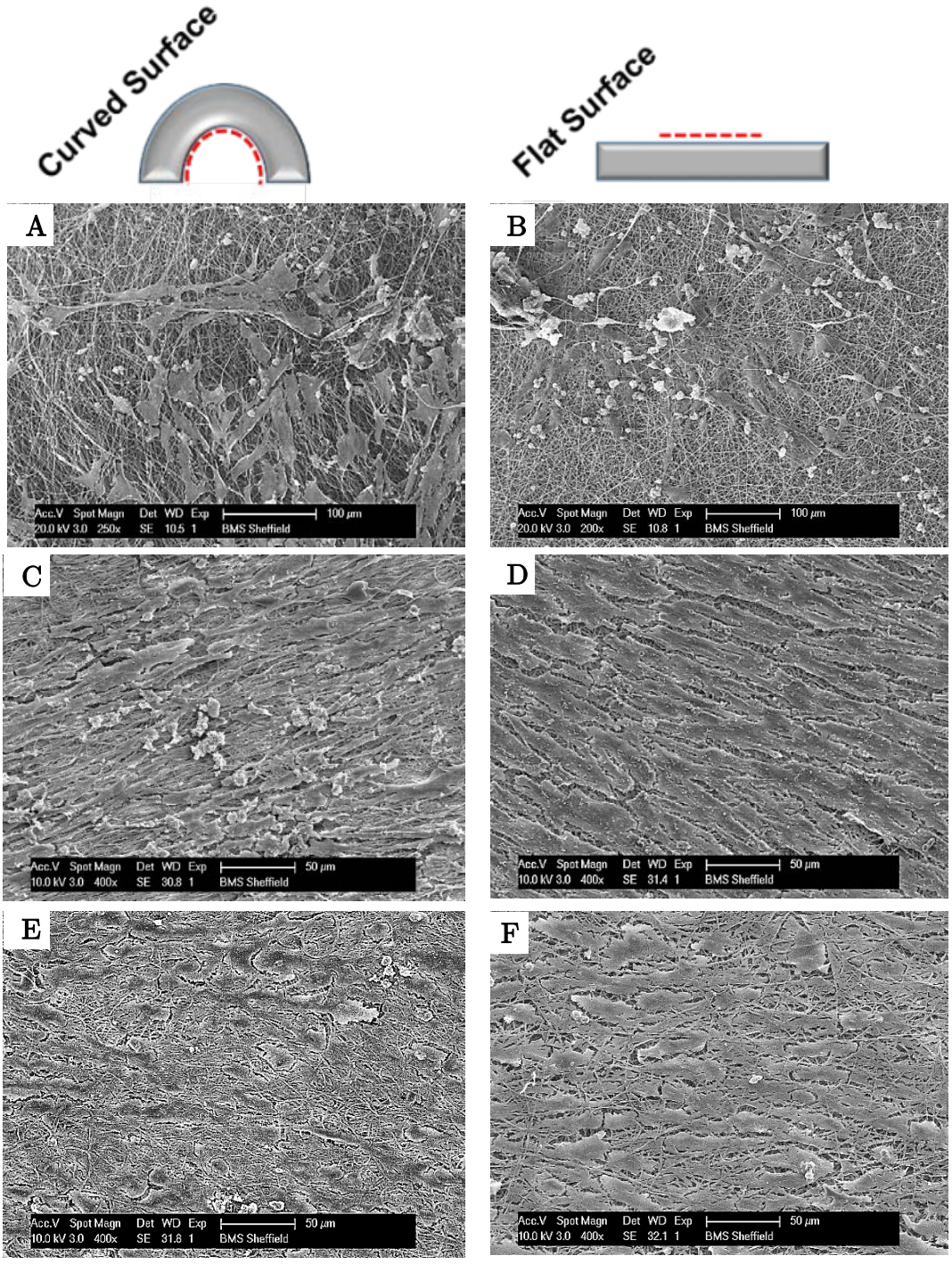


Figure 57 – SEM images of the curved and flat inner surfaces of the scaffolds recellularised with HDMECs only (A, B), HDMECs and HDFs both inside the channels (C, D) and HDMECs within the channels and HDFs on the outer surfaces (E, F). All samples were cultured under static conditions for 7 days.

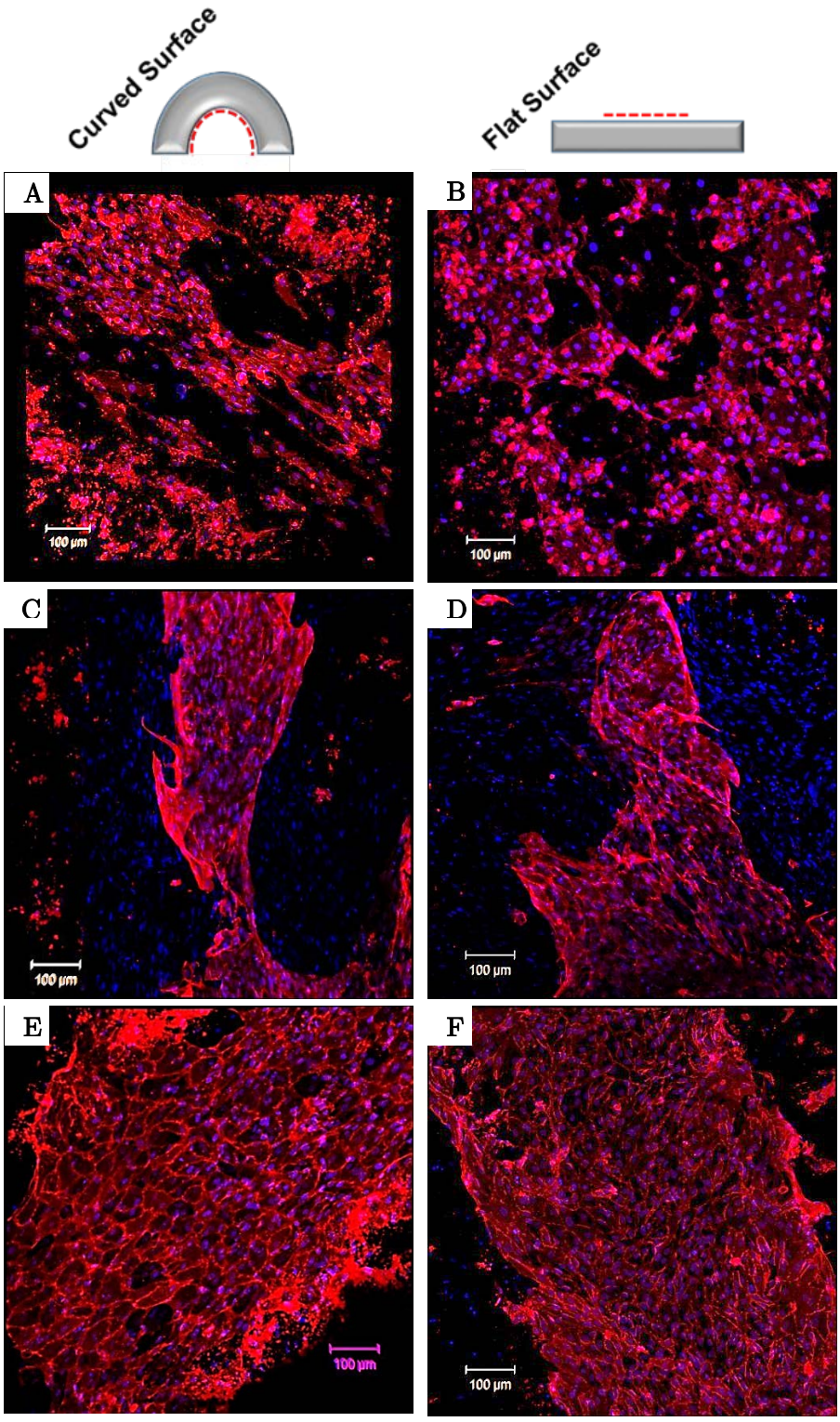


Figure 58 – Immunostained sections of the curved and flat surfaces of the scaffolds recellularised with HDMECs only (A, B), HDMECs and HDFs both inside the channels (C, D) and HDMECs within the channels and HDFs on the outer surfaces (E, F). All samples were cultured under static conditions for 7 days. CD31+ (red) and DAPI (blue).

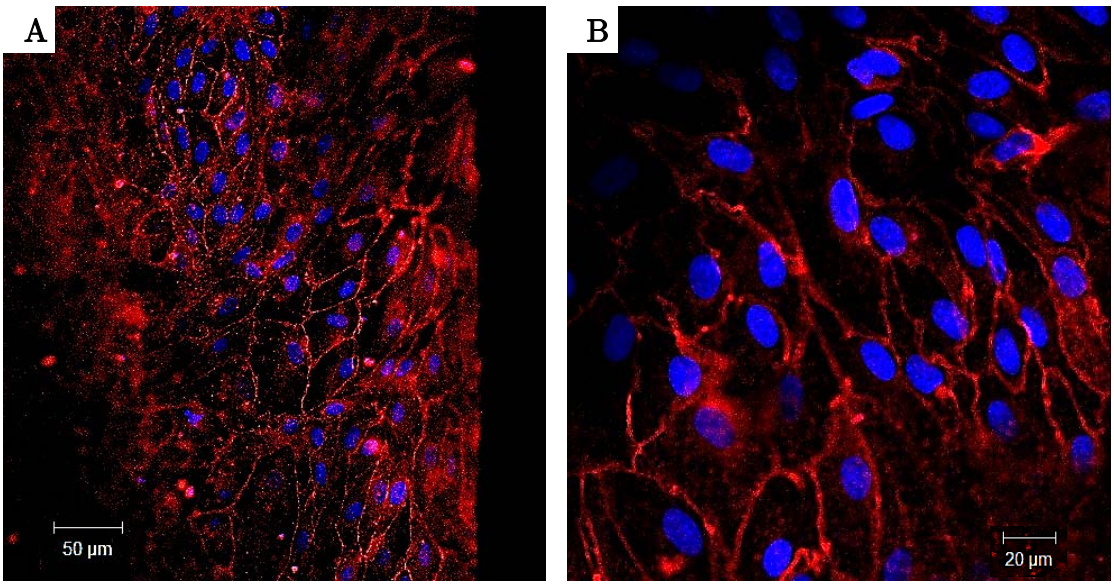


Figure 59 – Immunostained sections of the curved (A) and flat (B) surfaces of the scaffolds for CD144 (red) on samples recellularised with HDMECs within the channels and HDFs on the outer surfaces. All samples were cultured under static conditions for 7 days. Samples were counterstained with DAPI (blue).

In an attempt to try and understand why adding HDFs resulted in HDMECs transforming to produce a monolayer distribution, samples were stained for alpha smooth muscle actin (αSMA). Mature fibroblasts do not express this marker, however it is upregulated in myofibroblasts [234–236]. Myofibroblasts play a key part in tissue remodelling by both exerting and responding to mechanical stimuli but also by producing ECM components such as collagens, fibronectin and others in response to growth factor stimuli [234]. Scaffolds that had HDFs seeded either within the channels or on the outer surfaces were sectioned and in both cases showed positive staining for αSMA (Figure 60 and Figure 61 respectively). Interestingly, HDMECs also stained positive in certain areas of both scaffolds. This suggests that the HDFs and a proportion of HDMECs differentiate into myofibroblasts. Genetic labelling and RT-PCR may help determine whether this is actually the case. As a control, HDMECs and HDFs cultured on TCP were also stained for αSMA and both showed negative staining (Figure 63A and Figure 63B respectively).

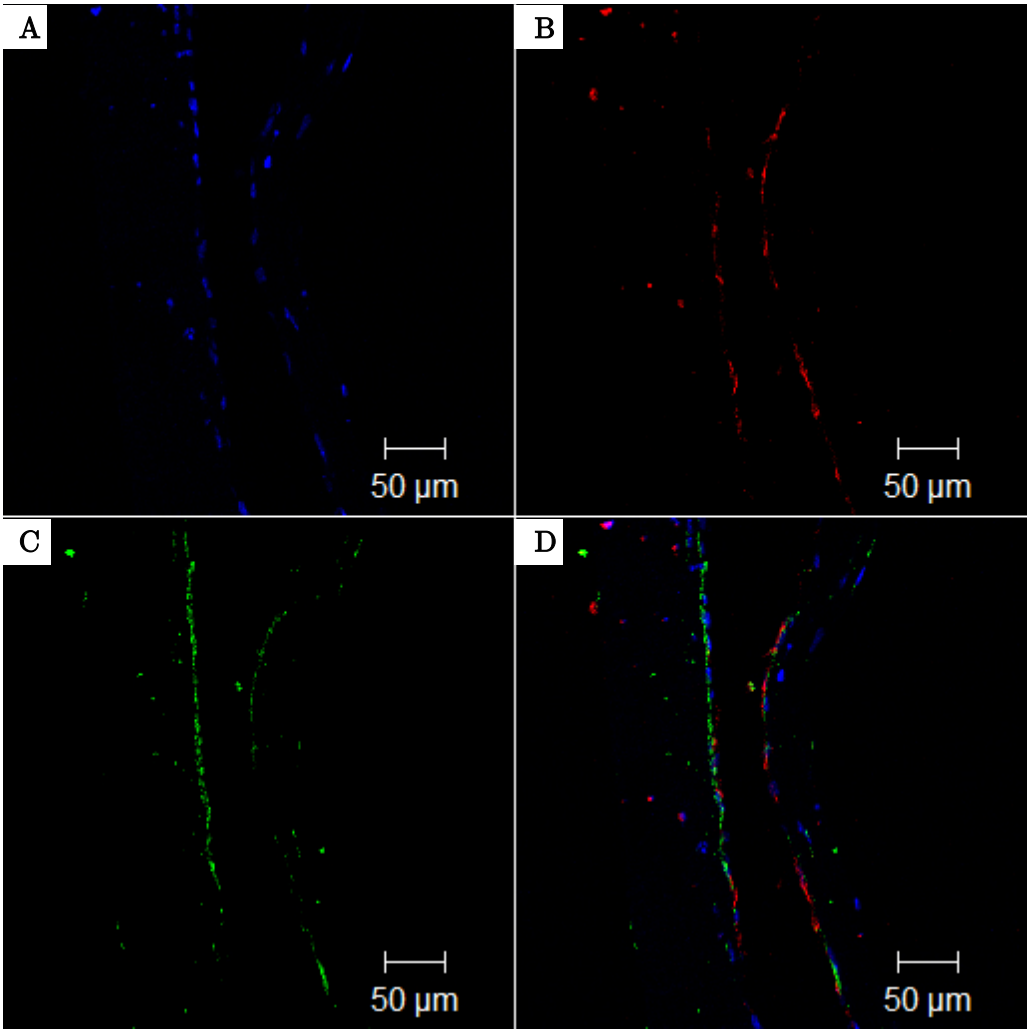


Figure 60 – Immunostained sections of scaffold recellularised with HDMECS and HDFs within the channels. DAPI staining (blue) of cells is shown in (A) with CD31+ staining (red) (B) and αSMA staining (green) (C). A merged image of all three channels is shown in (D).

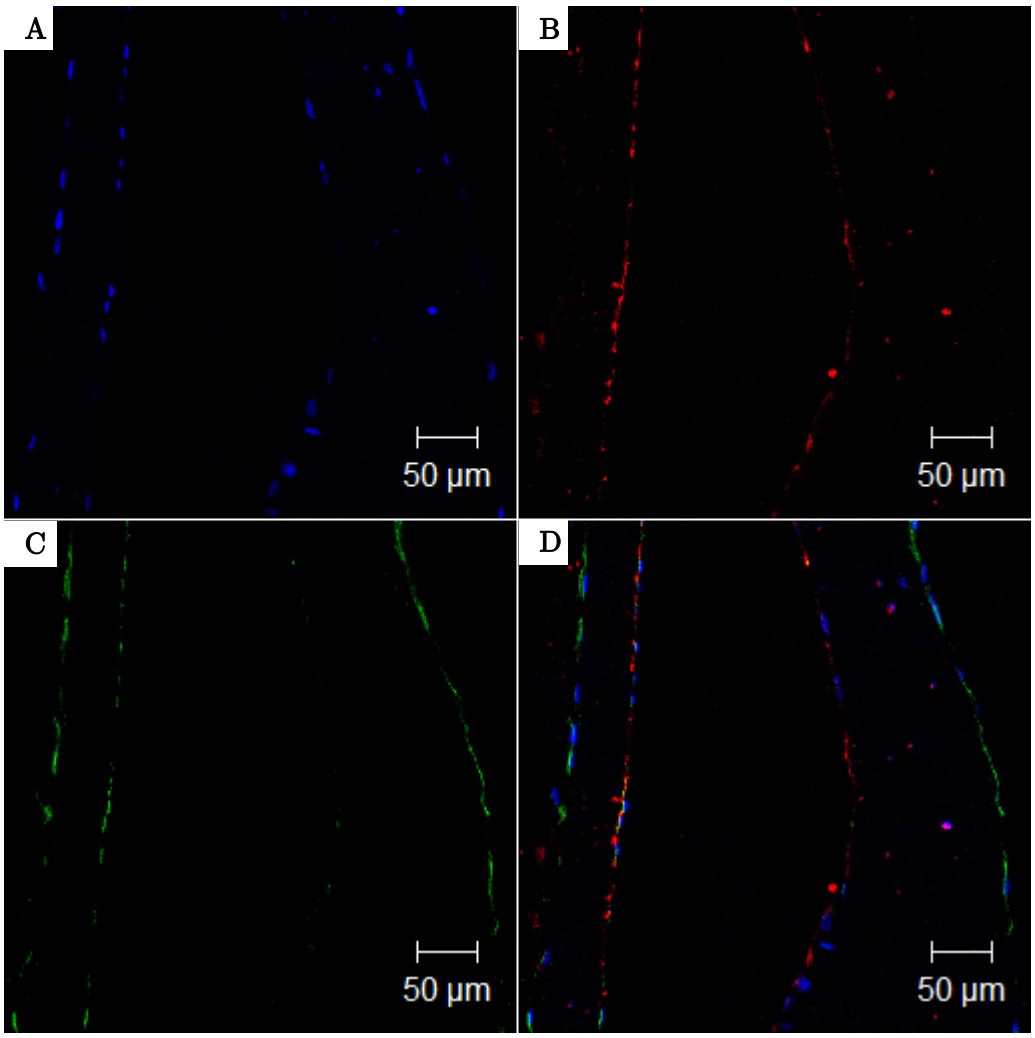


Figure 61 - Immunostained sections of scaffold recellularised with HDMECS within the channels and HDFs on the outer surfaces. DAPI staining (blue) of cells is shown in (A) with CD31+ staining (red) (B) and αSMA staining (green) (C). A merged image of all three channels is shown in (D).

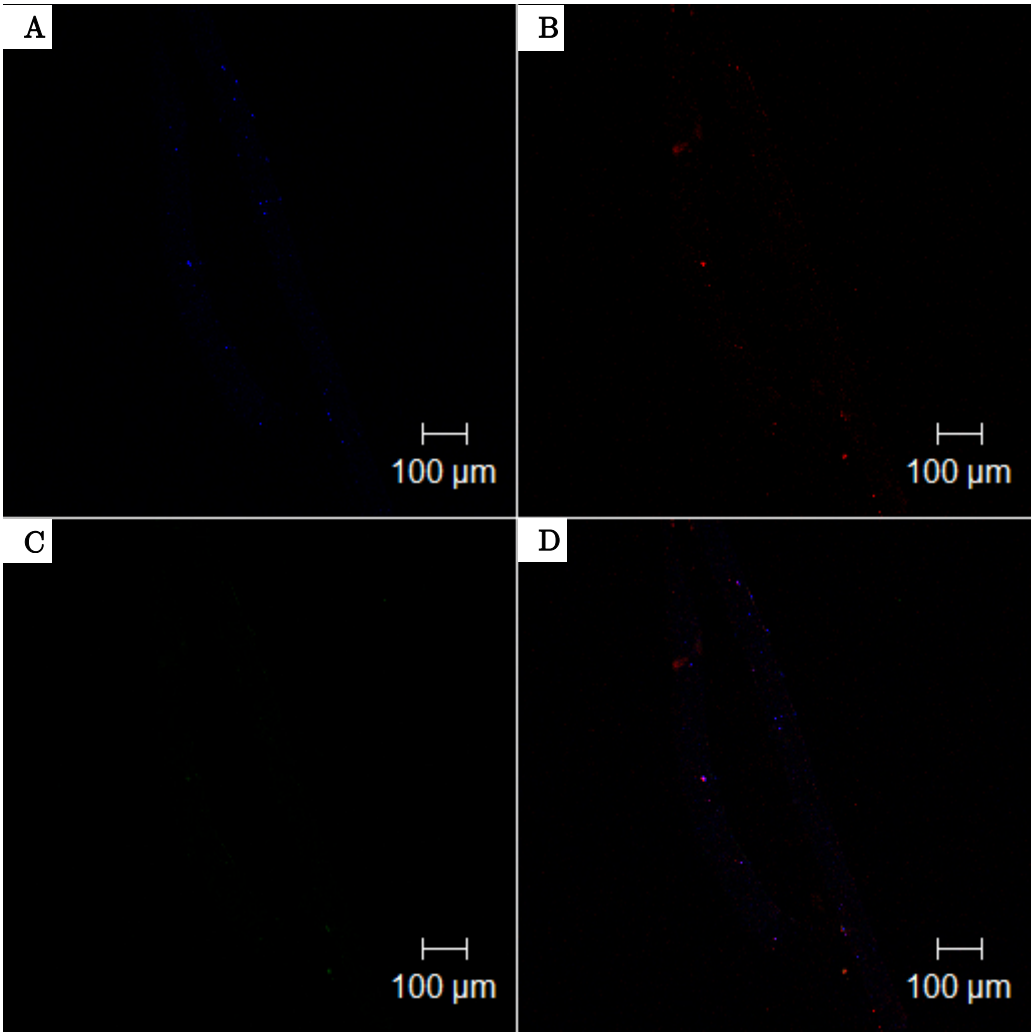


Figure 62 - Immunostained sections of scaffold recellularised with HDMECS only shows the presence of very few cells. DAPI staining (blue) of cells is shown in (A) with CD31+ staining (red) (B) and αSMA staining (green) (C). A merged image of all three channels is shown in (D).

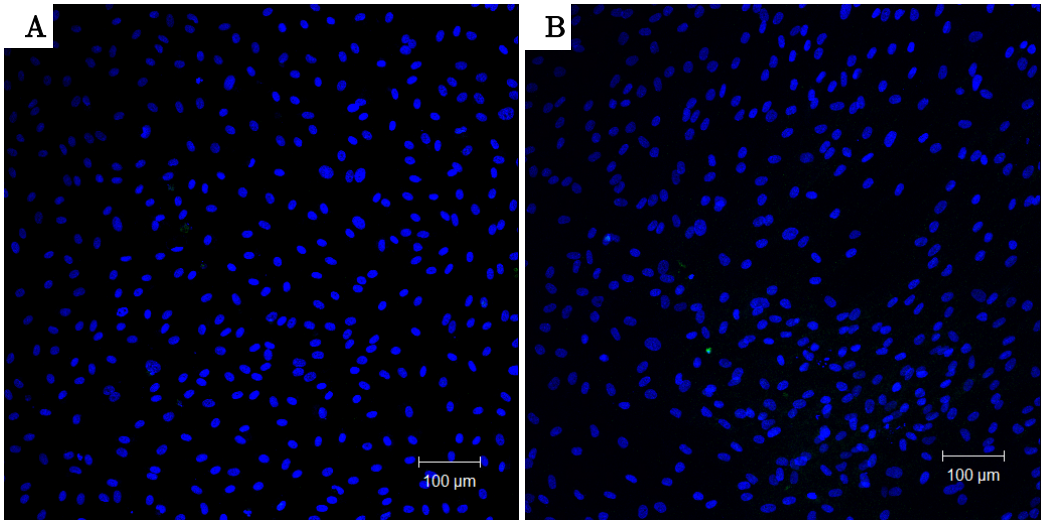


Figure 63 – Immunostaining for αSMA (green) of HDMECs (A) and HDFs (B) cultured on TCP. Counterstained with DAPI (blue) to show cell nuclei.

### 4.3.5. Use of the recellularised synthetic vascular net as an angiogenesis model

Experiments showed that recellularising the scaffolds with HDMECs inside the channels and HDFs on the outer surfaces resulted in a monolayer of HDMECs evenly distributed on both the curved and flat surfaces. This cell combination was therefore taken forward and used in the development of the angiogenesis model.

VEGF is a potent and well known stimulator of angiogenesis. To test whether HDMECs would be stimulated into sprouting, holes were pierced into the sides of the recellularised channels (due to the nanofibrous nature of the scaffold which prevents migration of cells) after 7 days before placing VEGF and non-VEGF loaded collagen gels on top of the scaffolds and culturing for a further 7 days, as illustrated in Figure 64.

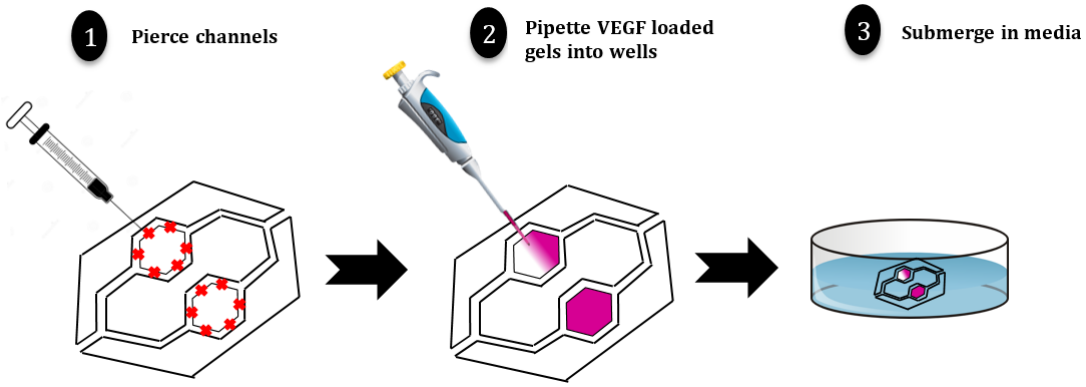


Figure 64 – Schematic showing addition of VEGF and non-VEGF loaded gels onto the surface of the recellularised pseudo-vascular scaffolds.

After 7 days in culture (after the addition of the gels) the scaffolds were fixed and immunostained (as a whole) for CD31. Confocal microscopy was used and images were taken within the collagen gel, close to the edge of the channels, as indicated by the schematic shown in Figure 65A. HDMECs were found to form interconnected networks branching outwards from the channels of the scaffold and into the VEGF loaded collagen gel (Figure 65 (B, C)). A z-stack from this area showed that the HDMECs

had in fact formed 3D capillary like structures (Figure 65D). No such structures were formed when the gel was not loaded with VEGF (Figure 65E). To determine whether these capillary like structures could be perfused FITC-lectin was injected through the scaffolds. Figure 66 shows that the FITC-lectin (green) co-localises with the CD31 staining (red) indicating that the solution has passed through the structures. Some FITC-lectin can be seen to be dispersed through the gel implying that the capillary like structures are leaky and have not developed a fully impermeable layer of HDMECs. To confirm that this is indeed the case, FITC-BSA or FITC-Dextran could also be perfused. Please note that these experiments were repeated 5 times with at least 6 replicates per experiment. However vascular network formation such as this was witnessed in the range of 25-50% of samples per experiment (i.e. 25% in experiment 1, 33% in experiment 2 etc.).

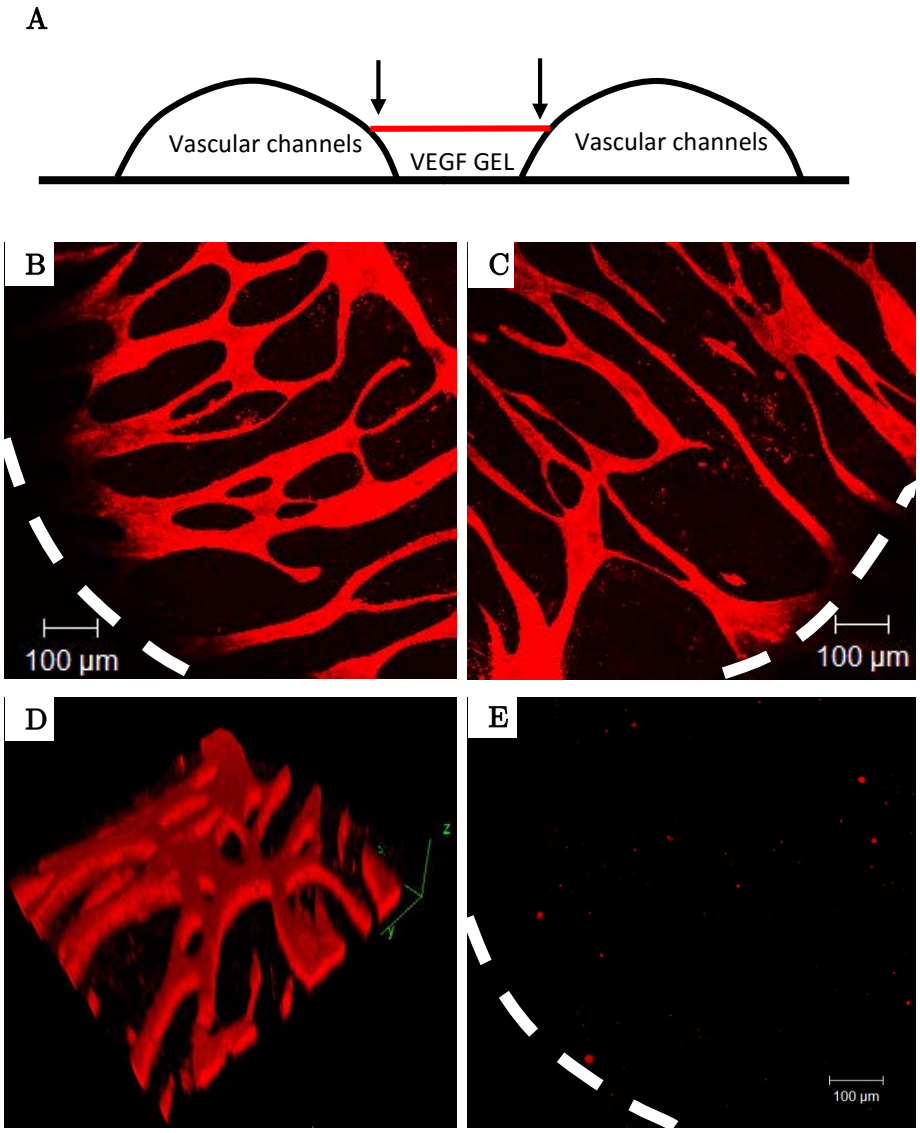


Figure 65 – Immunostained recellularised scaffolds cultured for 7 days with VEGF loaded gels placed on top. Images were taken near the boundaries between the channels and the gels as indicated by the arrows in the schematic (A). CD31 staining (red) shows the formation of an interconnected network of HDMECs (B, C) whilst a z-stack shows the formation of 3D capillary like structures (D). No such structures were formed when the gel was not loaded with VEGF (E).

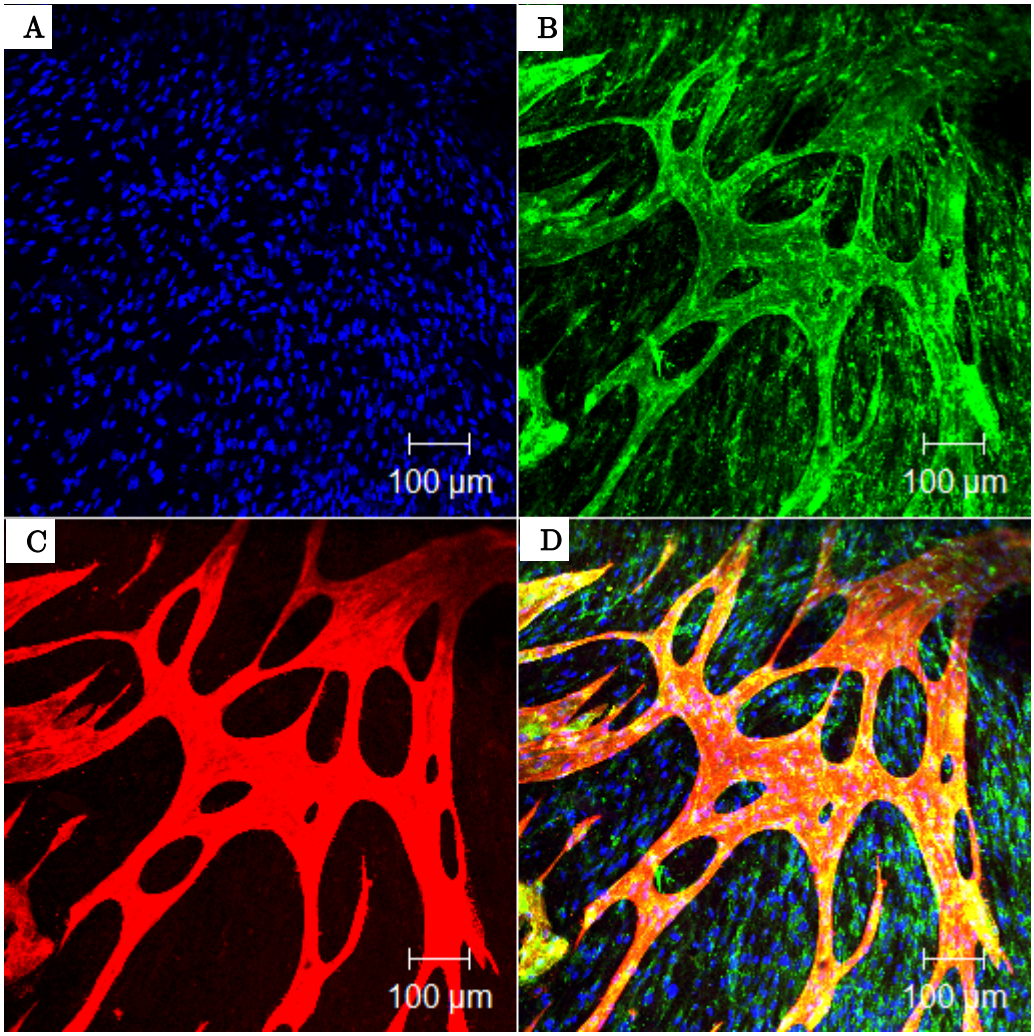


Figure 66 – Perfusion of FITC-Lectin through the recellularised (HDMECs within scaffold channels and HDMECs on the outer surface) pseudo-vascular scaffold. DAPI staining (blue) of cells is shown in (A) with FITC-Lectin (green) (B) and CD31+ staining (red) (C). A merged image of all three channels is shown in (D). Note that the cells shown in blue that are not co-localised with HDMECs (shown in red) are HDFs.

## 4.4. Discussion

### 4.4.1. Synthetic pseudo-vascular network production

Both electrospinning and innovative additive manufacturing techniques such as robocasting are used regularly for tissue engineering applications [237,238]. Combining these two approaches offers a range of advantages for future medical device design. In this study the use of robocasting allows us to readily tune the geometrical design of the vascular networks in terms of size, thickness and morphology. In addition, electrospinning allows us to create scaffolds with a range of degradation rates, fibre diameters and porosity levels [230,231,239]. By combining these approaches the production of pseudo-vascular networks such as this can be readily scaled up and sterilised for large experiments and even future clinical applications.

The polymer chosen to produce the electrospun scaffold layers was PHBV since previous work carried out in our group has found it to be biocompatible and biodegradable [230]. Not only that but it also forms nanofibers with small pore sizes which was a prerequisite of the material needed for this application. Studies have shown that cells cannot penetrate nanofibrous scaffolds due to their small fibre thickness and small pore size but do allow for the passage of essential nutrients through the pores which are necessary for cell survival [230,240,241]. Since the initial aim of this study was to form a HDMEC monolayer within the pseudo-vascular structures it was necessary that the cells did not migrate through the thickness of the scaffold. In addition it has also been shown that irrespective of the polymer material, the nanofibrous topography of electrospun scaffolds has the ability to modulate cell behaviour in a similar way to ECM fibres by guiding cell migration, controlling differentiation, aiding in cell attachment etc. [241–243]. Electrospun layers with fibre diameters of ~0.7 μm were produced and used in this study. To create the 3D pseudo-vascular nets robocasting of alginate was used. Robocasting is a room temperature extrusion based technique [229] and was used instead of techniques such as fused deposition modelling because they do not

require elevated temperatures which could potentially alter the microstructural properties of the electrospun mat. Alginate, which is a natural polysaccharide used widely in the biomedical field due to its biocompatibility [244,245], was used as the sacrificial material to form the outline of the pseudo-vascular network. Not only can it form 3D scaffolds but it can also be easily removed using EDTA [246]. Using this combination of electrospinning and robocasting it was possible to produce a nanofibrous synthetic pseudo-vascular network comprised of interconnected hollow channels. This method quickly produced multiple scaffolds for experimentation which could easily be scaled up. However printing errors were encountered during the robocasting of the alginate paste and as a result the production efficiency was ~70%, with around 10 scaffolds being wasted for every 36 produced. Since this was a preliminary study that focussed upon the use of these networks as an angiogenesis model, the efficiency of the production was deemed satisfactory for our purposes.

Prior to cell culture mechanical properties of the PHBV scaffolds were tested results show that the bulk material has an average UTS of 0.6 MPa, similar to PEUU vascular graft scaffolds that have been used previously *in vivo* [232]. The suture retention strength of this material is also similar to scaffolds that have been used *in vivo* which have a typical range of between 35-59 MPa [233].

### 4.4.2. Recellularisation of the pseudo-vascular network

In order for the electrospun pseudo-vascular net to act as a model vascular structure for angiogenesis and potentially support neovascularisation within biological structures, optimisation of seeding and growth of an endothelial monolayer within the scaffold lumen was performed. As was the case in the natural angiogenesis model discussed in Chapter 3, HDMECs were used due to their microvascular nature. Initially HDMECs were injected at high density within the lumen alone and allowed to adhere to the upper and lower surfaces for 7 days. After this time results showed the presence of CD31 and therefore HDMECs but the distribution was discontinuous with HDMECs appearing rounded and little evidence of

CD31 at cell-cell junctions. Since HDFs had been used effectively to improve the re-endothelialisation of the natural vascular channels, it was decided to apply similar techniques to the synthetic pseudo-vascular network. Therefore HDFs were co-cultured with HDMECs both inside the vascular channels and on the outer surfaces of the scaffolds. Results echoed those found when analysing the natural vascular networks. H&E staining of scaffold sections indicated that the greatest improvement in cellular coverage was observed when HDFs were cultured within the channels when compared to seeding HDFs onto the outer surfaces. In order to further characterise the cell coverage to confirm the results indicated via H&E staining the vascular nets were peeled apart to reveal the upper and lower surfaces of the channels. Immunostaining of the entire scaffold for CD31 was then performed and the samples were analysed using confocal microscopy. These technique, unlike H&E staining was able to discern between HDMECs and HDFs and did indeed show improved HDMEC coverage when HDFs were seeded within the channels of the nets but unlike H&E staining it showed that the coverage was patchy with some areas of HDMECs appearing to have detached from the pseudo-vascular net. This suggested poor cell adhesion and a potential competition for space within the channels between the two cell types. Although not very well identified through H&E staining, possibly due to their thin monolayer distribution, HDMEC coverage was vastly improved when HDFs were cultured on the outer surface of the scaffolds. In this instance HDMECs formed a continuous endothelial monolayer with a characteristic 'cobblestone' appearance and exhibited clear cell-cell junction staining of CD31, particularly on the curved surface. Furthermore, staining for the endothelial adherens junction protein VE-Cadherin confirmed the establishment of a confluent monolayer on the inside of the lumen when HDFs were cultured on the outside. This shows that HDMECs had formed funtional intercellular junctions which are a key determinant in the cellular permeabiltiy and therefore functionality of an endothlium. As was the case with the results attained from the natural vascular network, this implies that HDFs and HDMECs do not need to be in direct contact for the HDFs to act as 'helper' cells and that they communicate via soluble mediators that can penetrate through the synthetic scaffold.

Even though fibroblasts were described over 100 years ago it is their location and 'what they are not' that still defines them. Their lack of distinguishable markers means that they are often identified as 'non-SMCs', 'non-ECs' etc. [191]. Gene analysis has found that fibroblasts can be quite different depending on their location but their main purpose of synthesising and maintaining the ECM remains a common property of such cells [247]. Research looking into gene expression of fibroblasts in tumours and in locations of active wound healing have found that they are activated into myofibroblasts [248]. Unlike fibroblasts these cells can be recognised by their expression of αSMA [191]. Myofibroblasts play a key part in tissue remodelling by both exerting and responding to mechanical stimuli but also by producing ECM components such as collagens, fibronectin and others in response to growth factor stimuli [234]. Studies investigating tumour growth have also shown increased angiogenesis in xenograft models when tumour cells were co-cultured with myofibroblasts [249,250]. They have been found to enhance angiogenesis by secreting a range of growth factors including VEGF, bFGF, TGF-β, PDGFs etc. [251–255]. In an attempt to try and determine whether HDFs had been activated into myofibroblasts, which could have potentially promoted the HDMECs into producing an evenly distributed monolayer, samples were stained for αSMA. Scaffolds that had HDFs seeded either within the channels or on the outer surfaces were sectioned and in both cases showed positive staining for αSMA suggesting that they had indeed been activated into myofibroblasts. Interestingly, HDMECs also stained positive in certain areas of both scaffolds. Several studies have shown that ECs can undergo a transition towards myofibroblast like cells and deposit ECM components [256–258]. Although HDFs and a proportion of HDMECs have expressed αSMA which may indicate that growth factors and ECM proteins are being deposited leading to a more even distribution of HDMECs, much more work needs to be done to confirm if this is indeed the reason and if so what growth factors and mechanisms are involved.

### 4.4.3. The use of the recellularised pseudo-vascular network as an angiogenesis model

Since the combination of HDMECs within the channels and HDFs on the outer surface of the scaffold resulted in a uniformly distributed monolayer of interconnected HDMECs, this cell combination was used when developing the angiogenesis model (again with particular focus placed on sprouting angiogenesis). The advantage of using a scaffold such as this is that it has two hexagonal wells in the centre that can be used to deposit test substances. For the same reasons as were discussed Chapter 3 when developing the angiogenesis model from the natural vascular network, collagen loaded with VEGF was used in an attempt to induce the outgrowth of HDMECs from the re-endothelialised channels. Prior to loading the gels onto the scaffold, holes had to be pierced into the sides of the channels since the scaffold was nanofibrous. The nanfibrous properties are advantageous when initially seeding HDMECs into the channels since the small fibre diameters and pore sizes prevents migration of cells. However this is a disadvantage when the aim is to allow for the migration of cells. Gels with concentration of 2 mg/ml of collagen containing 10 ng/ml of VEGF were pipetted into the wells and allowed to set before culturing the scaffolds under static conditions for 7 days. Results showed the presence of a CD31 positive network within the collagen I gel with the appearance of a simple vascular network. This network was found in locations close to the pierced channels and extended a small way into the gel, but not entirely into the centre. Perhaps if cultured for a longer period of time migration throughout the entire gel may have been seen. To determine whether the vascular structures had formed patent tubes and could be perfused, FITC-lectin was infused through the vascular scaffold. Lectins are proteins that have been found to specifically bind to sugar complexes attached to lipids and proteins [178,179] and have been found to be extremely useful for microvascular labelling [180–182]. When conjugated with a fluorescent dye (FITC), any lectin that binds to the vascular endothelium can be visualised using fluorescence microscopy. In this study confocal imaging was used to visualise FITC-lectin and showed significant overlap with CD31. A possible justification for this could be that perfusion had occurred through the newly formed vascular network. Diffusion of FITC-lectin to areas not stained with CD31 could imply that

the vessels are leaky and HDMECs have not formed an impermeable layer. To confirm that this is indeed the case FITC-BSA or FITC-Dextran (due to their larger molecular weights) could be perfused in a repeat experiment to rule out the possibility that FITC-lectin had diffused through the scaffold first before binding to the endothelium instead of being perfused through the channels. Nevertheless these observations are validated by what has been reported in the literature where VEGF has been shown to regulate angiogenic outgrowth of ECs [226–228]. It is important to note that these experiments were repeated 5 times with at least 6 replicates per experiment and vessel formation was found in around 25-50% of samples. This variability indicates that the angiogenesis model as it stands is not reliable enough to perform large scale studies to investigate angiogenesis. Improving the reproducibility of this assay is paramount before it can be developed further. The reason for this variability could have stemmed from a number of factors including the thickness of the collagen gel used. Unfortunately the thickness was not very well controlled since the dimensions of the hexagonal well of the scaffold varied between samples and even though the same volume of collagen gel was used this variation in geometry would have resulted in a variation in thickness of the gel from sample to sample. Gel thickness has been shown to lead to the death of ECs and fibroblasts in certain studies [97]. The batch of HDMECs may have also been a contributing factor to the variations observed. Half way through this study the batch of HDMECs was changed. Batch-to-batch variation has been noted as a cause for irreproducibility in other studies that have developed *in vitro* angiogenesis assays [259]. In addition the position of the holes pierced into the channels of the nanofibrous scaffolds to allow for cellular migration differed in their position and size for each sample. This was because the holes were pierced manually with a sterile needle which did not allow for precision control of such parameters. This could have led to a variation in results if the pierced holes were above the level of the collagen gel for instance. Much more work therefore needs to be done to standardise the techniques used to perform this assay and ensure that it is reliable. However, these promising preliminary results indicate that through further development this technique offers real potential for use as a model to investigate angiogenesis *in vitro*.

### 4.4.4. Limitations

The main limitation of this model is the poor reproducibility associated with it with respect to the formation of new vessels sprouting from the channels. In developing the model re-endothelialisation of the channels was reasonably consistent. Probably more work needs to be undertaken in relation to the use of flow - certainly it can be perfused but the lack of reproducibility in the development of new vessels may relate to the response of the cells to flow which may not be optimum in this model as yet. However the fact that some evidence of new vessels was seen in approximately 50% of the experiments shows that the potential is there. As it can be perfused and can be seeded with a variety of cells which can secrete ECM components and subjected to external pro-angiogenic stimuli it has considerable potential. However, to obtain reproducible results clearly more work must be done to optimise the current variables to achieve more consistent results.

## 4.5. Summary

In this chapter robocasting and electrospinning were used to produce perfusable synthetic networks for use as an angiogenesis model. Analysis showed that nanofibrous scaffolds with hollow channels capable of perfusion were produced with similar mechanical properties as those used as vascular grafts *in vivo*. Recellularisation showed that the vascular network could be evenly re-endothelialised with HDMECs when HDFs were physically separated by seeding them on the outer surfaces of the scaffolds. Placing VEGF loaded gels onto the scaffolds caused HDMEC outgrowth to occur from within the channels into the collagen gel showing that the engineered vasculature maintains its capacity for angiogenesis. Furthermore the HDMECs appeared to have formed perfusable tubules within the gel. Unfortunately these results were not found in every experiment and indicate the need for further work to guarantee reproducible results. However, these results indicate promising steps towards the development of an *in vitro* platform in which to study angiogenesis and vascular biology in a tissue engineering context.

# Chapter 5

# Conclusions and Future Work

This project reports the development of two *in vitro* models to study sprouting angiogenesis that have the capability of combining pro-angiogenic cells with ECM components which can be monitored under flow conditions to learn more about the 'rules' of angiogenesis.

The first model was developed through the decellularisation of a rat jejunum. Initial experiments focussed on characterising the matrix to determine what it was composed of and whether the native vasculature remained patent for eventual recellularisation. Results showed that after decellularisation ~97% of the DNA content had been removed whilst preserving the vascular network. Analysis of the ECM components showed an increase in the proportion of collagen with respect to the dry weight (~30%), the retention of GAGs and laminin but did show the removal of elastin and fibronectin. Placing segments of decellularised jejunum onto the CAM model showed cell and blood vessel infiltration into the matrix indicating that it had inherent angiogenic potential. Further work could be carried out to characterise the matrix in order to determine if and what growth factors had been retained in the matrix and their quantities using an ELISA. After characterising the decellularised jejunum, experiments were carried out to determine whether the vascular network could be re-endothelialised and if so what conditions were optimal. Recellularisation showed that the vascular network could be evenly re-endothelialised with HDMECs when HDFs were seeded into the lumen and the jejunum was continuously perfused at a rate of 0.025 ml/min. Higher flow rates resulted in the loss and subsequent uneven coverage of HDMECs within the channels. Once satisfactory re-endothelialisation was observed the next step of the project was to determine whether the scaffold could be used as a test bed to model angiogenesis. Placing VEGF loaded gels onto the recellularised jejunum led to the expression of DLL4 by HDMECs indicating their transformation

into tip cells. Tip cells are synonymous with sprouting angiogenesis since they allow for the exploration of the surrounding environment to sense chemoattractants, such as VEGF, emitted as a result of hypoxia [226–228]. These results indicated the potential of this technique to model angiogenesis and overcome the shortcomings of current angiogenesis assays by allowing the inclusion of supporting cells, an ECM component and the ability to perfuse the whole scaffold. In the future, experiments could be carried out for longer time periods to see whether the HDMECs that had migrated into the collagen gels would form tubules that could subsequently be perfused with FITC-lectin (as used for the synthetic model). A host of other experiments could also be carried out to observe the effects of other growth factors (individually or in combination with others), mechanical forces (through the variation of flow rates), cellular mechanical forces (through the manipulation of Rho/ROCK pathway), tumour samples or hypoxic tissue (such as skin taken from biopsies) on the angiogenic outgrowth of HDMECs. Furthermore this model offers the potential to be repopulated with a range of other cells such as EPCs, iPSCs, SMCs etc. which may or may not show better re-endothelialisation and angiogenic outgrowth.

The second model was developed through the combination of electrospinning and robocasting to produce a synthetic pseudo-vascular network. Again, initial experiments aimed to characterise the synthetic scaffolds. Analysis showed that nanofibrous PHBV scaffolds with hollow channels capable of perfusion were produced with similar mechanical properties as those used as vascular grafts *in vivo*. After characterising the scaffold, experiments were performed to see if HDMECs would attach to the scaffold and form an interconnected monolayer. Recellularisation showed that the vascular network could be evenly re-endothelialised with HDMECs when HDFs were physically separated by seeding them on the outer surfaces of the scaffolds. This echoed the results obtained from the natural model, indicating the necessity for fibroblasts to act as helper cells to ECs. Further experiments showed that HDFs expressed the marker αSMA which is known to be upregulated upon transformation to myofibroblasts [191]. Myofibroblasts play a key part in tissue remodelling by both exerting and responding to mechanical stimuli but also by producing ECM components such as collagens, fibronectin and others in

response to growth factor stimuli [234]. They have been found to enhance angiogenesis by secreting a range of growth factors including VEGF, bFGF, TGF-β, PDGFs [251–255]. This could explain the reason for the enhanced HDMEC distribution when co-cultured with HDFs. Further work could be done to truly understand what mechanisms and cross-talk is going on between the HDMECs and HDFs to produce this enhanced cellular distribution. Once a uniform monolayer distribution of HDMECs was obtained within the channels, VEGF loaded collagen gels were placed onto the scaffold to determine whether HDMECs would migrate towards this pro-angiogenic growth factor, as was previously observed in the natural model. Results showed that HDMEC outgrowth did indeed occur from within the channels into the collagen gel. Furthermore the HDMECs appeared to have formed perfusable tubules within the gel. Unfortunately these results were not found in every experiment and indicate the need for further work to achieve reproducible results. The reason for the variation in the results was not determined and clearly indicates the complexity of these models. Nevertheless, these results indicated promising steps towards the development of a synthetic *in vitro* platform upon which to study angiogenesis and vascular biology in a tissue engineering context. In the future, studies trying to standardise the thickness of the collagen gel, position of the holes pierced into the channels and the source of ECs could be trialled in an attempt to increase the reliability of this model. If this could be improved to satisfactory levels the breath of experimentation that could be performed using this model is extensive. As in the case of the natural net, different cell combinations, growth factors, perfusion conditions etc. could be studied in relation to angiogenesis. Perfusion was not focussed upon when developing this model due to the even monolayer HDMEC distribution obtained under static conditions but it would be very interesting to observe the effects of perfusion on HDMEC distribution and outgrowth into the VEGF loaded collagen gel. In addition, the link between inflammatory cells and the angiogenic process is gaining increasing interest with recent studies showing macrophage mediated angiogenic activation [260–262]. Indeed recent data from the Fitzpatrick laboratory have shown differing responses to M1 and M2 macrophages in 3D models [263]. This model would be a useful platform to further study the effects of such cells on the angiogenic outgrowth of ECs from the

vascular channels and expand knowledge in this critical area. This is a substantial challenge but should be achievable using this model.

In the development of both of these models the majority of data obtained has been qualitative. Future experiments would aim to convert many of the fluorescent images into quantitative measures of cell viability, distribution etc. via the measurement and comparison of fluorescence to arrive at objective conclusions.

Overall, these two models offer novel ways to investigate factors affecting the angiogenic process. The advantages and disadvantages of both models are summarised in Table 24. They overcome limitations of current *in vitro* models since they offer the capability of combining pro-angiogenic cells with ECM components that can be monitored under flow conditions. This could be very useful not only in understanding the basic science underlying angiogenesis but also in pre-clinical studies to develop and evaluate therapeutic treatments for tissue engineering and related applications.

Table 24 – Summary of the pros and cons associated with the synthetic and naturally derived angiogenesis models.

| | Synthetic Net | Natural Net |
|---|---|---|
| **Pros** | Easy manufacture and scale up | Contains ECM components (and growth factors) |
| | Simple to cannulate | Has physiologically relevant architecture |
| | Can vary geometry | Cells are able to break down matrix and sprout 'naturally' |
| | Can introduce flow | Can introduce flow |
| | Can combine different cell types Can alter material choice/properties<br>Simple to post process and analyse | Can combine different cell types |
| **Cons** | Doesn't contain any inherent ECM components | Can't vary geometry/size easily |
| | Requires holes to be punctured in scaffold for gel outgrowth experiments | Difficult to cannulate – requires dissection microscope and practise |
| | Doesn't contain as much geometrical detail as physiological vasculature | Time consuming to retrieve tissue/decellularise/sterilise |
| | | Batch-to-batch variation |
| | | Requires a source of animals – relatively expensive |

# References


[1] K.R. Stevens, K.L. Kreutziger, S.K. Dupras, F.S. Korte, M. Regnier, V. Muskheli, et al., Physiological function and transplantation of scaffold-free and vascularized human cardiac muscle tissue, Proc. Natl. Acad. Sci. U. S. A. 106 (2009) 16568–16573.

[2] P. Carmeliet, Manipulating angiogenesis in medicine, J. Intern. Med. 255 (2004) 538–561.

[3] S. Patan, Vasculogenesis and angiogenesis as mechanisms of vascular network formation, growth and remodeling, J. Neurooncol. 50 (2000) 1–15.

[4] P. Carmeliet, Mechanisms of angiogenesis and arteriogenesis, Nat. Med. 6 (2000) 389–395.

[5] P.H. Burri, R. Hlushchuk, V. Djonov, Intussusceptive angiogenesis: Its emergence, its characteristics, and its significance, Dev. Dyn. 231 (2004) 474–488.

[6] Y.T. Shiu, S. Li, W.A. Marganski, S. Usami, M.A. Schwartz, Y.L. Wang, et al., Rho mediates the shear-enhancement of endothelial cell migration and traction force generation, Biophys. J. 86 (2004) 2558–2565.

[7] E.M. Conway, D. Collen, P. Carmeliet, Molecular mechanisms of blood vessel growth, Cardiovasc. Res. 49 (2001) 507-521.

[8] M. Potente, H. Gerhardt, P. Carmeliet, Basic and Therapeutic Aspects of Angiogenesis, Cell. 146 (2011) 873–887.

[9] S. Germain, C. Monnot, L. Muller, A. Eichmann, Hypoxia-driven angiogenesis: role of tip cells and extracellular matrix scaffolding, Curr. Opin. Hematol. 17 (2010) 245–251.

[10] A.S. Chung, N. Ferrara, Developmental and Pathological Angiogenesis, in: R. Schekman, L. Goldstein, R. Lehmann (Eds.), Annu. Rev. Cell Dev. Biol. Vol 27, Annual Reviews, Palo Alto, 2011: pp. 563–584.

[11] W.G. Kaelin, P.J. Ratcliffe, Oxygen sensing by metazoans: the central role of the HIF hydroxylase pathway., Mol. Cell. 30 (2008) 393–402.

[12] B.H. Jiang, J.Z. Zheng, S.W. Leung, R. Roe, G.L. Semenza, Transactivation and inhibitory domains of hypoxia-inducible factor 1alpha. Modulation of transcriptional activity by oxygen tension., J. Biol. Chem. 272 (1997) 19253–60.

[13] C.W. Pugh, J.F. O'Rourke, M. Nagao, J.M. Gleadle, P.J. Ratcliffe, Activation of hypoxia-inducible factor-1; definition of regulatory domains within the alpha subunit., J. Biol. Chem. 272 (1997) 11205–14.

[14] B.L. Krock, N. Skuli, M.C. Simon, Hypoxia-induced angiogenesis: good and evil, Genes Cancer. 2 (2011) 1117–1133.

[15] D.G. Duda, D. Fukumura, R.K. Jain, Role of eNOS in neovascularization: NO for endothelial progenitor cells, Trends Mol. Med. 10 (2004) 143–145.

[16] K. Doi, T. Ikeda, A. Marui, T. Kushibiki, Y. Arai, K. Hirose, et al., Enhanced angiogenesis by gelatin hydrogels incorporating basic fibroblast growth factor in rabbit model of hind limb ischemia, Heart Vessels. 22 (2007) 104–108.

[17] M. Przybylski, A review of the current research on the role of bFGF and VEGF in angiogenesis, J. Wound Care. 18 (2009) 516–519.

[18] R.O. Hynes, The extracellular matrix: not just pretty fibrils, Science (80-. ). 326 (2009) 1216–1219.

[19] N. Ferrara, Role of vascular endothelial growth factor in regulation of physiological angiogenesis, Am J Physiol Cell Physiol. 280 (2001) C1358–1366.

[20] S. Soker, S. Takashima, H.Q. Miao, G. Neufeld, M. Klagsbrun, Neuropilin-1 is expressed by endothelial and tumor cells as an isoform-specific receptor for vascular endothelial growth factor., Cell. 92 (1998) 735–45.

[21] A.M. Byrne, D.J. Bouchier-Hayes, J.H. Harmey, Angiogenic and cell

survival functions of Vascular Endothelial Growth Factor (VEGF), J. Cell. Mol. Med. 9 (2005) 777–794.

[22] N. Ferrara, H.P. Gerber, The role of vascular endothelial growth factor in angiogenesis, Acta Haematol. 106 (2001) 148–156.

[23] A. Ahluwalia, A. S Tarnawski, Critical role of hypoxia sensor-HIF-1α in VEGF gene activation. Implications for angiogenesis and tissue injury healing, Curr. Med. Chem. 19 (2012) 90–97.

[24] C. Hellberg, A. Ostman, C.H. Heldin, PDGF and Vessel Maturation, in: R. Liersch, W.E. Berdel, T. Kessler (Eds.), Angiogenes. Inhib., Springer-Verlag Berlin, Berlin, 2010: pp. 103–114.

[25] V. V Orlova, Z. Liu, M.-J.M.-J. Goumans, P. ten Dijke, Controlling angiogenesis by two unique TGF-beta type I receptor signaling pathways, Histol. Histopathol. 26 (2011) 1219–1230.

[26] J.F. Santibanez, M. Quintanilla, C. Bernabeu, TGF-beta/TGF-beta receptor system and its role in physiological and pathological conditions, Clin. Sci. 121 (2011) 233–251.

[27] M.T. Holderfield, C.C.W. Hughes, Crosstalk between vascular endothelial growth factor, notch, and transforming growth factor-beta in vascular morphogenesis, Circ. Res. 102 (2008) 637–652.

[28] P. Carmeliet, Angiogenesis in health and disease, Nat. Med. 9 (2003) 653–660.

[29] C. Frantz, K.M. Stewart, V.M. Weaver, The extracellular matrix at a glance, J. Cell Sci. 123 (2010) 4195–4200.

[30] L. Krishnan, J.B. Hoying, H. Nguyen, H. Song, J.A. Weiss, Interaction of angiogenic microvessels with the extracellular matrix, Am. J. Physiol. Circ. Physiol. 293 (2007) H3650–H3658.

[31] E.L. Pardue, S. Ibrahim, A. Ramamurthi, Role of hyaluronan in angiogenesis and its utility to angiogenic tissue engineering, Organogenesis. 4 (2008) 203–214.

[32] C.J. Avraamides, B. Garmy-Susini, J.A. Varner, Integrins in angiogenesis and lymphangiogenesis, Nat. Rev. Cancer. 8 (2008) 604–617.

[33] A. Seker, O. Yildirim, O. Kurtkaya, A. Sav, M. Gunel, M.N. Pamir, et al., Expression of integrins in cerebral arteriovenous and cavernous malformations, Neurosurgery. 58 (2006) 159–167.

[34] S.M. Weis, D.A. Cheresh, alpha v Integrins in Angiogenesis and Cancer, Cold Spring Harb. Perspect. Med. 1 (2011).

[35] D. Marmé, N. Fusenig, Tumor angiogenesis: basic mechanisms and cancer therapy, Heidelberg: Springer, 2007.

[36] J.H.C. Wang, J.-S. Lin, Cell traction force and measurement methods, Biomech. Model. Mechanobiol. 6 (2007) 361–371.

[37] Y. Shiu, J.A. Weiss, J.B. Hoying, M.N. Iwamoto, I.S. Joung, C.T. Quam, The role of mechanical stresses in angiogenesis., Crit. Rev. Biomed. Eng. 33 (2005) 431.

[38] R. Ananthakrishnan, A. Ehrlicher, The forces behind cell movement, Int. J. Biol. Sci. 3 (2007) 303–317.

[39] M. Amano, M. Nakayama, K. Kaibuchi, Rho-kinase/ROCK: A key regulator of the cytoskeleton and cell polarity., Cytoskeleton (Hoboken). 67 (2010) 545–54.

[40] R. van der Meel, M.H. Symons, R. Kudernatsch, R.J. Kok, R.M. Schiffelers, G. Storm, et al., The VEGF/Rho GTPase signalling pathway: A promising target for anti-angiogenic/anti-invasion therapy, Drug Discov. Today. 16 (2011) 219–228.

[41] C.J. Underwood, L.T. Edgar, J.B. Hoying, J.A. Weiss, Cell-generated traction forces and the resulting matrix deformation modulate microvascular alignment and growth during angiogenesis, Am. J. Physiol. Circ. Physiol. 307 (2014) H152–H164.

[42] L. Lamalice, F. Le Boeuf, J. Huot, Endothelial cell migration during angiogenesis, Circ. Res. 100 (2007) 782–794.

[43] A.L. Sieminski, R.P. Hebbel, K.J. Gooch, The relative magnitudes of endothelial force generation and matrix stiffness modulate capillary morphogenesis in vitro, Exp. Cell Res. 297 (2004) 574–584.

[44] P.A. Galie, D.H.T. Nguyen, C.K. Choi, D.M. Cohen, P.A. Janmey, C.S. Chen, Fluid shear stress threshold regulates angiogenic

sprouting, Proc. Natl. Acad. Sci. U. S. A. 111 (2014) 7968–7973.

[45] A.L. Zhou, S. Egginton, M.D. Brown, O. Hudlicka, Capillary growth in overloaded, hypertrophic adult rat skeletal muscle: An ultrastructural study, Anat. Rec. 252 (1998) 49–63.

[46] Z. Yan, M. Okutsu, Y.N. Akhtar, V.A. Lira, Regulation of exercise-induced fiber type transformation, mitochondrial biogenesis, and angiogenesis in skeletal muscle, J. Appl. Physiol. 110 (2011) 264–274.

[47] G.L. Semenza, Vasculogenesis, angiogenesis, and arteriogenesis: Mechanisms of blood vessel formation and remodeling, J. Cell. Biochem. 102 (2007) 840–847.

[48] M. Heil, I. Eitenmuller, T. Schmitz-Rixen, W. Schaper, Arteriogenesis versus angiogenesis: similarities and differences, J. Cell. Mol. Med. 10 (2006) 45–55.

[49] J.R. Fuchs, B.A. Nasseri, J.P. Vacanti, Tissue engineering: A 21st century solution to surgical reconstruction, Ann. Thorac. Surg. 72 (2001) 577–591.

[50] A. Atala, Tissue engineering and regenerative medicine: Concepts for clinical application, Rejuvenation Res. 7 (2004) 15–31.

[51] C.K. Griffith, C. Miller, R.C.A. Sainson, J.W. Calvert, N.L. Jeon, C.C.W. Hughes, et al., Diffusion limits of an in vitro thick prevascularized tissue, Tissue Eng. 11 (2005) 257–266.

[52] H. Sekine, T. Shimizu, K. Sakaguchi, I. Dobashi, M. Wada, M. Yamato, et al., In vitro fabrication of functional three-dimensional tissues with perfusable blood vessels, Nat. Commun. 4 (2013) 1399.

[53] S. Sekiya, T. Shimizu, M. Yamato, A. Kikuchi, T. Okano, Bioengineered cardiac cell sheet grafts have intrinsic angiogenic potential, Biochem. Biophys. Res. Commun. 341 (2006) 573–582.

[54] A. Atala, S.B. Bauer, S. Soker, J.J. Yoo, A.B. Retik, Tissue-engineered autologous bladders for patients needing cystoplasty, Lancet. 367 (2006) 1241–1246.

[55] T. Dvir, A. Kedem, E. Ruvinov, O. Levy, I. Freeman, N. Landa, et

al., Prevascularization of cardiac patch on the omentum improves its therapeutic outcome, Proc. Natl. Acad. Sci. U. S. A. 106 (2009) 14990–14995.

[56] Y. Tanaka, A. Tsutsumi, D.M. Crowe, S. Tajima, W.A. Morrison, Generation of an autologous tissue (matrix) flap by combining an arteriovenous shunt loop with artificial skin in rats: preliminary report, Br. J. Plast. Surg. 53 (2000) 51–57.

[57] Y. Asano, S. Ichioka, M. Shibata, J. Ando, T. Nakatsuka, Sprouting from arteriovenous shunt vessels with increased blood flow, Med. Biol. Eng. Comput. 43 (2005) 126–130.

[58] H.L.M. Cheng, C. Wallis, Z.P. Shou, W.A. Farhat, Quantifying angiogenesis in VEGF-enhanced tissue-engineered bladder constructs by dynamic contrast-enhanced MRI using contrast agents of different molecular weights, J. Magn. Reson. Imaging. 25 (2007) 137–145.

[59] W. Chen, C.Y. Shi, S.H. Yi, B. Chen, W.W. Zhang, Z.Q. Fang, et al., Bladder Regeneration by Collagen Scaffolds With Collagen Binding Human Basic Fibroblast Growth Factor, J. Urol. 183 (2010) 2432–2439.

[60] L.H. Zhou, B. Yang, C. Sun, X.F. Qiu, Z.Y. Sun, Y. Chen, et al., Coadministration of Platelet-Derived Growth Factor-BB and Vascular Endothelial Growth Factor with Bladder Acellular Matrix Enhances Smooth Muscle Regeneration and Vascularization for Bladder Augmentation in a Rabbit Model, Tissue Eng. Part A. 19 (2013) 264–276.

[61] M.K. Smith, K.W. Riddle, D.J. Mooney, Delivery of hepatotrophic factors fails to enhance longer-term survival of subcutaneously transplanted hepatocytes, Tissue Eng. 12 (2006) 235–244.

[62] T.P. Richardson, M.C. Peters, A.B. Ennett, D.J. Mooney, Polymeric system for dual growth factor delivery, Nat. Biotechnol. 19 (2001) 1029–1034.

[63] K. Ohashi, T. Yokoyama, M. Yamato, H. Kuge, H. Kanehiro, M. Tsutsumi, et al., Engineering functional two- and three-dimensional liver systems in vivo using hepatic tissue sheets, Nat. Med. 13 (2007)

880–885.

[64] N. Kanda, N. Morimoto, A.A. Ayvazyan, S. Takemoto, K. Kawai, Y. Nakamura, et al., Evaluation of a Novel Collagen-Gelatin Scaffold for Achieving the Sustained Release of Basic Fibroblast Growth Factor in a Diabetic Mouse Model, J. Tissue Eng. Regen. Med. 8 (2014) 29–40.

[65] N. Morimoto, K. Yoshimura, M. Niimi, T. Ito, R. Aya, J. Fujitaka, et al., Novel Collagen/Gelatin Scaffold with Sustained Release of Basic Fibroblast Growth Factor: Clinical Trial for Chronic Skin Ulcers, Tissue Eng. Part A. 19 (2013) 1931–1940.

[66] K. Kawai, S. Suzuki, Y. Tabata, Y. Ikada, Y. Nishimura, Accelerated tissue regeneration through incorporation of basic fibroblast growth factor-impregnated gelatin microspheres into artificial dermis, Biomaterials. 21 (2000) 489–499.

[67] N. Kanda, N. Morimoto, S. Takemoto, A. Ayvazyan, K. Kawai, Y. Sakamoto, et al., Deliberation of the concentration of basic fibroblast growth factor impregnated into collagen gelatin sponges, Wound Repair Regen. 18 (2010) A5–A5.

[68] B. Hendrickx, J.J. Vranckx, A. Luttun, Cell-Based Vascularization Strategies for Skin Tissue Engineering, Tissue Eng. Part B-Reviews. 17 (2011) 13–24.

[69] D.M. Supp, A.P. Supp, S.M. Bell, S.T. Boyce, Enhanced vascularization of cultured skin substitutes genetically modified to overexpress vascular endothelial growth factor, J. Invest. Dermatol. 114 (2000) 5–13.

[70] R.J. Trent, Molecular Medicine: Genomics to Personalized Healthcare, San Diego: Elsevier Academic Press, 2012 4th Edition.

[71] G. Vunjak-Noyakovic, K.O. Lui, N. Tandon, K.R. Chien, G. Vunjak-Novakovic, K.O. Lui, et al., Bioengineering heart muscle: a paradigm for regenerative medicine, Annu. Rev. Biomed. Eng. 13 (2011) 245-267.

[72] D. Schultheiss, A.I. Gabouev, S. Cebotari, I. Tudorache, T. Walles, N. Schlote, et al., Biological vascularized matrix for bladder tissue

engineering: Matrix preparation, reseeding technique and short-term implantation in a porcine model, J. Urol. 173 (2005) 276–280.

[73] F. Wezel, J. Southgate, D.F.M. Thomas, Regenerative medicine in urology, Bju Int. 108 (2011) 1046–1065.

[74] U. Sarig, G.C.T. Au-Yeung, Y. Wang, T. Bronshtein, N. Dahan, F.Y.C. Boey, et al., Thick Acellular Heart Extracellular Matrix with Inherent Vasculature: A Potential Platform for Myocardial Tissue Regeneration, Tissue Eng. Part A. 18 (2012) 2125–2137.

[75] B.E. Uygun, A. Soto-Gutierrez, H. Yagi, M.L. Izamis, M.A. Guzzardi, C. Shulman, et al., Organ reengineering through development of a transplantable recellularized liver graft using decellularized liver matrix, Nat. Med. 16 (2010) 814–U120.

[76] S.F. Badylak, D. Taylor, K. Uygun, Whole-Organ Tissue Engineering: Decellularization and Recellularization of Three-Dimensional Matrix Scaffolds, Annu. Rev. Biomed. Eng. 13 (2011) 27–53.

[77] P.M. Baptista, M.M. Siddiqui, G. Lozier, S.R. Rodriguez, A. Atala, S. Soker, The Use of Whole Organ Decellularization for the Generation of a Vascularized Liver Organoid, Hepatology. 53 (2011) 604–617.

[78] J. Bao, Y. Shi, H. Sun, X. Yin, R. Yang, L. Li, et al., Construction of a Portal Implantable Functional Tissue-Engineered Liver Using Perfusion-Decellularized Matrix and Hepatocytes in Rats, Cell Transplant. 20 (2011) 753-766.

[79] P.M. Crapo, T.W. Gilbert, S.F. Badylak, An overview of tissue and whole organ decellularization processes, Biomaterials. 32 (2011) 3233–3243.

[80] D.M. Hoganson, H.I. Pryor, J.P. Vacanti, Tissue Engineering and Organ Structure: A Vascularized Approach to Liver and Lung, Pediatr Res. 63 (2008) 520–526.

[81] E. Leclerc, Y. Sakai, T. Fujii, Microfluidic PDMS (polydimethylsiloxane) bioreactor for large-scale culture of hepatocytes, Biotechnol. Prog. 20 (2004) 750–755.

[82] M.J. Powers, K. Domansky, M.R. Kaazempur-Mofrad, A. Kalezi, A. Capitano, A. Upadhyaya, et al., A microfabricated array bioreactor for perfused 3D liver culture, Biotechnol. Bioeng. 78 (2002) 257–269.

[83] A. Marsano, R. Maidhof, J. Luo, K. Fujikara, E.E. Konofagou, A. Banfi, et al., The effect of controlled expression of VEGF by transduced myoblasts in a cardiac patch on vascularization in a mouse model of myocardial infarction, Biomaterials. 34 (2013) 393–401.

[84] J.S. Miller, K.R. Stevens, M.T. Yang, B.M. Baker, D.-H.T. Nguyen, D.M. Cohen, et al., Rapid casting of patterned vascular networks for perfusable engineered three-dimensional tissues, Nat. Mater. 11 (2012) 768–774.

[85] E.F. Kung, F. Wang, J.S. Schechner, In vivo perfusion of human skin substitutes with microvessels formed by adult circulating endothelial progenitor cells, Dermatologic Surg. 34 (2008) 137–146.

[86] E.M. Brey, Vascularization: Regenerative Medicine and Tissue Engineering, Boca Raton: CRC Press, 2014 1st Edition.

[87] A. Lesman, M. Habib, O. Caspi, A. Gepstein, G. Arbel, S. Levenberg, et al., Transplantation of a Tissue-Engineered Human Vascularized Cardiac Muscle, Tissue Eng. Part A. 16 (2009) 115–125.

[88] J.R. Hurley, S. Balaji, D.A. Narmoneva, Complex temporal regulation of capillary morphogenesis by fibroblasts, Am. J. Physiol. Physiol. 299 (2010) C444–C453.

[89] R.E. Unger, S. Ghanaati, C. Orth, A. Sartoris, M. Barbeck, S. Halstenberg, et al., The rapid anastomosis between prevascularized networks on silk fibroin scaffolds generated in vitro with cocultures of human microvascular endothelial and osteoblast cells and the host vasculature, Biomaterials. 31 (2010) 6959–6967.

[90] M. Markowicz, E. Koellensperger, S. Neuss, S. Koenigschulte, C. Bindler, N. Pallua, Human bone marrow mesenchymal stem cells seeded on modified collagen improved dermal regeneration in vivo, Cell Transplant. 15 (2006) 723–732.

[91] M. Sasaki, R. Abe, Y. Fujita, S. Ando, D. Inokuma, H. Shimizu, Mesenchymal stem cells are recruited into wounded skin and contribute to wound repair by transdifferentiation into multiple skin cell type, J. Immunol. 180 (2008) 2581–2587.

[92] T. Kinnaird, E. Stabile, M.S. Burnett, C.W. Lee, S. Barr, S. Fuchs, et al., Marrow-derived stromal cells express genes encoding a broad spectrum of arteriogenic cytokines and promote in vitro and in vivo arteriogenesis through paracrine mechanisms, Circ. Res. 94 (2004) 678–685.

[93] A.M. Altman, Y.S. Yan, N. Matthias, X.W. Bai, C. Rios, A.B. Mathur, et al., IFATS Collection: Human Adipose-Derived Stem Cells Seeded on a Silk Fibroin-Chitosan Scaffold Enhance Wound Repair in a Murine Soft Tissue Injury Model, Stem Cells. 27 (2009) 250–258.

[94] M.D. Herreros, M. Garcia-Arranz, H. Guadalajara, P. De-La-Quintana, D. Garcia-Olmo, F.C. Grp, Autologous Expanded Adipose-Derived Stem Cells for the Treatment of Complex Cryptoglandular Perianal Fistulas: A Phase III Randomized Clinical Trial (FATT 1: Fistula Advanced Therapy Trial 1) and Long-term Evaluation, Dis. Colon Rectum. 55 (2012) 762–772.

[95] A. Bura, V. Planat-Benard, P. Bourin, J.-S. Silvestre, F. Gross, J.-L. Grolleau, et al., Phase I trial: the use of autologous cultured adipose-derived stroma/stem cells to treat patients with non-revascularizable critical limb ischemia, Cytotherapy. 16 (2014) 245–257.

[96] T. Takebe, K. Sekine, M. Enomura, H. Koike, M. Kimura, T. Ogaeri, et al., Vascularized and functional human liver from an iPSC-derived organ bud transplant, Nature. 499 (2013) 481–484.

[97] C.A. Staton, M.W.R. Reed, N.J. Brown, A critical analysis of current in vitro and in vivo angiogenesis assays, Int. J. Exp. Pathol. 90 (2009) 195–221.

[98] G. Alessandri, K. Raju, P. Gullino, Mobilization of capillary endothelium in vitro induced by effectors of angiogenesis in vivo, cancer Res. 43 (1983) 1790–1797.

[99] A. Albini, R. Benelli, D.M. Noonan, C. Brigati, The “chemoinvasion assay”: a tool to study tumor and endothelial cell invasion of basement membranes., Int. J. Dev. Biol. 48 (2004) 563–71.

[100] W. Falk, R.H. Goodwin, E.J. Leonard, A 48-well micro chemotaxis assembly for rapid and accurate measurement of leukocyte migration, J. Immunol. Methods. 33 (1980) 239–247.

[101] L.A. Cary, J.L. Guan, Focal adhesion kinase in integrin-mediated signaling., Front. Biosci. 4 (1999) D102–D113.

[102] J.T. Smith, J.K. Tomfohr, M.C. Wells, T.P. Beebe, T.B. Kepler, W.M. Reichert, Measurement of cell migration on surface-bound fibronectin gradients., Langmuir. 20 (2004) 8279–86.

[103] M. Wong, A. Gotlieb, In vitro Reendothelialization of a Single-Cell Wound - Role of Microfilament Bundles in Rapid Lamellipodia-Mediated Wound Closure, Lab. Investig. 51 (1984) 75–81.

[104] M.S. Pepper, Transforming growth factor-beta 1 modulates basic fibroblast growth factor-induced proteolytic and angiogenic properties of endothelial cells in vitro, J. Cell Biol. 111 (1990) 743–755.

[105] R. Auerbach, W. Auerbach, I. Polakowski, Assays for angiogenesis: A review, Pharmacol. Ther. 51 (1991) 1–11.

[106] G. Cai, J. Lian, S.S. Shapiro, D.A. Beacham, Evaluation of endothelial cell migration with a novel in vitro assay system., Methods Cell Sci. 22 (2000) 107–114.

[107] J.S. Lee, B.S. Oum, S.H. Lee, Mitomycin c influence on inhibition of cellular proliferation and subsequent synthesis of type I collagen and laminin in primary and recurrent pterygia., Ophthalmic Res. 33 (2001) 140–146.

[108] J.L. Obeso, R. Auerbach, A new microtechnique for quantitating cell movement in vitro using polystyrene bead monolayers, J. Immunol. Methods. 70 (1984) 141–152.

[109] R. Auerbach, Angiogenesis Assays: A Critical Overview, Clin. Chem. 49 (2003) 32–40.

[110] P. Ariano, C. Distasi, A. Gilardino, P. Zamburlin, M. Ferraro, A simple method to study cellular migration., J. Neurosci. Methods. 141 (2005) 271–6.

[111] J.A. Madri, Capillary endothelial cell cultures: phenotypic modulation by matrix components, J. Cell Biol. 97 (1983) 153–165.

[112] T.J. Lawley, Y. Kubota, Induction of Morphologic Differentiation of Endothelial Cells in Culture., J. Invest. Dermatol. 93 (1989) 59S–61S.

[113] D. Donovan, N.J. Brown, E.T. Bishop, C.E. Lewis, Comparison of three in vitro human "angiogenesis" assays with capillaries formed in vivo, Angiogenesis. 4 (n.d.) 113–121.

[114] H. Emonard, A. Calle, J.-A. Grimaud, S. Peyrol, V. Castronovo, A. Noel, et al., Interactions Between Fibroblasts and a Reconstituted Basement Membrane Matrix., J. Invest. Dermatol. 89 (1987) 156–163.

[115] A. Bikfalvi, E.M. Cramer, D. Tenza, G. Tobelem, Phenotypic modulations of human umbilical vein endothelial cells and human dermal fibroblasts using two angiogenic assays, Biol. Cell. 72 (1991) 275–278.

[116] R. Montesano, M. Pepper, L. Orci, Paracrine Induction of Angiogenesis In-Vitro By Swiss 3T3 Fibroblasts, J. Cell Sci. 105 (1993) 1013–1024.

[117] K.K. Hirschi, PDGF, TGF-beta , and Heterotypic Cell-Cell Interactions Mediate Endothelial Cell-induced Recruitment of 10T1/2 Cells and Their Differentiation to a Smooth Muscle Fate, J. Cell Biol. 141 (1998) 805–814.

[118] T. Korff, S. Kimmina, G. Martiny-Baron, H.G. Augustin, Blood vessel maturation in a 3-dimensional spheroidal coculture model: direct contact with smooth muscle cells regulates endothelial cell quiescence and abrogates VEGF responsiveness., Faseb J. 15 (2001) 447–57.

[119] D. Darland, L. Massingham, S. Smith, E. Piek, M. St-Geniez, P. D'Amore, Pericyte production of cell-associated VEGF is

differentiation-dependent and is associated with endothelial survival, Dev. Biol. 264 (2003) 275–288.

[120] S. Akimoto, M. Mitsumata, T. Sasaguri, Y. Yoshida, Laminar shear stress inhibits vascular endothelial cell proliferation by inducing cyclin-dependent kinase inhibitor p21(Sdi1/Cip1/Waf1), Circ. Res. 86 (2000) 185–190.

[121] Z. Tahergorabi, M. Khazaei, A Review on Angiogenesis and Its Assays, Iran. J. Basic Med. Sci. 15 1110–1126.

[122] V. Muthukkaruppan, B. Shinners, R. Lewis, The chick embryo aortic arch assay: a new, rapid, quantifiable in vitro method for testing the efficacy of angiogenic and anti-angiogenic factors in a three-, Proc Am Assoc Cancer Res. (2000).

[123] S.J. Leibovich, P.J. Polverini, H.M. Shepard, D.M. Wiseman, V. Shively, N. Nuseir, Macrophage-induced angiogenesis is mediated by tumour necrosis factor-alpha., Nature. 329 (1987) 630–2.

[124] M. Gimbrone, R. Cotran, S. Leapman, J. Folkman, Tumor-growth and neovascularization - experimental model using rabbit cornea, J. Natl. Cancer Inst. 52 (1974) 413–427.

[125] S. Shan, A. Lockhart, W. Saito, A. Knapp, K. Laderoute, M. Dewhirst, The novel tubulin-binding drug BTO-956 inhibits R3230Ac mammary carcinoma growth and angiogenesis in Fischer 344 rats, Clin. Cancer Res. 7 (2001) 2590–2596.

[126] O. Klotz, J.-K. Park, U. Pleyer, C. Hartmann, H. Baatz, Inhibition of corneal neovascularization by α v -integrin antagonists in the rat, Graefe's Arch. Clin. Exp. Ophthalmol. 238 (2000) 88–93.

[127] A. Rubinstein, Zebrafish: From disease modeling to drug discovery, Curr. Opin. Drug Discov. Devel. 6 (2003) 218–223.

[128] S. Childs, J. Chen, D. Garrity, M. Fishman, Patterning of angiogenesis in the zebrafish embryo, Development. 129 (2002) 973–982.

[129] B.M. Weinstein, D.L. Stemple, W. Driever, M.C. Fishman, gridlock, a localized heritable vascular patterning defect in the zebrafish, Nat.

Med. 1 (1995) 1143–1147.

[130] T.J.A. Chico, P.W. Ingham, D.C. Crossman, Modeling cardiovascular disease in the zebrafish., Trends Cardiovasc. Med. 18 (2008) 150–5.

[131] N.D. Lawson, B.M. Weinstein, Arteries and veins: making a difference with zebrafish., Nat. Rev. Genet. 3 (2002) 674–82.

[132] T. Motoike, S. Loughna, E. Perens, B.L. Roman, W. Liao, T.C. Chau, et al., Universal GFP reporter for the study of vascular development., Genesis. 28 (2000) 75–81.

[133] L.M. Cross, M.A. Cook, S. Lin, J.-N. Chen, A.L. Rubinstein, Rapid analysis of angiogenesis drugs in a live fluorescent zebrafish assay., Arterioscler. Thromb. Vasc. Biol. 23 (2003) 911–2.

[134] P.D. Currie, P.W. Ingham, Induction of a specific muscle cell type by a hedgehog-like protein in zebrafish., Nature. 382 (1996) 452–5.

[135] P. Vajkoczy, M.D. Menger, B. Vollmar, L. Schilling, P. Schmiedek, K.P. Hirth, et al., Inhibition of tumor growth, angiogenesis, and microcirculation by the novel Flk-1 inhibitor SU5416 as assessed by intravital multi-fluorescence videomicroscopy., Neoplasia. 1 (1999) 31–41.

[136] H.D. Papenfuss, J.F. Gross, M. Intaglietta, F.A. Treese, A transparent access chamber for the rat dorsal skin fold, Microvasc. Res. 18 (1979) 311–318.

[137] B. Endrich, K. Asaishi, A. Götz, K. Meßmer, Technical report—a new chamber technique for microvascular studies in unanesthetized hamsters, Res. Exp. Med. 177 (1980) 125–134.

[138] H. Lehr, M. Leunig, M. Menger, D. Nolte, K. Messmer, Dorsal skinfold chamber technique for intravital microscopy in nude-mice, Am. J. Pathol. 143 (1993) 1055–1062.

[139] M.D. Menger, H.A. Lehr, Scope and perspectives of intravital microscopy--bridge over from in vitro to in vivo., Immunol. Today. 14 (1993) 519–22.

[140] M.W. Laschke, A. Elitzsch, B. Vollmar, P. Vajkoczy, M.D. Menger,

Combined inhibition of vascular endothelial growth factor (VEGF), fibroblast growth factor and platelet-derived growth factor, but not inhibition of VEGF alone, effectively suppresses angiogenesis and vessel maturation in endometriotic lesions., Hum. Reprod. 21 (2006) 262–8.

[141] J. Schilling, W. Joel, H. Shurley, Wound healing - a comparative study of the histochemical changes in granulation tissue contained in stainless steel wire mesh and polyvinyl sponge cylinders, Surgery. 46 (1959) 702–710.

[142] K. Sprugel, J. Mcpherson, A. Clowes, R. Ross, Effects of growth-factors in vivo, cell ingrowth into porous subcutaneous chambers, Am. J. Pathol. 129 (1987) 601–613.

[143] H.K. Kleinman, J. Graf, Y. Iwamoto, G.T. Kitten, R.C. Ogle, M. Sasaki, et al., Role of Basement Membranes in Cell Differentiation, Ann. N. Y. Acad. Sci. 513 (1987) 134–145.

[144] A. Passaniti, R. Taylor, R. Pili, Y. Guo, P. Long, J. Haney, et al., Methods in laboratory investigation - a simple, quantitative method for assessing angiogenesis and antiangiogenic agents using reconstituted basement-membrane, heparin, and fibroblast growth-factor, Lab. Investig. 67 (1992) 519–528.

[145] J.M. Davidson, Accelerated wound repair, cell proliferation, and collagen accumulation are produced by a cartilage-derived growth factor, J. Cell Biol. 100 (1985) 1219–1227.

[146] R. Edwards, S. Sarmenta, G. Hass, Stimulation of granulation tissue growth by tissue extracts, Arch. Pathol. 69 (1960) 286–302.

[147] Y. Chang, H.-C. Liang, H.-J. Wei, C.-P. Chu, H.-W. Sung, Tissue regeneration patterns in acellular bovine pericardia implanted in a canine model as a vascular patch., J. Biomed. Mater. Res. A. 69 (2004) 323–33.

[148] J. Hodde, Naturally occurring scaffolds for soft tissue repair and regeneration., Tissue Eng. 8 (2002) 295–308.

[149] A. Lichtenberg, I. Tudorache, S. Cebotari, M. Suprunov, G. Tudorache, H. Goerler, et al., Preclinical testing of tissue-engineered

heart valves re-endothelialized under simulated physiological conditions., Circulation. 114 (2006) I559–65.

[150] B. Andree, A. Bar, A. Haverich, Small Intestinal Submucosa Segments as Matrix for Tissue Engineering: Review, 19 (2013) 279–291.

[151] D. Schultheiss, A.I. Gabouev, P.M. Kaufmann, N. Schlote, H. Mertsching, A. Haverich, et al., [Biological vascularized matrix (BioVaM): a new method for solving the perfusion problems in tissue engineering]., Urologe. A. 43 (2004) 1223–8.

[152] H. Mertsching, J. Schanz, V. Steger, M. Schandar, M. Schenk, J. Hansmann, et al., Generation and transplantation of an autologous vascularized bioartificial human tissue., Transplantation. 88 (2009) 203–10.

[153] K. Linke, J. Schanz, J. Hansmann, T. Walles, H. Brunner, H. Mertsching, Engineered liver-like tissue on a capillarized matrix for applied research., Tissue Eng. 13 (2007) 2699–707.

[154] J. Schanz, J. Pusch, J. Hansmann, H. Walles, Vascularised human tissue models: A new approach for the refinement of biomedical research, J. Biotechnol. 148 (2010) 56–63.

[155] G. Totonelli, P. Maghsoudlou, M. Garriboli, J. Riegler, G. Orlando, A.J. Burns, et al., A rat decellularized small bowel scaffold that preserves villus-crypt architecture for intestinal regeneration, Biomaterials. 33 (2012) 3401–3410.

[156] C. Moll, J. Reboredo, T. Schwarz, A. Appelt, S. Schürlein, H. Walles, et al., Tissue engineering of a human 3D in vitro tumor test system., J. Vis. Exp. (2013) 110-113.

[157] Z. Vukadinovic-Nikolic, B. Andree, S.E. Dorfman, M. Pflaum, T. Horvath, M. Lux, et al., Generation of Bioartificial Heart Tissue by Combining a Three-Dimensional Gel-Based Cardiac Construct with Decellularized Small Intestinal Submucosa, Tissue Eng. Part A. 20 (2014) 799–809.

[158] H.C. Ott, B. Clippinger, C. Conrad, C. Schuetz, I. Pomerantseva, L. Ikonomou, et al., Regeneration and orthotopic transplantation of a

bioartificial lung, Nat. Med. 16 (2010) 927–933.

[159] D.W. Courtman, C.A. Pereira, V. Kashef, D. McComb, J.M. Lee, G.J. Wilson, Development of a pericardial acellular matrix biomaterial: biochemical and mechanical effects of cell extraction., J. Biomed. Mater. Res. 28 (1994) 655–66.

[160] M. Kasimir, E. Rieder, G. Seebacher, G. Silberhumer, E. Wolner, G. Weigel, et al., Comparison of different decellularization procedures of porcine heart valves, Int. J. Artif. Organs. 26 (2003) 421–427.

[161] S. Cebotari, I. Tudorache, T. Jaekel, A. Hilfiker, S. Dorfman, W. Ternes, et al., Detergent decellularization of heart valves for tissue engineering: toxicological effects of residual detergents on human endothelial cells., Artif. Organs. 34 (2010) 206–10.

[162] G. Feil, M. Christ-Adler, S. Maurer, S. Corvin, H.-O. Rennekampff, J. Krug, et al., Investigations of urothelial cells seeded on commercially available small intestine submucosa, Eur. Urol. 50 (2006) 1330–1337.

[163] T.W. Hudson, S.Y. Liu, C.E. Schmidt, Engineering an Improved Acellular Nerve Graft via Optimized Chemical Processing, Tissue Eng. 10 (2004) 1346–1358.

[164] B. Andrée, K. Bela, T. Horvath, M. Lux, R. Ramm, L. Venturini, et al., Successful re-endothelialization of a perfusable biological vascularized matrix (BioVaM) for the generation of 3D artificial cardiac tissue., Basic Res. Cardiol. 109 (2014) 441.

[165] K. Chwalek, L.J. Bray, C. Werner, Tissue-engineered 3D tumor angiogenesis models: potential technologies for anti-cancer drug discovery., Adv. Drug Deliv. Rev. 79-80 (2014) 30–9.

[166] M. Alemany-Ribes, C.E. Semino, Bioengineering 3D environments for cancer models., Adv. Drug Deliv. Rev. 79-80 (2014) 40–9.

[167] K. Chwalek, M. V Tsurkan, U. Freudenberg, C. Werner, Glycosaminoglycan-based hydrogels to modulate heterocellular communication in in vitro angiogenesis models., Sci. Rep. 4 (2014) 4414.

[168] E.M. Jeffries, S. Nakamura, K.-W. Lee, J. Clampffer, H. Ijima, Y.

Wang, Micropatterning Electrospun Scaffolds to Create Intrinsic Vascular Networks, Macromol. Biosci. 14 (2014) 1514–1520.

[169] D.W. Hutmacher, T. Schantz, I. Zein, K.W. Ng, S.H. Teoh, K.C. Tan, Mechanical properties and cell cultural response of polycaprolactone scaffolds designed and fabricated via fused deposition modeling., J. Biomed. Mater. Res. 55 (2001) 203–16.

[170] N. Bhardwaj, S.C. Kundu, Electrospinning: a fascinating fiber fabrication technique., Biotechnol. Adv. 28 (2010) 325–347.

[171] S. Badylak, The extracellular matrix as a scaffold for tissue reconstruction, Semin. Cell Dev. Biol. 13 (2002) 377–383.

[172] S. Miyamoto, H. Teramoto, O.A. Coso, J.S. Gutkind, P.D. Burbelo, S.K. Akiyama, et al., Integrin Function - Molecular Hierarchies Of Cytoskeletal And Signaling MoleculeS, J. Cell Biol. 131 (1995) 791–805.

[173] J. Schwarzbauer, Basement membrane: Putting up the barriers, Curr. Biol. 9 (1999) R242–R244.

[174] T.B. McPherson, S.F. Badylak, Characterization of Fibronectin Derived from Porcine Small Intestinal Submucosa, Tissue Eng. 4 (1998) 75–83.

[175] G.K. Reddy, C.S. Enwemeka, A simplified method for the analysis of hydroxyproline in biological tissues, Clin. Biochem. 29 (1996) 225–229.

[176] R.W. Farndale, D.J. Buttle, A.J. Barrett, Improved Quantitation And Discrimination Of Sulfated Glycosaminoglycans By Use Of Dimethylmethylene Blue, Biochim. Biophys. Acta. 883 (1986) 173–177.

[177] K. Modjarrad, S. Ebnesajjad, Handbook of Polymer Applications in Medicine and Medical Devices, San Diego: Elsevier (2013) 1st Edition.

[178] C. Bies, C.-M. Lehr, J.F. Woodley, Lectin-mediated drug targeting: history and applications., Adv. Drug Deliv. Rev. 56 (2004) 425–35.

[179] N. Jährling, K. Becker, H.-U. Dodt, 3D-reconstruction of blood

vessels by ultramicroscopy., Organogenesis. 5 (2009) 227–30.

[180] G. Thurston, T.J. Murphy, P. Baluk, J.R. Lindsey, D.M. McDonald, Angiogenesis in mice with chronic airway inflammation: strain-dependent differences., Am. J. Pathol. 153 (1998) 1099–112.

[181] T. Ezaki, P. Baluk, G. Thurston, A. La Barbara, C. Woo, D.M. McDonald, Time course of endothelial cell proliferation and microvascular remodeling in chronic inflammation., Am. J. Pathol. 158 (2001) 2043–55.

[182] S. Mazzetti, S. Frigerio, M. Gelati, A. Salmaggi, L. Vitellaro-Zuccarello, Lycopersicon esculentum lectin: an effective and versatile endothelial marker of normal and tumoral blood vessels in the central nervous system, Eur. J. Histochem. 48 423–428.

[183] L. Junqueira, W. Cossermelli, R. Brentani, Differential Staining Of Collagens Type-I, Type-Ii And Type-Iii By Sirius Red And Polarization Microscopy, Arch. Histol. Jpn. 41 (1978) 267–274.

[184] G. Montes, L. Junqueira, The use of the picrosirus-polarization method for the study of the biopathology of collagen, Mem. Inst. Oswaldo Cruz. 86 (1991) 1–11.

[185] R. Montesano, In vitro rapid organization of endothelial cells into capillary-like networks is promoted by collagen matrices, J. Cell Biol. 97 (1983) 1648–1652.

[186] F. Goto, K. Goto, K. Weindel, J. Folkman, Synergistic effects of vascular endothelial growth factor and basic fibroblast growth factor on the proliferation and cord formation of bovine capillary endothelial cells within collagen gels., Lab. Invest. 69 (1993) 508–17.

[187] V. Thumwanit, U. Kedjarune, Cytotoxicity of polymerized commercial cyanoacrylate adhesive on cultured human oral fibroblasts., Aust. Dent. J. 44 (1999) 248–52.

[188] C.E. Evans, G.C. Lees, I.A. Trail, Cytotoxicity of cyanoacrylate adhesives to cultured tendon cells., J. Hand Surg. Br. 24 (1999) 658–61.

[189] F. Pourageaud, J.G. De Mey, Structural properties of rat mesenteric small arteries after 4-wk exposure to elevated or reduced blood flow.,

Am. J. Physiol. 273 (1997) H1699–706.

[190] F. Dietrich, P. Lelkes, Fine-tuning of a three-dimensional microcarrier-based angiogenesis assay for the analysis of endothelial-mesenchymal cell co-cultures in fibrin and collagen gels, Angiogenesis. 9 (2006) 111-125.

[191] C. Hughes, Endothelial–stromal interactions in angiogenesis, Curr. Opin. Hematol. 15 (2008) 204-209.

[192] L.A. Kunz-Schughart, J.A. Schroeder, M. Wondrak, F. van Rey, K. Lehle, F. Hofstaedter, et al., Potential of fibroblasts to regulate the formation of three-dimensional vessel-like structures from endothelial cells in vitro., Am. J. Physiol. Cell Physiol. 290 (2006) C1385–98.

[193] S. MacNeil, Progress and opportunities for tissue-engineered skin, Nature. 445 (2007) 874–880.

[194] S. Bhargava, J.M. Patterson, R.D. Inman, S. MacNeil, C.R. Chapple, Tissue-engineered buccal mucosa urethroplasty - Clinical outcomes, Eur. Urol. 53 (2008) 1263–1271.

[195] P. Macchiarini, P. Jungebluth, T. Go, M.A. Asnaghi, L.E. Rees, T.A. Cogan, et al., Clinical transplantation of a tissue-engineered airway, Lancet. 372 (2008) 2023–2030.

[196] S. Miyamoto, B.-Z. Kathz, R.M. Lafrenie, K.m. Yamada, Fibronectin and Integrins in Cell Adhesion, Signaling, and Morphogenesis, Ann. N. Y. Acad. Sci. 857 (1998) 119–129.

[197] R. Janvier, A. Sourla, M. Koutsilieris, C.J. Doillon, Stromal fibroblasts are required for PC-3 human prostate cancer cells to produce capillary-like formation of endothelial cells in a three-dimensional co-culture system, Anticancer Res. 17 (1997) 1551–1557.

[198] X. Chen, A.S. Aledia, S.A. Popson, L. Him, C.C.W. Hughes, S.C. George, Rapid Anastomosis of Endothelial Progenitor Cell-Derived Vessels with Host Vasculature Is Promoted by a High Density of Cotransplanted Fibroblasts, Tissue Eng. Part A. 16 (2010) 585–594.

[199] M.T. Cerqueira, R.P. Pirraco, A.R. Martins, T.C. Santos, R.L. Reis, A.P. Marques, Cell sheet technology-driven re-epithelialization and neovascularization of skin wounds., Acta Biomater. 10 (2014) 3145–

55.

[200] K.G. Neiva, K.A. Warner, M.S. Campos, Z. Zhang, J. Moren, T.E. Danciu, et al., Endothelial cell-derived interleukin-6 regulates tumor growth., BMC Cancer. 14 (2014) 99-102.

[201] R. Walser, W. Metzger, A. Goerg, T. Pohlemann, M.D. Menger, M.W. Laschke, Generation Of Co-Culture Spheroids As Vascularisation Units For Bone Tissue Engineering, Eur. Cell. Mater. 26 (2013) 222–233.

[202] C.E. Tanase, A. Sartoris, M.I. Popa, L. Verestiuc, R.E. Unger, C.J. Kirkpatrick, In vitro evaluation of biomimetic chitosan-calcium phosphate scaffolds with potential application in bone tissue engineering., Biomed. Mater. 8 (2013) 250-252.

[203] F. Jin, U. Brockmeier, F. Otterbach, E. Metzen, New insight into the SDF-1/CXCR4 axis in a breast carcinoma model: hypoxia-induced endothelial SDF-1 and tumor cell CXCR4 are required for tumor cell intravasation., Mol. Cancer Res. 10 (2012) 1021–31.

[204] T. Ziegler, R.W. Alexander, R.M. Nerem, An endothelial cell-smooth muscle cell co-culture model for use in the investigation of flow effects on vascular biology, Ann. Biomed. Eng. 23 (1995) 216–225.

[205] J.W. Wragg, S. Durant, H.M. McGettrick, K.M. Sample, S. Egginton, R. Bicknell, Shear stress regulated gene expression and angiogenesis in vascular endothelium., Microcirculation. 21 (2014) 290–300.

[206] J. Ando, T. Komatsuda, A. Kamiya, Cytoplasmic calcium response to fluid shear stress in cultured vascular endothelial cells, Vitr. Cell. Dev. Biol. 24 (1988) 871–877.

[207] B. Nilius, G. Droogmans, Ion channels and their functional role in vascular endothelium., Physiol. Rev. 81 (2001) 1415–59.

[208] S.P. Olesen, D.E. Clapham, P.F. Davies, Haemodynamic shear stress activates a K+ current in vascular endothelial cells., Nature. 331 (1988) 168–70.

[209] G. Schwarz, G. Droogmans, B. Nilius, Shear stress induced membrane currents and calcium transients in human vascular

endothelial cells, Pflgers Arch. Eur. J. Physiol. 421 (1992) 394–396.

[210] B. Nilius, F. Viana, G. Droogmans, Ion channels in vascular endothelium., Annu. Rev. Physiol. 59 (1997) 145–70.

[211] Y. Zhao, P.M. Vanhoutte, S.W.S. Leung, Vascular nitric oxide: Beyond eNOS., J. Pharmacol. Sci. 129 (2015) 83–94.

[212] A. Hoeben, B. Landuyt, M.S. Highley, H. Wildiers, A.T. Van Oosterom, E.A. De Bruijn, Vascular endothelial growth factor and angiogenesis., Pharmacol. Rev. 56 (2004) 549–80.

[213] N. Ferrara, H.-P. Gerber, J. LeCouter, The biology of VEGF and its receptors., Nat. Med. 9 (2003) 669–76.

[214] A.-K. Olsson, A. Dimberg, J. Kreuger, L. Claesson-Welsh, VEGF receptor signalling - in control of vascular function., Nat. Rev. Mol. Cell Biol. 7 (2006) 359–71.

[215] T. Mirzapoiazova, I. Kolosova, P. V Usatyuk, V. Natarajan, A.D. Verin, Diverse effects of vascular endothelial growth factor on human pulmonary endothelial barrier and migration., Am. J. Physiol. Lung Cell. Mol. Physiol. 291 (2006) L718–24.

[216] X. Liu, C.S. Lin, T. Graziottin, J. Resplande, T.F. Lue, Vascular endothelial growth factor promotes proliferation and migration of cavernous smooth muscle cells., J. Urol. 166 (2001) 354–60.

[217] A. Weisz, B. Koren, T. Cohen, G. Neufeld, T. Kleinberger, B.S. Lewis, et al., Increased Vascular Endothelial Growth Factor 165 Binding to Kinase Insert Domain-Containing Receptor After Infection of Human Endothelial Cells by Recombinant Adenovirus Encoding the Vegf165 Gene, Circulation. 103 (2001) 1887–1892.

[218] M. Morales-Ruiz, D. Fulton, G. Sowa, L.R. Languino, Y. Fujio, K. Walsh, et al., Vascular Endothelial Growth Factor-Stimulated Actin Reorganization and Migration of Endothelial Cells Is Regulated via the Serine/Threonine Kinase Akt, Circ. Res. 86 (2000) 892–896.

[219] K. Bayless, H. Kwak, S. Su, Investigating endothelial invasion and sprouting behavior in three-dimensional collagen matrices, Nat. Protoc. 4 (2009) 1888-1898.

[220] K.J. Bayless, G.E. Davis, Sphingosine-1-phosphate markedly induces matrix metalloproteinase and integrin-dependent human endothelial cell invasion and lumen formation in three-dimensional collagen and fibrin matrices, Biochem. Biophys. Res. Commun. 312 (2003) 903–913.

[221] S. Bell, A. Mavila, R. Salazar, K. Bayless, S. Kanagala, S. Maxwell, et al., Differential gene expression during capillary morphogenesis in 3D collagen matrices: regulated expression of genes involved in basement membrane matrix assembly, cell cycle progression, cellular differentiation and G-protein signaling, J. Cell Sci. 114 (2001) 2755–2773.

[222] S. Vukicevic, H.K. Kleinman, F.P. Luyten, A.B. Roberts, N.S. Roche, A.H. Reddi, Identification of multiple active growth factors in basement membrane matrigel suggests caution in interpretation of cellular activity related to extracellular matrix components, Exp. Cell Res. 202 (1992) 1–8.

[223] C.S. Szot, C.F. Buchanan, J.W. Freeman, M.N. Rylander, In vitro angiogenesis induced by tumor-endothelial cell co-culture in bilayered, collagen I hydrogel bioengineered tumors., Tissue Eng. Part C. Methods. 19 (2013) 864–74.

[224] Y. Shin, S. Han, J.S. Jeon, K. Yamamoto, I.K. Zervantonakis, R. Sudo, et al., Microfluidic assay for simultaneous culture of multiple cell types on surfaces or within hydrogels., Nat. Protoc. 7 (2012) 1247–59.

[225] A. Das, D. Lauffenburger, H. Asada, R.D. Kamm, A hybrid continuum-discrete modelling approach to predict and control angiogenesis: analysis of combinatorial growth factor and matrix effects on vessel-sprouting morphology., Philos. Trans. A. Math. Phys. Eng. Sci. 368 (2010) 2937–60.

[226] H. Gerhardt, M. Golding, M. Fruttiger, C. Ruhrberg, A. Lundkvist, A. Abramsson, et al., VEGF guides angiogenic sprouting utilizing endothelial tip cell filopodia., J. Cell Biol. 161 (2003) 1163–77.

[227] R. Blanco, H. Gerhardt, VEGF and Notch in tip and stalk cell selection., Cold Spring Harb. Perspect. Med. 3 (2013) 657-659.

[228] L. Jakobsson, C.A. Franco, K. Bentley, R.T. Collins, B. Ponsioen, I.M. Aspalter, et al., Endothelial cells dynamically compete for the tip cell position during angiogenic sprouting., Nat. Cell Biol. 12 (2010) 943–53.

[229] R. Narayan, Rapid Prototyping of Biomaterials: Principles and Applications, Cambridge: Woodhead Publishing, (2014) 1st Edition.

[230] F.J. Bye, J. Bissoli, L. Black, A.J. Bullock, S. Puwanun, K. Moharamzadeh, et al., Development of bilayer and trilayer nanofibrous/microfibrous scaffolds for regenerative medicine, Biomater. Sci. 1 (2013) 942-951.

[231] F.J. Bye, A.J. Bullock, R. Singh, F. Sefat, S. Roman, S. MacNeil, Development of a Basement Membrane Substitute Incorporated Into an Electrospun Scaffold for 3D Skin Tissue Engineering, J. Biomater. Tissue Eng. 4 (2014) 686–692.

[232] W. He, A. Nieponice, L. Soletti, Y. Hong, B. Gharaibeh, M. Crisan, et al., Pericyte-based human tissue engineered vascular grafts., Biomaterials. 31 (2010) 8235–44.

[233] Y. Hong, K. Takanari, N.J. Amoroso, R. Hashizume, E.P. Brennan-Pierce, J.M. Freund, et al., An elastomeric patch electrospun from a blended solution of dermal extracellular matrix and biodegradable polyurethane for rat abdominal wall repair., Tissue Eng. Part C. Methods. 18 (2012) 122–32.

[234] S.A. Eming, B. Brachvogel, T. Odorisio, M. Koch, Regulation of angiogenesis: wound healing as a model., Prog. Histochem. Cytochem. 42 (2007) 115–70.

[235] G.K. Owens, M.S. Kumar, B.R. Wamhoff, Molecular regulation of vascular smooth muscle cell differentiation in development and disease., Physiol. Rev. 84 (2004) 767–801.

[236] B. Hinz, Formation and function of the myofibroblast during tissue repair., J. Invest. Dermatol. 127 (2007) 526–37.

[237] I. Ortega, L. Dew, A.G. Kelly, C.K. Chong, S. MacNeil, F. Claeyssens, Fabrication of biodegradable synthetic perfusable vascular networks via a combination of electrospinning and

robocasting, Biomater. Sci. 3 (2015) 592–596.

[238] Q.P. Pham, U. Sharma, A.G. Mikos, Electrospinning of polymeric nanofibers for tissue engineering applications: A review, TISSUE Eng. 12 (2006) 1197–1211.

[239] K.A. Blackwood, R. McKean, I. Canton, C.O. Freeman, K.L. Franklin, D. Cole, et al., Development of biodegradable electrospun scaffolds for dermal replacement., Biomaterials. 29 (2008) 3091–104.

[240] M. Rampichová, M. Buzgo, J. Chvojka, E. Prosecká, O. Kofroňová, E. Amler, Cell penetration to nanofibrous scaffolds: Forcespinningff, an alternative approach for fabricating 3D nanofibers., Cell Adh. Migr. 8 (2014) 36–41.

[241] V. Beachley, X. Wen, Polymer nanofibrous structures: Fabrication, biofunctionalization, and cell interactions., Prog. Polym. Sci. 35 (2010) 868–892.

[242] R.G. Ellis-Behnke, Y.-X. Liang, S.-W. You, D.K.C. Tay, S. Zhang, K.-F. So, et al., Nano neuro knitting: peptide nanofiber scaffold for brain repair and axon regeneration with functional return of vision., Proc. Natl. Acad. Sci. U. S. A. 103 (2006) 5054–9.

[243] J. Venugopal, S. Low, A.T. Choon, S. Ramakrishna, Interaction of cells and nanofiber scaffolds in tissue engineering., J. Biomed. Mater. Res. B. Appl. Biomater. 84 (2008) 34–48.

[244] J. Sun, H. Tan, Alginate-Based Biomaterials for Regenerative Medicine Applications, Materials (Basel). 6 (2013) 1285–1309.

[245] K.Y. Lee, D.J. Mooney, Alginate: properties and biomedical applications., Prog. Polym. Sci. 37 (2012) 106–126.

[246] B. Chueh, Y. Zheng, Y. Torisawa, A.Y. Hsiao, C. Ge, S. Hsiong, et al., Patterning alginate hydrogels using light-directed release of caged calcium in a microfluidic device., Biomed. Microdevices. 12 (2010) 145–51.

[247] H.Y. Chang, J.-T. Chi, S. Dudoit, C. Bondre, M. van de Rijn, D. Botstein, et al., Diversity, topographic differentiation, and positional memory in human fibroblasts., Proc. Natl. Acad. Sci. U. S. A. 99

(2002) 12877–82.

[248] M. Allinen, R. Beroukhim, L. Cai, C. Brennan, J. Lahti-Domenici, H. Huang, et al., Molecular characterization of the tumor microenvironment in breast cancer., Cancer Cell. 6 (2004) 17–32.

[249] A. Orimo, P.B. Gupta, D.C. Sgroi, F. Arenzana-Seisdedos, T. Delaunay, R. Naeem, et al., Stromal fibroblasts present in invasive human breast carcinomas promote tumor growth and angiogenesis through elevated SDF-1/CXCL12 secretion., Cell. 121 (2005) 335–48.

[250] J. Tuxhorn, S. McAlhany, T. Dang, G. Ayala, D. Rowley, Stromal cells promote angiogenesis and growth of human prostate tumors in a differential reactive stroma (DRS) xenograft model, CANCER Res. 62 (2002) 3298–+.

[251] J. Dong, J. Grunstein, M. Tejada, F. Peale, G. Frantz, W.-C. Liang, et al., VEGF-null cells require PDGFR alpha signaling-mediated stromal fibroblast recruitment for tumorigenesis., EMBO J. 23 (2004) 2800–10.

[252] Y. Crawford, I. Kasman, L. Yu, C. Zhong, X. Wu, Z. Modrusan, et al., PDGF-C mediates the angiogenic and tumorigenic properties of fibroblasts associated with tumors refractory to anti-VEGF treatment., Cancer Cell. 15 (2009) 21–34.

[253] L. Hlatky, C. Tsionou, P. Hahnfeldt, C. Coleman, Mammary fibroblasts may influence breast-tumor angiogenesis via hypoxia-induced vascular endothelial growth-factor up-regulation and protein expression, Cancer Res. 54 (1994) 6083–6086.

[254] J. Fang, L. Yan, Y. Shing, M. Moses, HIF-1 alpha-mediated up-regulation of vascular endothelial growth factor, independent of basic fibroblast growth factor, is important in the switch to the angiogenic phenotype during early tumorigenesis, Cancer Res. 61 (2001) 5731–5735.

[255] S. Vong, R. Kalluri, The role of stromal myofibroblast and extracellular matrix in tumor angiogenesis., Genes Cancer. 2 (2011) 1139–45.

[256] E.M. Zeisberg, S. Potenta, L. Xie, M. Zeisberg, R. Kalluri, Discovery of endothelial to mesenchymal transition as a source for carcinoma-associated fibroblasts., Cancer Res. 67 (2007) 10123–8.

[257] K. Azuma, K. Ichimura, T. Mita, S. Nakayama, W.L. Jin, T. Hirose, et al., Presence of alpha-smooth muscle actin-positive endothelial cells in the luminal surface of adult aorta., Biochem. Biophys. Res. Commun. 380 (2009) 620–6.

[258] H. Ando, T. Kubin, W. Schaper, J. Schaper, Cardiac microvascular endothelial cells express alpha-smooth muscle actin and show low NOS III activity., Am. J. Physiol. 276 (1999) H1755–68.

[259] M. Bahramsoltani, T. Harms, B. Drewes, J. Plendl, Searching for markers to identify angiogenic endothelial cells: a proteomic approach., Clin. Hemorheol. Microcirc. 55 (2013) 255–69.

[260] E. Dohle, I. Bischoff, T. Boese, A. Marsano, A. Banfi, R.E. Unger, et al., Macrophage-Mediated Angiogenic Activation Of Outgrowth Endothelial Cells In Co-Culture With Primary Osteoblasts, Eur. Cell. Mater. 27 149–165.

[261] Y. Yamaguchi, M. Kuwana, Proangiogenic hematopoietic cells of monocytic origin: roles in vascular regeneration and pathogenic processes of systemic sclerosis, Histol. Histopathol. 28 (2013) 175–183.

[262] A.S. Jaipersad, G.Y.H. Lip, S. Silverman, E. Shantsila, The role of monocytes in angiogenesis and atherosclerosis., J. Am. Coll. Cardiol. 63 (2014) 1–11.

[263] J.Y. Kasper, M.I. Hermanns, R.E. Unger, C.J. Kirkpatrick, A responsive human triple-culture model of the air-blood barrier: incorporation of different macrophage phenotypes., J. Tissue Eng. Regen. Med. (2015).

# Appendix

## A. Materials list

### I. Bioscaffold preparation

| Chemical/Reagent | Cat No. | Supplier |
|---|---|---|
| Isofluorane | CDS019936 | Sigma Aldrich |
| Heparin sodium salt from porcine intestinal mucosa | H3149-250KU | Sigma Aldrich |
| Penicillin/streptomycin | P0781 | Sigma Aldrich |
| Amphotericin B | A2942 | Sigma Aldrich |
| PBS (Dulbecco A) tablets | BR0014 | Oxoid Ltd. |

| Material | Cat No. | Supplier |
|---|---|---|
| 24 gauge cannula | 381212 | BD Insyte |
| Ethicon 4/0 sutures (Mersilk) | W501H | Medisave |
| Universal tubes | P4333 | Sigma Aldrich |
| 10ml syringe | 302188 | BD Plastipak |
| Syringe filter (0.2 μm) | 83.1826.001 | Sarstedt |
| Straight sample container | 216-2595 | VWR International |
| Measuring cylinder | 1129469 | Camlab |
| 500 ml Duran® glass bottle | Z305197 | Sigma Aldrich |

| Equipment | Model | Supplier |
|---|---|---|
| Dissection kit | N/A | Thackeray |
| Analytical balance | AB204 | Mettler Toledo |

### II. Decellularisation

| Chemical/Reagent | Cat No. | Supplier |
|---|---|---|
| Triton-X 100 | BP151 | Fisher Scientific |
| Ammonium hydroxide | 320145 | Sigma Aldrich |

| Material | Cat No. | Supplier |
|---|---|---|
| 2 L glass beaker (tall) | BEA1166 | SLS |
| 1 L Duran® glass bottle | Z305200 | Sigma Aldrich |
| Tubing Versilic 2x4 mm BxOD | TUB1944 | SLS |
| ADCF male luer barb adapter | EW-30800-24 | Cole Parmer |
| Petri dish (90 mm) | SLS2000 | SLS |
| Magnetic stir bar | VWR1442-0521 | VWR International |
| Syringe (1 ml) | 300013 | BD Plastipak |
| Blue food colouring | 2680374 | Asda |

| Equipment | Model | Supplier |
|---|---|---|
| Dissection microscope | M 3Z | Wild Heerbrugg |
| Multi-channel cassette pump | 205U | Watson Marlow |
| Magnetic stirrer | CD162 | Bibby Scientific |
| Forceps | Prestige | Morton medical supplies |
| Automatic pipettes | Various | Gilson |

| Chemical/Reagent | Cat No. | Supplier |
|---|---|---|
| Peracetic acid (40% v/v) | BP151 | Fisher Scientific |
| PBS (Dulbecco A) tablets | BR0014 | Oxoid Ltd. |

| Material | Cat No. | Supplier |
|---|---|---|
| Petri dish (90 mm) | SLS2000 | SLS |
| 5 ml syringe | 302187 | BD Plastipak |

| Equipment | Model | Supplier |
|---|---|---|
| Forceps | Prestige | Morton medical supplies |
| Automatic pipettes | Various | Gilson |

III. Bioscaffold sterilisation

IV. Bioscaffold Characterisation

*Vascular patency*

| Chemical/Reagent | Cat No. | Supplier |
|---|---|---|
| Blue food colouring | 2680374 | Asda |
| Fluorescein isothiocyanate (FITC)–dextran (250 kDa) | FD250S | Sigma Aldrich |

| Material | Cat No. | Supplier |
|---|---|---|
| Petri dish (90 mm) | SLS2000 | SLS |
| Syringe (1 ml) | 300013 | BD Plastipak |

| Equipment | Model | Supplier |
|---|---|---|
| Forceps | Prestige | Morton medical supplies |
| Dissection microscope | M 3Z | Wild Heerbrugg |
| Confocal microscope | Zeiss LSM 510 | Zeiss |

*Preparation of histological slides*

| Chemical/Reagent | Cat No. | Supplier |
|---|---|---|
| Industrial methylated spirits (IMS) | M/4450/17 | Fisher Scientific |
| Xylene | X/0100/17 | Fisher Scientific |
| Paraffin wax | P3558 | Sigma Aldrich |
| Formaldehyde (37%) | F8775 | Sigma Aldrich |
| PBS (Dulbecco A) tablets | BR0014 | Oxoid Ltd. |

| Material | Cat No. | Supplier |
|---|---|---|
| SuperFrost® Plus slides | 48311-703 | VWR International |

| Equipment | Model | Supplier |
|---|---|---|
| Benchtop tissue processor | TP1020 | Leica |
| Embedding centre, dispenser & hot plate | EG1160 | Leica |
| Microtome | RM2235 | Leica |
| Microtome blades | S35 | Feather |
| Hot plate | HI1210 | Leica |
| Water bath | MH8516 | Electrothermal |
| Forceps | Prestige | Morton medical supplies |

*Hematoxylin and Eosin (H&E) staining*

| Chemical/Reagent | Cat No. | Supplier |
|---|---|---|
| Xylene | X/0100/17 | Fisher Scientific |
| Harris haematoxylin solution | HHS16 | Sigma Aldrich |
| IMS | M/4450/17 | Fisher Scientific |
| Eosin Y solution | HT110232 | Sigma Aldrich |
| DPX mountant | D/5319/05 | Fisher Scientific |

| Material | Cat No. | Supplier |
|---|---|---|
| Slide rack | 70312-24 | EMS |
| Staining dish | 70312-23 | EMS |
| Cover slips | MNJ350020 | Thermo Fisher Scientific |
| Measuring cylinder | 1129469 | Camlab |
| Pasteur pipette | PIP4208 | SLS |

| Equipment | Model | Supplier |
|---|---|---|
| Light microscope | DM-B1 | Motic |

*Glycosaminoglycan (GAG) staining*

| Chemical/Reagent | Cat No. | Supplier |
|---|---|---|
| Xylene | X/0100/17 | Fisher Scientific |
| IMS | M/4450/17 | Fisher Scientific |
| Ethanol | 10048291 | Fisher Scientific |
| Alcian blue 8GX | A3157 | Sigma Aldrich |
| Glacial acetic acid | 27222 | Sigma Aldrich |
| Periodic acid | 395132 | Sigma Aldrich |
| Schiffs reagent | 3952016 | Sigma Aldrich |
| Gills no. 3 hematoxylin | GH5316 | Sigma Aldrich |
| DPX mountant | D/5319/05 | Fisher Scientific |

| Material | Cat No. | Supplier |
|---|---|---|
| Slide rack | 70312-24 | EMS |
| Staining dish | 70312-23 | EMS |
| Cover slips | MNJ350020 | Thermo Fisher Scientific |
| Measuring cylinder | 1129469 | Camlab |
| Pasteur pipette | PIP4208 | SLS |

| Equipment | Model | Supplier |
|---|---|---|
| pH meter | SevenMulti | Mettler Toledo |
| Light microscope | DM-B1 | Motic |

*Collagen staining*

| Chemical/Reagent | Cat No. | Supplier |
|---|---|---|
| Xylene | X/0100/17 | Fisher Scientific |
| IMS | M/4450/17 | Fisher Scientific |
| Ethanol | 10048291 | Fisher Scientific |
| Glacial acetic acid | 27222 | Sigma Aldrich |
| Direct red 80 | 365548 | Sigma Aldrich |
| Picric acid | 36011 | Sigma Aldrich |
| Weigert's hematoxylin | HX384843 | Merck |
| DPX mountant | D/5319/05 | Fisher Scientific |

| Material | Cat No. | Supplier |
|---|---|---|
| Slide rack | 70312-24 | EMS |
| Staining dish | 70312-23 | EMS |
| Cover slips | MNJ350020 | Thermo Fisher Scientific |
| Measuring cylinder | 1129469 | Camlab |
| Pasteur pipette | PIP4208 | SLS |

| Equipment | Model | Supplier |
|---|---|---|
| Light microscope (with polarised filter) | BX50 | Olympus |

*Elastin staining*

| Chemical/Reagent | Cat No. | Supplier |
|---|---|---|
| Xylene | X/0100/17 | Fisher Scientific |
| IMS | M/4450/17 | Fisher Scientific |
| Ethanol | 10048291 | Fisher Scientific |
| Hematoxylin solution | HT25A | Sigma Aldrich |
| Weigert's iodine solution | HT25A | Sigma Aldrich |
| Ferric chloride solution | HT25A | Sigma Aldrich |
| Van Gieson solution | HT25A | Sigma Aldrich |
| DPX mountant | D/5319/05 | Fisher Scientific |

| Material | Cat No. | Supplier |
|---|---|---|
| Slide rack | 70312-24 | EMS |
| Staining dish | 70312-23 | EMS |
| Cover slips | MNJ350020 | Thermo Fisher Scientific |

| | | |
|---|---|---|
| Measuring cylinder | 1129469 | Camlab |
| Pasteur pipette | PIP4208 | SLS |

| Equipment | Model | Supplier |
|---|---|---|
| Light microscope | DM-B1 | Motic |

Masson-Goldner trichrome staining

| Chemical/Reagent | Cat No. | Supplier |
|---|---|---|
| Xylene | X/0100/17 | Fisher Scientific |
| IMS | M/4450/17 | Fisher Scientific |
| Ethanol | 10048291 | Fisher Scientific |
| Weigert's iron haematoxylin kit | 115973 | Merck Millipore |
| Glacial acetic acid | 27222 | Sigma Aldrich |
| Azophloxine solution | 100485 | Merck Millipore |
| Tungstophosphoric acid orange G solution | 100485 | Merck Millipore |
| Light green SF solution | 100485 | Merck Millipore |
| DPX mountant | D/5319/05 | Fisher Scientific |

| Material | Cat No. | Supplier |
|---|---|---|
| Slide rack | 70312-24 | EMS |
| Staining dish | 70312-23 | EMS |
| Cover slips | MNJ350020 | Thermo Fisher Scientific |
| Measuring cylinder | 1129469 | Camlab |
| Pasteur pipette | PIP4208 | SLS |

| Equipment | Model | Supplier |
|---|---|---|
| Light microscope | DM-B1 | Motic |

Staining of cell nuclei

| Chemical/Reagent | Cat No. | Supplier |
|---|---|---|
| Xylene | X/0100/17 | Fisher Scientific |
| IMS | M/4450/17 | Fisher Scientific |
| 4',6-diamidino-2-phenylindole (DAPI) | D8417 | Sigma Aldrich |
| PBS (Dulbecco A) tablets | BR0014 | Oxoid Ltd. |
| DPX mountant | D/5319/05 | Fisher Scientific |

| Material | Cat No. | Supplier |
|---|---|---|
| Universal container | 1048636-1 | SLS |
| Aluminium foil | 11247 | Terinex |
| PAP pen | ab2601 | abcam |
| Pasteur pipette | PIP4208 | SLS |

| Equipment | Model | Supplier |
|---|---|---|
| Confocal microscope | Zeiss LSM 510 | Zeiss |

Immunolabeling of laminin and fibronectin

| Chemical/Reagent | Cat No. | Supplier |
|---|---|---|
| Xylene | X/0100/17 | Fisher Scientific |
| IMS | M/4450/17 | Fisher Scientific |
| Triton-X 100 | BP151 | Fisher Scientific |
| Bovine serum albumin (BSA) | A7030 | Sigma Aldrich |
| Polyclonal rabbit anti-fibronectin primary antibody | ab2413 | Abcam |
| Polyclonal rabbit anti-laminin primary antibody | ab11575 | Abcam |
| FITC anti-rabbit secondary antibody | A-11008 | Life Technologies |
| 4',6-diamidino-2-phenylindole (DAPI) | D8417 | Sigma Aldrich |
| PBS (Dulbecco A) tablets | BR0014 | Oxoid Ltd. |
| DPX mountant | D/5319/05 | Fisher Scientific |

| Material | Cat No. | Supplier |
|---|---|---|
| Slide rack | 70312-24 | EMS |
| Staining dish | 70312-23 | EMS |
| Cover slips | MNJ350020 | Thermo Fisher Scientific |
| Measuring cylinder | 1129469 | Camlab |
| Universal container | 1048636-1 | SLS |
| Microcentrifuge tube 1.5 ml | 11558232 | Fisher Scientific |
| Pasteur pipette | PIP4208 | SLS |
| Aluminium foil | 11247 | Terinex |

| | | |
|---|---|---|
| PAP pen | ab2601 | abcam |

| Equipment | Model | Supplier |
|---|---|---|
| Confocal microscope | Zeiss LSM 510 | Zeiss |
| Analytical balance | AB204 | Mettler Toledo |
| Automatic pipettes | Various | Gilson |

Contact cytotoxicity assay

| Chemical/Reagent | Cat No. | Supplier |
|---|---|---|
| Collagen type I (rat tail) | A10483-01 | Gibco |
| Cyanoacrylate contact adhesive | Z105880 | Sigma Aldrich |
| Sodium hydroxide pellets | 221465 | Sigma Aldrich |
| Dulbecco's Modified Eagle Medium (DMEM) | D6546 | Sigma Aldrich |
| Fetal calf serum (FCS) | F9565 | Sigma Aldrich |
| Penicillin/Streptomycin | P0781 | Sigma Aldrich |
| Amphotericin B | A2942 | Sigma Aldrich |
| L-Glutamine | G7513 | Sigma Aldrich |
| Trypsin ethylenediaminetetraacetic acid (EDTA) | T3924 | Sigma Aldrich |
| Giemsa's stain solution | 352603R | VWR International |
| Formaldehyde | F8775 | Sigma Aldrich |
| PBS (Dulbecco A) tablets | BR0014 | Oxoid Ltd. |

| Material | Cat No. | Supplier |
|---|---|---|
| 6 well plate | CC7682-7506 | CytoOne |
| Pasteur pipette | PIP4208 | SLS |
| Syringe (50 ml) | 300866 | BD Plastipak |
| Syringe filter (0.2 μm) | 83.1826.001 | Sarstedt |
| Magnetic stir bar | VWR1442- | VWR International |

| | | |
|---|---|---|
| | 0521 | |

| Equipment | Model | Supplier |
|---|---|---|
| Pipette boy | Pipetboy acu | Integra Biosciences |
| Automatic pipette | Various | Gilson |
| Haemocytometer | AC1000 | Hawksley |
| Inverted microscope | CK40 | Olympus |
| Magnetic stirrer | CD162 | Bibby Scientific |
| Analytical balance | AB204 | Mettler Toledo |
| Dissection kit | N/A | Thackeray |

## V. Quantitative analysis

*DNA quantification*

| Chemical/Reagent | Cat No. | Supplier |
|---|---|---|
| DNeasy kit | 69504 | Qiagen |
| Ethanol | 10048291 | Fisher Scientific |
| Calf thymus DNA (5 mg lyophilised) | D4522 | Sigma Aldrich |
| Nuclease free water | 436912C | VWR International |
| L-cysteine hydrochloride | C1276 | Sigma Aldrich |
| Di-sodium ethylenediaminetetraacetic acid | E5134 | Sigma Aldrich |
| PBS containing calcium and magnesium | 14040-133 | Life Technologies |

| Material | Cat No. | Supplier |
|---|---|---|
| Micro centrifuge tube 1.5 ml | 11558232 | Fisher Scientific |

| Equipment | Model | Supplier |
|---|---|---|
| Automatic pipettes | Various | Gilson |
| Analytical balance | AB204 | Mettler Toledo |
| Freeze dryer | FreeZone Triad | Spectrum |
| Centrifuge | CL10 | Thermo Scientific |
| Dissection kit | N/A | Thackeray |
| Nanodrop spectrophotometer | NanoDrop 1000 | Thermo Scientific |
| Pipette boy | Pipetboy acu | Integra Biosciences |
| Whirlimixer | MS2 | IKA |

*Collagen Quantification*

| Chemical/Reagent | Cat No. | Supplier |
|---|---|---|
| Hydrochloric acid | 2611.5000 | VWR International |
| Citric acid (monohydrate) | C1909 | Sigma Aldrich |
| Glacial acetic acid | 27222 | Sigma Aldrich |
| Sodium acetate (trihydrate) | BP334 | Fisher Scientific |
| Sodium hydroxide pellets | 221465 | Sigma Aldrich |
| Propan-1-ol | 20861.294 | VWR International |
| Chloramine T hydrate | 857319 | Sigma Aldrich |
| p-dimethylaminobenzaldehyde | 109762 | Sigma Aldrich |
| Perchloric acid (70%) | **244252** | Sigma Aldrich |
| Trans-4-hydroxy-L-proline | H54409 | Sigma Aldrich |

| Material | Cat No. | Supplier |
|---|---|---|
| Flat bottomed 96 well plate | 139006 | Thermo Scientific |
| Polypropylene universal container | E1412-3020 | Starlab Group |
| Micro centrifuge tube 1.5 ml | 11558232 | Fisher Scientific |

| Equipment | Model | Supplier |
|---|---|---|
| Automatic pipettes | Various | Gilson |
| Freeze dryer | FreeZone Triad | Spectrum |
| Magnetic stirrer | CD162 | Bibby Scientific |
| Absorbance microplate reader | ELx800 | BioTek |
| pH meter | SevenMulti | Mettler Toledo |
| Pipette boy | Pipetboy acu | Integre Biosciences |
| Table shaker | PSU-10i | SLS |

*GAG quantification*

| Chemical/Reagent | Cat No. | Supplier |
|---|---|---|
| Sodium di-hydrogen orthophosphate | S5011 | Sigma Aldrich |
| Di-sodium hydrogen orthophosphate | S9763 | Sigma Aldrich |
| 1,9 dimethylene blue | 341088 | Sigma Aldrich |
| Formic acid | F0507 | Sigma Aldrich |
| Papain | A3824 | PanReac ApplChem |
| L-cysteine hydrochloride | C1276 | Sigma Aldrich |
| Di-sodium ethylenediaminetetraacetic acid | E5134 | Sigma Aldrich |
| PBS containing calcium and magnesium | 14040-133 | Life Technologies |
| Ethanol | 10048291 | Fisher Scientific |
| Sodium formate | 30142LN | VWR International |
| Hydrochloric acid (6 M) | 2611.5000 | VWR International |
| Sodium hydroxide pellets | 221465 | Sigma Aldrich |
| Chondroitin sulphate B | C3788 | Sigma Aldrich |

| Material | Cat No. | Supplier |
|---|---|---|
| Flat bottomed 96 well plate | 139006 | Thermo Scientific |
| Polypropylene universal container | E1412-3020 | Starlab Group |

| Equipment | Model | Supplier |
|---|---|---|
| Automatic pipettes | Various | Gilson |
| Magnetic stirrer | CD162 | Bibby Scientific |
| Absorbance microplate reader | ELx800 | BioTek |
| pH meter | SevenMulti | Mettler Toledo |
| Pipette boy | Pipetboy acu | Integra Biosciences |
| Table shaker | PSU-10i | SLS |
| Water bath | Fisherbrand | Fisher Scientific |

## VI. General cell culture

### HDF culture

| Chemical/Reagent | Cat No. | Supplier |
|---|---|---|
| Difco-trypsin powder | 215240 | BD |
| Trypsin EDTA | T3924 | Sigma Aldrich |
| D-glucose | G8270 | Sigma Aldrich |
| Collagenase A | 10103578001 | Roche |
| Phenol red | P0290 | Sigma Aldrich |

| | | |
|---|---|---|
| DMEM | D6546 | Sigma Aldrich |
| FCS | F9565 | Sigma Aldrich |
| Penicillin/Streptomycin | P0781 | Sigma Aldrich |
| Amphotericin B | A2942 | Sigma Aldrich |
| L-Glutamine | G7513 | Sigma Aldrich |
| Dimethyl sulphoxide (DMSO) | 472301 | Sigma Aldrich |
| Sodium hydroxide pellets | 221465 | Sigma Aldrich |

| Material | Cat No. | Supplier |
|---|---|---|
| T25 flask | 82051-074 | VWR International |
| T75 flask | BD353136 | VWR International |
| Universal container | 1048636-1 | SLS |
| Cryovial | 72.377.992 | Sarstedt |
| Mr Frosty™ freezing container | 5100-0001 | Thermo Scientific |
| Syringe filter (0.2 μm) | 83.1826.001 | Sarstedt |
| Syringe (50 ml) | 300866 | BD Plastipak |
| Magnetic stir bar | VWR1442-0521 | VWR International |

| Equipment | Model | Supplier |
|---|---|---|
| Centrifuge | CL10 | Thermo Scientific |
| Inverted microscope | CK40 | Olympus |
| Automatic pipette | Various | Gilson |
| Pipette boy | Pipetboy acu | Integra Biosciences |
| Dissection kit | N/A | Thackeray |
| pH meter | SevenMulti | Mettler Toledo |
| Magnetic stirrer | CD162 | Bibby Scientific |
| Water bath | MH8516 | Electrothermal |
| Haemocytometer | AC1000 | Hawksley |

Human dermal microvascular endothelial cell culture

| Chemical/Reagent | Cat No. | Supplier |
|---|---|---|
| Proliferating HDMECs derived from human juvenile foreskin | C-12260 | PromoCell |
| Endothelial cell growth medium MV kit | C-22120 | PromoCell |
| Penicillin/streptomycin | P0781 | Sigma Aldrich |
| Amphotericin B | A2942 | Sigma Aldrich |
| DetachKit (contains hepesBSS, trypsin/EDTA, trypsin neutralising solution) | C-41210 | PromoCell |
| Pig skin gelatin | G-2500 | Sigma Aldrich |
| Cryo-SFM | C-29912 | PromoCell |
| PBS (Dulbecco A) tablets | BR0014 | Oxoid Ltd. |

| Material | Cat No. | Supplier |
|---|---|---|
| T25 flask | 82051-074 | VWR International |
| Universal container | 1048636-1 | SLS |
| Cryovial | 72.377.992 | Sarstedt |
| Mr Frosty™ freezing container | 5100-0001 | Thermo Scientific |
| Syringe filter (0.2 µm) | 83.1826.001 | Sarstedt |
| Syringe (50 ml) | 300866 | BD Plastipak |

| Equipment | Model | Supplier |
|---|---|---|
| Centrifuge | CL10 | Thermo Scientific |
| Inverted microscope | CK40 | Olympus |
| Pipette boy | Pipetboy acu | Integra Biosciences |
| Automatic pipette | Various | Gilson |
| Dissection kit | N/A | Thackeray |
| Analytical balance | AB204 | Mettler Toledo |
| Water bath | MH8516 | Electrothermal |

## VII. Melanin infusion of dermal fibroblasts

| Chemical/Reagent | Cat No. | Supplier |
|---|---|---|
| Melanin | M0418 | Sigma |
| DMEM | D6546 | Sigma Aldrich |
| FCS | F9565 | Sigma Aldrich |
| Penicillin/Streptomycin | P0781 | Sigma Aldrich |
| Amphotericin B | A2942 | Sigma Aldrich |
| Trypsin/EDTA | T3924 | Sigma Aldrich |
| FCS | F9565 | Sigma Aldrich |

| Material | Cat No. | Supplier |
|---|---|---|
| T75 flask | BD353136 | VWR International |
| Universal container | 1048636-1 | SLS |
| Pipette straw | 13-676-10H<br>13-676-10J<br>13-676-10K | Fisher Scientific |

| Equipment | Model | Supplier |
|---|---|---|
| Centrifuge | CL10 | Thermo Scientific |
| Pipette boy | Pipetboy acu | Integra Biosciences |
| Ultrasonic bath | Fisherbrand | Fisher Scientific |

## VIII. Bioscaffold recellularisation

| Chemical/Reagent | Cat No. | Supplier |
|---|---|---|
| Endothelial cell growth medium MV kit | C-22120 | PromoCell |
| Penicillin/streptomycin | P0781 | Sigma Aldrich |
| Amphotericin B | A2942 | Sigma Aldrich |
| DetachKit (contains hepesBSS, trypsin/EDTA, trypsin neutralising solution) | C-41210 | PromoCell |
| Pig skin gelatin | G-2500 | Sigma Aldrich |
| DMEM | D6546 | Sigma Aldrich |
| L-Glutamine | G7513 | Sigma Aldrich |
| FCS | F9565 | Sigma Aldrich |
| Trypsin EDTA | T3924 | Sigma Aldrich |

| Material | Cat No. | Supplier |
|---|---|---|
| Universal container | 1048636-1 | SLS |
| Pipette straw | 13-676-10H<br>13-676-10J<br>13-676-10K | Fisher Scientific |
| Syringe filter (0.2 μm) | 83.1826.001 | Sarstedt |
| Syringe (50 ml) | 300866 | BD Plastipak |
| Syringe (1 ml) | 300013 | BD Plastipak |
| Syringe (5 ml) | 302187 | BD Plastipak |

| Equipment | Model | Supplier |
|---|---|---|
| Centrifuge | CL10 | Thermo Scientific |
| Pipette boy | Pipetboy acu | Integra Biosciences |
| Haemocytometer | AC1000 | Hawksley |
| Forceps | Prestige | Morton medical supplies |
| Automatic pipettes | Various | Gilson |

## IX. Bioreactor design and preparation

| Chemical/Reagent | Cat No. | Supplier |
|---|---|---|

| | | |
|---|---|---|
| PA (40% v/v) | BP151 | Fisher Scientific |

| Material | Cat No. | Supplier |
|---|---|---|
| A4 stainless M5 12 mm socket head cap screw | - | Westfield fasteners |
| Lexan medical grade polycarbonate | - | The Plastic Shop |
| Tubing Versilic 2x 4 mm BxOD | TUB1944 | SLS |
| PharMed BPT tubing (1/8" × 3/16") | EW-96880-05 | Cole Parmer |
| Stainless steel grid | - | - |
| Pipe fittings (plug), 10-32 UNF, 9/32", 1/4" | TW-31503-30 | Cole Parmer |
| Barbed to threaded adapters | TW-40621-07 | Cole Parmer |
| Straight barbed tubing connector | WZ-06365-22 | Cole Parmer |
| Silicon elastomer kit | 1673921 | Dow Corning |
| 2 L glass beaker (tall) | BEA1166 | SLS |
| Square petri dish | 10489282 | Thermo Fisher Scientific |
| Straight sample container | 216-2595 | VWR International |

| Equipment | Model | Supplier |
|---|---|---|
| Oven | Heraeus vacutherm | Thermo Scientific |
| Laser cutter | Epilog Laser Mini | Epilog |
| Analytical balance | AB204 | Mettler Toledo |
| Autoclave | Touchclave II Osprey 100 | LTE |

X. Perfusion of recellularised bioscaffold

| Chemical/Reagent | Cat No. | Supplier |
|---|---|---|
| Endothelial cell growth medium MV kit | C-22120 | PromoCell |
| Penicillin/streptomycin | P0781 | Sigma Aldrich |
| Amphotericin B | A2942 | Sigma Aldrich |

| Material | Cat No. | Supplier |
|---|---|---|
| Pipette straw | 13-676-10K | Fisher Scientific |
| Syringe filter (0.2 μm) | 83.1826.001 | Sarstedt |
| Bioreactor base and lid | - | - |
| Silicon gasket | - | - |
| Tubing Versilic 2 x 4 mm B x OD | TUB1944 | SLS |

| | | |
|---|---|---|
| PharMed BPT tubing<br>(1/8" × 3/16") | EW-96880-05 | Cole Parmer |
| Stainless steel grid | - | - |
| Pipe fittings (plug), 10-32 UNF, 9/32", 1/4" | TW-31503-30 | Cole Parmer |
| Barbed to threaded adapters | TW-40621-07 | Cole Parmer |
| Straight barbed tubing connector | WZ-06365-22 | Cole Parmer |
| A4 stainless M5 12 mm socket head cap screw | - | Westfield fasteners |

| Equipment | Model | Supplier |
|---|---|---|
| Pipette boy | Pipetboy acu | Integra Biosciences |
| Forceps | Prestige | Morton medical supplies |
| Allen key | 6867C | Screwfix |
| Multi-channel cassette pump | 205U | Watson Marlow |

## XI. LIVE/DEAD cell staining

| Chemical/Reagent | Cat No. | Supplier |
|---|---|---|
| Propidium iodide | P3566 | Life Technologies |
| Syto® 9 | S-34854 | Life Technologies |
| DMEM | D6546 | Sigma Aldrich |

| Material | Cat No. | Supplier |
|---|---|---|
| 6 well plate | CC7682-7506 | CytoOne |
| Universal container | 1048636-1 | SLS |
| Aluminium foil | 11247 | Terinex |
| Pipette straw | 13-676-10J | Fisher Scientific |

| Equipment | Model | Supplier |
|---|---|---|
| Automatic pipette | Various | Gilson |
| Pipette boy | Pipetboy acu | Integra Biosciences |
| Dissection kit | N/A | Thackeray |
| Confocal microscope | Zeiss LSM 510 | Zeiss |

## XII. Collagen gel preparation

| Chemical/Reagent | Cat No. | Supplier |
|---|---|---|
| Collagen type I (rat tail) | A10483-01 | Gibco |
| Sodium hydroxide pellets | 221465 | Sigma Aldrich |
| Endothelial cell growth medium MV kit | C22120 | Sigma Aldrich |
| Penicillin/streptomycin | P0781 | Sigma Aldrich |
| Amphotericin B | A2942 | Sigma Aldrich |
| PBS (Dulbecco A) tablets | BR0014 | Oxoid Ltd. |
| VEGF 165 human | V7259 | Sigma Aldrich |

| Material | Cat No. | Supplier |
|---|---|---|
| Magnetic stir bar | VWR1442-0521 | VWR International |
| Syringe (50 ml) | 300866 | BD Plastipak |
| Syringe filter (0.2 μm) | 83.1826.001 | Sarstedt |
| Microcentrifuge tube 1.5 ml | 11558232 | Fisher Scientific |

| Equipment | Model | Supplier |
|---|---|---|
| Automatic pipette | Various | Gilson |
| Magnetic stirrer | CD162 | Bibby Scientific |

## XIII. Production of natural angiogenesis model

| Chemical/Reagent | Cat No. | Supplier |
|---|---|---|
| Collagen type I (rat tail) | A10483-01 | Gibco |
| Sodium hydroxide pellets | 221465 | Sigma Aldrich |
| Endothelial cell growth medium MV kit | C22120 | Sigma Aldrich |
| Penicillin/streptomycin | P0781 | Sigma Aldrich |
| Amphotericin B | A2942 | Sigma Aldrich |
| PBS (Dulbecco A) tablets | BR0014 | Oxoid Ltd. |
| VEGF human | V7259 | Sigma Aldrich |

| Material | Cat No. | Supplier |
|---|---|---|

| | | |
|---|---|---|
| Magnetic stir bar | VWR1442-0521 | VWR International |
| Syringe (50 ml) | 300866 | BD Plastipak |
| Syringe filter (0.2 μm) | 83.1826.001 | Sarstedt |
| Microcentrifuge tube 1.5 ml | 11558232 | Fisher Scientific |
| 24 gauge cannula | 381212 | BD Insyte |
| Stainless steel rings | - | - |

| Equipment | Model | Supplier |
|---|---|---|
| Automatic pipette | Various | Gilson |
| Magnetic stirrer | CD162 | Bibby Scientific |
| Forceps | Prestige | Morton medical supplies |

| Chemical/Reagent | Cat No. | Supplier |
|---|---|---|
| IMS | M/4450/17 | Fisher Scientific |

| Material | Cat No. | Supplier |
|---|---|---|
| Fertilised chick eggs | - | Henry Stewart & Co. |
| Parafilm | P7793 | Sigma Aldrich |
| Masking tape | 378-98 29 | RS |

| Equipment | Model | Supplier |
|---|---|---|
| Chick egg incubator | RCOM Suro | Amazon |
| Dissection kit | N/A | Thackeray |
| Hacksaw blade | 05260140 | B&Q |
| Digital microscope | N43HH | Maplin |

## XIV. Chick CAM assay

## XV. Synthetic scaffold production

### Electrospinning PHBV

| Chemical/Reagent | Cat No. | Supplier |
|---|---|---|
| Poly(3-hydroxybutyrate-*co*-3-hydroxyvalerate) (PHBV) pellets | BV326301 | Goodfellow |
| Methanol | M/4058/17 | Fisher Scientific |
| Dichloromethane (DCM) | D/1850/17 | Fisher Scientific |

| Material | Cat No. | Supplier |
|---|---|---|
| Magnetic stir bar | VWR1442-0521 | VWR International |
| 50ml Duran® glass bottle | 11782282 | Fisher Scientific |
| Syringe (5 ml) | 302187 | BD Plastipak |
| Blunt tip needles (0.6 mm ID) | FIS5601098 | AMS Ltd. |
| Flat metal sheet | 3232636003958 | B&Q |
| Rule | 12969084 | Fisher Scientific |

| Equipment | Model | Supplier |
|---|---|---|
| Magnetic stirrer | CD162 | Bibby Scientific |
| Syringe pump | Genie Plus | Kent Scientific |
| High voltage power pack | 7XX30 | Genvolt |
| Mandrel | SSCY30X120 | Linari engineering |
| Retort stand | 11548092 | Fisher Scientific |
| Retort stand clamp | 11517722 | Fisher Scientific |

Alginate printing

| Chemical/Reagent | Cat No. | Supplier |
|---|---|---|
| Alginic acid sodium salt from brown algae | A2033 | Sigma Aldrich |
| Calcium chloride dihydrate | 100704Y | BDH |
| Glycerol | G/0650/17 | Fisher Scientific |
| Eosin Y | E4009 | Sigma Aldrich |

| Material | Cat No. | Supplier |
|---|---|---|
| Glass beaker | 13127374 | Fisher Scientific |
| Magnetic stir bar | VWR1442-0521 | VWR International |
| Syringe barrel | 7012072 | Nordson |
| Blunt tip needles (0.6 mm ID) | FIS5601098 | AMS Ltd. |

| Equipment | Model | Supplier |
|---|---|---|
| Magnetic stirrer | CD162 | Bibby Scientific |
| Positive displacement dispensing system | Ultra2800 | Nordson |
| 3D printer | RepRap | Mendel |

Alginate removal

| Chemical/Reagent | Cat No. | Supplier |
|---|---|---|
| Anhydrous acid free ethylenediaminetetraacetic acid (EDTA) | E6758 | Sigma Aldrich |
| Sodium hydroxide pellets | 221465 | Sigma Aldrich |

| Material | Cat No. | Supplier |
|---|---|---|
| Straight sample container | 216-2595 | VWR International |
| Magnetic stir bar | VWR1442-0521 | VWR International |
| Measuring cylinder | 1129469 | Camlab |

| Equipment | Model | Supplier |
|---|---|---|
| Magnetic stirrer | CD162 | Bibby Scientific |
| pH meter | SevenMulti | Mettler Toledo |
| See-saw rocker | Stuart | Fisher Scientific |

## XVI. Scanning electron microscopy

| Chemical/Reagent | Cat No. | Supplier |
|---|---|---|
| Glutaraldehyde | G6257 | Sigma Aldrich |
| Ethanol | 10048291 | Fisher Scientific |
| Hexamethyldisilazane (HMDS) | 440191 | Sigma Aldrich |
| PBS (Dulbecco A) tablets | BR0014 | Oxoid Ltd. |

| Material | Cat No. | Supplier |
|---|---|---|
| Pipette straw | 13-676-10H<br>13-676-10J<br>13-676-10K | Fisher Scientific |
| 6 well plate | CC7682-7506 | CytoOne |

| Equipment | Model | Supplier |
|---|---|---|
| Pipette boy | Pipetboy acu | Integra Biosciences |
| Gold sputter coater | Emscope SC500 | Philips |
| SEM | Inspect F | FEI |

## XVII. Synthetic scaffold sterilisation

| Chemical/Reagent | Cat No. | Supplier |
|---|---|---|
| Ethanol | 10048291 | Fisher Scientific |
| PBS (Dulbecco A) tablets | BR0014 | Oxoid Ltd. |

| Material | Cat No. | Supplier |
|---|---|---|
| Petri dish (90mm) | SLS2000 | SLS |
| 24 gauge cannula | 381212 | BD Insyte |
| Ethicon 4/0 sutures (Mersilk) | W501H | Medisave |

| Equipment | Model | Supplier |
|---|---|---|
| Dissection kit | N/A | Thackeray |
| Dissection microscope | M 3Z | Wild Heerbrugg |

## XVIII. Mechanical testing

| Material | Cat No. | Supplier |
|---|---|---|
| Ethicon 4/0 sutures (Mersilk) | W501H | Medisave |
| Digital callipers | 11787105 | Fisher Scientific |

| Equipment | Model | Supplier |
|---|---|---|
| Uniaxial load test system | Electroforce 3100 | Bose |

## XIX. Synthetic scaffold recellularisation

| Chemical/Reagent | Cat No. | Supplier |
|---|---|---|
| Endothelial cell growth medium MV kit | C-22120 | PromoCell |
| Penicillin/streptomycin | P0781 | Sigma Aldrich |
| Amphotericin B | A2942 | Sigma Aldrich |
| DetachKit (contains hepesBSS, trypsin/EDTA, trypsin neutralising solution) | C-41210 | PromoCell |
| Pig skin gelatin | G-2500 | Sigma Aldrich |
| DMEM | D6546 | Sigma Aldrich |
| L-Glutamine | G7513 | Sigma Aldrich |
| FCS | F9565 | Sigma Aldrich |
| Trypsin EDTA | T3924 | Sigma Aldrich |

| Material | Cat No. | Supplier |
|---|---|---|
| Syringe (1 ml) | 300013 | BD Plastipak |
| Universal container | 1048636-1 | SLS |
| Pipette straw | 13-676-10H<br>13-676-10J<br>13-676-10K | Fisher Scientific |

| Equipment | Model | Supplier |
|---|---|---|
| Centrifuge | CL10 | Thermo Scientific |
| Pipette boy | Pipetboy acu | Integra Biosciences |
| Haemocytometer | AC1000 | Hawksley |
| Forceps | Prestige | Morton medical supplies |
| Automatic pipettes | Various | Gilson |

## XX. Production of synthetic angiogenesis model

| Chemical/Reagent | Cat No. | Supplier |
|---|---|---|
| Collagen type I (rat tail) | A10483-01 | Gibco |
| Sodium hydroxide pellets | 221465 | Sigma Aldrich |
| Endothelial cell growth medium MV kit | C22120 | Sigma Aldrich |
| Penicillin/streptomycin | P0781 | Sigma Aldrich |
| Amphotericin B | A2942 | Sigma Aldrich |
| PBS (Dulbecco A) tablets | BR0014 | Oxoid Ltd. |
| VEGF human | V7259 | Sigma Aldrich |

| Material | Cat No. | Supplier |
|---|---|---|
| Magnetic stir bar | VWR1442-0521 | VWR International |
| Syringe (50 ml) | 300866 | BD Plastipak |
| Syringe filter (0.2 μm) | 83.1826.001 | Sarstedt |
| Microcentrifuge tube 1.5 ml | 11558232 | Fisher Scientific |
| 24 gauge cannula | 381212 | BD Insyte |

| Equipment | Model | Supplier |
|---|---|---|
| Automatic pipette | Various | Gilson |
| Magnetic stirrer | CD162 | Bibby Scientific |
| Forceps | Prestige | Morton medical supplies |

## XXI. Immunohistochemistry

| Chemical/Reagent | Cat No. | Supplier |
|---|---|---|
| Monoclonal mouse anti-human CD31 primary antibody | M082329 | Dako |
| Polyclonal rabbit anti-alpha smooth muscle Actin (αSMA) primary antibody | ab5694 | abcam |
| Mouse anti-VE-cadherin (CD144) primary antibody | 610252 | BD Biosciences |
| Goat anti-mouse IgG secondary antibody, Alexa Fluor® 546 conjugate | A-11030 | Life Technologies |
| Goat anti-mouse IgG secondary antibody, Alexa Fluor® 488 conjugate | A-11001 | Life Technologies |
| DAPI | D8417 | Sigma Aldrich |
| Glycine | 23390 | Serva |
| BSA | A9418 | Sigma Aldrich |
| TWEEN® 20 | P9416 | Sigma Aldrich |
| Xylene | X/0100/17 | Fisher Scientific |
| IMS | M/4450/17 | Fisher Scientific |
| PBS (Dulbecco A) tablets | BR0014 | Oxoid Ltd. |
| Paraformaldehyde (PFA) | 158127 | Sigma Aldrich |
| Hanks Balanced Salt Solution (HBSS) with calcium and magnesium | 14025050 | Life Technologies |
| Sodium hydroxide pellets | 221465 | Sigma Aldrich |

| Material | Cat No. | Supplier |
|---|---|---|
| Slide rack | 70312-24 | EMS |
| Staining dish | 70312-23 | EMS |
| Cover slips | MNJ350020 | Thermo Fisher Scientific |
| SuperFrost® Plus slides | 48311-703 | VWR International |
| Measuring cylinder | 1129469 | Camlab |
| Universal container | 1048636-1 | SLS |
| Microcentrifuge tube 1.5 ml | 11558232 | Fisher Scientific |
| Pasteur pipette | PIP4208 | SLS |
| Aluminium foil | 11247 | Terinex |
| PAP pen | ab2601 | abcam |
| 24 well plate | 3524 | SLS |
| Magnetic stir bar | VWR1442-0521 | VWR International |

| Equipment | Model | Supplier |
|---|---|---|
| Automatic pipettes | Various | Gilson |
| Confocal microscope | Zeiss LSM 510 | Zeiss |
| Forceps | Prestige | Morton medical supplies |
| Magnetic stirrer | CD162 | Bibby Scientific |

## XXII. FITC-lectin perfusion

| Chemical/Reagent | Cat No. | Supplier |
|---|---|---|
| PFA | 158127 | Sigma Aldrich |
| HBSS with calcium and magnesium | 14025050 | Life Technologies |
| FITC conjugated lectin from Lycopersicon esculentum (tomato) | L0401 | Sigma Aldrich |

| Material | Cat No. | Supplier |
|---|---|---|
| Petri dish (90 mm) | SLS2000 | SLS |
| Syringe (1 ml) | 300013 | BD Plastipak |

| Equipment | Model | Supplier |
|---|---|---|
| Automatic pipette | Various | Gilson |
| Syringe pump | Genie Plus | Kent Scientific |
| Forceps | Prestige | Morton medical supplies |

## B. Preparation of general reagents

### I. PBS solution

To prepare PBS solution, one PBS tablet (Dulbecco A) was added to every 100 ml of distilled water in a bottle able to withstand autoclaving. PBS was autoclaved for 10 minutes at 115 °C and stored at room temperature.

Supplemented PBS was prepared by adding 5ml of penicillin/streptomycin and 1.5 ml of amphotericin B to 500 ml of PBS to give final concentrations of 100 U/ml, 0.1 mg/ml and 0.75 μg/ml respectively.

### II. 0.1% Peracetic acid (PA) solution

PA solution was prepared to a final concentration of 0.1% (v/v) by adding 1.25 ml of PA stock solution (40% v/v) to 500 ml of distilled water.

### III. Formaldehyde (3.7% w/v)

A formaldehyde working solution was prepared by adding 50 ml of formaldehyde stock solution (37% w/v) to 450 ml of PBS to give a final concentration of 3.7% (w/v).

### IV. IMS

Absolute IMS was diluted in distilled water to produce solutions with final concentrations of 70%, 80%, 90% and 95% (v/v).

V. Sodium hydroxide (1M) solution

To prepare a 1 M sodium hydroxide solution, 4 g of sodium hydroxide pellets were added to a clean bottle containing 100 ml of distilled water. A magnetic stir bar was added and the solution was stirred using a magnetic stirrer until the pellets had completely dissolved. The solution was filter sterilised in a class II biological safety cabinet.

VI. Gluteraldehyde (2.5%) solution

Gluteraldehyde stock solution was diluted in PBS at a ratio of 1:10 to obtain a 2.5% (w/v) glutaraldehyde working solution.

# C. Bioscaffold characterisation

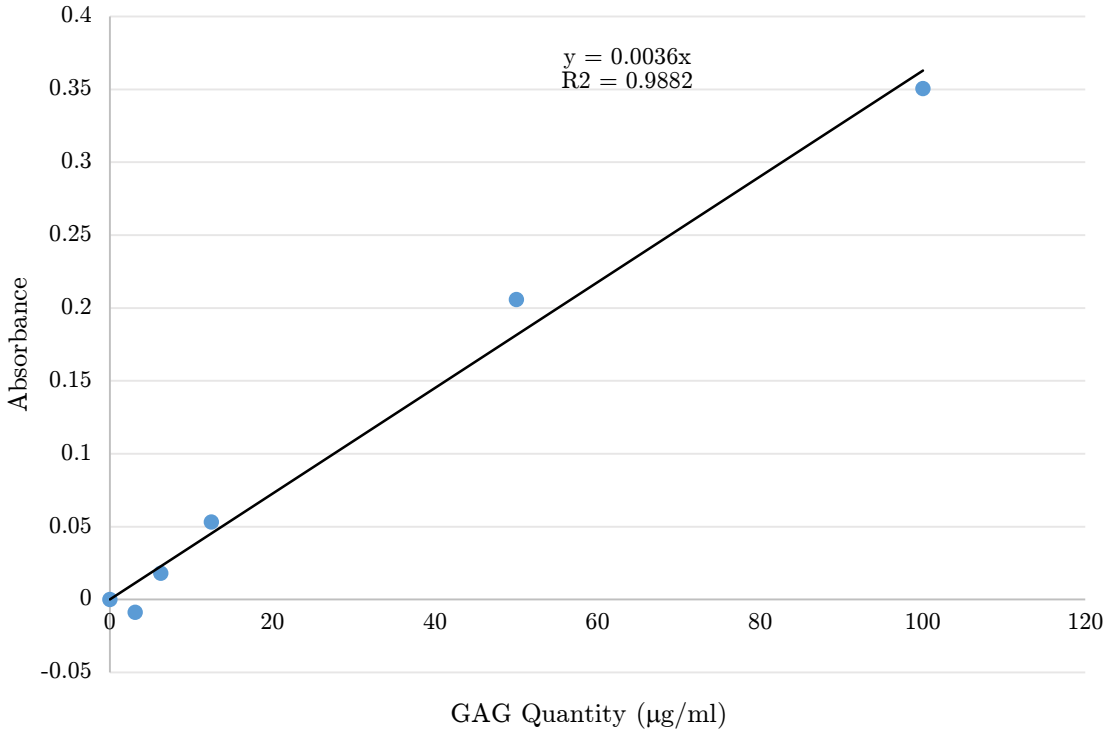


Figure 67 – Calibration curve used to determine the GAG content in the decellularized jejunum.

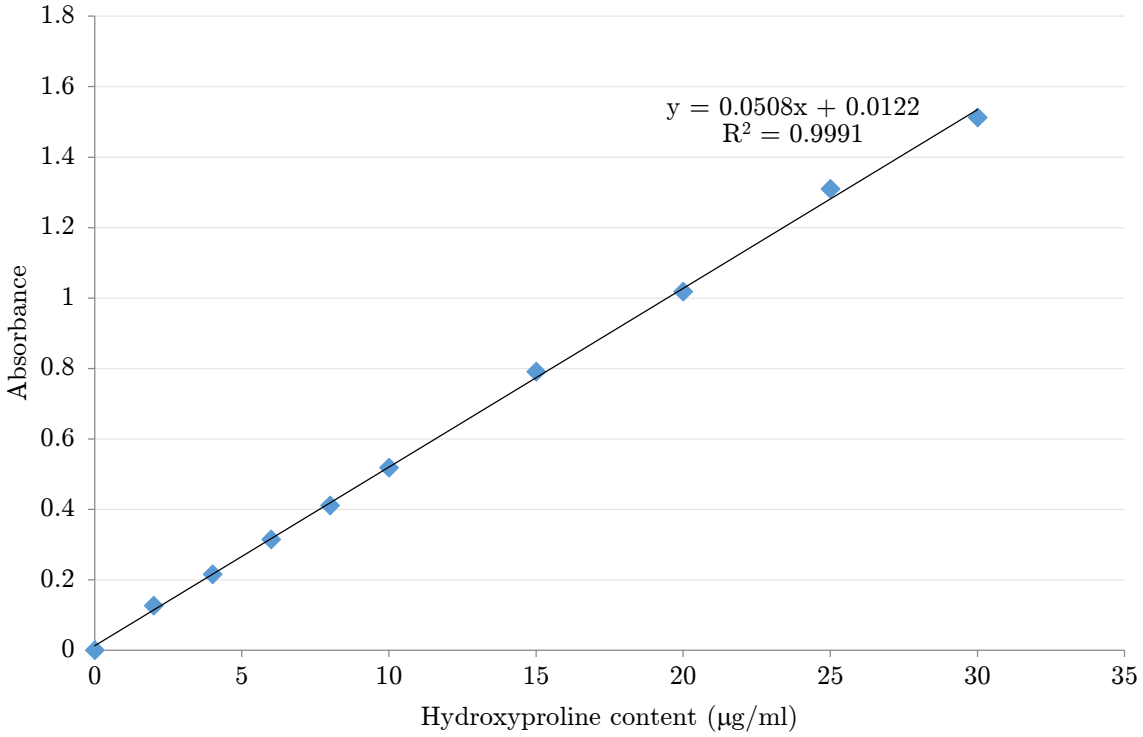


Figure 68 – Calibration curve used to determine the hydroxyproline content in the decellularised jejunal segments.

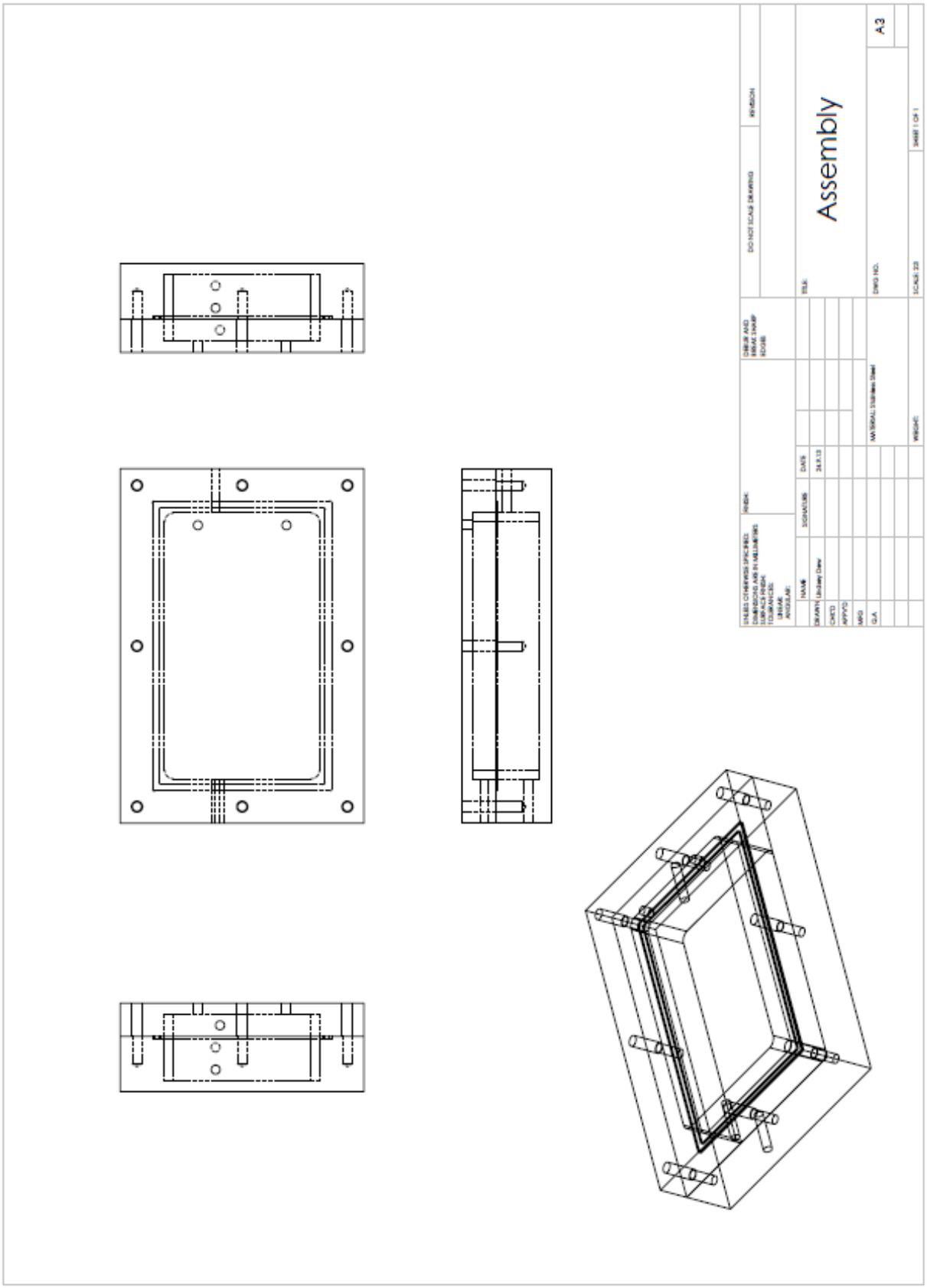


Figure 69 – CAD drawing of the assembled bioreactor produced using the software SolidWorks.

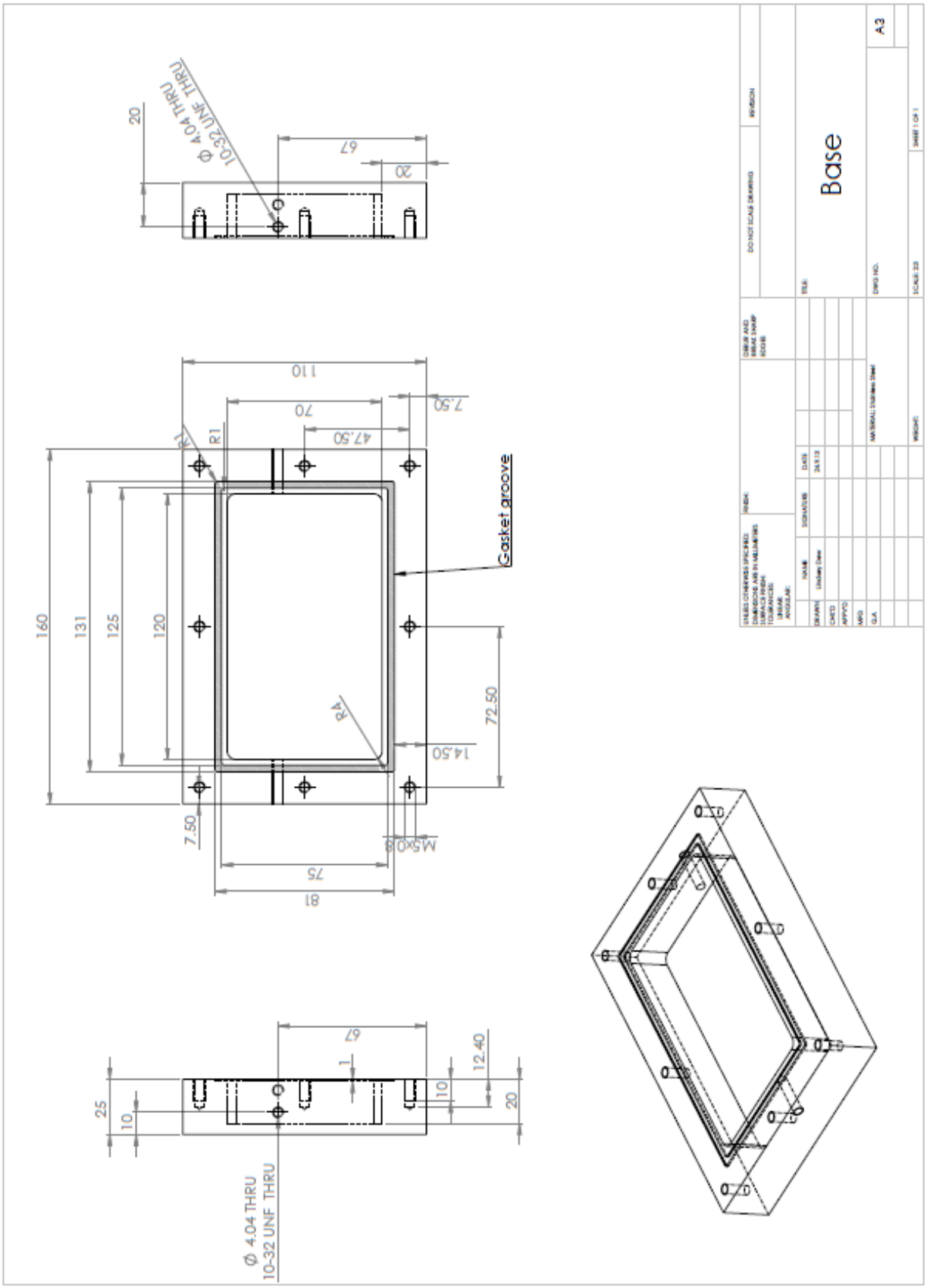


Figure 70 – CAD drawing of the base of the bioreactor produced using the software package SolidWorks.

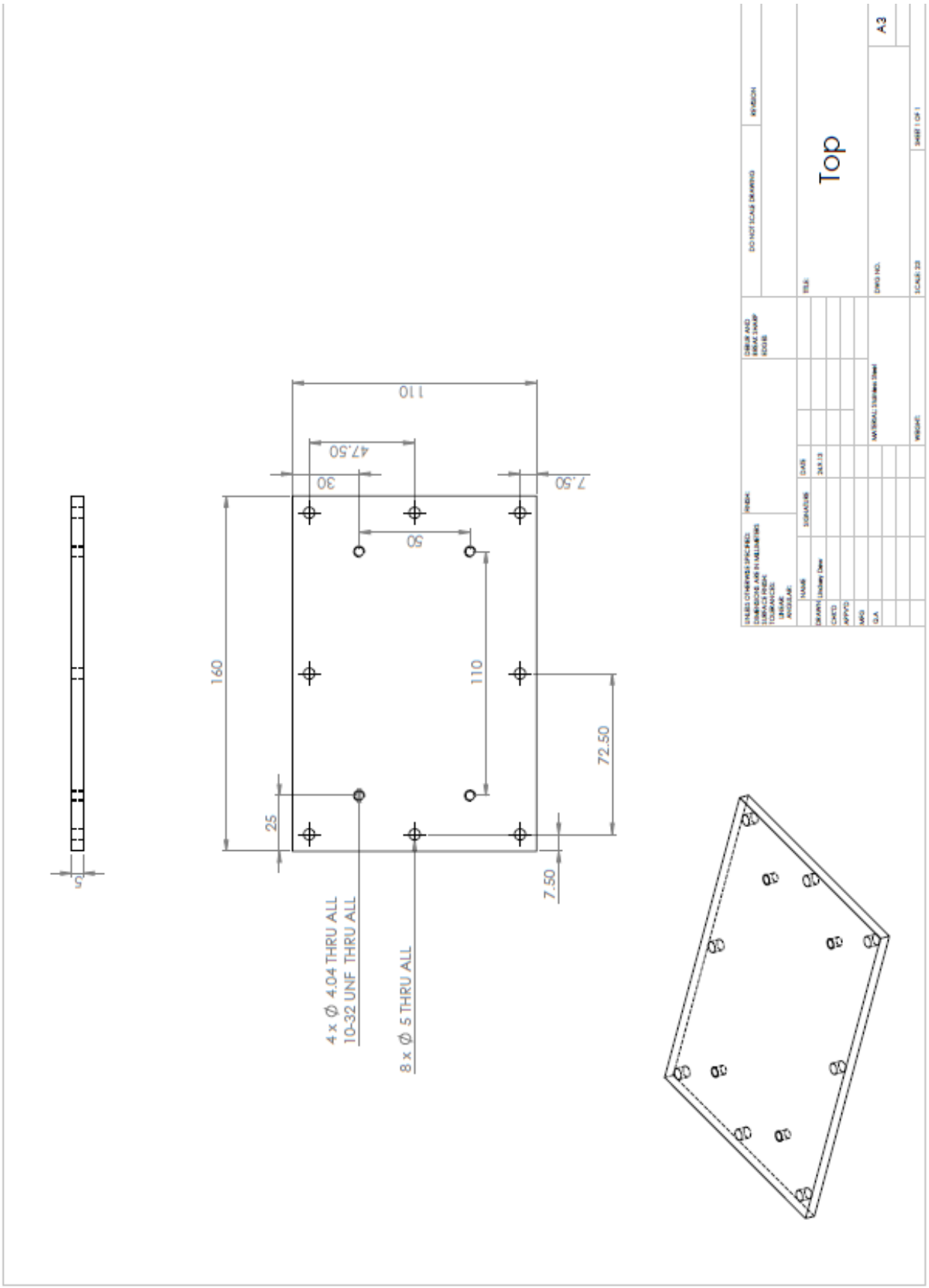


Figure 71 – CAD drawing of the lid of the bioreactor produced using the software package SolidWorks.

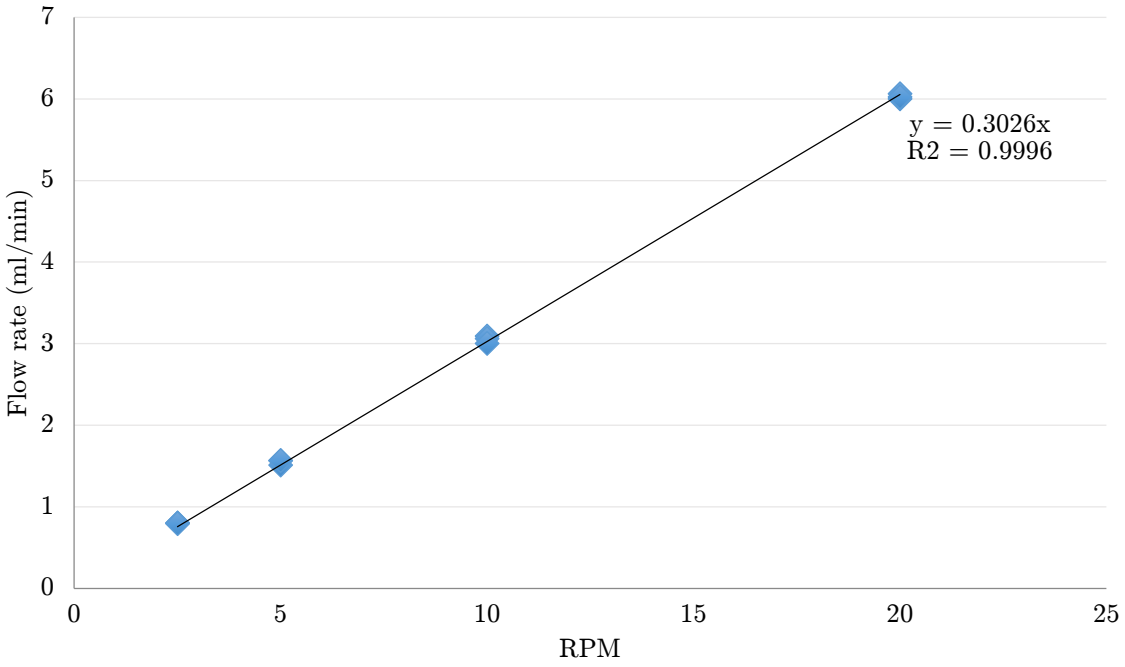


Figure 72 – Calibration curve for Watson Marlow pump attached to the assembled bioreactor to determine the required RPM setting associated with the desired flow rate.